Utilization of Thermoplastic Mounting Studs for Simple Performance Testing on Hot Mix Asphalt

by

Dirk BeGell

A Thesis Presented in Partial Fulfilment
of the Requirements for the Degree
Master of Science

Approved April 2018 by the
Graduate Supervisory Committee

Kamil E. Kaloush, Chair
Michael Mamlouk
Jeffery Stempihar

ARIZONA STATE UNIVERSITY

May 2018

ABSTRACT

The objective of the research is to test the use of 3D printed thermoplastic to produce fixtures which affix instrumentation to asphalt concrete samples used for Simple Performance Testing (SPT). The testing is done as part of materials characterization to obtain properties that will help in future pavement designs. Currently, these fixtures (mounting studs) are made of expensive brass and cumbersome to clean with or without chemicals.

Three types of thermoplastics were utilized to assess the effect of temperature and applied stress on the performance of the 3D printed studs. Asphalt concrete samples fitted with thermoplastic studs were tested according to AASHTO & ASTM standards. The thermoplastics tested are: Polylactic acid (PLA), the most common 3D printing material; Acrylonitrile Butadiene Styrene (ABS), a typical 3D printing material which is less rigid than PLA and has a higher melting temperature; Polycarbonate (PC), a strong, high temperature 3D printing material.

A high traffic volume Marshal mix design from the City of Phoenix was obtained and adapted to a Superpave mix design methodology. The mix design is dense-graded with nominal maximum aggregate size of ¾" inch and a PG 70-10 binder. Samples were fabricated and the following tests were performed: Dynamic Modulus |E*| conducted at five temperatures and six frequencies; Flow Number conducted at a high temperature of $50°C$, and axial cyclic fatigue test at a moderate temperature of $18°C$.

The results from SPT for each 3D printed material were compared to results using brass mounting studs. Validation or rejection of the concept was determined from statistical analysis on the mean and variance of collected SPT test data.

The concept of using 3D printed thermoplastic for mounting stud fabrication is a promising option; however, the concept should be verified with more extensive research using a variety of asphalt mixes and operators to ensure no bias in the repeatability and reproducibility of test results. The Polycarbonate (PC) had a stronger layer bonding than ABS and PLA while printing. It was recommended for follow up studies.

DEDICATION

To Nancy Almanza for trying so hard.

Thank you

ACKNOWLEDGMENTS

This thesis would not have been possible without the support of the following:

Dr. Kamil E. Kaloush

Dr Michael Mamlouk

Dr. M. W. Witczak

Dr. Jeffrey Stempihar

Ramadan Salim

Jose Medina

Hossein Noorvand

Akshay Gundla

Gonzalo Arredondo

Phani Sasank Kaligotla

Janak Shah

Aswin Srinivasan

Southwest Asphalt

Trey Billingsley

Tom Waters

Austin Bolze

TABLE OF CONTENTS

Page

CHAPTER Page

LIST OF TABLES

Table Page

Table Page

Table Page

Table Page

LIST OF FIGURES

Figure Page

Figure Page

Figure Page

Figure Page

Figure Page

Figure Page

1. INTRODUCTION AND OBJECTIVE

Laboratory testing on asphalt concrete is valuable for predicting pavement performance in the field. The viscoelastic-plastic nature of asphalt concrete is very difficult to model and is still not fully understood. There is a plethora of variables involved with the prediction of pavement performance; temperature, frequency of loading, pavement structure, aggregate gradation, choice of binder, and aging are a few of the variables that must be incorporated into pavement performance modeling.

Years of research has led to almost universally accepted laboratory testing methodology for asphalt concrete. Various Simple Performance Testing (SPT) protocols, that complement the Superpave Mix Design method, were originally developed at Arizona State University (ASU) [1,4]. SPT included several carefully controlled experiments performed on laboratory prepared specimens. The collected data is analyzed and yields results that are used to predict the behavior and performance, both short term and long term, of asphalt pavements in nearly any climate.

Permanent deformation tests such as, Triaxial Dynamic Modulus, AASHTO TP 62-07 and T 342-11, Repeated Load Permanent Deformation, AASHTO TP 79-13 and Direct Tension Cyclic Fatigue, AASHTO TP 107-14, require specimens to be instrumented with Linear Variable Differential Transformers (LVDTs) to accurately measure deformation that occurs under the various loading conditions. The current method for affixing LVDT instrumentation to specimens requires gluing of brass mounting studs to cored specimens using a five-minute, two-part epoxy. The fixtures are made of expensive brass and cumbersome to clean with or without chemicals. Utilizing

the emerging technology of additive manufacturing (3D Printing) to produce mounting studs from thermoplastics, may potentially yield comparable results to the current SPT instrumentation practices at a fraction of the cost. The rapid manufacturing process allows more time for experimentation and less time cleaning studs with harmful chemicals. Additionally, the opportunity to recycle the thermoplastic material after use suggests a level of sustainability previously not recognized for the asphalt testing industry.

The objective of this research is to manufacture thermoplastic studs using desktop 3D printers, then perform simple performance tests on samples fitted with 3D printed studs, as well as the traditional brass studs. The SPT tests include a variety of strain levels, load frequencies and temperatures. The results are compared to ascertain if there is a statistical difference between additively manufactured studs and currently used brass studs. For this investigation, a single asphalt mixture and three types of thermoplastics were tested. Comparison to brass studs was analyzed using statistical hypothesis testing on the mean and variance of collected SPT data, and comparison of fatigue testing models.

2. LITERATURE REVIEW

2.1 Superpave Mix Design System

The Superpave mix design system is a comprehensive method of designing paving mixes tailored to the unique performance requirements influenced by the traffic, environment (climate), and structural section at a particular pavement site [1]. It is

designed along with performance-based properties collected from a potential mix, to determine the most economical asphalt mix design that achieves the performance requirements that are required from that location. The method is valid for virgin or modified Hot Mix Asphalt (HMA) and facilitates the use of recycled materials if desired. The method is applicable for construction of new surface and base layers, as well as overlay design. Through materials selection and mix design, it directly addresses the reduction and control of permanent deformation, fatigue cracking, and low-temperature cracking. It also explicitly considers the effects of aging and moisture sensitivity in promoting or arresting the development of these three distresses [1]. The basic workflow of the design method can be broken down into three sequential categories, volumetric design, mechanical properties, and finally field control. The first two components are iterated until the optimal mix has been determined, then field control verifies the mix design. Figure *1* below outlines the basic workflow of the Superpave mix design method.

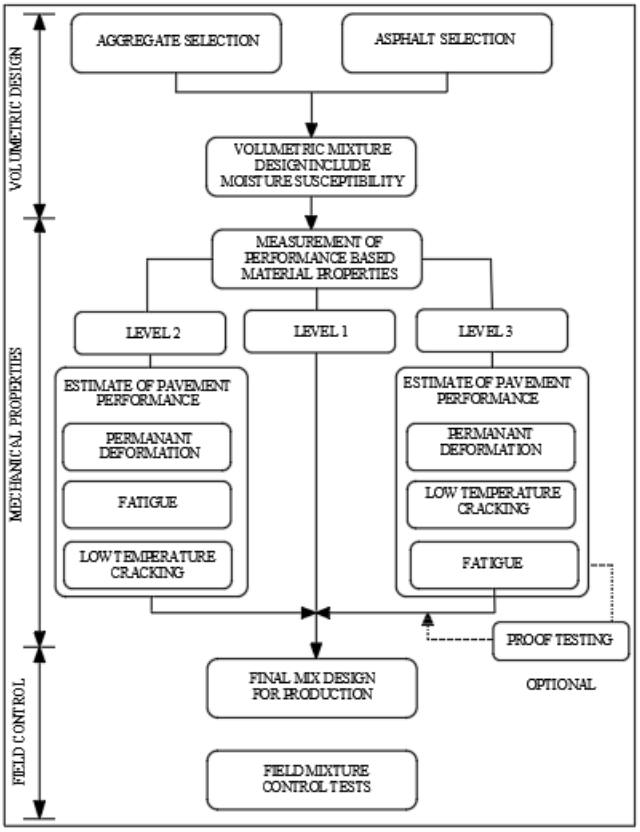

Figure 1: Workflow of Superpave Mix Design Method *[1]*

Superpave is an acronym for SUperior PERforming asphalt PAVEment [2]. The design methods and tools are being implemented by many state agencies to replace the Marshall and Hveem design methods, although some state agencies, such as Phoenix, still hold tight to the older design methods. For this reason, the Marshall design obtained for this research had to be modified to the equipment and design methodology used at Arizona State University.

2.2 Simple Performance Testing

Research completed by Witczak and Kaloush, at the University of Maryland and Arizona State University, led to the development of standardized laboratory testing procedures for performance-based mix design. The main objective of the research was to

develop testing procedures that accurately correlate laboratory tests to measurable field rutting and fatigue cracking behaviors. Three candidate tests and sixteen test parameters were evaluated using mixtures and performance data from three experimental sites: the Minnesota Road Project (MnRoad), the Federal Highway (FHWA) Accelerated Loading Facility Study (ALF), and the FHWA Performance-Related Specifications Study (WesTrack) [3]. The research also outlines development in laboratory specimen instrumentation techniques and minimum specimen dimensions that would provide true measured material responses. Preliminary recommendations for specific laboratory tests were defined in Phase II of a FHWA contract with the University of Maryland and are outlined in The National Cooperative Highway Research Project (NCHRP) 465 report, Simple Performance Tests for Superpave Mix Design, published by the Transportation Research Board – National Research Council in 2002 [4]. The NCHRP 465 report defines SPT as follows:

A test method(s) that accurately and reliably measures a mixture response characteristic or parameter that is highly correlated to the occurrence of pavement distress (e.g., cracking and rutting) over a diverse range of traffic and climatic conditions [4].

Considering this definition, SPT must assess a mixture's ability to resist permanent deformation and fracture given criteria specific to the location where the pavement is to be placed. The researchers determined there is no "Perfect" test for all HMA mixtures at varying temperatures and loading scenarios.

Referencing several years of research, as well as information collected from industry professionals, it was determined that rutting, fatigue cracking, and thermal cracking were the most important distresses to simulate for SPT; of these three distresses,

rutting and fatigue cracking were the main focus of concern for pavement design and testing. From the NCHRP 465 study, five laboratory tests were found to have good-to-excellent correlation to field measured rutting and three laboratory tests were found to have a fair correlation to fatigue and thermal cracking.

A summary of these tests are as follows:

For Rutting

- Repeated Shear Permanent Deformation
- Triaxial Compression, at high temperatures
- Triaxial Creep
- Permanent Shear Strain.
- Triaxial Repeated Load

For Cracking

- Triaxial Compression at lower temperatures
- Indirect Tensile Creep
- Indirect Tensile Strength

Based on the results of the NCHRP testing program, the research team recommended three test-parameter combinations for further field validation as an SPT for permanent deformation: (1) the dynamic modulus term, $E^*/\sin\varphi$, (determined from the triaxial dynamic modulus test); (2) the flow time, *Ft*, determined from the triaxial static creep test; and (3) the flow number, *Fn*, determined from the triaxial repeated load test. All combinations exhibit a coefficient of determination, R^2 value, of 0.9 or greater for the combined correlation of the laboratory test results with performance in the MnRoad, Wes-Track, and FHWA ALF experiments [4].

2.2.1 Dynamic Modulus |E*|

The procedure for sample preparation and testing for the Dynamic Modulus |E*| test is outlined in the AASHTO TP 62-07, “Determining the Dynamic Modulus of Hot Mix Asphalt (HMA)”, and the ASTM D3497-79, “Standard Test Method for Dynamic

Modulus of Asphalt Concrete Mixtures.”. The test consists of a sinusoidal (haversine) axial compression stress being applied to a specimen of asphalt concrete at a given temperature and loading frequency. The resulting recoverable axial strain response of the specimen is measured and used to calculate dynamic modulus [9]. This test is considered to be a non-destructive test (NDT) method as the amount of applied stress experienced by the sample does not exceed the linear viscoelastic limit of the material; however, along with recoverable strain, the sample does experience a small amount of permanent deformation as a result of the applied stress.

The test is performed at several temperatures and frequencies. The data collected is then shifted to fit a sigmoidal curve. The shifted data forms a master curve which allows the behavior of the asphalt concrete to be predicted at any given temperature and frequency. The sigmoidal E* model correlates to rutting, at high temperature and low frequency of loading, and to fatigue damage, low to mid-range temperature at repeated high frequency of loading. The samples are instrumented with LVDTs and conditioned in a temperature- controlled chamber until test temperature is achieved at the sample core. An actuator loading device inside the chamber applies the stress while the LVDTs collect deformations on the sample. shows the machine setup for running the Dynamic Modulus Test and an instrumented sample fitted with three LVDTs.

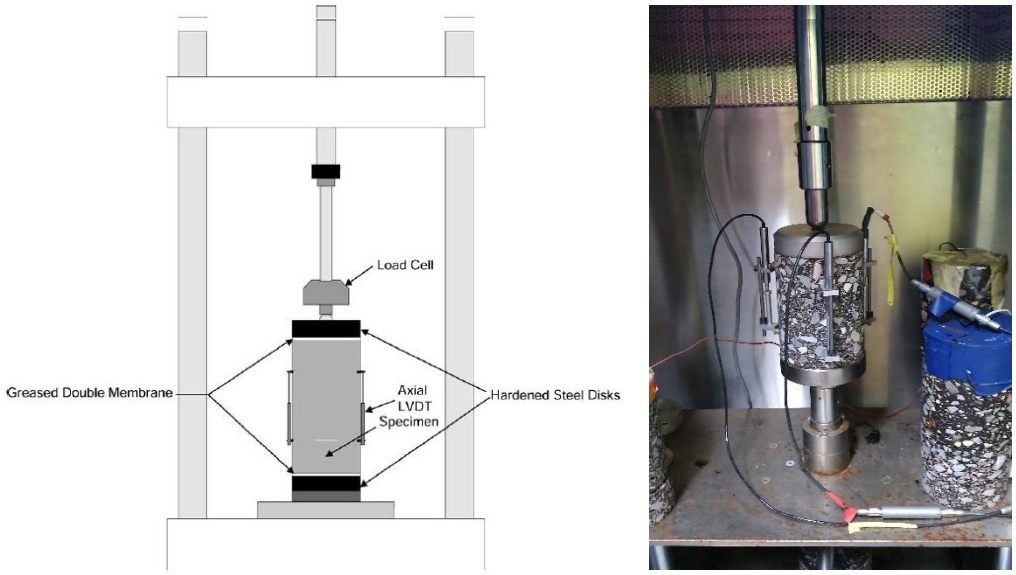

Figure 2. Machine Setup For The Dynamic Modulus Test [10]

The number of replicates that must be tested depends on the number of LVDTs used to collect data and the desired level of accuracy. AASHTO standard TP 62-7 states "Three replicate specimens should be tested to obtain a desired accuracy limit (e.g., less than 15% percent of the true dynamic modulus)." [10]. Table *1* summarizes the effect of estimated accuracy depending on the number of replicates and LVDTs. To achieve an acceptable level of accuracy of $\pm 12\%$ three replicates fitted with three LVDTs were tested.

Table 1. Estimated Accuracy Associated with The Number of Replicates [10].

LVDTs per Specimen	Number of Specimens	Estimated Limit of Accuracy
2	2	±18.0%
2	3	±15.0%
2	4	±13.4%
3	2	±13.1%
3	3	±12.0%
3	4	±11.5%

The procedure for analysis of raw data collected is given in the AASHTO TP 62-07 standard [10]. The first step is to analyze the collected stress data. The process is performed on centered stress data, which is calculated by subtracting average stress. Equation (1) is used to determine the average stress.

$$\bar{\sigma} = \frac{\sum_{i=1}^{n} \sigma_1}{n} \quad (1)$$

Where:
$\bar{\sigma}$ = Average Stress
σ_1 = Raw Stress point i in the data array
n = Number of points in the data array

Equation (2) is used to compute the centered stress by subtracting the average stress from each measured stress.

$$\sigma_1' = \sigma_1 - \bar{\sigma} \quad (2)$$

Where:
σ_1' = Centered stress point in the array
σ_1 = Raw Stress point i in the data array
$\bar{\sigma}$ = Average Stress

Three stress coefficients are the computed from the centered stress data, offset, in-phase magnitude, and out-of-phase magnitude, by using equations (3) – (5).

$$A_{\sigma 0} = \frac{\sum_{i=1}^{n} \sigma_i'}{n} \tag{3}$$

$$A_{\sigma 1} = \frac{2}{n} \sum_{i=1}^{n} \sigma_i' \cos(\omega_0 t_i) \tag{4}$$

$$B_{\sigma 1} = \frac{2}{n} \sum_{i=1}^{n} \sigma_i' \sin(\omega_0 t_i) \tag{5}$$

Where:
$A_{\sigma 0}$ = Stress offset coefficient, kPa (psi)
σ_1' = Centered Stress point i in the data array
$A_{\sigma 1}$ = Stress in − phase magnitude coefficient, kPa (psi)
ω_0 = Frequency of applied stress, rad, sec
t_i = Time at point i in the data array, sec
$B_{\sigma 1}$ = Stress out − of − phase magnitude coefficient, kPa (psi)

Equations (6) and (7) are used to compute the stress magnitude and the stress phase using the stress coefficients angle.

$$|\sigma^*| = \sqrt{A_{\sigma 1}^2 + B_{\sigma 1}^2} \tag{6}$$

$$\theta_\sigma = \arctan\left(-\frac{B_{\sigma 1}}{A_{\sigma 1}}\right) \tag{7}$$

Where:
$|\sigma^*|$ = Stress magnitude, kPa (psi)
$A_{\sigma 1}$ = Stress in − phase magnitude coefficient, kPa (psi)
$B_{\sigma 1}$ = Stress out − of − phase magnitude coefficient, kPa (psi)
θ_σ = Stress phase angle, degrees

Equations (8) and (9) are used to compute an array of predicted centered stresses and the standard error of applied stress.

$$\hat{\sigma}_i' = A_{\sigma 0} + A_{\sigma 1}\cos(\omega_0 t_i) + B_{\sigma 1}\sin(\omega_0 t_i) \quad (8)$$

$$SE(\sigma) = \sqrt{\frac{\sum_{i-1}^{n}\left(\hat{\sigma}_i' - \sigma_1'\right)^2}{n-4}}\left(\frac{100\%}{|\sigma^*|}\right) \quad (9)$$

Where:
$\hat{\sigma}_i'$ = Predicted centered stress at point i, kPa (psi)
$A_{\sigma 0}$ = Stress offset coefficient, kPa (psi)
$A_{\sigma 1}$ = Stress in − phase magnitude coefficient, kPa (psi)
ω_0 = Frequency of applied stress, rad, sec
t_i = Time at point i in the data array, sec
$B_{\sigma 1}$ = Stress out − of − phase magnitude coefficient, kPa (psi)
$SE(\sigma)$ = Standard error for applied stress, percent
σ_1' = Centered Stress point i in the data array
n = Number of points in the data array
$|\sigma^*|$ = Stress magnitude, kPa (psi)

The second step is to analyze collected strain data which is corrected for drift caused by permanent deformation during the test, and centered data based on average strain for the transducers. Drift estimation is made by identifying the slope of local minimum and maximum values with respect to time by linear regression. The average of the two slopes is the rate of drift D_j for transduce j. Equation (10) is used to calculate average strain.

$$\overline{\epsilon_j} = \frac{\sum_{j=1}^{n}\epsilon_{j_i}}{n} \quad (10)$$

Where:
$\overline{\epsilon_j}$ = Average strain for transducer j
ϵ_{j_i} = Raw strain for transducer j at point in the data array
n = Number of points in the data array

Equation (11) is used to compute the centered strain by subtracting the rate of drift times, loading time, and the average strain from the measured strain for that transducer.

$$\epsilon'_{ji} = \epsilon_{ji} - D_j t_i - \overline{\epsilon_j} \tag{11}$$

Where:
ϵ'_{j_i} = Centered strain for transducer j at point in the data array
ϵ_{j_i} = Raw strain for transducer j at point in the data array
D_j = Rate of drift for transducer j
t_i = Time for point i in the data array
$\overline{\epsilon_j}$ = Average strain for transducer j

Three strain coefficients are the computed from the centered strain data, offset, in-phase magnitude, and out-of-phase magnitude, by using equations (12) – (14).

$$A_{\epsilon_{j0}} = \frac{\sum_{j=1}^{n} \epsilon'_{j_i}}{n} \tag{12}$$

$$A_{\epsilon_{ji}} = \frac{2}{n} \sum_{j=1}^{n} \epsilon'_{j_i} \cos(\omega_0 t_i) \tag{13}$$

$$B_{\epsilon_{ji}} = \frac{2}{n} \sum_{j=1}^{n} \epsilon'_{j_i} \sin(\omega_0 t_i) \tag{14}$$

Where:
$A_{\epsilon_{j0}}$ = Strain offset coefficient, kPa (psi)
ϵ'_{j_i} = Centered strain for transducer j at point in the data array
$A_{\epsilon_{ji}}$ = Strain in − phase magnitude coefficient, kPa (psi)
ω_0 = Frequency of applied stress, rad, sec
t_i = Time at point i in the data array, sec
$B_{\epsilon_{ji}}$ = Strain out − of − phase magnitude coefficient, kPa (psi)

Equations (15) and (16) are used to compute the strain magnitude and the strain phase using the stress coefficients angle.

$$\left|\epsilon_j^*\right| = \sqrt{A_{\epsilon_{ji}}^2 + B_{\epsilon_{ji}}^2} \tag{15}$$

$$\theta_{\epsilon_{ji}} = \arctan\left(-\frac{B_{\epsilon_{ji}}}{A_{\epsilon_{ji}}}\right) \tag{16}$$

Where:
$\left|\epsilon_j^*\right| =$ Stress magnitude, kPa (psi)
$A_{\epsilon_{ji}} =$ Strain in $-$ phase magnitude coefficient for transducer j, kPa (psi)
$B_{\epsilon_{ji}} =$ Strain out $-$ of $-$ phase magnitude for transducer j, , kPa (psi)
$\theta_{\epsilon_{ji}} =$ Strain phase angle for transducer j, , degrees

Equations (17) and (18) are used to compute an array of predicted centered strains and the standard error of strain data for each transducer.

$$\hat{\epsilon}'_{ji} = A_{\epsilon_{j0}} + A_{\epsilon_{ji}}\cos(\omega_0 t_i) + B_{\epsilon_{ji}}\sin(\omega_0 t_i) \tag{17}$$

$$SE(\epsilon_j) = \sqrt{\frac{\sum_{j=1}^{n}\left(\hat{\epsilon}'_{ji} - \epsilon_{ji}\right)^2}{n-4}}\left(\frac{100\%}{\left|\epsilon_j^*\right|}\right) \tag{18}$$

Where:
$\hat{\epsilon}'_{ji} =$ Predicted centered strain for transducer j at point i
$A_{\epsilon_{j0}} =$ Strain offset coefficient for transducer j
$A_{\epsilon_{ji}} =$ Strain in $-$ phase magnitude coefficient for transducer j
$\omega_0 =$ Frequency of applied stress, rad, sec
$t_i =$ Time at point i in the data array, sec
$B_{\epsilon_{ji}} =$ Strain out $-$ of $-$ phase magnitude coefficient for transducer j
$SE(\epsilon_j) =$ Standard error for strain transducer j response, percent
$\epsilon'_{ji} =$ Centered Strain for transducer j point i in the data array
n = Number of points in the data array
$\left|\epsilon_j^*\right| =$ Strain magnitude for transducer j

Equations (19) – (23) are used to calculate the average phase angle, strain magnitude, standard error for all m strain transducers, and two uniformity coefficients representing the variation among transducers.

$$\overline{\theta_\epsilon} = \frac{\sum_{j=1}^{m} \theta_{\epsilon j}}{m} \tag{19}$$

$$|\epsilon^*| = \frac{\sum_{j=1}^{m} |\epsilon_j^*|}{m} \tag{20}$$

$$se(\epsilon) = \frac{\sum_{j=1}^{m} se(\epsilon_j)}{m} \tag{21}$$

$$U_\epsilon = \sqrt{\frac{\sum_{j=1}^{n} \left(|\epsilon_j^*| - |\epsilon^*|\right)^2}{m-1}} \left(\frac{100\%}{|\epsilon^*|}\right) \tag{22}$$

$$U_\theta = \sqrt{\frac{\sum_{j=1}^{n} \left(\theta_{\epsilon j} - \theta_\epsilon\right)^2}{m-1}} \tag{23}$$

Where:
$\overline{\theta_\epsilon}$ = Average phase angle for all strain transducers, degrees
m = Number of transducers
$|\epsilon^*|$ = Average strain magnitude
$se(\epsilon)$ = Average standard error for all strain transducer , percent
U_ϵ = Uniformity coefficient for strain transducers, percent
U_ϵ = Uniformity coefficient phase angle, degree

The final step in analysis is to calculate overall phase angle, the complex modulus at a selected frequency. Equations (24) and (25) are used to calculate these parameters.

$$\theta(\omega) = \overline{\theta_\epsilon} - \theta_\sigma \tag{24}$$

$$|E^*(\omega)| = \frac{|\sigma*|}{|\epsilon*|} \tag{25}$$

Where:
$\theta(\omega) =$ Phase angle betweenapplied stress and strain for frequency ω, degrees
$\bar{\theta}_{\epsilon} =$ Average phase angle for all strain transducers, degrees
$\theta_{\sigma} =$ Strain phase angle, degrees
$|E^*(\omega)| =$ Dynamic modulus for frequency ω, kPa (psi)
$U_{\epsilon} =$ Uniformity coefficient for strain transducers, percent
$U_{\epsilon} =$ Uniformity coefficient phase angle, degree
$|\bar{\epsilon^*}| =$ Average strain magnitude

2.2.3 Repeated Load Permanent Deformation

NCHRP Project 9-19 recommends the Flow Number (FN) test as a simple performance test for the evaluation of rutting in asphalt mixtures. The FN test results have shown good correlation with rutting under various traffic levels on pavements. A significant parameter for the evaluation of rutting in the field is shear deformation in asphalt mixtures, and this value can be identified by the Flow Number test. This value is obtained from the Repeated Load Permanent Deformation (RLPD) lab test as outlined in the AASHTO TP 79-13 standard test document.

The flow number represents a measure of rutting potential and can be determined by applying a uniaxial compressive load, using a 0.1s haversine pulse with a 0.9s dwell time, to a compacted lab specimen. The test is conducted by exposing the specimen to the repeated compressive load at a specific temperature, determined by the effective temperature of the location where the asphalt is to be placed. The number of cycles of the applied load is plotted against the cumulative permanent deformation (strain percent) and yields a graph with three distinct sections, a primary section that describes the shear deformation accumulated during compaction and initial traffic loads, a secondary section that mimics the behavior of the asphalt over the majority of the life span of a pavement,

and a tertiary section that describes the point at which the threshold of shear deformation is overcome and rutting begins. The flow number is the cycle number that corresponds to the point where tertiary flow begins.

The test for flow number also yields more valuable information about an asphalt mix. The resilient modulus is also calculated from application of the repeated load permanent deformation test. The resilient modulus is a measure of the material strength and is often used similarly to Young's modulus. The resilient modulus and Poisson's ratio are two parameters used in linear elastic analysis. The amount of resilient strain is also a parameter that results from the test for flow number. The resilient strain is the amount of recoverable axial strain experienced by the material during the rest period of the loading process. After the sample is loaded the material recovers a portion of the strain during the rest period. The value is recorded and cumulative percentages are reported. This parameter shows the elasticity of the sample and corresponds to the field performance of the asphalt. The permanent strain measured from the flow number and the recoverable strain provide the strain ratio parameter, which is the ratio of permanent strain to recoverable strain. This parameter gives an overall view of how the material will behave, taking into account both forms of strain the material experiences. A higher strain ratio shows a material does not recover much, which can indicate more rutting potential in the field.

The flow number test is a valuable tool in simple performance testing of asphalt materials as it provides a great deal of information about the strength and performance of a complex material. The Francken model is used to determine the flow number (FN) or

tertiary flow. Nonlinear regression analysis is used to fit the model to the test data. Equation (26) is the model used to describe the behavior of deformation of the material under a certain number of cycles of the haversine applied load (0.1s of load and 0.9s of rest period), giving the strain for each cycle of load.

$$\varepsilon_p(N) = a \cdot N^b + c(e^{d \cdot N} - 1) \tag{26}$$

Where:
ε_p(N) = Permanent strain at N cycles
N = Number of cycles
a, b, c, d = regression coefficients

The intercept, a, represents the permanent strain at N = 1, and the slope, b, represents the rate of change in permanent strain as a function of the change in loading cycles (log(N)). An alternative form of the model used to characterize the permanent strain per load repetition (ε_{pn}) can be derived as shown in Equation (27) and can be expressed by Equation (28):

$$\frac{\partial \varepsilon_p}{\partial N} = \varepsilon_{pn} = \frac{\partial (aN^b)}{\partial N} \tag{27}$$

$$\varepsilon_{pn} = ab \cdot N^{(b-1)} \tag{28}$$

The first derivative of the permanent strain function will provide the slope of the tangent line to the function at some point N, and shows whether a function is increasing or decreasing, and by what rate the change is occurring. Zero slope indicates a local maximum or minimum is defined at that point or that a turning point was defined. A positive derivative signifies the function is increasing, and a negative derivative signifies the function is decreasing. Equation (29) shows the first derivative of the strain model:

$$\frac{\partial \varepsilon_p}{\partial N} = abN^{b-1} + cde^{dN} \quad (29)$$

The second derivate of the strain function shows where the Flow Number (inflection point) is given. If the second derivative is positive, it means that the first derivative is increasing, and that the slope of the tangent line to the function is increasing as N increases. Thus, the second derivative of the strain function will tell when N is a local maximum or minimum. The second derivative is shown in Equation (30):

$$\frac{\partial^2 \varepsilon_p}{\partial N^2} = ab(b-1)N^{b-2} + cd^2e^{dN} \quad (30)$$

The procedure for performing the RLPD test as outlined in the AASHTO TP 79-13 standard uses and Asphalt Mixture Performance Tester (AMPT) [11]. The test performed at ASU used a loading frame contained in a temperature-controlled chamber. The procedure is outlined as follows:

1. The compacted sample is cut and cored into specimens 100 mm in diameter and 150 mm in height. The specimen is instrumented for performing flow number test.
2. Thermoplastic studs were glued to sample at three positions with 120^0 angle between each on top and bottom. One set of each thermoplastic studs were used to attach LVDT instrumentation. The performance of each set of studs were compared to the measured actuator strain.
3. The LVDT instruments were attached to studs with the help of screws.
4. The sample is placed into the universal testing machine and is conditioned at the required temperature for eight hours.

5. Three LVDT's are attached to sample to measure displacements.
6. The conditioned sample is tested by applying 0.1s haversine pulse with 0.9s dwell time.
7. A deviatoric stress must be set in such a magnitude that tertiary flow occurs within 2000 and 10000 number of load cycles.
8. The flow number is determined by the point at which the specimen exhibits tertiary flow, which is shear deformation at constant volume. The test procedure destroys the samples.

The test temperature was determined from the average 7-day max pavement surface temperature where the asphalt is to be placed, termed the effective temperature. For this research the effective temperature was determined to be 122°F (50°C). The amount of deviatoric stress to be applied to the sample and the corresponding flow number was estimated based on the Flow Number Prediction Model proposed by Rodezno and Kaloush [12].

Viscosity and gradation information was found from in the mix design provided by Southwest Asphalt. The value of deviatoric stress predicted by the model was 457 kPa and yielded a flow number of approximately 680 cycles. The results suggest the predictive model was unsuccessful in predicting the flow number, however yielded a starting point for the applied stress to be used for testing. As a precaution, an applied stress of 300 kPa was used for testing. Equation (31) shows the strength relationship based on Mohr-Coulomb failure theory.

$$\sigma_1 = \sigma_3 \tan^2\left(45° + \frac{\phi}{2}\right) + 2c \tan^2\left(45° + \frac{\phi}{2}\right) \quad (31)$$

Where:
σ_1 = Major principle stress at failure
σ_3 = Minor principle stress at failure
$\phi = Friction\ angle$

The statistical analysis was based on the relationship and degree of interaction of the different variable. The predictor variables originally selected also included volumetrics and binder properties for each mix [12]. The following terms are included in the approximation of the c and phi parameters.

- Binder Viscosity at the test temperature, and at 70°F; defined in terms of A_i and VTS_i
- Aggregate Gradation (%R_{34}, R_{38}, R_{04} and Passing 200 sieve)
- Air Voids (V_a%)
- Binder Content (AC%)
- Effective Binder Content (V_{beff}%)
- Voids in the Mineral Aggregate (VMA)
- Voids Filled with Asphalt (VFA)
- Test Temperature (°F)

The final form of the c and phi models is shown in equations (32) and (33); The final regression model is shown in Equation (34).

$$c = 65.493 + 3.48 \times 10^{-7}V_2 - 0.595V_a - 0.442T - 1.324.4AC + 1.37P_{200} \quad (32)$$

$$\phi = 28.18 + 0.354R_{04} - 0.476VMA + 0.075T - 0.090R_{38} + 0.112R_{34} \quad (33)$$

$$Log(FN) = 0.485 + 0.644Log(V_1) + 0.0874P_{200} - 3.323Log(p) + 0.0129R_{04} - 0.080V_a + 2.593Log(q) - 0.0142R_{34} \quad (34)$$

Where:
$FN =$ Flow Number
$V_1 =$ Viscosity at 100°F, Poise
$P_{200} =$ Percent passing the #200 seive
$P =$ Vertical Stress, psi
$R_{04} =$ Percent passing the #4 seive
$V_a =$ Air void content, percent
$q =$ Horizontal stress, psi
$R_{34} =$ Percent passing the 3/4" sieve

2.2.4 Direct Tension Cyclic Fatigue

The test method for determination of the damage characteristic curve resulting from the Direct Tension Cyclic Fatigue test are outlined in the AASHTO TP 107-14 standard. Software used at Arizona State University, called the Viscoelastic Cyclic Data test and analysis software, Asphalt Pavement Hierarchical Analysis Toolbox-Materials at Multiple Scales (ALPHAMAT), was developed by Underwood [13].

AASHTO TP 107-14 summarizes the test as a controlled and repeated cyclic loading is applied to a cylindrical asphalt concrete specimen until failure. The applied stress and on-specimen axial strain response are measured and used to calculate the necessary quantities. The relationship between the damage (*S*) and the pseudo secant modulus (*C*) is determined and expressed as the damage characteristic curve [14]. The test utilizes a temperature-controlled chamber kept at 18°C and a Universal Testing Machine which applies the cyclic compressive and tensile load. The 75mm diameter, 150mm tall sample is fitted with loading end plates and mounting studs which are glued with a 5-minute two-part epoxy. The sample is fitted with six LVDTs, four loose-core styles at 90° apart and two spring style LVDTs at 180° apart; All have a gage length of 100mm.

The test first collects dynamic modulus data at one temperature and one frequency (10Hz) which is used as a linear viscoelastic fingerprint for the cyclic test. The fingerprint test is performed in the tension-compression mode of loading. A minimum of three tests must be completed at different strain levels for each treatment. The first test is run at 300 $\mu\varepsilon$ (microstrains). The following tests are run at microstrain values of either $\pm 50\ \mu\varepsilon$ or $\pm 100\ \mu\varepsilon$, depending on the number of cycles necessary until failure (N_f) of the first test. *Table 2* summarizes the choice for micro-strain setting for the second and third tests.

Table 2: On-specimen Strain Levels for Samples Two and Three.

Case	$\varepsilon os2$	$\varepsilon os3$
$500 < Nf1 < 1{,}000$	$\varepsilon os1 - 100$	$\varepsilon os1 - 150$
$1{,}000 < Nf1 < 5{,}000$	$\varepsilon os1 - 50$	$\varepsilon os1 - 100$
$5{,}000 < Nf1 < 20{,}000$	$\varepsilon os1 + 50$	$\varepsilon os1 - 50$
$20{,}000 < Nf1 < 100{,}000$	$\varepsilon os1 + 100$	$\varepsilon os1 + 50$
$100{,}000 < Nf1$	$\varepsilon os1 + 150$	$\varepsilon os1 + 100$

The standard procedure for calculating the pseudo strain, pseudo secant modulus, and damage for fatigue tests are automatically performed using ALPHAMAT software. The detailed calculation procedure is outlined using the following equations. First, it is necessary to determine the E(t) Prony coefficients from the measured dynamic modulus and phase angle outlined in AASHTO T342 [15]. Next determine the specimen-to-specimen normalization parameter using Equation (35).

$$DMR = \frac{|E^*|fingerprint}{|E^*|_{LVE}} \tag{35}$$

Where:
$|E^*|$fingerprint = Dynamic modulus, kPa or psi
$|E^*|$LVE = Average representation dynamic modulus for the mixture of interest
At the temperature and frequency of interest, kPa or psi, and computed from Equation (36)
DMR = Dynamic modulus ratio, which is the specimenvariability compensation parameter, kPa or psi

$$|E^*|_{LVE} = \sqrt{\left[E_\infty + \sum_{m=1}^{N} \frac{E_m \omega_R^2 \rho_m^2}{\omega_R^2 \rho_m^2 + 1}\right]^2 + \left[\sum_{m=1}^{N} \frac{E_m \omega_R \rho_m}{\omega_R^2 \rho_m^2 + 1}\right]^2} \quad (36)$$

Where:
ω = Angular frequency used in the fingerprint experiment
a_T = Time − temperature shift factor for the fingerprint test temperature
ω_R = Reduced angular frequency, Equation (37), used in the fingerprint experiment
E_∞, E_m, ρ_m = Prony coefficient terms

$$\omega_R = \omega \times a_T \quad (37)$$

Separate the data into two parts. The first part, referred to as data set 1, comprises the data for the first half of the first loading path (from zero to first peak stress). The second part, referred to as data set 2, comprises the rest of the data. 12.5. For data set 1, average all sensor readings and compute the average strain for all data points using Equation (38).

$$\varepsilon = \frac{\delta}{GL} \quad (38)$$

Where:
ε = Average axial strain
$\delta\varepsilon$ = Average axial displacement measured by the sensors, mm or in.
GL = Sensor gage length, mm or in.

Compute the axial stress using Equation (39) for each data point in set 1

$$\sigma = \frac{F}{\pi r^2} \tag{39}$$

Where:
σ = Axial stress, kPa or psi
F = Axial force measured by the load transducers, kN or lb.
r = Specimen radius mm or in.

Compute the reduced time for each data point in data set 1 using Equation (40)

$$t_R = \frac{t}{a_T} \tag{40}$$

Where:
a_T = Time − temperature shift factor at a given temperature
t = Time measured from the experiment, s
t_R = Reduced time, s

Compute the pseudo strain for each data point in data set 1 using the state of variable formulation in Equation (41).

$$\varepsilon^{R(n+1)} = \frac{1}{E_R}\left[\eta_0^{n+1} + \sum_{m=1}^{N} \eta_m^{n+1}\right] \tag{41}$$

Where:
$\varepsilon^{R(n+1)}$ = Pseudo strain at the next time step
E_R = Reference modulus, a value of 1 should be chosen
η = Elastic component of the pseudo strain (Equation (42))
η_m = Pseudo strain contribution of Prony element m (Equation (43))
n = Time step used in the calculation
ε = Strain calculated for the current or subsequent time step using Equation (38)
Δ_{t_r} = Duration of the reduced time step, $t_R^{n+1} - t_R^n$
t_R = Reduced time

$$\eta_0^{n+1} = E_\infty(\varepsilon^{n+1}) \tag{42}$$

$$\eta_m^{n+1} = e^{-\frac{\Delta t_R}{\rho_m}}\eta_m^n + \rho_m\left(\frac{\varepsilon^{n+1}-\varepsilon^n}{\Delta_{t_R}}\right)\left[1 - e^{-\frac{\Delta t_R}{\rho_m}}\right] \tag{43}$$

Compute the normalized pseudo secant strain for each data point in data set 1 using Equation (44).

$$C = \frac{\sigma}{\varepsilon^R \times DMR} \tag{44}$$

Compute the change in damage, ΔS, for each step using Equation (45).

$$\Delta S_1 = \left(-\frac{DMR}{2}(\varepsilon^R)(C_i - C_{i-1})\right)^{\frac{\alpha}{\alpha+1}} \left(\Delta_{t_R}\right)^{\frac{1}{\alpha+1}} \tag{45}$$

Where:
$C_i =$ Pseudo secant modulus at the current time step
$C_{i-1} =$ Pseudo secant modulus at the previous time step
$\Delta_{t_R} =$ Change in the reduced time step
$\alpha =$ Continuum damage power term related to material time dependence, Equation (47)

$$\Delta S_1 = \begin{cases} \left(-\frac{DMR}{2}(\varepsilon^R)(C_i - C_{i-1})\right)^{\frac{\alpha}{\alpha+1}} \left(\Delta_{t_R}\right)^{\frac{1}{\alpha+1}} & \begin{matrix} C_i \leq C_{i-1} \\ C_i \geq C_{i-1} \end{matrix} \\ 0 \end{cases} \tag{46}$$

$$\alpha = \frac{1}{n} + 1 \tag{47}$$

Where:
$n =$ Maximum $\log - \log$ slope of the relaxation modulus

Determine the damage at each time step using Equation (48).

$$S_i = \sum_{i=1}^{N} \Delta S_i \tag{48}$$

Where:
$S_i =$ Cumulative damage at the current time step
$\Delta S_i =$ Incremental damage for all time steps to be summed from the initial time step, $\mathrm{i} = 1,$ to the current time step

Define the damage at the final point in data set 1 as $S_{dataset\ 1}$. Compute the peak-to-peak strain for each sensor and each cycle in data set 2 using Equation (49).

$$\varepsilon_{pp}^{i} = \frac{\delta_{peak}^{i} - \delta_{valley}^{i}}{GL} \quad (49)$$

Where:
$i =$ Index to denote that the calculation is performed for all four sensors
$\varepsilon_{pp}^{i} =$ Peak $-$ to $-$ peak axial strain for sensor, i
$\delta_{peak}^{i} =$ Peak axial displacement measured by sensor, i, mm or in.
$\delta_{valley}^{i} =$ Valley axial displacement measured by sensor, i, mm or in.

For each cycle in data set 2, average all sensor strains and denote this as the test peak-to-peak strain amplitude, ε_{pp}. Compute the peak-to-peak stress for each cycle in data set 2 using Equation (50).

$$\sigma_{pp} = \frac{F_{peak} - F_{valley}}{\pi r^2} \quad (50)$$

Where:
$\sigma =$ Axial stress, kPa or psi
$F_{peak} =$ Peak axial force measured by the load transducer, kN or lb.
$\delta_{valley}^{i} =$ Valley axial force measured by the load transducer, kN or lb.
$r =$ Specime radius, mm or in.

Compute the peak-to-peak pseudo strain for each cycle in data set 2 using Equation (51).

$$\varepsilon_{pp}^{R} = \varepsilon_{pp} \times |E^*|_{LVE} \quad (51)$$

Where:
$\varepsilon_{pp}^{i} =$ Peak $-$ to $-$ peak pseudo strain

Compute the cyclic pseudo secant modulus for each cycle in data set 2 using Equation (52).

$$C^* = \frac{\sigma_{pp}}{\varepsilon_{pp} \times DMR} \quad (52)$$

Reduce the number of data points in data set 2 using the filtering scheme, define this data set as reduced data set 2. Then compute the functional form factor, β, for each cycle in reduced data set 2 using Equation (53).

$$\beta = \frac{F_{peak}+F_{valley}}{|F_{peak}|+|F_{valley}|} \tag{53}$$

Compute the tension amplitude pseudo strain for each cycle in reduced data set 2 using Equation (54).

$$\varepsilon_{ta}^{R} = \frac{\beta+1}{2}\varepsilon_{pp}^{R} \tag{54}$$

Where:
$\varepsilon_{ta}^{R} =$ Tension amplitude pseudo strain

Compute the time within a cycle when tensile loading begins, t_b for each cycle in reduced data set 2 using Equation (55).

$$t_b = \frac{\cos^{-1}(\beta)}{62.83} \tag{55}$$

Compute the time within a cycle when tensile loading ends, t_e for each cycle in reduced data set 2 using Equation (56).

$$t_e = \frac{2\pi-\cos^{-1}(\beta)}{62.83} \tag{56}$$

Compute the form adjustment factor for each cycle in reduced data set 2 using Equation (57). Equation (57) should be solved for each cycle, but generally β does not change significantly after the first few cycles, and a constant value may be applied after this transient period. Values of *K*1 have been tabulated for typical values of β and α in *Table 3*.

Table 3: Compiled K1 Values for Typical Material and Test Conditions.

				Alpha			
Beta	4.333	4.077	3.857	3.667	3.500	3.353	3.222
–0.5	0.277	0.285	0.293	0.300	0.306	0.312	0.318
0.0	0.263	0.271	0.278	0.285	0.291	0.297	0.302
0.2	0.256	0.264	0.271	0.277	0.284	0.289	0.295
0.4	0.248	0.256	0.262	0.269	0.275	0.280	0.286
0.6	0.238	0.245	0.252	0.258	0.264	0.269	0.274
0.8	0.225	0.231	0.238	0.243	0.249	0.254	0.259
1.0	0.189	0.195	0.200	0.205	0.209	0.214	0.218

$$K_1 = \frac{1}{t_e - t_b}\left[\left(\frac{1}{\beta+1}\right)^{2\alpha}\int_{t_b}^{t_e}(\beta - \cos(62.83 \times t))^{2\alpha}dt\right] \tag{57}$$

Compute the average reduced time for each cycle in reduced data set 2 using Equation (58) or (29) depending on the data acquisition history.

$$t_R = \frac{1}{a_T}\left[\frac{t_{peak}+t_{valley}}{2}\right] \tag{58}$$

Where:
t_{peak} = Time at the peak force
t_{valley} = Time at the valley force

$$t_R = \frac{1}{a_T}\left[\frac{N}{10}\right] \tag{59}$$

Where:
N = Cycle number

Compute the change in damage, ΔS, for each cycle in the reduced data set 2 using Equation (60). Even with data reduction, a few sequential data points may have positive ΔC values. A few of these spurious data points do not negatively affect the overall value of *S*, but they do complicate the calculation. An efficient method that accounts for these

spurious data points is to use the piecewise function shown in Equation (61). This piecewise function can be included in a spreadsheet by using the *if* (…) function.

$$\Delta S_n = \left(-\frac{DMR}{2}(\varepsilon_m^R)^2(C_n^* - C_{n-1}^*)\right)^{\frac{\alpha}{\alpha+1}}(\Delta t_R)^{\frac{1}{\alpha+1}}(K_1)^{\frac{1}{\alpha+1}} \tag{60}$$

Where:
C_{n}^* = The cycle pseudo secant modulus at the current analysis cycle
$C_{\mathrm{n-1}}^*$ = The cycle pseudo secant modulus at the previous analysis cycle
Δt_R = The change in the average reduced time between analysis cycles

$$\Delta S_n = \begin{cases} \left(-\frac{DMR}{2}(\varepsilon_m^R)^2(C_n^* - C_{n-1}^*)\right)^{\frac{\alpha}{\alpha+1}}(\Delta t_R)^{\frac{1}{\alpha+1}}(K_1)^{\frac{1}{\alpha+1}} & C_{\mathrm{n}}^* \le C_{n-1}^* \\ 0 & C_n^* > C_{n-1}^* \end{cases} \tag{61}$$

Determine the damage at each analysis cycle using Equation (62).

$$S_R = S_{dataset1+}\sum_{i=1}^{N}\Delta S_R \tag{62}$$

Where:
S_R = Cumulative damage at the current analysis cycle
ΔS_n = Incremental damage for all analysis cycles to be summed from the initial analysis cycle step, $\mathrm{n} = 1$, to the current time step, N

Combine the damage and pseudo secant modulus from each time step in the first with the cyclic pseudo secant moduli and damage values into a single data set. Determine the damage characteristic relationship by fitting one of the following equations to the plot of the pseudo secant modulus and damage from all of the fatigue tests.

$$C = e^{aS^b} \tag{63}$$

Or

$$C = 1 - yS^z \tag{64}$$

Where:
a, b = The fitting coefficients for the exponential model
y, z = The fitting coefficients for the power model

2.3 Specimen Instrumentation

A key aspect of the SPT is specimen instrumentation for laboratory testing. Instrumentation is a combination of small interconnected hardware components used to affix LVDTs to asphalt concrete specimens. LVDTs are used to accurately measure miniscule deformation that occurs in test samples as a result of applied loading. To collect the most accurate data while performing tests, and reduce any noise produced from testing machinery, all pieces of the instrumentation must be tightly installed. Proper procedures for instrumenting asphalt concrete samples are summarized in the paper: Specimen Instrumentation Techniques for Permanent Deformation Testing of Asphalt Mixtures, published in the Journal of Testing and Evaluation in 2001 [5]. The instrumentation techniques outlined in the paper facilitate the capture of true test parameters without restraint or alteration to anticipated stress states.

A variety of instrumentation systems can be used to measure strains and displacement. The systems can be separated into two classifications: local and whole body [5]. Local systems measure strain and displacement over a discrete gage length, while whole body systems measure response of the entire specimen, or the majority of the entire specimen. Whole body systems are typically comprised of imaging devices such as optical or X-ray. Local systems are comprised of components that are either in direct contact with the specimen, such as strain gages, LVDTs, or fiber optics, or non-contact devices such as lasers and proximity sensors. *Figure 3* below illustrates the classification for each system.

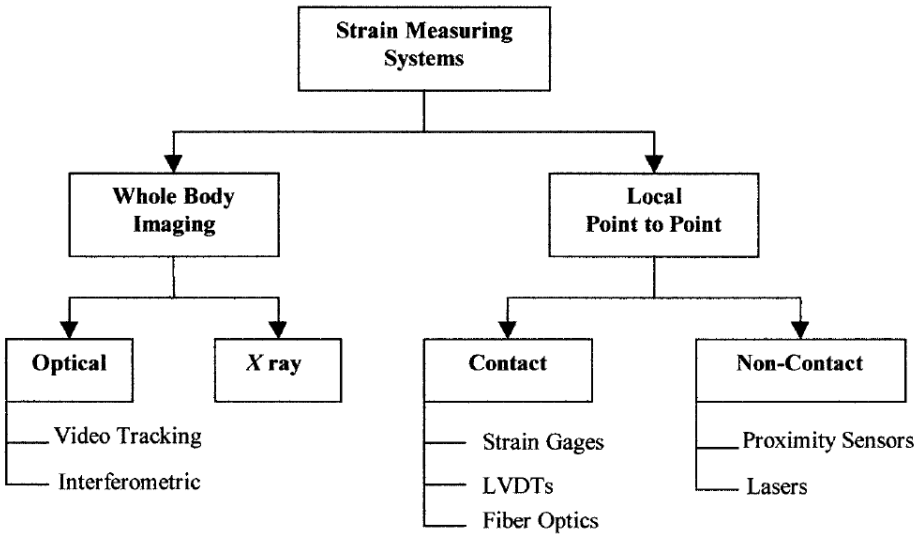

Figure 3: Strain Measurement System Classification *[5]*.

No matter the system chosen for measurement, there are sources of error associated with the collection of strain data. Historically, both whole body and local instrumentation have been used for triaxial tests. For soil testing, it was found that whole body systems result in significant error, including seating, alignment, bedding, and compliance errors, which are also true for testing asphalt concrete [5]. Unlike soil samples, asphalt concrete samples facilitate direct contact instrumentation systems as they can be easily attached to specimens using a two-part 5-minute epoxy resin. Consideration of errors associated with whole body systems, the ease of application of direct contact systems, and the benefits associated with the use of LVDTs (such as reusability, range of deformation measurement, and the availability of a many shapes and sizes), make using affixed LVDT instrumentation an attractive and relatively low-cost option for deformation measurements.

With direct contact systems, split collar clamps, such as seen in Figure *4*, have been the most popular when connecting LVDTs to samples and measuring axial strains. The collars are attached to the samples and held in place by spring mechanisms which allow for radial strain measurements. Bracelet-type devices have also been used for radial deformation measurements. However, it has been recognized that significant error due to the forces required to hold the LVDTs in place results from the use of these devices.

Figure 4: Split Spring Collars Used to Attach LVDTs To Asphalt Concrete Samples [5].

A report from the Strategic Highway Research Program (SHRP) recommended the use of small blocks glued to samples to avoid these errors [13]. In accordance with the SHRP report, and as a part of the extensive research outlined in the previously mentioned 2001 ASTM paper, new equipment was developed to affix LVDTs instrumentation to asphalt concrete samples used for permanent deformation tests. The new design consists of brass mounting studs, which are glued to the samples, aluminum

brackets that hold LVDTs, and frictionless linear bushings used with steel alignment rods which maintain stud alignment during extreme failure conditions. The brackets are fastened to the mounting studs using 4 x 40 hex-head screws. The newly designed instrumentation, as seen in Figure 5, was tested under specific geometric conditions using several cored and sawed gyratory compacted samples [5].

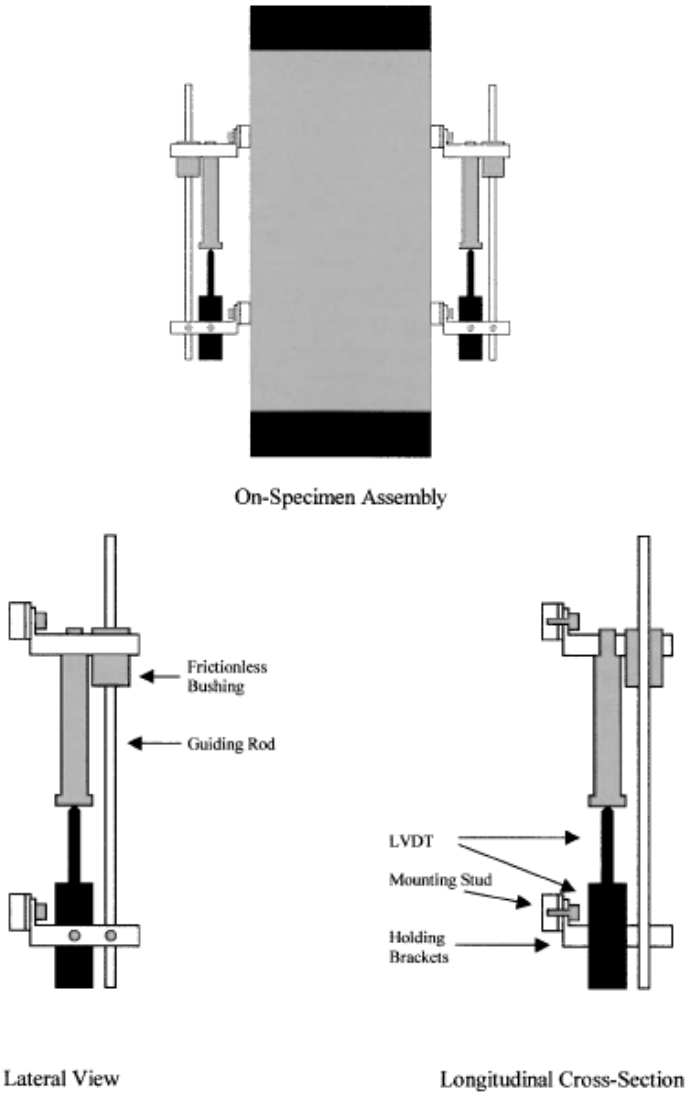

Figure 5: Redesigned LVDT Instrumentation Including On-Specimen Assembly [5].

Preliminary permanent deformation tests at high temperature and stress levels were performed to ascertain the viability of glued brass studs. The tests showed the glued brass studs performed well. Secondary tests were performed with varying instrumentation and boundary conditions. The results were analyzed in terms of consistency in the individual LVDT readings, failure mechanism, and comparison of several permanent deformation response parameters [5]. Table *4* shows the results of the various conditions tested as part of the research. Figure *6* displays the comparison between clamped samples and samples with brass studs for each of the following test parameters, slope (*b*), cumulative permanent strain, and the number of cycles at which tertiary flow occurred (F_N).

Table 4: Results for Various Test Instrumentations and Boundary Conditions [5].

Test Instrumentation and Preparation Method	**Asphalt Content, %**	**Air Voids, %**	**Intercept (α x 10^-6)**	**Slope, *b***	**Flow Number, *FN***	**Permanent Strain, %, at *N* = 600 cycles**
Studs, Sawed, No Capping	5.2	6.3	977	0.478	420	2.08
Clamps, Sawed, No Capping	5.2	5.7	1678	0.343	850	1.51
Studs, "as is," No Capping	5.2	6.1	1158	0.354	600	1.11
Clamps, "as is," No Capping	5.2	5.3	982	0.399	1000	1.26
Studs, Sawed, No Capping	5.2	6.2	677	0.482	350	1.48
Studs, Sawed, and Capped	5.2	6.5	993	0.320	1000	0.77

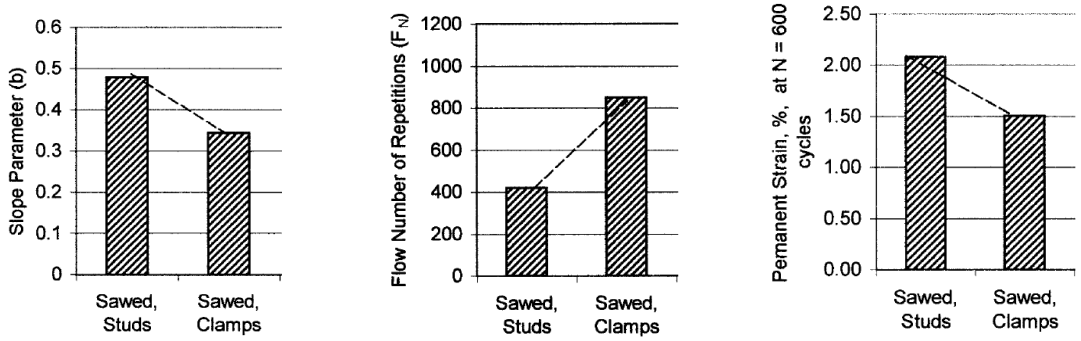

Figure 6: Comparison of Test Parameters Between Clamp and Stud Instrumentation [5].

As seen in the chart on the left in Figure *6* for sawed samples, there is significant difference of 0.15 for the slope between clamped and studded samples. Previous research from the same authors showed that even a 0.05 variation in slope values can result in ranking a mixture in different performance categories [7]. The results indicate the use of studs for instrumentation greatly increases the accuracy of the deformation measurements. The center chart from Figure *6* shows the flow number is increased by a factor of two for clamed samples. This indicates using clamp instrumentation restrains the samples from freely deforming and produces inaccurate results. The chart on the right in Figure *6* verifies the restraining effect of using clamp instrumentation by recording a 0.5% reduction in the cumulative strain percent at 600 cycles. The final recommendation from the research, due to the restraining effect of using clamp instrumentation, was to use mounting stud instrumentation for all permanent deformation tests that utilize a frictionless alignment rod to maintain stud alignment during extreme failure conditions.

2.4 3D Printing

3D printing refers to a variety of processes that utilize building layers of materials on the top of a previously built layers. The additive process of construction can be seen in many applications throughout history. Structures such as block buildings and pyramids are built by stacking large stone blocks on top of previously laid blocks. Pavement structures utilize the additive concept for construction by establishing a strong foundation layer then placing additional layers, or lifts, on top of the base layer. Even layer cakes are made using the same concept. Additive construction seems to be the underlying basis for the creation of nearly everything.

3D printing, more recently known as additive manufacturing, emerged as a prototype manufacturing process in 1986 with the invention of the stereolithography (STL) machine. A man named Charles “Chuck” Hull, who was working for an ultraviolet lamp company at the time, developed the technology in his lab during his spare time and later created his own company, 3D Systems [8]. The STL machine cures photopolymer with ultraviolet light layer by layer until an object is formed. Stereolithography laid the foundation for the development of a variety of new additive technologies used today for manufacturing. Shortly after the release of the stereolithography machine, in 1988 Scott Crump developed a new technique to additively manufacture objects, fused deposition modeling (FDM). FDM uses thermoplastic filament forced through a computer controlled heated extruder and is laid down on a build platform layer by layer. Scott and his wife founded the company Stratasys based on FDM technology [9]. 3D Systems and Stratasys became the leaders in the 3D printing industry for the next twenty years; However, the industry quietly developed over that time. In 1989 Carl Deckard, working at the University of Texas, patented a laser sintering technology which uses powdered substrate cured by a computer driven laser, Selective Laser Sintering (SLS). 1989 also saw the formation of EOS GmbH in Germany, founded by Hans Langer. EOS GmbH focuses on sintering technology as well, but with a focus on metal substrate, termed Direct Metal Laser Sintering (DMLS) [9].

As material science develops, the ability to 3D print with a wider range of materials is making the industry expand at a rapid rate. The 1990s and early 2000s saw a flood of development in 3D printing technologies. As the concept of rapidly producing

items spread, many industry specific machines were developed and marketed all over the world. Some of the materials currently being utilized for 3D printing are various types of metals, sand, ceramics, food, and even biological material. The technology is used by a wide variety of industries, from hobbyist to aviation and beyond. For example, if you have flown on a plane in the last ten years, chances are there has been a 3D printed part incorporated into that plane. Dental implants are created from specially designed 3D printers and jewelry is made with 3D printers designed to work with precious metals such as gold, platinum etc. Additionally, medical equipment manufacturers, movie special effects companies, machining shops, casting and molding companies, the gaming industries, and more are utilizing the additive process.

In 2005 the desktop 3D printer Makerbot, now owned by Stratasys, was developed by a Dr. Gordon as a part of the RepRap project. The RepRap project delivered the first fully assembled desktop 3D printer to its' clients and paved the way for open source 3D printing [8]. Since the RepRap project, there are countless desktop style 3D printers available at affordable prices and nearly everyone has at least a small amount of experience working with these devices.

The basic workflow of the 3D printing process is simple to understand. First, 3D model data must be obtained. The model is then imported to software that slices it into predetermined layer heights and is printed. Most 3D printed objects require some post-processing before they are considered an end-use part. 3D models can be obtained in three ways, a model can be developed using computer aided design (CAD) software, nearly all commercial CAD packages allow for the export of files to a 3D printing format.

Data can also be obtained using a 3D scanner. There are a variety of scanning options available, from handheld scanners used by hobbyist and reverse engineering industries, to scanners attached to drones that collect terrain data for surveying and topological applications. Lastly, the RepRap community has compiled a large database of open source models that can be downloaded for free, which can be modified or directly 3D printed.

No matter the method used to obtain a 3D model, all 3D printers work on dedicated software, either open source or proprietary, so it is necessary to have your model data in a common file format that can be imported into any 3D printing software. Charles Hull solved this issue with the creation of the stereolithography file format (.stl). The term "stereolithography" not only refers to the type of technology used to additively produce an object using ultraviolet cured photopolymers, but also became the standard file extension for files that are intended to be additively manufactured [8]. When a 3D model is saved in a stereolithography format, the model's outer surface is tessellated, or approximated, using millions of planar triangles, very similar to Triangular Irregular Networks (TIN), used by most CAD programs; which are used to represent existing terrain data.

Recently, with the release of various printing technologies and new machinery, more advanced files are being used to represent 3D models destined to be 3D printed. A few file types worth mentioning are additive manufacturing files (.amf) which tessellate the outer surface of a model as well; However, this file type allows for curvature in the triangles used to tessellate the model surface; curvature in the triangles facilitates a more

accurate representation of complex 3D models. Additionally, .amf files also include unit data to ease scaling issues that can arise when importing and exporting files between software. Object files (.obj) expand on the same concept by including color data and allow for full color 3D prints. There are many more file extensions currently being used, many of which are proprietary to specific machinery.

Once the model has been imported into the chosen 3D printing software, it is then sliced horizontally into layers by predetermined height settings and form a two-dimensional profile for each layer. A toolpath is then generated and the printing can begin. So, 3D printing is actually still 2D printing, just a series of 2D prints lain atop one another.

There are currently seven varieties of 3D printing technologies available, each technology has various limitations and benefits [10]:

- Stereolithography (SLA)
- Material extrusion or Fused Filament Fabrication (FFF)
- Material Jetting (MJ)
- Powder Bed Fusion (PBF)
- Selective Laser Sintering (SLS) or Direct Metal Laser Sintering (DMLS)
- Directed Energy (DE)
- Sheet Lamination (SL)

Out of the seven varieties of 3D printing, two technologies were available for use at ASU, SLA and FFF. SLA was the first form of 3D printing and is a type of vat-photopolymerization. This method uses a UV laser to cure a thin layer of photopolymer while the print-bed lowers or raises. The photopolymers used are not designed to withstand high temperatures and release toxic fumes when heated, so the use of SLA printing for the purposes of this research was not practical. On the other hand, material

extrusion or fused filament fabrication (FFF) forces a thermoplastic filament through a computer controlled heated extruder. Multiple extruders allow for printing of different materials simultaneously. The extruders can be moved in different directions, under computer control, to define the desired printed shape. Some of the thermoplastics used by FFF have high glass transition temperatures, are very affordable, and are safe to handle, which made this technology an attractive option for this research and led to the decision to use this technology to produce the mounting studs.

3. METHODOLOGY

The techniques described in the NCHRP 465 report for Simple Performance Testing for Superpave Mix Design, and finalized in AASHTO and ASTM Standards, were utilized for permanent deformation tests using both brass and thermoplastic studs. The variation between results produced by brass studs and the three types of thermoplastic studs were determined by statistical analysis of collected data.

3.1 Mounting Stud Fabrication

Three types of plastic studs were made using desktop 3D printers, a Da Vinci 1.0 and a CreatorBOT II Pro Series, with a solid infill and 0.2 mm layer height. The three types were: Polylactic acid (PLA), the most common 3D printing material; Acrylonitrile Butadiene Styrene (ABS), a typical 3D printing material which is less rigid than PLA and has a higher melting temperature; Polycarbonate (PC), a strong, high temperature 3D printing material. The test studs were designed using CAD software and exported to a Stereolithography (stl) format. Figure *7*Figure *7* shows the top and front view of the stud

design used for printing. All dimensions are displayed in millimeters. As seen in Figure *7*, a pilot hole was incorporated in the design to allow for fasteners which affix Linear Variable Displacement Transformer (LVDT) instrumentation to the specimens. The pilot hole was honed and 4 x 40 threads were added to each stud as a post processing technique. No additional post processing was applied to the test studs before testing. Figure 8 shows a brass stud and each 3D printed thermoplastic stud.

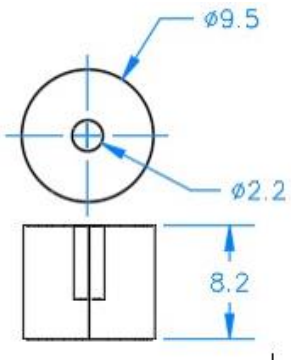

Figure 7: Design For 3D Printed Thermoplastic Mounting Studs, NTS

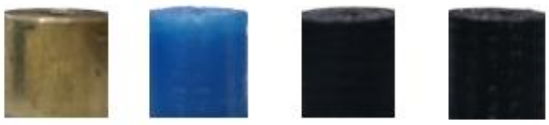

Figure 8. Mounting Studs, Left to Right: Brass, PLA, ABS, PC

3.2 Test Sample Preparation

All asphalt samples were prepared according to ASTM and AASHTO standards. The Superpave mix design method was utilized to determine aggregate gradation and optimal binder content. A high-volume Marshal mix design for the City of Phoenix, used by the Southwest Asphalt plant, was re-designed using the Superpave mix design as part of an ASU project using recycled asphalt pavement (RAP) for the City of Phoenix [11].

The mix design was used for all samples. The mix design is dense-graded with nominal maximum aggregate size of ¾ inch; Detailed information for the mix design and sample preparation is shown in Appendix A. The aggregate and hydrated lime used for sample preparation were also obtained from the Southwest Asphalt plant. The binder used is a PG70-10 and was obtained from Western Oil Company.

The ideal gradation was determined from sieve analysis and the optimal binder content of 5% was identified from volumetric calculations and test trials. Three samples were compacted for air void calibration. The optimal air voids for each specimen was targeted to be $6.5\% \pm 0.5\%$. To achieve the target air voids in each sample, it was determined that 7112 grams of the asphalt mixture need to be added to the gyratory mold for compaction. 7300 grams were prepared for each sample to account for material lost during the mixing process.

After compaction of 180mm tall and 150mm diameter gyratory plugs, test specimens were cored to a diameter of 100mm for Triaxial Dynamic Modulus tests and Repeated Load Permanent Deformation tests, and 75mm diameter for Direct Tension Cyclic Fatigue tests. All cored specimens were then sawed at each end to produce 150mm tall specimens.

Brass studs were used for control instrumentation and to provide a comparison for the 3 D printed stud materials. Variation of stud placement was conducted to ascertain the optimal stud locations to produce consistent results (i.e., plastic studs in the same location as the brass studs, plastic studs directly adjacent to the brass studs). It was determined for

Triaxial tests, that adjacent stud placement facilitated the most similar homogenous material within the gage length of 100mm on each sample.

3.3 Laboratory Tests

Three laboratory tests for asphalt concrete that utilize LVDT instrumentation were identified earlier and discussed as part of the simple performance tests. The data collected from these tests are intended to be correlated to rutting and fatigue cracking of pavements in the field. The following three tests were performed using both brass and three types of thermoplastic mounting studs:

- Dynamic Modulus |E*|, AASHTO TP 62-07 - This was considered as a low stress application; the test was conducted at five temperatures and six frequencies:

  Temperature ($°C$)
  - -10
  - 4.4
  - 21.1
  - 37.8
  - 54.4

  Frequency (Hz)
  - 25
  - 10
  - 5
  - 1
  - 0.5
  - 0.1

- Repeated Load Permanent Deformation, Flow Number (FN), AASHTO TP 79-13 - This was considered as a high stress application (300 KPa), and it was conducted at a high temperature of $50°C$
- Axial Cyclic Fatigue Test , AASHTP TP 107-14 - This test was considered to include varied compressive and tensile forces at constant stress levels with a moderate temperature ($18°C$).

4. DATA ANALYSIS AND RESULTS

4.1 Dynamic Modulus |E*|

The purpose of performing the Dynamic Modulus experiment was to examine the effect of test conditions, such as range of temperatures, on the performance of the thermoplastic studs. The collected data for the dynamic modulus tests for each type of mounting stud was fitted to a predicted master curve that conforms to a sigmoidal function by shifting the collected data for each temperature and frequency using Excel's Solver function, and by converting the temperature to a reduced time value. Equation (65) is a ratio of time and reduced time. Equation (66) was used to calculate the logarithm of reduced time factors based on optimized coefficients, which is used to plot the x-axis of the master curve charts. Equation (67) is the sigmoidal function used to plot the master curves. Equation (68) calculated the standard error of estimate (Se). As an indication of the quality of the data, the Se value is divided by the standard deviation (Sy) of the data. Equation (69) is the regression equation used to show how well the plotted data fits the predicted curve.

$$\alpha(T) = \frac{t}{t_r} \tag{65}$$

Where:
$\alpha(T) =$ Reduced time, s
$t =$ Time, s
$t_r =$ Reduced tme, s

$$Log\ \alpha(T) = aT_i^2 + bT_i + c \tag{66}$$

Where:
Log $\alpha(T) =$ Log of reduced time, s
$T_i =$ A given emperature, F°

$a, b, c =$ Optimized coefficients

$$Log\ |E^*| = \delta + \frac{\alpha}{1+e^{\beta+\gamma(\log(t_r))}} \quad (67)$$

Where:
$Log\ |E^*| =$ Sigmoidal function, psi
$T_i =$ A given emperature, F°
$\delta, \alpha, \beta, \gamma =$ Optimized coefficients
$t_r =$ Reduced tme, s

$$Se = \sqrt{\frac{\sum SE}{n-p}} \quad (68)$$

Where:
$Se =$ Standard error of estimate
$SE =$ Square of error for each data point
$n =$ Number of data points
$p =$ Number of regression constants
$n - p =$ Degree of freedom

$$R^2 = 1 - \frac{n-p}{n-1} \times \left(\frac{Se}{Sy}\right)^2 \quad (69)$$

Where:
$R^2 =$ Squared regression term
$Se =$ Standard error of estimate
$Sy =$ Standard deviation
$n =$ Number of data points
$p =$ Number of regression constants
$n - p =$ Degree of freedom

The following tables and charts correspond to the average data for master curve formation from the three replicates, and a comparison of the master curves for all stud types. Detailed information for each replicate can be found in Appendix C.

Brass

Table 5: Average Data for the Creation of Master Curve for Brass Studs

METAL (Brass)												
Temp, °C	Temp, °F	Frequency Hz	E* ksi	E* psi	Log E* psi	Time, t s	Log Time s	Log Red Time, t_r	Pred Log E* psi	Pred E* psi	Error	Error^2
-10.0	14 °F	25	4945.11	4.95E+06	6.6942	0.04	-1.39794	-6.1986	6.7042	5.06E+06	-0.0100	0.0001
-10.0	14 °F	10	4821.0544	4.82E+06	6.6831	0.1	-1	-5.8007	6.6832	4.82E+06	-0.0001	0.0000
-10.0	14 °F	5	4737.7061	4.74E+06	6.6756	0.2	-0.69897	-5.4997	6.6660	4.63E+06	0.0096	0.0001
-10.0	14 °F	1	4420.7019	4.42E+06	6.6455	1	0	-4.8007	6.6209	4.18E+06	0.0246	0.0006
-10.0	14 °F	0.5	4282.1425	4.28E+06	6.6317	2	0.30103	-4.4997	6.5991	3.97E+06	0.0325	0.0011
-10.0	14 °F	0.1	3958.3216	3.96E+06	6.5975	10	1	-3.8007	6.5423	3.49E+06	0.0552	0.0030
4.4	40 °F	25	3243.2372	3.24E+06	6.5110	0.04	-1.39794	-3.8828	6.5495	3.54E+06	-0.0385	0.0015
4.4	40 °F	10	3047.0978	3.05E+06	6.4839	0.1	-1	-3.4849	6.5136	3.26E+06	-0.0297	0.0009
4.4	40 °F	5	2901.2382	2.90E+06	6.4626	0.2	-0.69897	-3.1838	6.4842	3.05E+06	-0.0216	0.0005
4.4	40 °F	1	2502.0944	2.50E+06	6.3983	1	0	-2.4849	6.4079	2.56E+06	-0.0096	0.0001
4.4	40 °F	0.5	2352.5121	2.35E+06	6.3715	2	0.30103	-2.1838	6.3713	2.35E+06	0.0003	0.0000
4.4	40 °F	0.1	1987.0654	1.99E+06	6.2982	10	1	-1.4849	6.2768	1.89E+06	0.0214	0.0005
21.1	70 °F	25	1730.832	1.73E+06	6.2383	0.04	-1.39794	-1.3979	6.2640	1.84E+06	-0.0258	0.0007
21.1	70 °F	10	1493.0185	1.49E+06	6.1741	0.1	-1	-1.0000	6.2028	1.60E+06	-0.0287	0.0008
21.1	70 °F	5	1331.7849	1.33E+06	6.1244	0.2	-0.69897	-0.6990	6.1531	1.42E+06	-0.0286	0.0008
21.1	70 °F	1	992.83166	9.93E+05	5.9969	1	0	0.0000	6.0259	1.06E+06	-0.0290	0.0008
21.1	70 °F	0.5	867.5674	8.68E+05	5.9383	2	0.30103	0.3010	5.9657	9.24E+05	-0.0274	0.0008
21.1	70 °F	0.1	610.02873	6.10E+05	5.7854	10	1	1.0000	5.8130	6.50E+05	-0.0277	0.0008
38.7	100 °F	25	779.96461	7.80E+05	5.8921	0.04	-1.39794	0.8942	5.8374	6.88E+05	0.0547	0.0030
38.7	100 °F	10	627.09483	6.27E+05	5.7973	0.1	-1	1.2921	5.7436	5.54E+05	0.0537	0.0029
38.7	100 °F	5	524.21473	5.24E+05	5.7195	0.2	-0.69897	1.5931	5.6686	4.66E+05	0.0509	0.0026
38.7	100 °F	1	326.28656	3.26E+05	5.5136	1	0	2.2921	5.4802	3.02E+05	0.0334	0.0011
38.7	100 °F	0.5	258.11883	2.58E+05	5.4118	2	0.30103	2.5931	5.3931	2.47E+05	0.0187	0.0004
38.7	100 °F	0.1	142.42706	1.42E+05	5.1536	10	1	3.2921	5.1769	1.50E+05	-0.0233	0.0005
54.4	130 °F	25	193.72207	1.94E+05	5.2872	0.04	-1.39794	2.9800	5.2758	1.89E+05	0.0114	0.0001
54.4	130 °F	10	136.86728	1.37E+05	5.1363	0.1	-1	3.3779	5.1491	1.41E+05	-0.0128	0.0002
54.4	130 °F	5	105.97424	1.06E+05	5.0252	0.2	-0.69897	3.6789	5.0492	1.12E+05	-0.0240	0.0006
54.4	130 °F	1	57.289907	5.73E+04	4.7581	1	0	4.3779	4.8050	6.38E+04	-0.0469	0.0022
54.4	130 °F	0.5	45.590196	4.56E+04	4.6589	2	0.30103	4.6789	4.6949	4.95E+04	-0.0360	0.0013
54.4	130 °F	0.1	30.506271	3.05E+04	4.4844	10	1	5.3779	4.4294	2.69E+04	0.0550	0.0030
										ΣE	**0.0017**	**0.0308**
											Unbiased	Biased

Table 6: Original and Optimized Coefficient Parameters for Brass Studs

Parameter	Starting Values	Final Values
δ	4.0702	0.4954
α	2.5636	6.4118
β	-0.9307	-1.8366
γ	0.4992	0.2555
a	0.0002	0.0001
b	-0.1072	-0.0950
c	6.5581	6.1095

Table 7: Reduced Time Values for Each Test Temperature for Brass Studs

Temp., F		Log a(T)
T1 °F	14.0	4.8007
T2 °F	40.0	2.4849
T3 °F	70.0	0.0000
T4 °F	100.0	-2.2921
T5 °F	130.0	-4.3779

Table 8: Predicted Master Curve Data for Brass Studs

Log Red Time, t_r	**Reduced Frequency, f_r**	**Predicted**	
		Log E* psi	**E* psi**
-8	8	6.7776	5,991,998
-7	7	6.7408	5,505,704
-6	6	6.6940	4,942,913
-5	5	6.6345	4,310,690
-4	4	6.5595	3,626,358
-3	3	6.4652	2,918,832
-2	2	6.3478	2,227,161
-1	1	6.2028	1,595,006
0	0	6.0259	1,061,340
1	-1	5.8130	650,184
2	-2	5.5613	364,194
3	-3	5.2696	186,020
4	-4	4.9391	86,917
5	-5	4.5745	37,545
6	-6	4.1838	15,270
7	-7	3.7779	5,997
8	-8	3.3695	2,341

Table 9: Regression Parameters for Brass Stud Curve Fit

n	30
p	8
n-p	22
n-1	29
ΣSE	0.0308
Se	0.0374
Sy	0.6669
Se/Sy	0.0561
R^2	0.9976

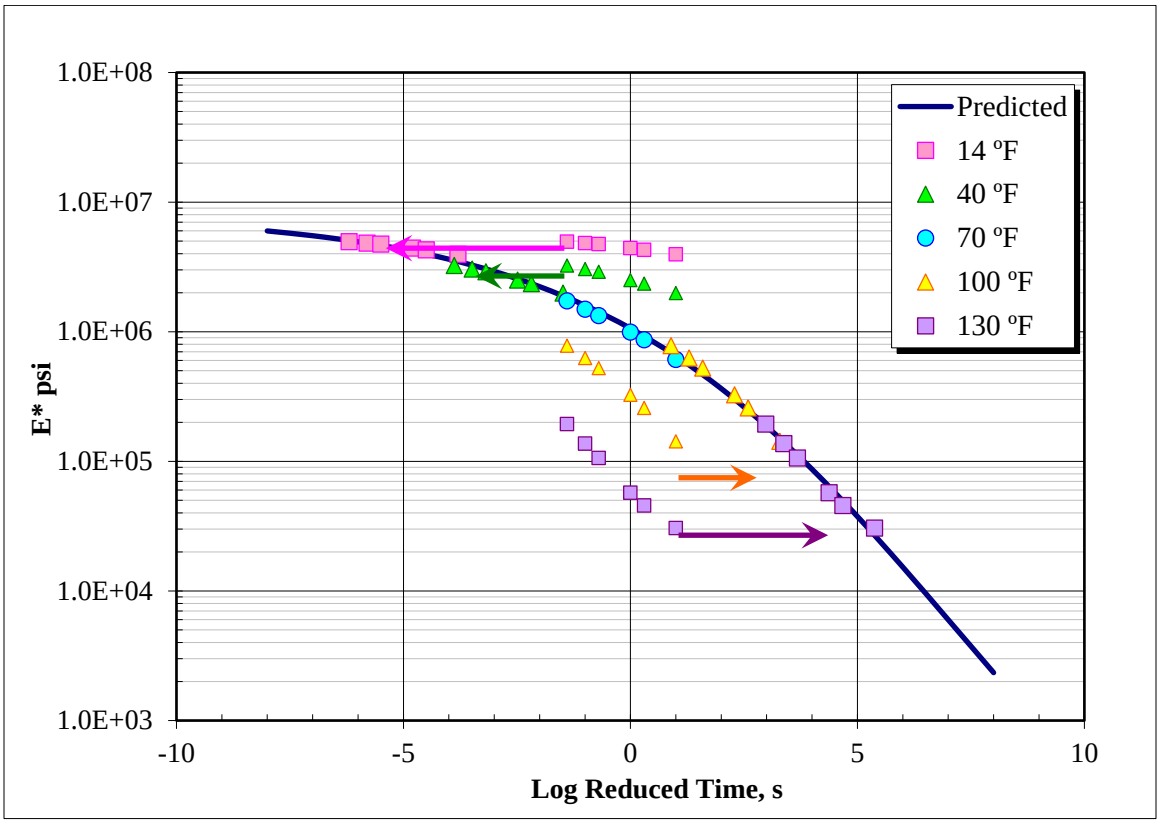

Figure 8. Initial Master Curve for Brass Studs

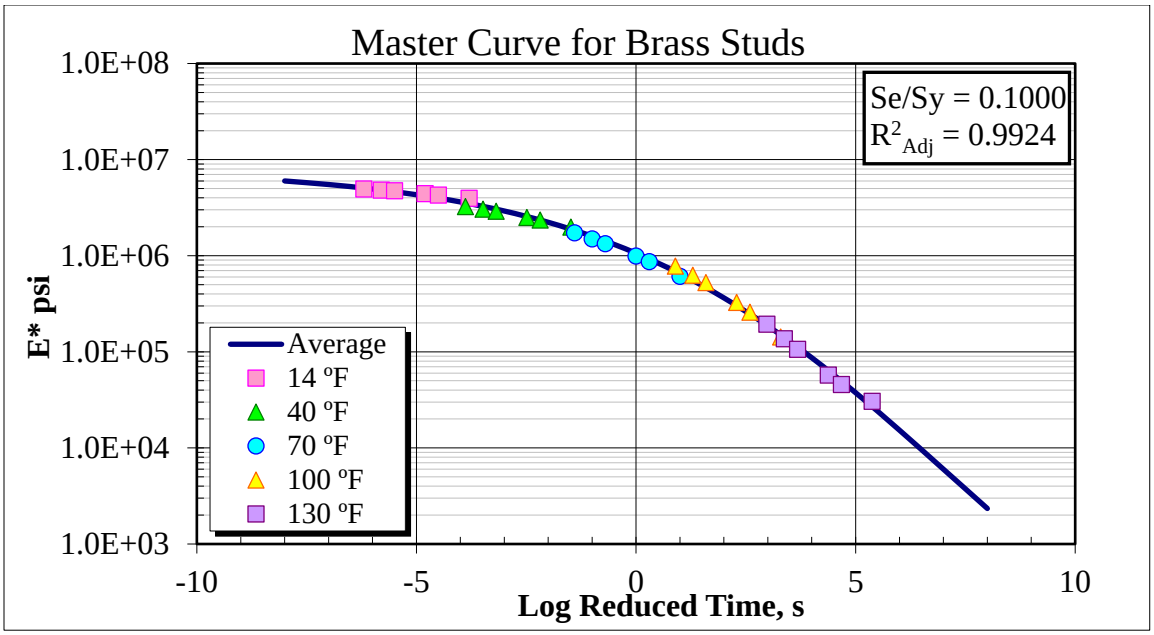

Figure 9: Final Master Curve for Brass Studs

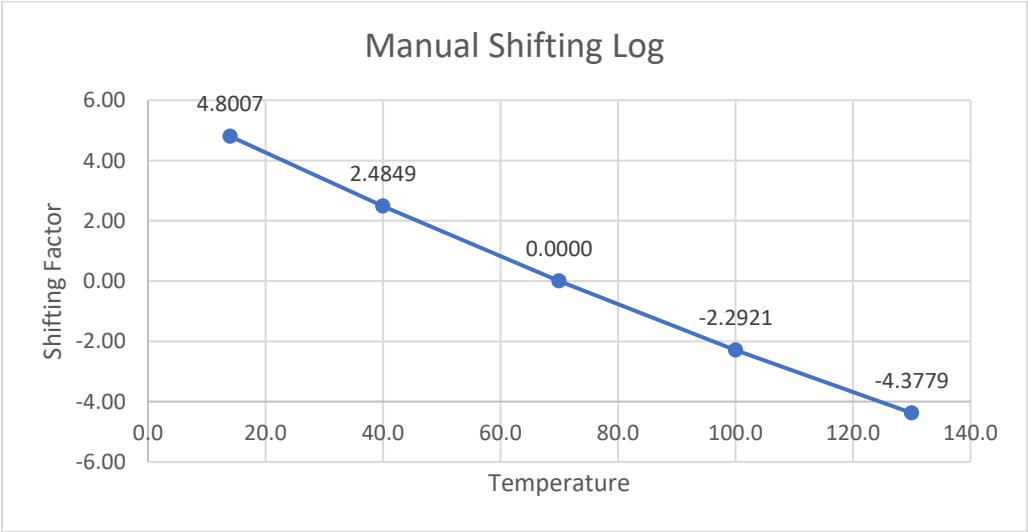

Figure 9: Manual Shift Log for Brass Studs

PLA

Table 10: Average Data for The Creation of Master Curve for PLA Studs

PLA												
Temp, °C	Temp, °F	Frequency Hz	E* ksi	E* psi	Log E* psi	Time, t s	Log Time s	Log Red Time, t_r	Pred Log E* psi	Pred E* psi	Error	Error^2
-10.0	14 °F	25	5820.5095	5.82E+06	6.7650	0.04	-1.39794	-6.7890	6.7722	5.92E+06	-0.0073	0.0001
-10.0	14 °F	10	5545.5179	5.55E+06	6.7439	0.1	-1	-6.3910	6.7544	5.68E+06	-0.0105	0.0001
-10.0	14 °F	5	5472.5156	5.47E+06	6.7382	0.2	-0.69897	-6.0900	6.7397	5.49E+06	-0.0015	0.0000
-10.0	14 °F	1	5112.2418	5.11E+06	6.7086	1	0	-5.3910	6.7011	5.02E+06	0.0075	0.0001
-10.0	14 °F	0.5	4944.2398	4.94E+06	6.6941	2	0.30103	-5.0900	6.6824	4.81E+06	0.0117	0.0001
-10.0	14 °F	0.1	4532.1392	4.53E+06	6.6563	10	1	-4.3910	6.6333	4.30E+06	0.0230	0.0005
4.4	40 °F	25	4014.1128	4.01E+06	6.6036	0.04	-1.39794	-4.1115	6.6112	4.09E+06	-0.0076	0.0001
4.4	40 °F	10	3766.9685	3.77E+06	6.5760	0.1	-1	-3.7136	6.5773	3.78E+06	-0.0013	0.0000
4.4	40 °F	5	3583.6891	3.58E+06	6.5543	0.2	-0.69897	-3.4125	6.5494	3.54E+06	0.0049	0.0000
4.4	40 °F	1	3075.6219	3.08E+06	6.4879	1	0	-2.7136	6.4768	3.00E+06	0.0111	0.0001
4.4	40 °F	0.5	2883.0602	2.88E+06	6.4599	2	0.30103	-2.4125	6.4418	2.77E+06	0.0180	0.0003
4.4	40 °F	0.1	2456.5042	2.46E+06	6.3903	10	1	-1.7136	6.3511	2.24E+06	0.0392	0.0015
21.1	70 °F	25	1798.2262	1.80E+06	6.2548	0.04	-1.39794	-1.3979	6.3054	2.02E+06	-0.0505	0.0026
21.1	70 °F	10	1599.4762	1.60E+06	6.2040	0.1	-1	-1.0000	6.2432	1.75E+06	-0.0393	0.0015
21.1	70 °F	5	1442.352	1.44E+06	6.1591	0.2	-0.69897	-0.6990	6.1927	1.56E+06	-0.0337	0.0011
21.1	70 °F	1	1062.8849	1.06E+06	6.0265	1	0	0.0000	6.0629	1.16E+06	-0.0364	0.0013
21.1	70 °F	0.5	941.4883	9.41E+05	5.9738	2	0.30103	0.3010	6.0013	1.00E+06	-0.0275	0.0008
21.1	70 °F	0.1	666.98021	6.67E+05	5.8241	10	1	1.0000	5.8443	6.99E+05	-0.0202	0.0004
38.7	100 °F	25	808.00524	8.08E+05	5.9074	0.04	-1.39794	0.9210	5.8630	7.30E+05	0.0444	0.0020
38.7	100 °F	10	642.90395	6.43E+05	5.8081	0.1	-1	1.3189	5.7658	5.83E+05	0.0423	0.0018
38.7	100 °F	5	535.2376	5.35E+05	5.7285	0.2	-0.69897	1.6200	5.6878	4.87E+05	0.0408	0.0017
38.7	100 °F	1	330.87943	3.31E+05	5.5197	1	0	2.3189	5.4912	3.10E+05	0.0285	0.0008
38.7	100 °F	0.5	260.72951	2.61E+05	5.4162	2	0.30103	2.6200	5.3998	2.51E+05	0.0164	0.0003
38.7	100 °F	0.1	144.50593	1.45E+05	5.1599	10	1	3.3189	5.1723	1.49E+05	-0.0124	0.0002
54.4	130 °F	25	224.08331	2.24E+05	5.3504	0.04	-1.39794	2.8318	5.3331	2.15E+05	0.0173	0.0003
54.4	130 °F	10	158.81632	1.59E+05	5.2009	0.1	-1	3.2297	5.2025	1.59E+05	-0.0016	0.0000
54.4	130 °F	5	121.05817	1.21E+05	5.0830	0.2	-0.69897	3.5307	5.0991	1.26E+05	-0.0162	0.0003
54.4	130 °F	1	62.656303	6.27E+04	4.7970	1	0	4.2297	4.8448	6.99E+04	-0.0478	0.0023
54.4	130 °F	0.5	49.167793	4.92E+04	4.6917	2	0.30103	4.5307	4.7293	5.36E+04	-0.0377	0.0014
54.4	130 °F	0.1	31.279805	3.13E+04	4.4953	10	1	5.2297	4.4493	2.81E+04	0.0460	0.0021
										ΣE	**0.0000**	**0.0237**
											Unbiased	Biased

Table 11: Original and Optimized Coefficient Parameters for PLA Studs

Parameter	Starting Values	Final Values
δ	4.0702	0.0932
α	2.5636	6.8474
β	-0.9307	-1.9172
γ	0.4992	0.2597
a	0.0002	0.0002
b	-0.1072	-0.1150
c	6.5581	6.9574

Table 12: Reduced Time Values for Each Test Temperature for PLA Studs

Temp., F		Log a(T)
T1 °F	14.0	5.3910
T2 °F	40.0	2.7136
T3 °F	70.0	0.0000
T4 °F	100.0	-2.3189
T5 °F	130.0	-4.2297

Table 13: Predicted Master Curve Data for PLA Studs

Log Red Time, t_r	**Reduced Frequency, f_r**	**Predicted**	
		Log E* psi	**E* psi**
-8	8	6.8169	6,559,299
-7	7	6.7810	6,039,611
-6	6	6.7351	5,433,668
-5	5	6.6765	4,747,761
-4	4	6.6020	3,999,678
-3	3	6.5079	3,220,675
-2	2	6.3899	2,454,368
-1	1	6.2432	1,750,836
0	0	6.0629	1,155,898
1	-1	5.8443	698,677
2	-2	5.5835	383,309
3	-3	5.2787	189,991
4	-4	4.9305	85,215
5	-5	4.5431	34,920
6	-6	4.1244	13,317
7	-7	3.6861	4,854
8	-8	3.2422	1,747

Table 14: Regression Parameters for PLA Stud Curve Fit

n	30
p	8
n-p	22
n-1	29
ΣSE	0.0237
Se	0.0328
Sy	0.6836
Se/Sy	0.0480
R^2	0.9983

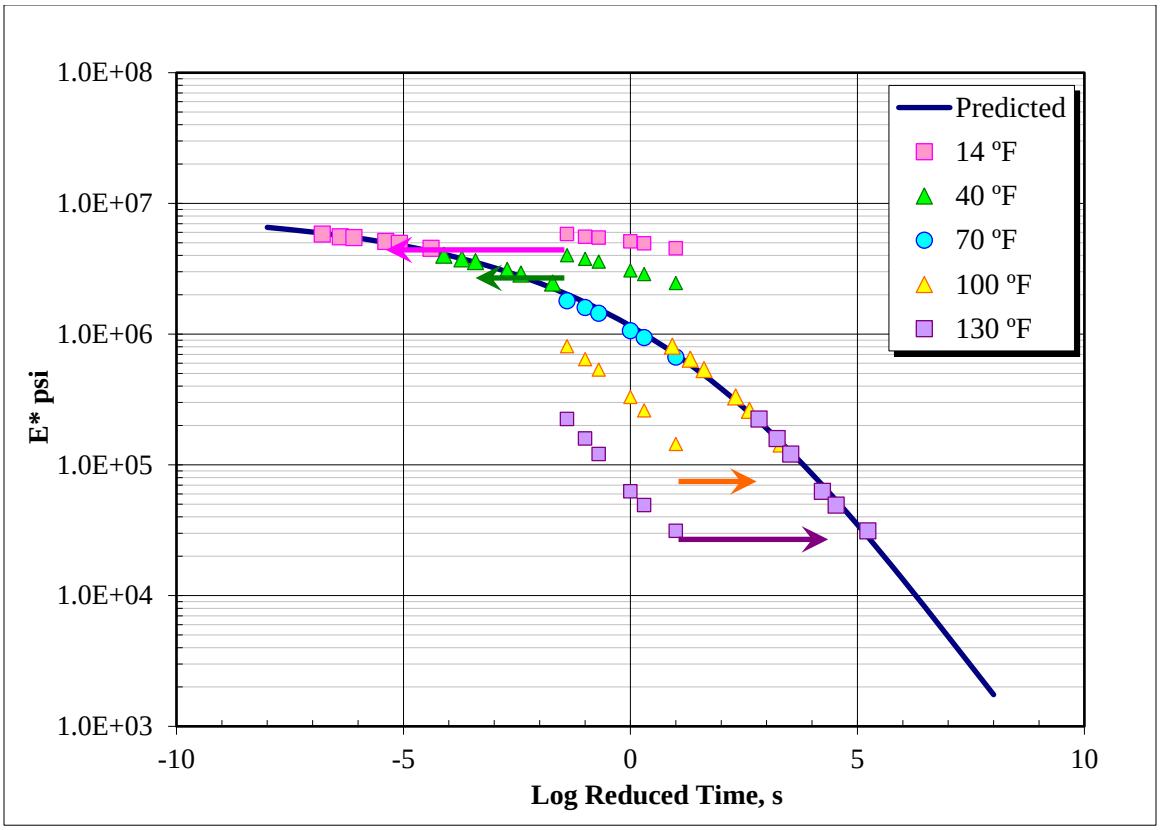

Figure 10: Initial Master Curve for PLA Studs

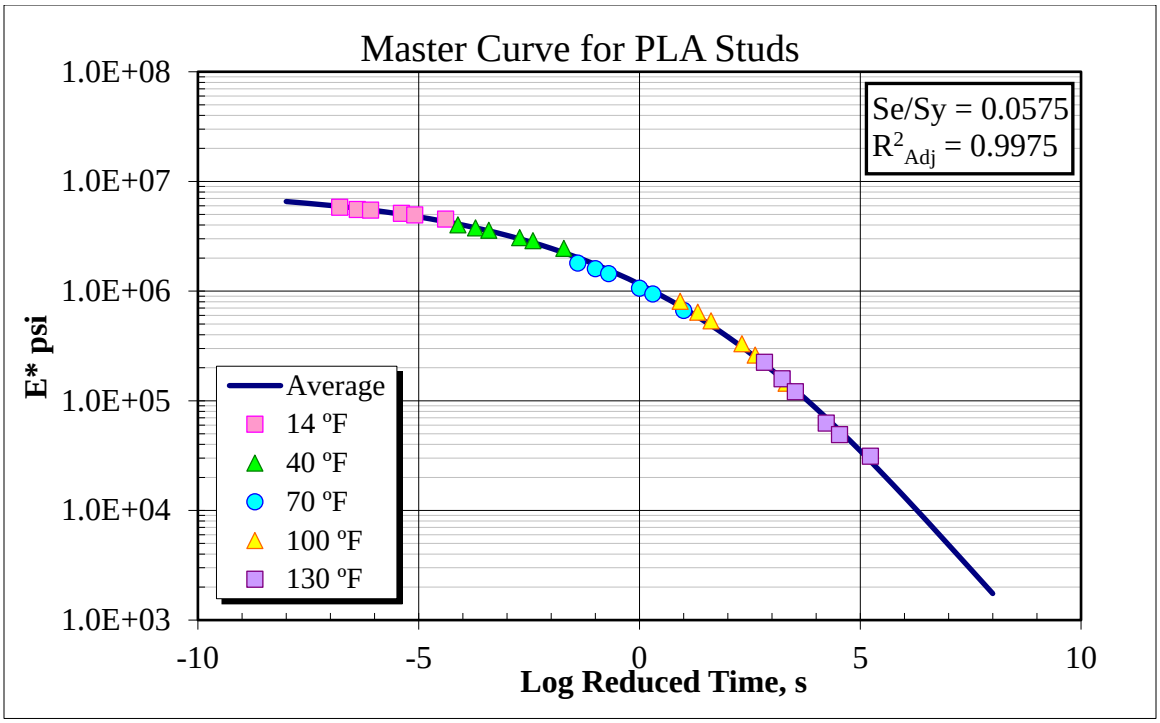

Figure 11: Final Master Curve for PLA Studs

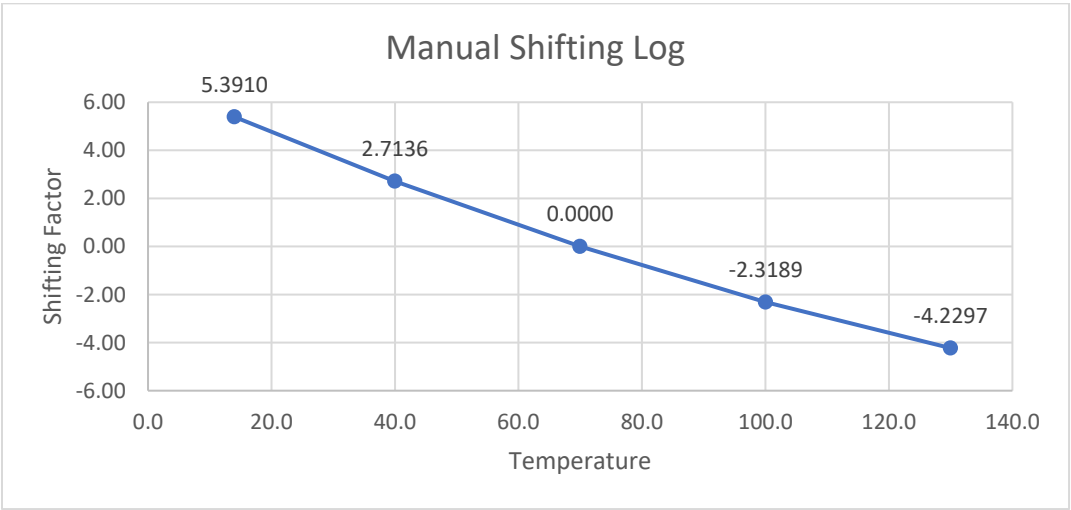

Figure 12: Manual Shifting Log for PLA Studs

ABS

Table 15: Average Data for The Creation of Master Curve for ABS Studs

ABS												
Temp, °C	Temp, °F	Frequency Hz	E* ksi	E* psi	Log E* psi	Time, t s	Log Time s	Log Red Time, t_r	Pred Log E* psi	Pred E* psi	Error	Error^2
-10.0	14 °F	25	6673.0896	6673089.634	6.824327	0.04	-1.39794	-6.734513	6.812131692	6.49E+06	0.0122	0.0001
-10.0	14 °F	10	6286.274	6286273.987	6.7983933	0.1	-1	-6.336573	6.794349169	6.23E+06	0.0040	0.0000
-10.0	14 °F	5	6071.038	6071037.983	6.783263	0.2	-0.69897	-6.035543	6.779626655	6.02E+06	0.0036	0.0000
-10.0	14 °F	1	5579.215	5579215.014	6.7465731	1	0	-5.336573	6.740722567	5.50E+06	0.0059	0.0000
-10.0	14 °F	0.5	5370.2156	5370215.633	6.7299917	2	0.30103	-5.035543	6.721718217	5.27E+06	0.0083	0.0001
-10.0	14 °F	0.1	4908.1737	4908173.746	6.6909199	10	1	-4.336573	6.671650943	4.70E+06	0.0193	0.0004
4.4	40 °F	25	4195.4583	4195458.301	6.6227794	0.04	-1.39794	-4.085704	6.651461006	4.48E+06	-0.0287	0.0008
4.4	40 °F	10	3985.0569	3985056.889	6.6004345	0.1	-1	-3.687764	6.616787753	4.14E+06	-0.0164	0.0003
4.4	40 °F	5	3760.5385	3760538.471	6.57525	0.2	-0.69897	-3.386734	6.588254938	3.87E+06	-0.0130	0.0002
4.4	40 °F	1	3253.4865	3253486.539	6.512349	1	0	-2.687764	6.513605302	3.26E+06	-0.0013	0.0000
4.4	40 °F	0.5	3045.4057	3045405.731	6.4836452	2	0.30103	-2.386734	6.477528822	3.00E+06	0.0061	0.0000
4.4	40 °F	0.1	2580.2214	2580221.359	6.411657	10	1	-1.687764	6.383683932	2.42E+06	0.0280	0.0008
21.1	70 °F	25	2047.8362	2047836.169	6.3112952	0.04	-1.39794	-1.397939	6.340339966	2.19E+06	-0.0290	0.0008
21.1	70 °F	10	1786.8649	1786864.932	6.2520917	0.1	-1	-0.999999	6.276292958	1.89E+06	-0.0242	0.0006
21.1	70 °F	5	1609.242	1609242.049	6.2066214	0.2	-0.69897	-0.698969	6.224199318	1.68E+06	-0.0176	0.0003
21.1	70 °F	1	1191.9685	1191968.477	6.0762648	1	0	5.538E-07	6.090452634	1.23E+06	-0.0142	0.0002
21.1	70 °F	0.5	1040.5491	1040549.078	6.0172626	2	0.30103	0.3010305	6.027102459	1.06E+06	-0.0098	0.0001
21.1	70 °F	0.1	735.38968	735389.6776	5.8665175	10	1	1.0000006	5.866096049	7.35E+05	0.0004	0.0000
38.7	100 °F	25	829.27744	829277.44	5.9186999	0.04	-1.39794	0.9028489	5.889656233	7.76E+05	0.0290	0.0008
38.7	100 °F	10	670.17104	670171.0414	5.8261857	0.1	-1	1.3007889	5.790709194	6.18E+05	0.0355	0.0013
38.7	100 °F	5	556.55815	556558.1466	5.7455105	0.2	-0.69897	1.6018189	5.711558276	5.15E+05	0.0340	0.0012
38.7	100 °F	1	337.74455	337744.5459	5.5285883	1	0	2.3007889	5.513614227	3.26E+05	0.0150	0.0002
38.7	100 °F	0.5	267.01448	267014.4757	5.4265348	2	0.30103	2.6018189	5.422412705	2.64E+05	0.0041	0.0000
38.7	100 °F	0.1	148.22857	148228.5682	5.1709319	10	1	3.3007889	5.197658199	1.58E+05	-0.0267	0.0007
54.4	130 °F	25	241.92295	241922.947	5.3836771	0.04	-1.39794	2.8032773	5.359451145	2.29E+05	0.0242	0.0006
54.4	130 °F	10	168.29212	168292.122	5.2260638	0.1	-1	3.2012173	5.230732865	1.70E+05	-0.0047	0.0000
54.4	130 °F	5	128.60013	128600.1277	5.1092414	0.2	-0.69897	3.5022473	5.129729486	1.35E+05	-0.0205	0.0004
54.4	130 °F	1	70.246611	70246.61111	4.8466254	1	0	4.2012173	4.884470978	7.66E+04	-0.0378	0.0014
54.4	130 °F	0.5	55.065995	55065.99453	4.7408835	2	0.30103	4.5022473	4.774861365	5.95E+04	-0.0340	0.0012
54.4	130 °F	0.1	36.404472	36404.47224	4.5611547	10	1	5.2012173	4.513399932	3.26E+04	0.0478	0.0023
										ΣE	**-0.0005**	**0.0149**
											Unbiased	Biased

Table 16: Original and Optimized Coefficient Parameters for ABS Studs

Parameter	Starting Values	Final Values
δ	4.0702	1.3922
α	2.5636	5.5780
β	-0.9307	-1.6752
γ	0.4992	0.2761
a	0.0002	0.0002
b	-0.1072	-0.1137
c	6.5581	6.8852

Table 17: Reduced Time Values for Each Test Temperature for ABS Studs

Temp., F		Log a(T)
T1 °F	14.0	5.3366
T2 °F	40.0	2.6878
T3 °F	70.0	0.0000
T4 °F	100.0	-2.3008
T5 °F	130.0	-4.2012

Table 18: Predicted Master Curve Data for ABS Studs

Log Red Time, t_r	**Reduced Frequency, f_r**	**Predicted**	
		Log E* psi	**E* psi**
-8	8	6.8578	7,208,032
-7	7	6.8230	6,652,909
-6	6	6.7778	5,995,312
-5	5	6.7194	5,240,560
-4	4	6.6443	4,408,332
-3	3	6.5485	3,535,639
-2	2	6.4274	2,675,555
-1	1	6.2763	1,889,266
0	0	6.0905	1,231,552
1	-1	5.8661	734,677
2	-2	5.6012	399,207
3	-3	5.2965	197,936
4	-4	4.9565	90,467
5	-5	4.5895	38,859
6	-6	4.2075	16,124
7	-7	3.8244	6,675
8	-8	3.4546	2,849

Table 19: Regression Parameters for ABS Stud Curve Fit

n	30
p	8
n-p	22
n-1	29
ΣSE	0.0149
Se	0.0260
Sy	0.6840
Se/Sy	0.0380
R^2	0.9989

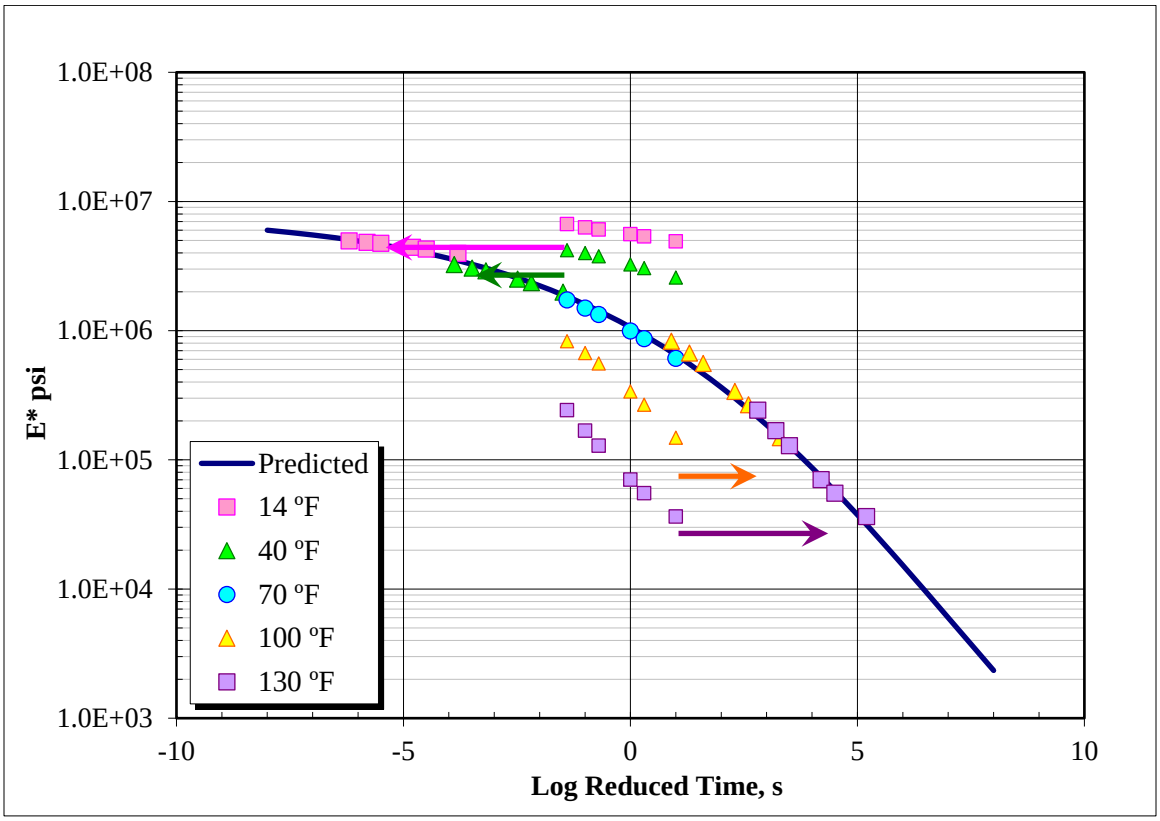

Figure 13: Initial Master Curve for ABS Studs

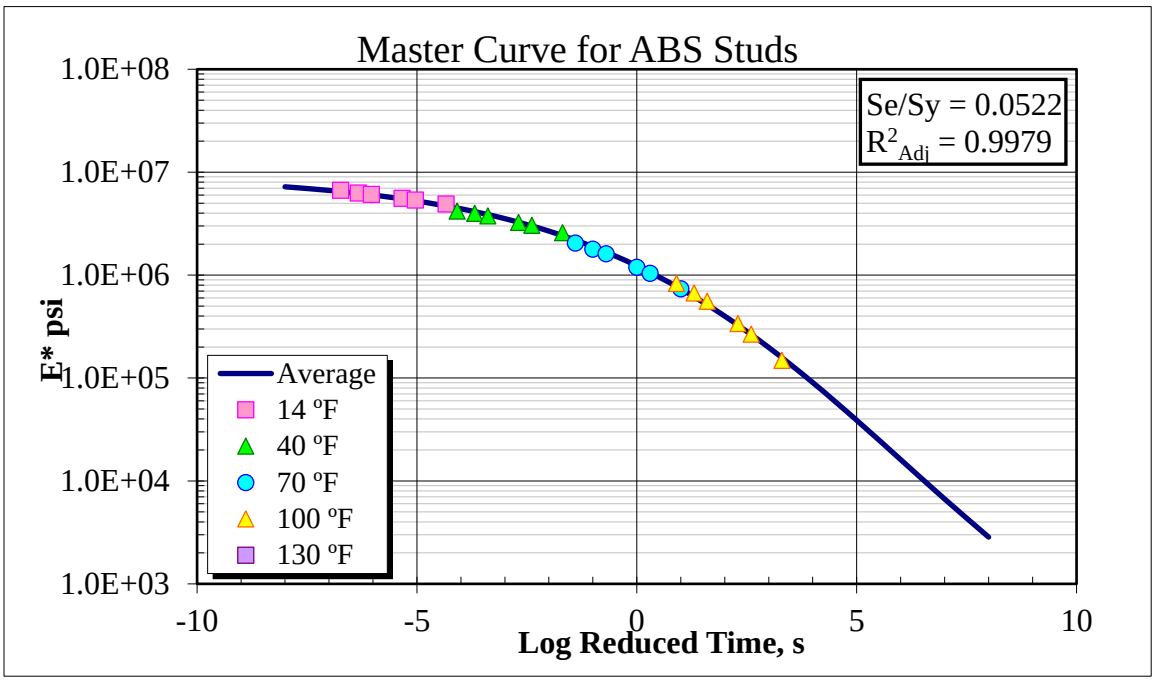

Figure 14: Final Master Curve for ABS Studs

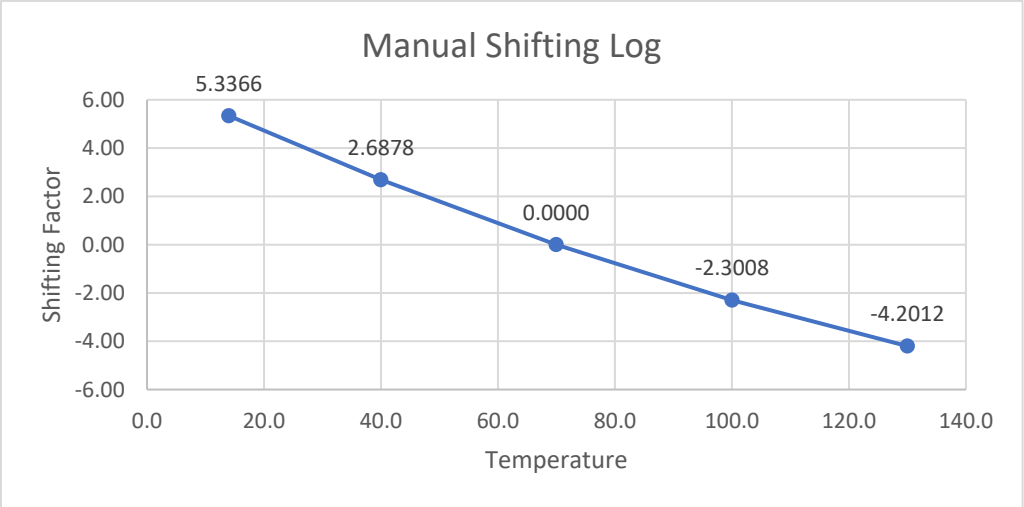

Figure 15: Manual Shifting Log for ABS Studs

PC

Table 20: Average Data for The Creation of Master Curve for PC Studs

PC												
Temp, °C	**Temp, °F**	**Frequency Hz**	**E* ksi**	**E* psi**	**Log E* psi**	**Time, t s**	**Log Time s**	**Log Red Time, t_r**	**Pred Log E* psi**	**Pred E* psi**	**Error**	**Error^2**
-10.0	14 °F	25	6411.2482	6411248.171	6.8069426	0.04	-1.39794	-6.702316	6.790365381	6.17E+06	0.0166	0.0003
-10.0	14 °F	10	5965.6197	5965619.721	6.7756556	0.1	-1	-6.304376	6.777086742	5.99E+06	-0.0014	0.0000
-10.0	14 °F	5	5785.8454	5785845.445	6.7623668	0.2	-0.69897	-6.003346	6.76587998	5.83E+06	-0.0035	0.0000
-10.0	14 °F	1	5364.2933	5364293.259	6.7295125	1	0	-5.304376	6.73542778	5.44E+06	-0.0059	0.0000
-10.0	14 °F	0.5	5184.3739	5184373.945	6.7146963	2	0.30103	-5.003346	6.720150055	5.25E+06	-0.0055	0.0000
-10.0	14 °F	0.1	4763.5469	4763546.948	6.6779304	10	1	-4.304376	6.678787914	4.77E+06	-0.0009	0.0000
4.4	40 °F	25	4617.4939	4617493.946	6.6644063	0.04	-1.39794	-4.082293	6.663720537	4.61E+06	0.0007	0.0000
4.4	40 °F	10	4365.1283	4365128.282	6.639997	0.1	-1	-3.684353	6.634114491	4.31E+06	0.0059	0.0000
4.4	40 °F	5	4138.9419	4138941.93	6.6168893	0.2	-0.69897	-3.383323	6.609312628	4.07E+06	0.0076	0.0001
4.4	40 °F	1	3526.375	3526375.043	6.5473285	1	0	-2.684353	6.54275837	3.49E+06	0.0046	0.0000
4.4	40 °F	0.5	3318.3184	3318318.408	6.5209181	2	0.30103	-2.383323	6.509823166	3.23E+06	0.0111	0.0001
4.4	40 °F	0.1	2838.171	2838170.976	6.4530386	10	1	-1.684353	6.42214189	2.64E+06	0.0309	0.0010
21.1	70 °F	25	2183.9783	2183978.259	6.3392483	0.04	-1.39794	-1.39794	6.381290248	2.41E+06	-0.0420	0.0018
21.1	70 °F	10	1968.3797	1968379.661	6.2941089	0.1	-1	-1	6.319378829	2.09E+06	-0.0253	0.0006
21.1	70 °F	5	1730.6628	1730662.809	6.2382125	0.2	-0.69897	-0.69897	6.268355037	1.86E+06	-0.0301	0.0009
21.1	70 °F	1	1312.8091	1312809.086	6.1182016	1	0	3.847E-07	6.135092249	1.36E+06	-0.0169	0.0003
21.1	70 °F	0.5	1151.092	1151092.008	6.06111	2	0.30103	0.3010304	6.071045088	1.18E+06	-0.0099	0.0001
21.1	70 °F	0.1	815.9098	815909.7952	5.9116421	10	1	1.0000004	5.90634349	8.06E+05	0.0053	0.0000
38.7	100 °F	25	880.45159	880451.5886	5.9447055	0.04	-1.39794	0.9314577	5.923490104	8.38E+05	0.0212	0.0005
38.7	100 °F	10	700.82235	700822.3501	5.8456079	0.1	-1	1.3293977	5.820934165	6.62E+05	0.0247	0.0006
38.7	100 °F	5	579.71584	579715.8388	5.7632152	0.2	-0.69897	1.6304277	5.738578743	5.48E+05	0.0246	0.0006
38.7	100 °F	1	354.61727	354617.2694	5.5497599	1	0	2.3293977	5.532212371	3.41E+05	0.0175	0.0003
38.7	100 °F	0.5	276.29689	276296.8909	5.441376	2	0.30103	2.6304277	5.437279913	2.74E+05	0.0041	0.0000
38.7	100 °F	0.1	154.03008	154030.0778	5.1876055	10	1	3.3293977	5.204860645	1.60E+05	-0.0173	0.0003
54.4	130 °F	25	238.87715	238877.1545	5.3781746	0.04	-1.39794	2.8923112	5.352029073	2.25E+05	0.0261	0.0007
54.4	130 °F	10	166.06821	166068.21	5.2202865	0.1	-1	3.2902512	5.21826648	1.65E+05	0.0020	0.0000
54.4	130 °F	5	124.22482	124224.8226	5.0942084	0.2	-0.69897	3.5912812	5.114179676	1.30E+05	-0.0200	0.0004
54.4	130 °F	1	67.660105	67660.10478	4.8303327	1	0	4.2902512	4.865556318	7.34E+04	-0.0352	0.0012
54.4	130 °F	0.5	53.083812	53083.81211	4.7249621	2	0.30103	4.5912812	4.756682004	5.71E+04	-0.0317	0.0010
54.4	130 °F	0.1	35.171651	35171.65147	4.5461928	10	1	5.2902512	4.503551242	3.19E+04	0.0426	0.0018
										ΣE	**-0.0001**	**0.0127**
											Unbiased	Biased

Table 21: Original and Optimized Coefficient Parameters for PC Studs

Parameter	Starting Values	Final Values
δ	4.0702	2.4949
α	2.5636	4.3924
β	-0.9307	-1.5768
γ	0.4992	0.3304
a	0.0002	0.0002
b	-0.1072	-0.1116
c	6.5581	6.8275

Table 22: Reduced Time Values for Each Test Temperature for PC Studs

Temp., F		Log a(T)
T1 °F	14.0	5.3044
T2 °F	40.0	2.6844
T3 °F	70.0	0.0000
T4 °F	100.0	-2.3294
T5 °F	130.0	-4.2903

Table 23: Predicted Master Curve for PC Studs

Log Red Time, t_r	**Reduced Frequency, f_r**	**Predicted**	
		Log E* psi	**E* psi**
-8	8	6.8237	6,663,060
-7	7	6.7993	6,298,879
-6	6	6.7657	5,831,085
-5	5	6.7200	5,247,739
-4	4	6.6579	4,548,622
-3	3	6.5745	3,753,626
-2	2	6.4638	2,909,168
-1	1	6.3194	2,086,310
0	0	6.1351	1,364,873
1	-1	5.9063	806,016
2	-2	5.6320	428,567
3	-3	5.3163	207,161
4	-4	4.9697	93,267
5	-5	4.6084	40,592
6	-6	4.2516	17,848
7	-7	3.9174	8,267
8	-8	3.6196	4,165

Table 24: Regression Parameters for PC Stud Curve Fit

n	30
p	8
n-p	22
n-1	29
ΣSE	0.0127
Se	0.0240
Sy	0.6899
Se/Sy	0.0348
R^2	0.9991

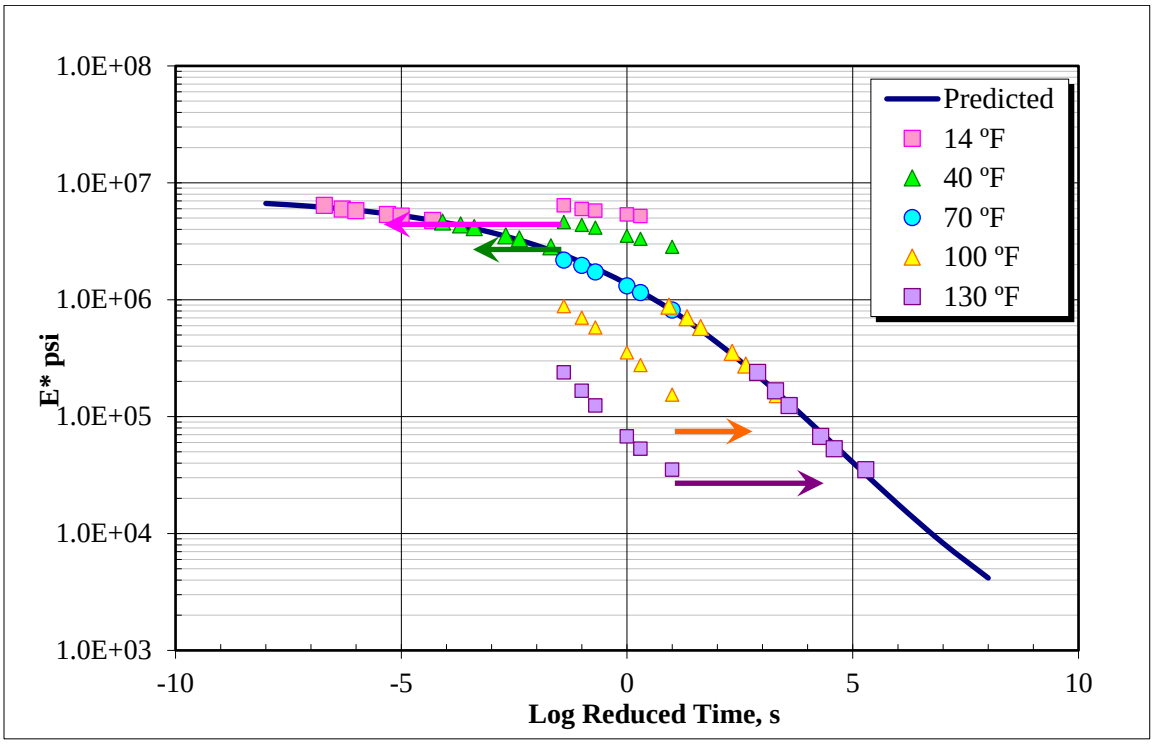

Figure 16: Initial Master Curve for PC Studs

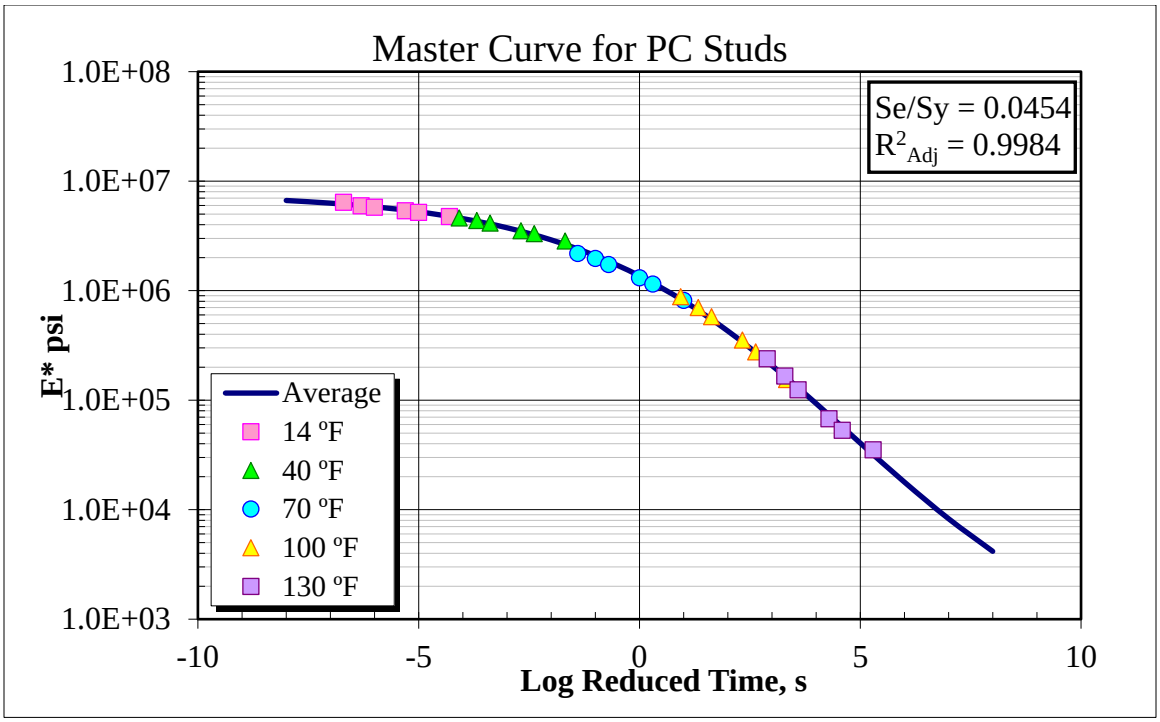

Figure 17: Final Master Curve for PC Studs

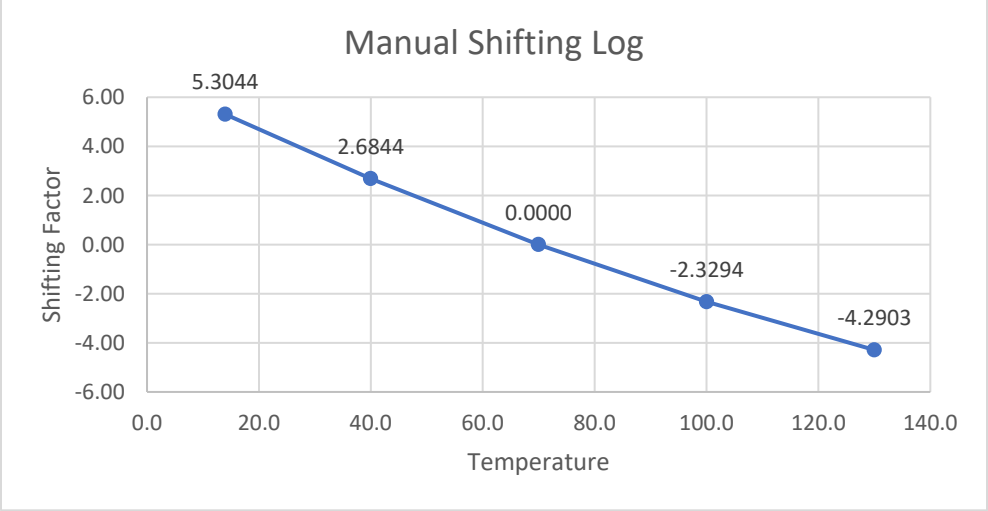

Figure 18: Manual Shifting Log for PC Studs

To form a basis for comparison between brass and thermoplastic mounting studs the difference in performance of the brass studs between replicates was investigated. Figure *19* Shows the master curves for each of the Brass replicates as well as the average of all three. It can be seen that a certain amount of variability is common between asphalt concrete replicates of the same treatment.

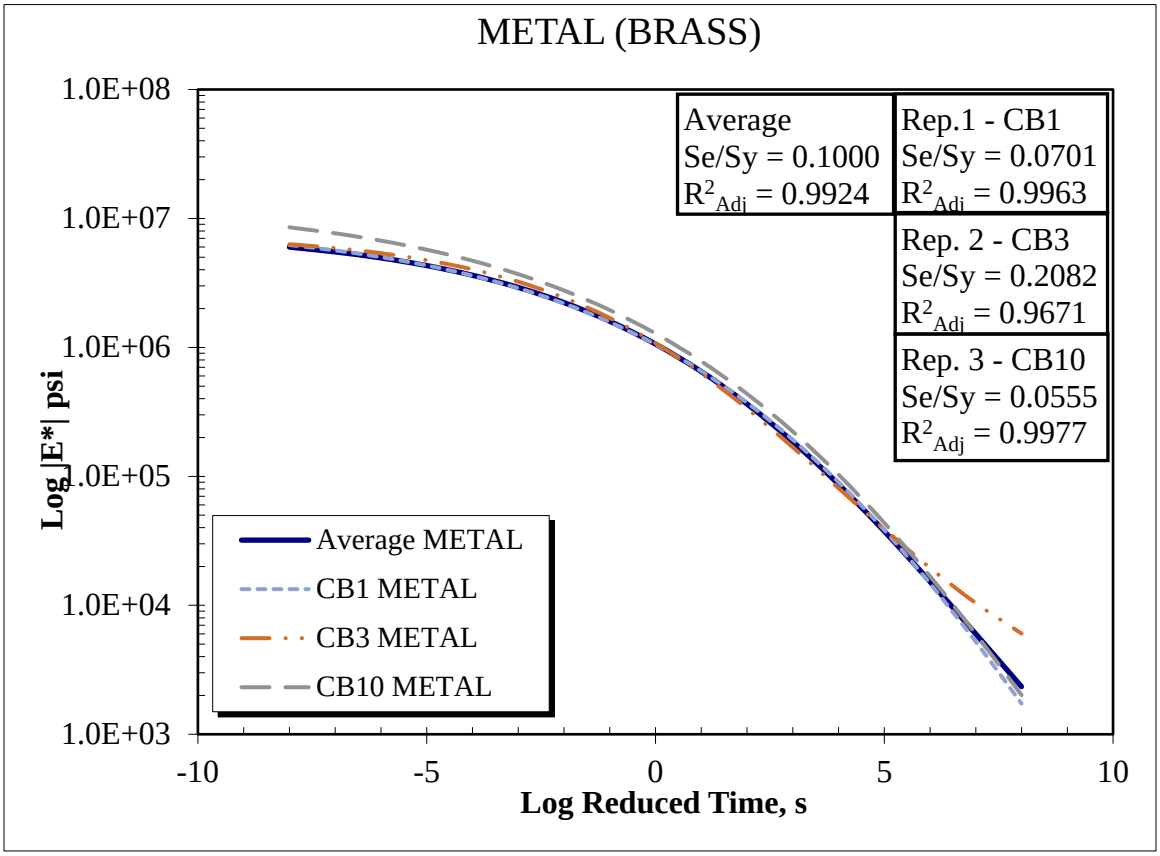

Figure 19. Comparison Between Brass Replicates for |E*|

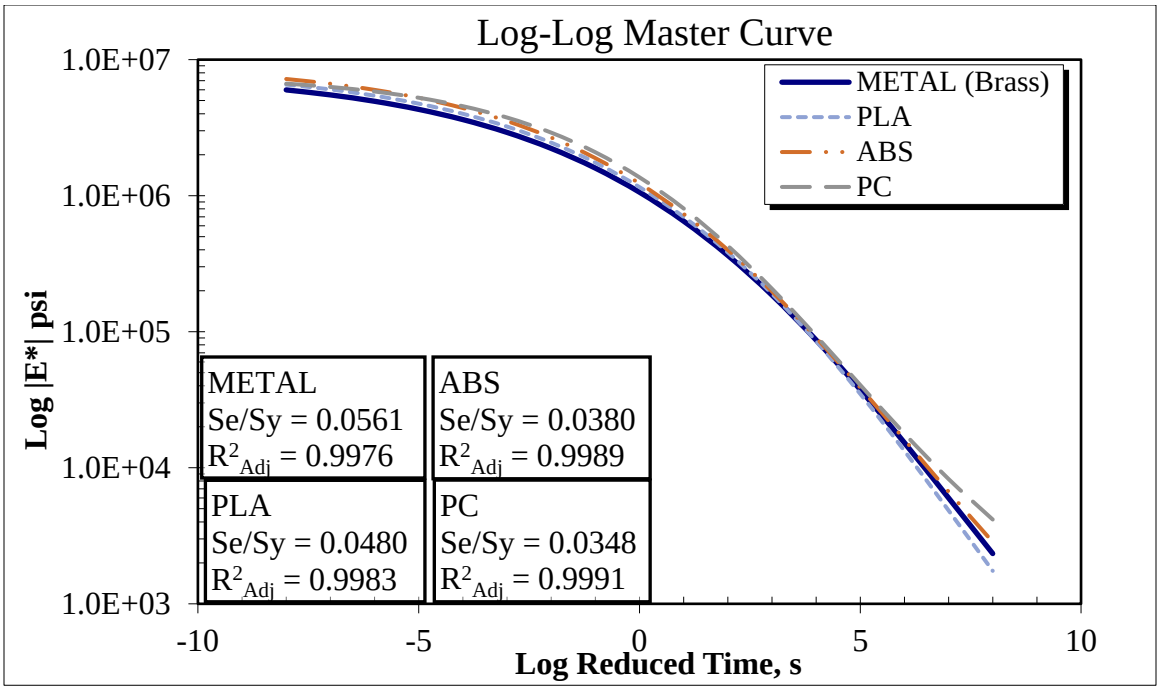

Figure 20: Log-Log Master Curve

The log-log master curve in Figure *20* shows nearly similar master curves for each stud type. Slight variation in the curves can be seen at negative reduced time values which corresponds to lower temperatures. The greatest variation can be seen at reduced time values larger than five which corresponds to higher temperatures. A more informative presentation of the data can be seen in Figure *21*, a semi-log master curve.

As seen in Figure *21* all stud types have very similar R^2 values. The Se/Sy ratios suggest that all thermoplastic studs performed equally or better than the brass studs in terms of model fit and accuracy of data. All studs had nearly the same modulus at reduced time values greater than zero, which corresponds to higher temperatures. The variation in the master curves is most notable at reduced time less than zero seconds and

is most extreme at the lowest reduced time. Reduced time values less than zero correspond to colder temperatures and yield a higher value for dynamic modulus.

The use of ABS studs yielded the highest modulus, followed by PC and PLA which produced very similar moduli. The PLA studs produced results closest to that of the brass studs at all temperatures, suggesting a good candidate for replacement studs. For ambient temperatures, the PC studs produces a higher modulus than all other studs and had a more pronounced curvature along its length. The performance of the PC studs also suggests a good candidate for replacement studs. The ABS studs produced a curve that constantly diverted from the brass curve, suggesting they are not a good option to replace brass studs.

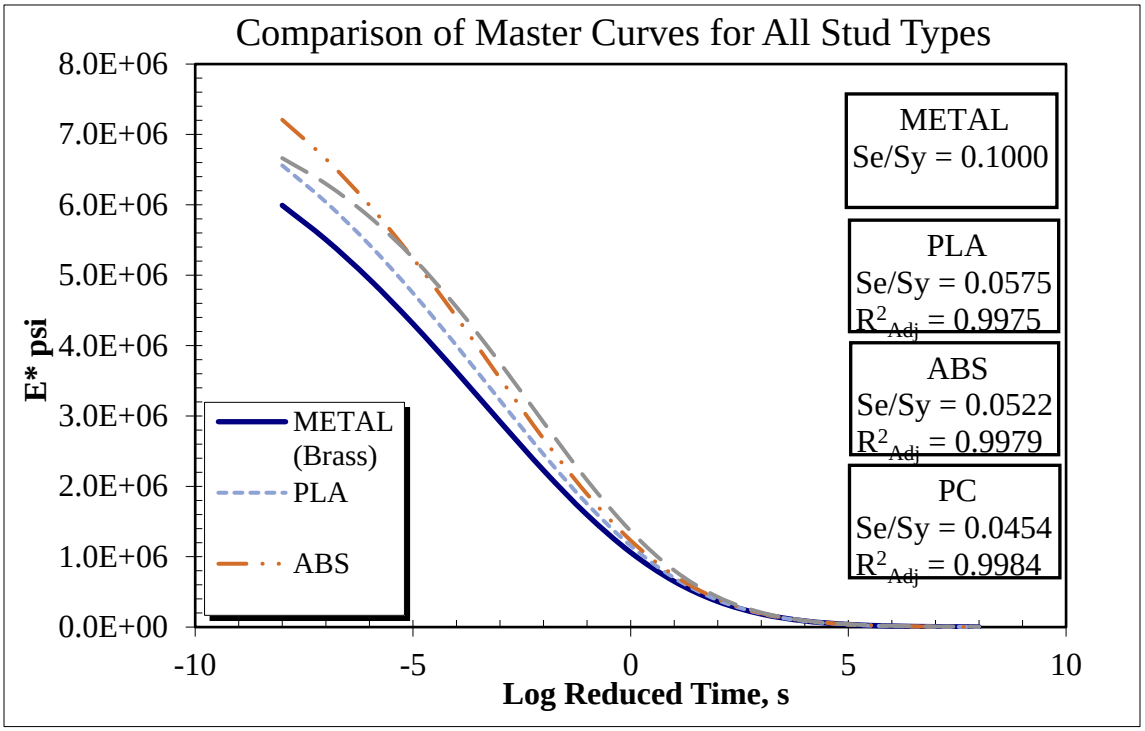

Figure 21: Comparison of Master Curves for All Stud Types

4.2 Repeated Load Permanent Deformation

The purpose of performing the Repeated Load Permanent deformation test was to examine the effect of high strain and temperature on the thermoplastic studs; three replicates were also tested. Each replicate was instrumented with all three types of thermoplastic studs, one type for each LVDT, totaling three LVDTs. The strain results were compared to the strain generated by the actuator of the loading device. All samples were tested at 122°F (50°C) and using a deviator stress of 300 kPa. The chosen temperature was based on the maximum average 7-day pavement temperature for the location in which the mix was intended to be placed. The deviatoric stress chosen was based upon Rodezno's predictive model [12], then adjusted based upon a previous research study by Arredondo at Arizona State University. This study used the same control mix design with identical parameters such as air voids, binder content, and aggregate gradation. Several control samples were tested and it was found that a deviator stress of approximately 300 kPa produced a flow number between 1000 and 5000 loading cycles.

Figure *22* - *26* show the average accumulated strain percentage, accumulated strain slope, measured strain and 2nd derivative strain, and predicted strain and 2nd derivative predicted curves for the average of all three replicates, for each stud type and the actuator value. Studies by Kaloush showed that the on-specimen LVDTs and actuator yield the same flow number value for the asphalt mixture.

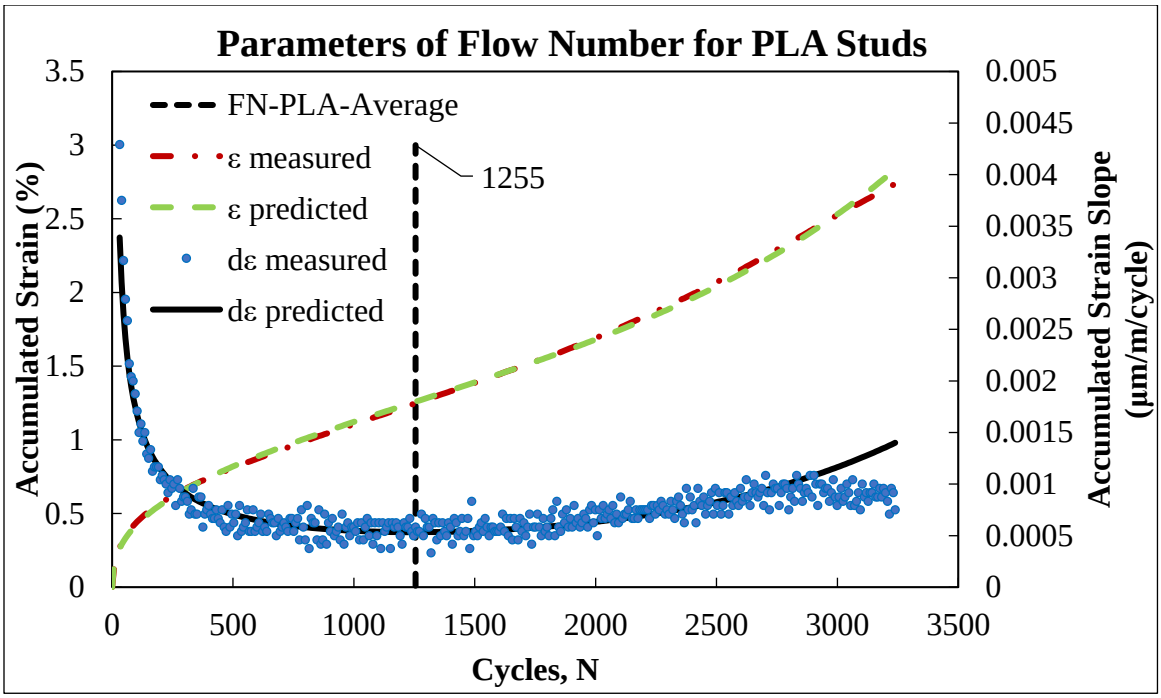

Figure 22: Parameters of Flow Number for PLA Studs

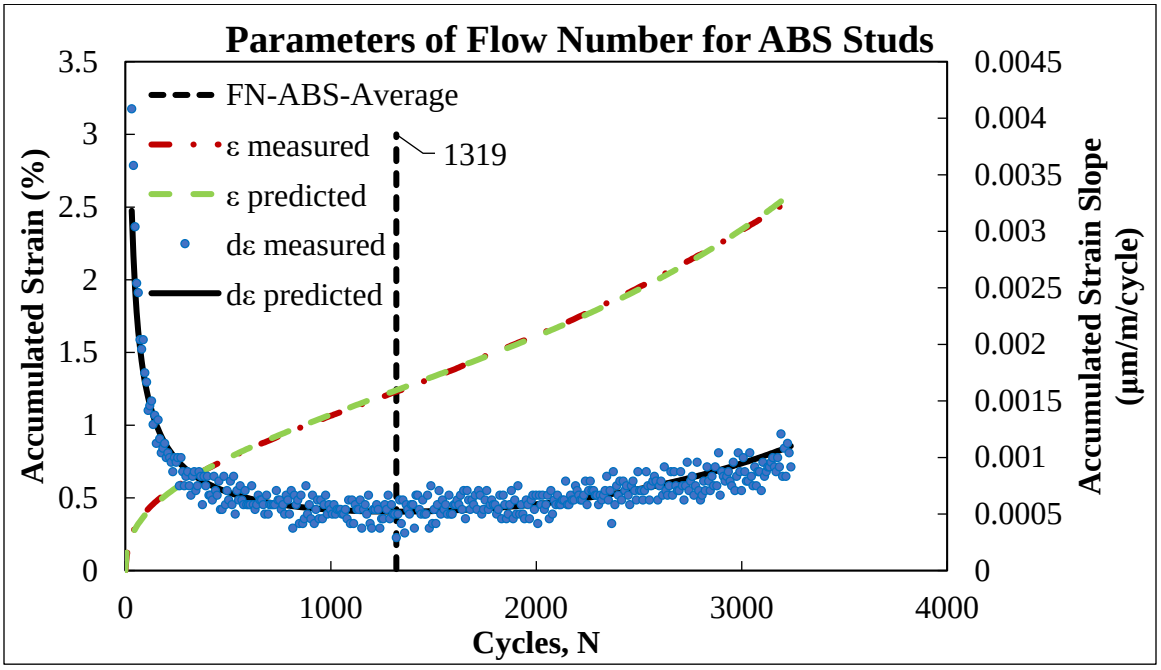

Figure 23: Parameters of Flow Number for ABS Studs

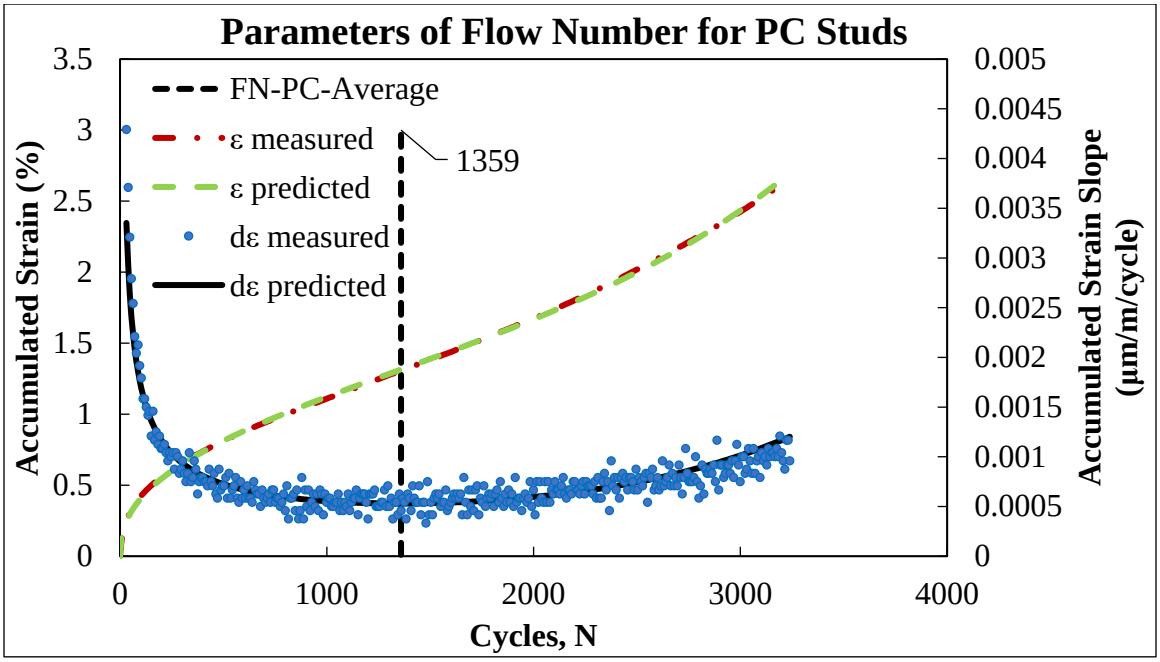

Figure 24: Parameters of Flow Number for PC Studs

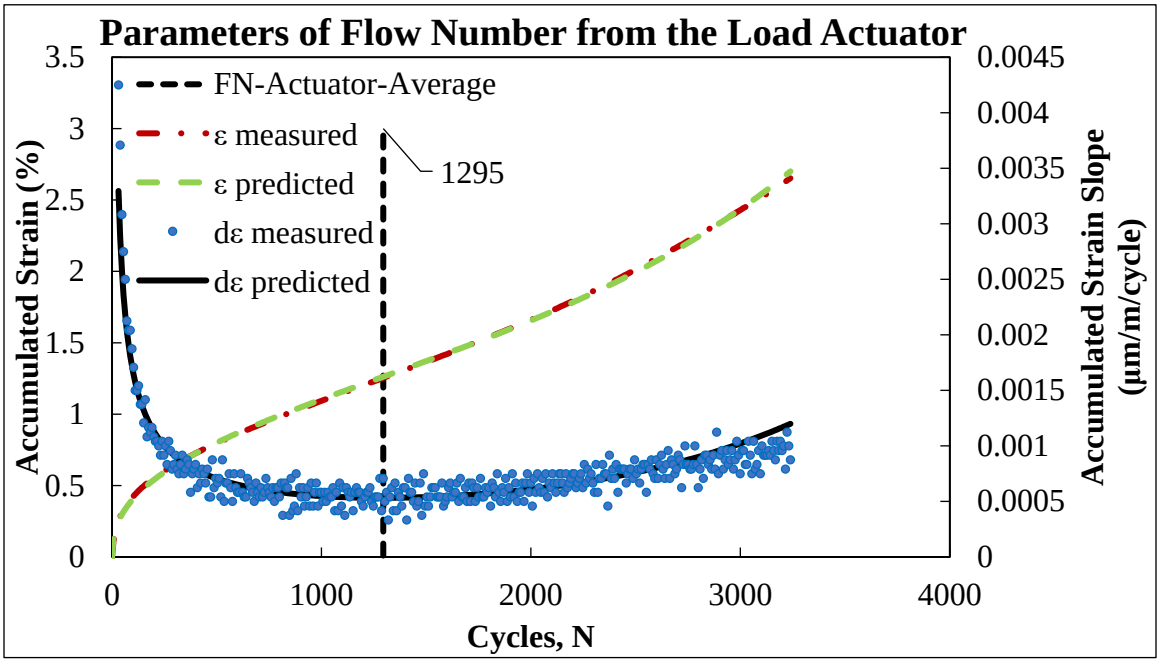

Figure 25: Parameters of Flow Number from the Load Actuator

A comparison between accumulator strain measurements for all replicates can be seen in Figure *26*. It can be seen that variability exists between replicates of the same treatment.

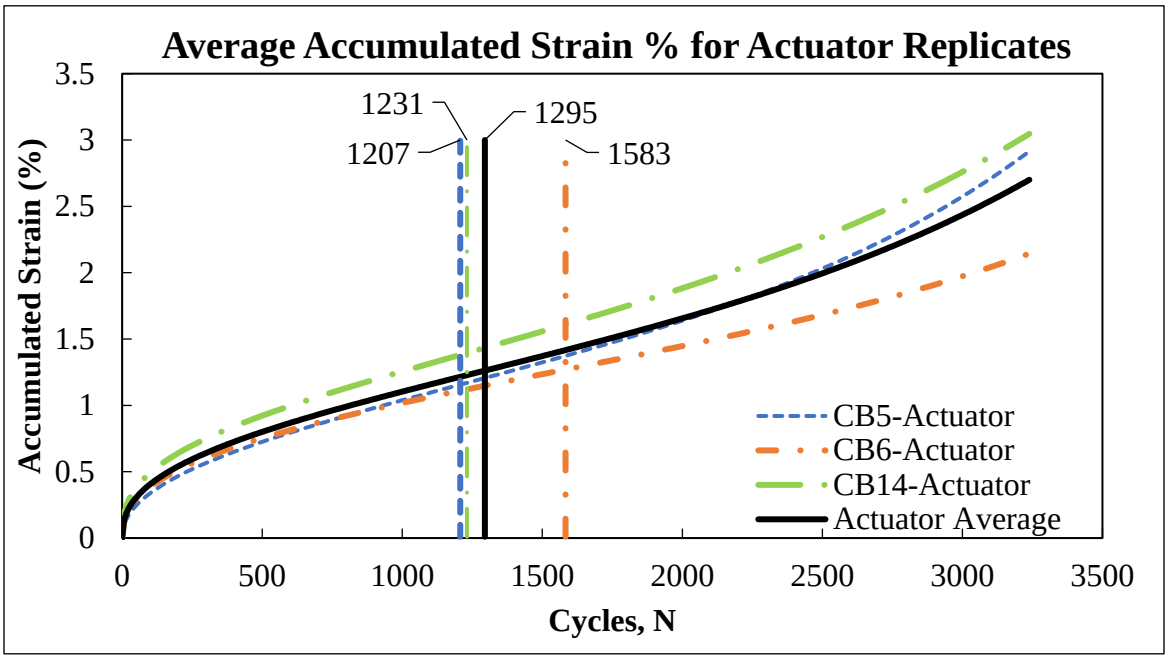

Figure 26. Accumulator Strains % for Each Replicate

Figure *27* shows the average accumulated strain percentage of all three replicates, for each stud type, as well as the average accumulated strain percentage recorded from the actuator of the loading device. As seen in Figure *27*, the flow number for each stud type are very similar. The highest variation occurs at the end of the tertiary section which corresponds to extreme shear deformation. Figure *28* shows the average for the percent strain ratio, permanent strain divided by the recoverable strain. Similar to the flow number curves, the strain ratio for each stud type produces similar results a in the primary

section of the curve. The strain ratio begins to diverge from each other while in the secondary section. The tertiary section displays the highest variation in the strain ratios. Charts corresponding to values recorded for all replicates can be found in Appendix C.

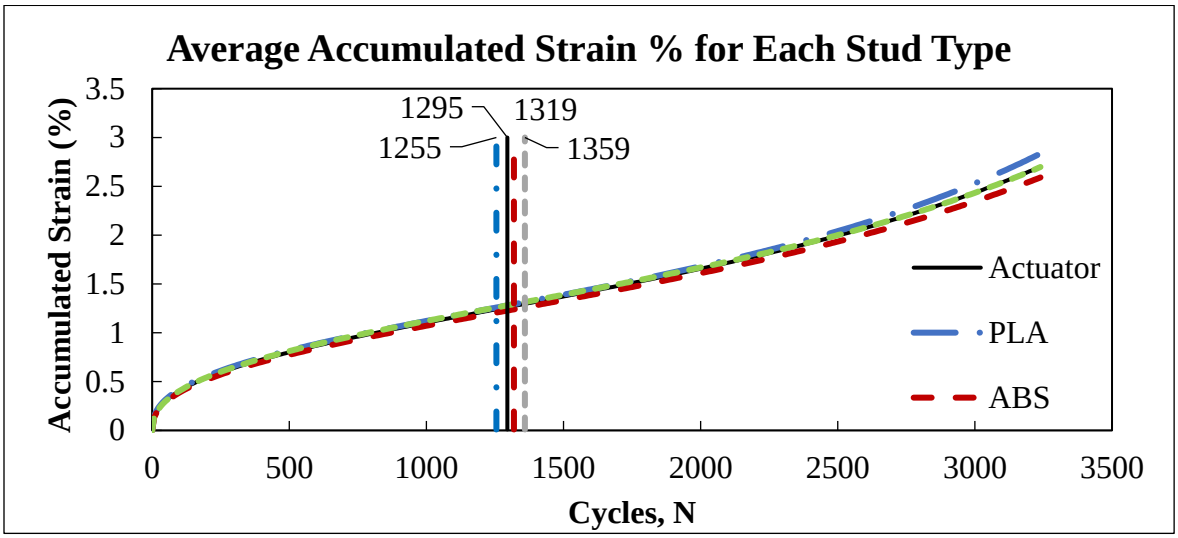

Figure 27: Average Flow Curve for All Stud Types

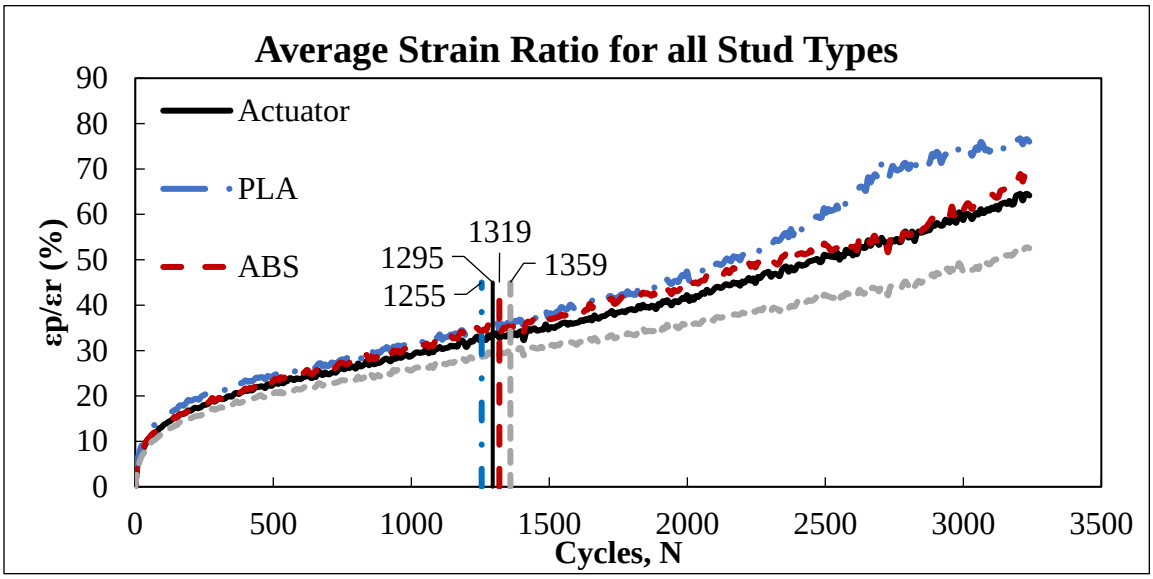

Figure 28: Average Strain Ration for All Stud Types

The similar performance of each thermoplastic stud suggests they are able to withstand high strain during permanent deformation testing and at high temperature. To further explore the validity of the suggested conclusion, statistical hypothesis tests were performed on several parameters relating to the flow number results. The details of the hypothesis testing can be seen in the Statistical Analysis section. Table *25 - 28* show initial statistical data related to the flow number results. A value to note in the following tables is the coefficient of variation (CV). The CV value is found by dividing the standard deviation by the average value and is a decent initial estimate of the variability of a data set.

Table 25: Parameters Measured from the Flow Number Curve for Replicate 1

Stud Type	Flow Number (Cycles)	Resilient Modulus at Failure (psi)	Axial Permanent Strain at Failure εp (%)	Axial Resilient Strain at Failure εr (%)	εp/εr (%)
CB5-Actuator	1207	95640	1.14	0.04	26.00
CB5-PLA	1135	131842	0.94	0.03	29.28
CB5-ABS	1319	85662	1.32	0.05	26.92
CB5-PC	1359	80967	1.30	0.05	24.94
Average	1271	99490	1.18	0.04	27.05
STD DEV	119	28116	0.214	0.011	2
CV%	**9.4%**	**28.3%**	**18.1%**	**24.3%**	**8.0%**

Table 26: Parameters Measured from the Flow Number Curve for Replicate 2

Stud Type	Flow Number (Cycles)	Resilient Modulus at Failure (psi)	Axial Permanent Strain at Failure εp (%)	Axial Resilient Strain at Failure εr (%)	εp/εr (%)
CB6-Actuator	1583	113891	1.27	0.04	34.22
CB6-PLA	1463	130734	1.17	0.03	36.69
CB6-ABS	1631	107121	1.31	0.04	32.73
CB6-PC	1727	106044	1.35	0.04	33.75
Average	1607	114633	1.28	0.04	34.39
STD DEV	134	13954	0.092	0.005	2
CV%	**8.3%**	**12.2%**	**7.2%**	**12.4%**	**6.0%**

Table 27: Parameters Measured from the Flow Number Curve for Replicate 3

Stud Type	Flow Number (Cycles)	Resilient Modulus at Failure (psi)	Axial Permanent Strain at Failure εp (%)	Axial Resilient Strain at Failure εr (%)	εp/εr (%)
CB14-Actuator	1231	133228	1.39	0.03	43.47
CB14-PLA	1143	96467	1.58	0.04	35.86
CB14-ABS	1327	240424	1.21	0.02	67.22
CB14-PC	1303	103269	1.40	0.04	34.12
Average	1258	146720	1.40	0.03	45.74
STD DEV	100	81221	0.184	0.014	19
CV%	**8.0%**	**55.4%**	**13.2%**	**41.4%**	**40.7%**

Table 28: Parameters Measured from the Flow Number Curve for the Average of all Replicates

Stud Type	Flow Number (Cycles)	Resilient Modulus at Failure (psi)	Axial Permanent Strain at Failure εp (%)	Axial Resilient Strain at Failure εr (%)	εp/εr (%)
Actuator	1295	113821	1.26	0.04	33.62
PLA	1255	119444	1.25	0.04	34.67
ABS	1319	137462	1.23	0.04	34.16
PC	1359	97397	1.31	0.04	29.46
Average	1311	118101	1.26	0.04	32.76
STD DEV	52	20066	0.040	0.005	3
CV%	**4.0%**	**17.0%**	**3.2%**	**12.4%**	**8.8%**

4.3 Direct Tension Cyclic Fatigue

The purpose of performing the Direct Tension Cyclic Fatigue test was to determine the effect of high stress and strain levels on the 3D printed studs, using both compressive and tensile forces. Four samples for each stud type were tested for Direct Tension Cyclic Fatigue. Three samples for each stud type were used to form pseudo secant modulus versus damage models, and strain verses number of load repetition to failure curves. Two samples for PLA studs yielded sufficient data to use for modelling purposes. Figure *29* shows the material integrity (C) verses damage (S) curves created from the modeling process for all stud types. Failure curves for each thermoplastic stud compared with brass studs can be found in Appendix C. Figure *30* shows the strain level at the 100^{th} cycle verses the number of load repetitions to failure for all stud types. Figure *31 – 34* show comparisons in failure curves between brass studs and each type of thermoplastic stud.

All stud types with the exception of PLA performed similarly in terms of damage response. In terms of failure curves, the ABS studs were almost identical to the brass studs, followed closely by the PLA studs, then the PC studs. It is difficult to determine any variation in performance of thermoplastic studs based solely on the damage models and failure curves. The failure curves in Figure *31 – 34* are a better indicator of the true response. It can be seen that PC studs showed slight variation from brass studs: However, PLA was the only stud type that clearly showed significant variation. Ideally, the same mix should produce curves that overlap. It is uncertain if the studs were responsible for any variation or if the difference in homogeneity of the samples is the main source of variation. Figure *34* shows a bar chart of the average micro-strain recorded for each stud type.

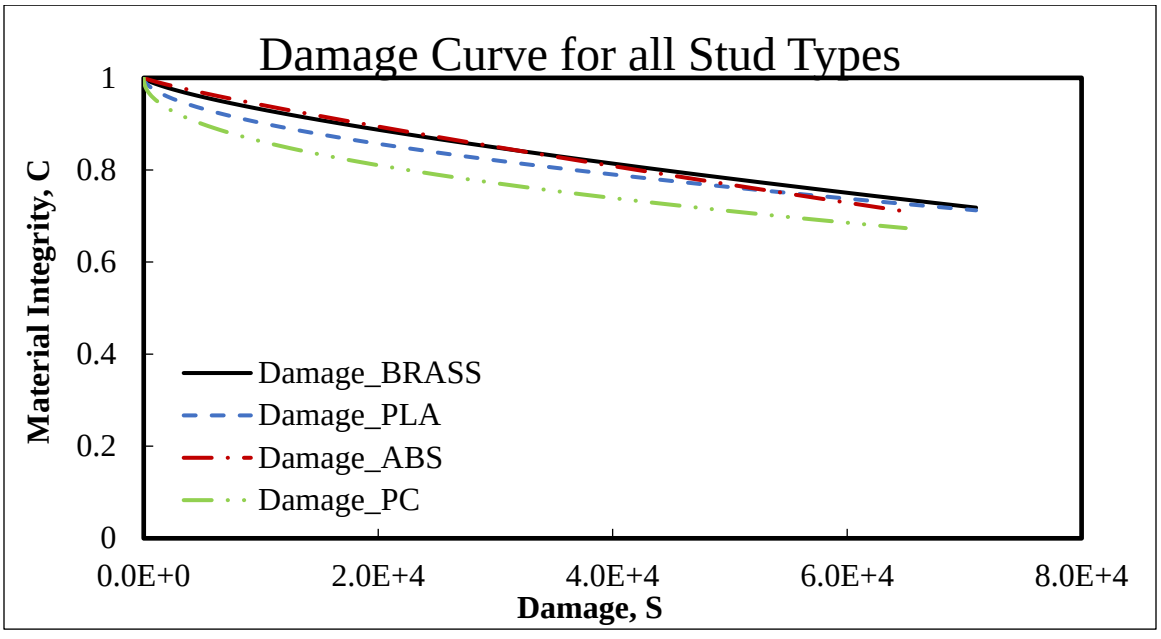

Figure 29: Damage Curve for All Stud Types

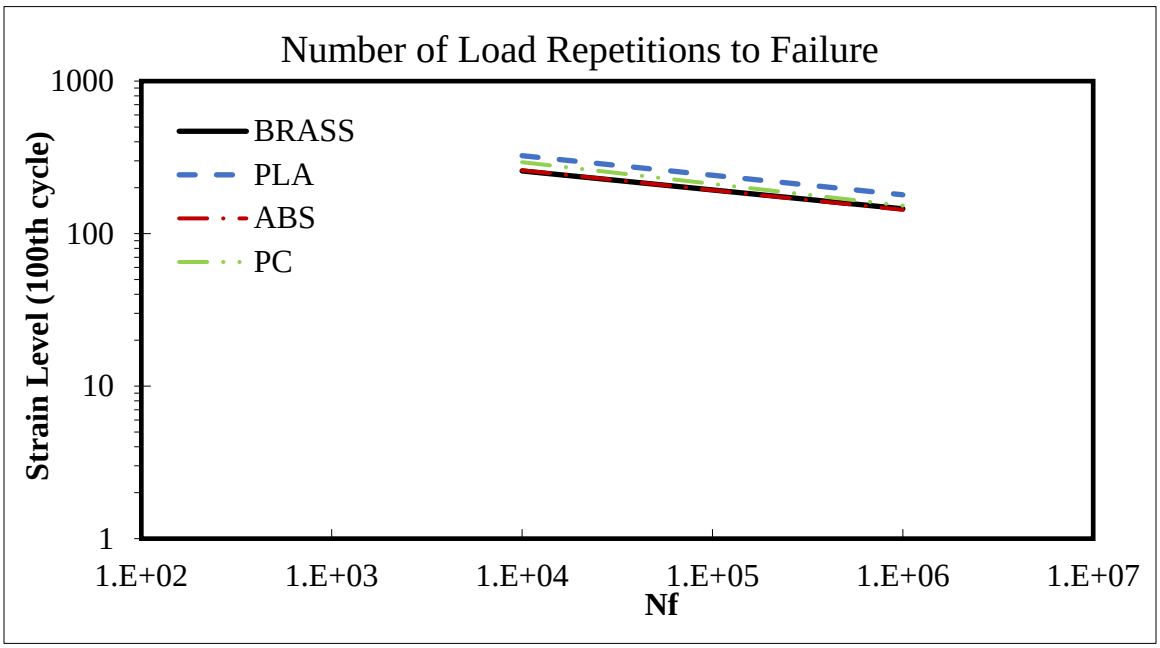

Figure 30: Number of Load Repetitions to Failure for All Stud Types

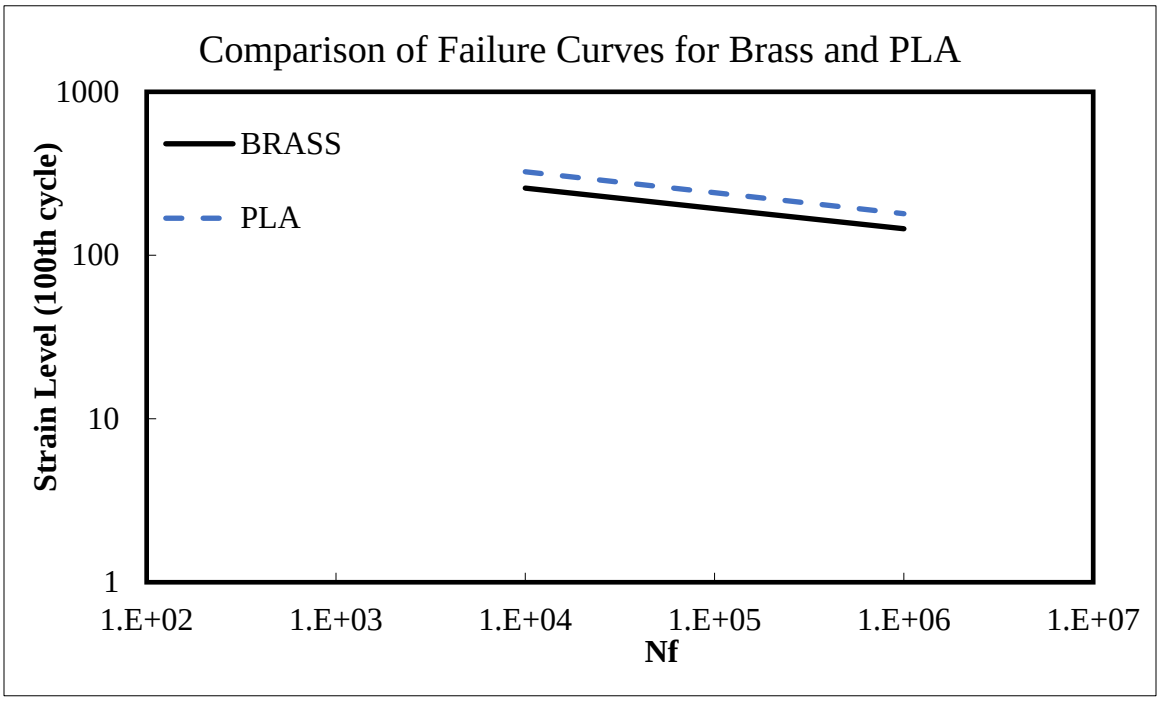

Figure 31: Comparison of Failure Curves for Brass and PLA

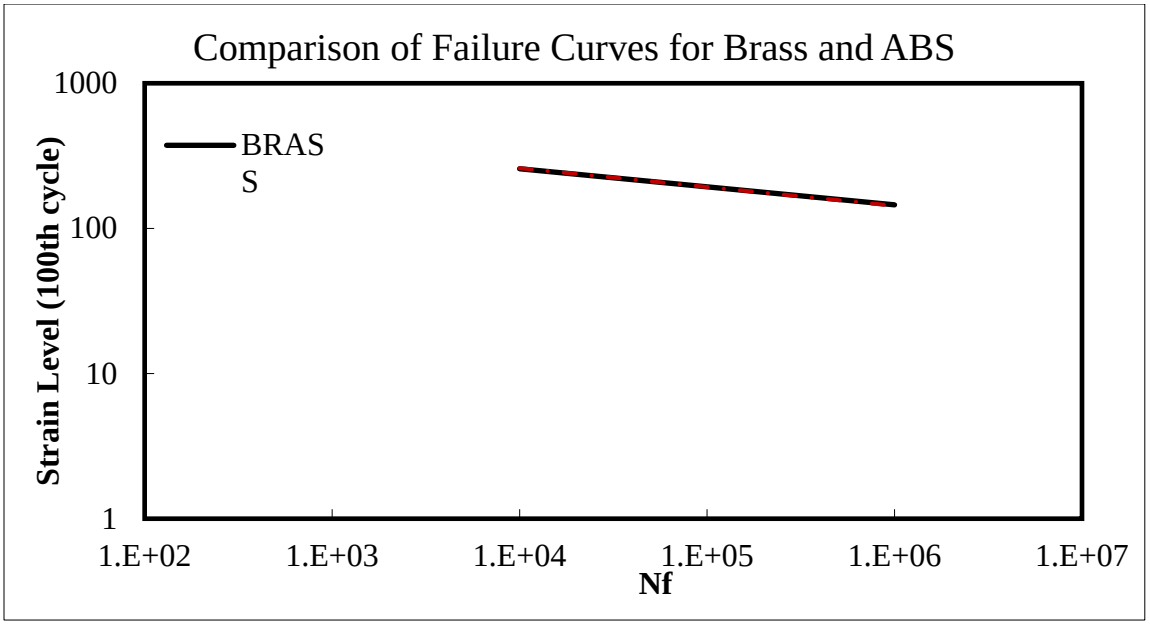

Figure 32: Comparison of Failure Curves for Brass and ABS

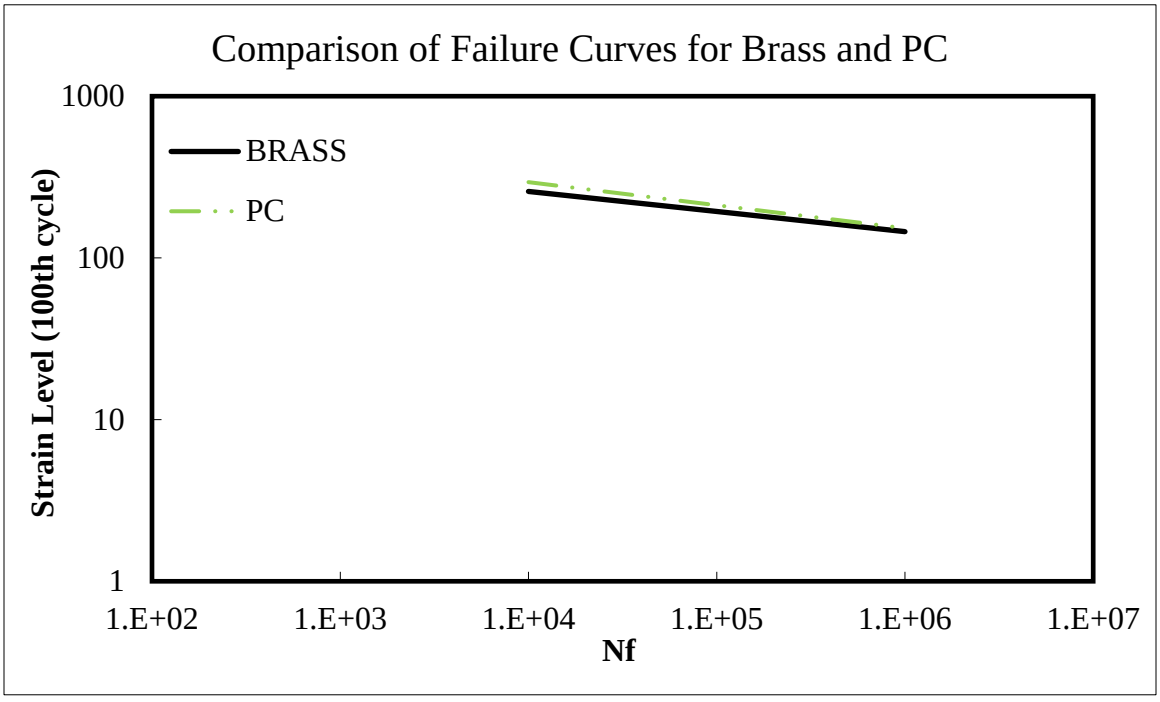

Figure 33: Comparison of Failure Curves for Brass and PC

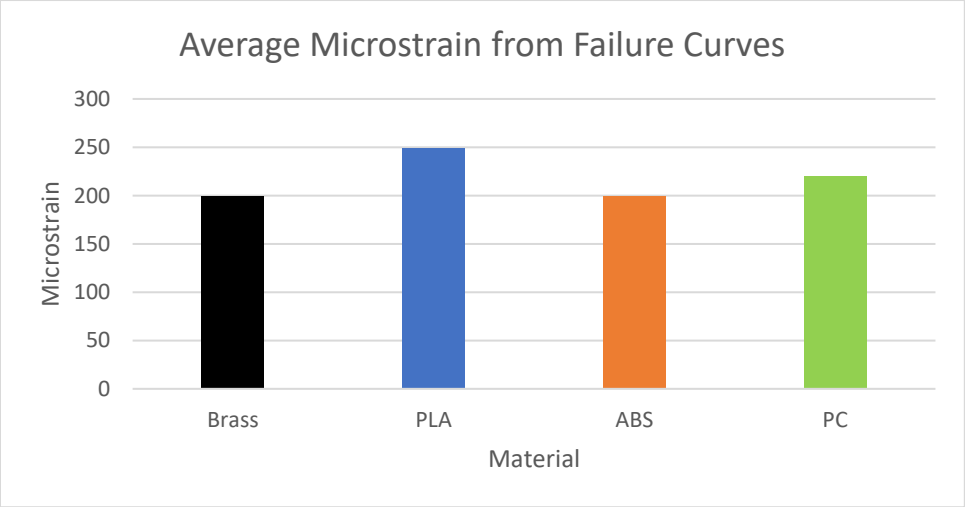

Figure 34: Average Macrostrains from Failure Curves

Figure *35* shows the failure curves for each brass LVDT. It can be seen that variability exists even between replicates that use the same stud type.

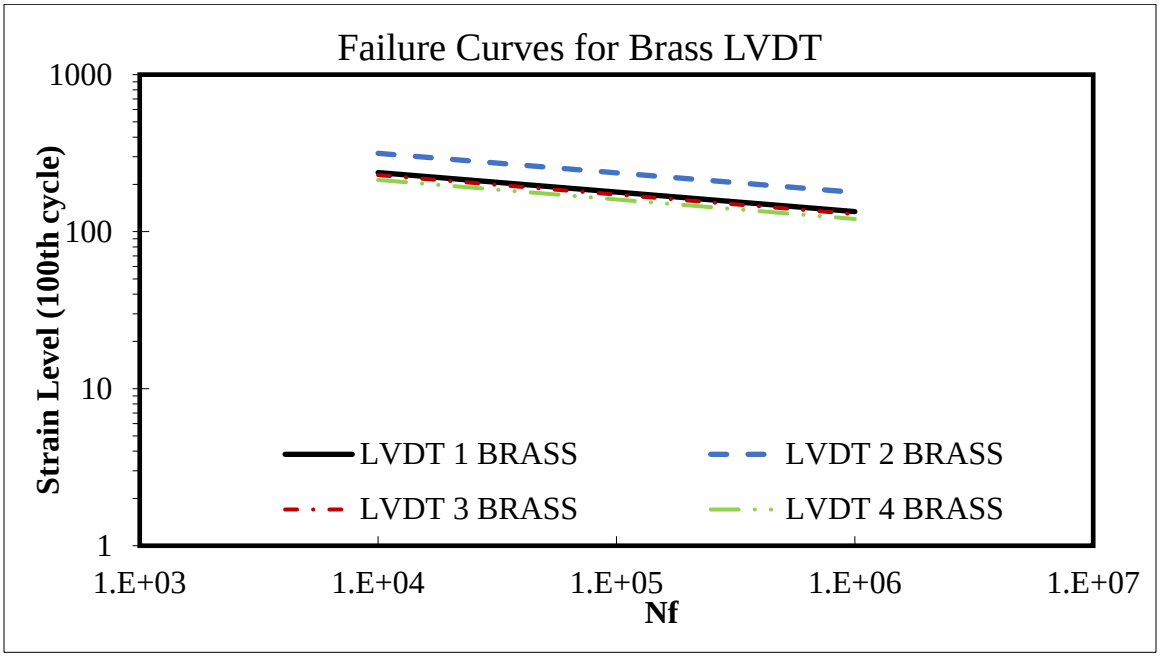

Figure 35. Failure Curves for Each Brass LVDT

5. STATISTICAL ANALYSIS

To determine the variation between brass studs and the various types of thermoplastic studs tested, Analysis of Variance (ANOVA) and hypothesis tests were performed for the mean and variance of the collected. The ANOVA test determines if there is a significant difference between a control treatment and additional treatments and was performed to validate the results of hypothesis testing. The hypothesis was formed from the assumption that the mean value of the brass stud results is equal to the mean value of each type of thermoplastic stud. Equations (70) and (71) were used to accept or reject the null hypothesis. By rejecting the null hypothesis, and accepting the alterative hypothesis, the means values are not equal, must be accepted. The same process was performed for the variance of collected data. For analysis of both the mean and the variance, the confidence level, (α), for full acceptance of the null hypothesis was identified when possible.

$$H:\ \mu_1 = \mu_2 \tag{70}$$

$$A:\ \mu_1 \neq \mu_2 \tag{71}$$

The criteria for rejection of the null hypothesis was adopted from the book, Engineering Statistics, written by A.H Bowker and G.J Lieberman, which was published in February 1963 [16]. Table *29* and Table *30* show the rejection criteria for the hypothesis test on mean and variance respectively.

Table 29: Rejection Criteria for the Hypothesis That the Means of Two Normal Distributions are Equal When STD Dev Is Unknown & Not Necessarily Equal.

Notation for the Hypothesis H: $\mu_z = \mu_y$	Test Statistic $t' = \frac{\bar{x} - \bar{y}}{\sqrt{\frac{S_z^2}{n_x} + \frac{S_y^2}{n_y}}}$ Formula for Obtaining the Degree of Freedom, ν $\nu = \frac{\left(\frac{S_z^2}{n_x} + \frac{S_y^2}{n_y}\right)^2}{\frac{\left(\frac{S_z^2}{n_x}\right)^2}{n_x + 1} + \frac{\left(\frac{S_y^2}{n_y}\right)^2}{n_y + 1}} - 2$
Criteria for Rejection $\lvert t' \rvert \geq t_{\alpha/2,\nu}$ if we wish to reject when μ_z is not equal to μ_y.	
$t' \geq t_{\alpha,\nu}$ if we wish to reject when $\mu_z > \mu_y$.	
$t' \leq -t_{\alpha,\nu}$ if we wish to reject when $\mu_z < \mu_y$.	

Table 30: Rejection Criteria for the Hypothesis That the Standard Deviations of Two Normal Distributions are Equal

Notation for Hypothesis $H: \sigma_z^2 = \sigma_y^2$ or $\sigma_z = \sigma_y$	Test Statistic $F = \frac{\sum_{i=1}^{n_z} \frac{(x_i - \bar{x})^2}{n_z - 1}}{\sum_{i=1}^{n_y} \frac{(y_i - \bar{y})^2}{n_y - 1}} = \frac{S_z^2}{S_y^2}$
Criteria for Rejection $F \leq 1/F_{\frac{\alpha}{2};n_y-1,n_z-1}$ or $F \geq 1/F_{\frac{\alpha}{2};n_z-1,n_y-1}$ if We wish to reject when σ_z is not equal to σ_y.	Method for Choosing Sample Sizes The OC Curve depends on $\lambda = \frac{\sigma_z}{\sigma_y}$. Choose a value of λ for which we wish to reject the hypothesis with given high probability. Enter figures corresponding to OC curves (not shown) to find the required sample size.

The modeling process for analysis of the Direct Tension Cyclic Fatigue test combines all replicates for a stud type into a single curve so damage and failure curves

were developed for each LVDT, for three samples per stud type, in order to perform hypothesis tests. Table *31* shows the statistical inputs used for hypothesis testing.

Table 31: Statistical Inputs for Hypothesis Testing

INPUTS		
	|E*| & Fn	Fatigue
REPLICATES n =	3	12
TREATMENTS a =	4	4
DoF	2	11
ni+1 =	4	13

5.1 Dynamic Modulus

5.1.1 ANOVA for Dynamic Modulus

The results for ANOVA analysis are outlined in Table *32*. The results show no significant difference for extreme temperatures and a significant difference for moderate temperatures.

Table 32. ANOVA Results for Dynamic Modulus

ANOVA on Dynamic Modulus |E*|					
Frequency (Hz)	Temperatures (°C)				
	-10	4.4	21.1	37.8	54.4
25	NS	S	S	S	NS
10	NS	S	S	S	NS
5	NS	S	S	S	NS
1	NS	S	S	S	NS
0.5	NS	S	S	S	NS
0.1	NS	S	S	S	NS

NS= Not Significant S= Significant

5.1.2 Mean

The average values for each frequency and every temperature were calculated using the first moment, Equation (72). The complete data sets for all statistical analysis can be found in Appendix D.

$$\frac{\sum_{i=1}^{n} x_i}{n_i} \tag{72}$$

Table *33* summarize the results of the average values for |E*|, Log |E*|, and Log Reduced Time (s).

Table 33: Sample of Average Values for Hypothesis Testing at 14°F

Temp. (°F)	Freq. (Hz)	|E*| (psi)				Log|E*|				Log Reduced Time (s)			
		METAL	**PLA**	**ABS**	**PC**	**METAL**	**PLA**	**ABS**	**PC**	**METAL**	**PLA**	**ABS**	**PC**
14	25	4945	5821	6673	7419	3.6934	3.7622	3.8213	3.8623	-5.9687	-6.2189	-6.5441	-6.6189
	10	4957	5537	6286	7080	3.6946	3.7405	3.7950	3.8394	-5.3855	-5.6788	-6.1462	-6.2209
	5	4738	5473	6071	7180	3.6747	3.7359	3.7807	3.8407	-5.2697	-5.5199	-5.8451	-5.9199
	1	4421	5112	5579	6356	3.6447	3.7057	3.7444	3.7930	-4.5708	-4.8209	-5.1462	-5.2209
	0.5	4282	4944	5370	6077	3.6308	3.6912	3.7280	3.7746	-4.2697	-4.5199	-4.8451	-4.9199
	0.1	3958	4532	4908	5232	3.5966	3.6535	3.6891	3.7151	-3.5708	-3.8209	-4.1462	-4.2209

The variance for each frequency and every temperature were calculated using the second moment, Equation (73) below.

$$S_i^2 = \frac{1}{n-1}\sum_{i=1}^{n}(x_i - \bar{x})^2 \tag{73}$$

Table *34* below summarizes the calculated values of variance for |E*|, Log |E*|, and Log Reduced Time (s).

Table 34: Sample of Calculated Variance Values for Hypothesis Testing at 14°F.

Temp. (°F)	Freq. (Hz)	|E*| (psi)				Log |E*|				Log Reduced Time (s)			
		METAL	**PLA**	**ABS**	**PC**	**METAL**	**PLA**	**ABS**	**PC**	**METAL**	**PLA**	**ABS**	**PC**
14	25	133797	665571	931270	3221157	0.0010	0.0035	0.0040	0.0103	0.1405	0.2038	0.8326	0.2867
	10	153103	384140	911224	3876224	0.0012	0.0024	0.0045	0.0134	0.1919	0.2341	0.8326	0.2867
	5	145081	474168	623225	5931261	0.0012	0.0030	0.0033	0.0193	0.1405	0.2038	0.8326	0.2867
	1	114364	512174	444602	3038135	0.0011	0.0038	0.0028	0.0129	0.1405	0.2038	0.8326	0.2867
	0.5	108253	487534	384347	2467791	0.0011	0.0038	0.0026	0.0115	0.1405	0.2038	0.8326	0.2867

Following the hypothesis test procedure is outlined in Table *29*, the test statistic was calculated according to Equation (74) for every frequency at each temperature.

$$t' = \frac{(\bar{x}-\bar{y})}{\sqrt{\frac{S_x^2}{n_x}+\frac{s_y^2}{n_y}}} \tag{74}$$

Where:
$\bar{x}$ = Average of Control Treatment
$\bar{y}$ = Average of Alternative Treatment
S_x^2 = Estimate of Variance for the Control Treatment
S_y^2 = Estimate of Variance for an Alternative Treatment
$n_x = n_y$ = Number of Test Replicates

Table 35 shows a sample the calculated values for the test statistic for every frequency at 14°F.

Table 35: Sample of Calculated Test Statistics for 14°F.

Temp. (°F)	Freq. (Hz)	|E*| (psi)			Log| E*|			Log Reduced Time (s)		
		t'1	**t'2**	**t'3**	**t'1**	**t'2**	**t'3**	**t'1**	**t'2**	**t'3**
14	25	1.7822	3.1271	2.7519	1.7822	3.1271	2.7519	0.7384	1.0103	1.7229
	10	1.3272	2.2934	2.0779	1.3272	2.2934	2.0779	0.7783	1.3016	2.0913
	5	1.6344	2.7340	2.0105	1.6344	2.7340	2.0105	0.7384	1.0103	1.7229
	1	1.5182	2.7733	2.1744	1.5182	2.7733	2.1744	0.7384	1.0103	1.7229
	0.5	1.4909	2.7592	2.2178	1.4909	2.7592	2.2178	0.7384	1.0103	1.7229
	0.1	1.4084	2.6666	2.6976	1.4084	2.6666	2.6976	0.7384	1.0103	1.7229

The degree of freedom was calculated according to Equation (75) below for every frequency for each temperature.

$$v = \frac{\left(\frac{S_x^2}{n_x}+\frac{S_y^2}{n_y}\right)^2}{\frac{\left(\frac{S_x^2}{n_x}\right)^2}{n_x-1}+\frac{\left(\frac{S_y^2}{n_y}\right)^2}{n_y-1}} - 2 \qquad (75)$$

Where:
S_x^2 = Estimate of Variance for the Control Treatment
S_y^2 = Estimate of Variance for an Alternative Treatment
$n_x = n_y$ = Number of Test Replicates

Table *36* summarizes the calculated values for the degree of freedom at 14°F.

Table 36: Calculated Degree of Freedom at $14°F$.

Temp. (°F)	Freq. (Hz)	|E*| (psi)			Log |E*|			Log Reduced Time (s)		
		Dof1	**Dof2**	**Dof3**	**Dof1**	**Dof2**	**Dof3**	**Dof1**	**Dof2**	**Dof3**
14	25	3.5457	3.1261	2.3317	4.1595	3.9063	2.7819	5.7382	3.3123	5.1607
	10	4.7514	3.3072	2.3155	5.2215	3.9902	2.7177	5.9225	3.7511	5.6981
	5	4.2382	3.7666	2.1956	4.6938	4.5027	2.4856	5.7382	3.3123	5.1607
	1	3.7015	3.9301	2.3007	4.0858	4.6470	2.6568	5.7382	3.3123	5.1607
	0.5	3.6929	4.0876	2.3503	4.0782	4.7918	2.7403	5.7382	3.3123	5.1607
	0.1	4.0079	4.5681	3.1703	4.3853	5.2335	3.9902	5.7382	3.3123	5.1607

To evaluate the tabulated value in which to compare the test statistic, $t_{0.025,\nu}$, must be used to locate the value in a standard table of values. For the hypothesis test on the mean, the degree of freedom was calculated and corresponds to varying values for each test. The tabulated solutions from the T-table that were used to compare the test statistic are summarized in Table *37*.

Table 37: Tabulated T-table Values for α = 0.05, at $14°F$.

Temp. (°F)	Freq. (Hz)	|E*| (psi)			Log |E*|			Log Reduced Time (s)		
		t Table 1	**t Table 2**	**t Table 3**	**t Table 1**	**t Table 2**	**t Table 3**	**t Table 1**	**t Table 2**	**t Table 3**
14	25	2.9604	3.1308	3.9311	2.7433	2.8140	3.4265	2.4795	3.0552	2.5511
	10	2.6220	3.0573	3.9493	2.5435	2.7800	3.4984	2.4566	2.8771	2.4844
	5	2.7272	2.8708	4.0838	2.6338	2.6729	3.7587	2.4795	3.0552	2.5511
	1	2.8972	2.8044	3.9659	2.7584	2.6434	3.5667	2.4795	3.0552	2.5511
	0.5	2.9007	2.7580	3.9104	2.7600	2.6137	3.4731	2.4795	3.0552	2.5511
	0.1	2.7744	2.6595	3.1129	2.6970	2.5420	2.7800	2.4795	3.0552	2.5511

The criteria for rejecting the hypothesis H: $(\mu_1 = \mu_2)$ is as follows. If the null hypothesis is rejected, the alternative A: $(\mu_1 \neq \mu_2)$ must be accepted. Equation (76) was used to accept or reject the null hypothesis.

$$|t'| \geq t_{\frac{\alpha}{2},\nu} \tag{76}$$

Table *38* summarizes the results of the hypothesis test for comparison of the mean of each treatment against the control treatment for all scenarios tested. As seen in the table the results of the hypothesis tests are inconclusive. All temperatures and frequencies accepted the null hypothesis for |E*| and Log reduced time, while many values rejected for Log |E*|.

Table 38: Results of Hypothesis Tests for the Mean of the Control Treatment to Alternative Treatments.

Frequency Hz	Temp ºF	|E*| (psi)			Log |E*|			Log Reduced Time (s)		
		H:μx = μy1	**H:μx = μy2**	**H:μx = μy3**	**H:μx = μy1**	**H:μx = μy2**	**H:μx = μy3**	**H:μx = μy1**	**H:μx = μy2**	**H:μx = μy3**
25	14 ºF	Accept	Accept	Accept	Accept	Reject	Accept	Accept	Accept	Accept
10	14 ºF	Accept	Accept	Accept	Accept	Accept	Accept	Accept	Accept	Accept
5	14 ºF	Accept	Accept	Accept	Accept	Reject	Accept	Accept	Accept	Accept
1	14 ºF	Accept	Accept	Accept	Accept	Reject	Accept	Accept	Accept	Accept
0.5	14 ºF	Accept	Accept	Accept	Accept	Reject	Accept	Accept	Accept	Accept
0.1	14 ºF	Accept	Accept	Accept	Accept	Reject	Accept	Accept	Accept	Accept
25	40 ºF	Reject	Reject	Reject	Reject	Reject	Reject	Accept	Accept	Accept
10	40 ºF	Reject	Reject	Reject	Reject	Reject	Reject	Accept	Accept	Accept
5	40 ºF	Reject	Reject	Reject	Reject	Reject	Reject	Accept	Accept	Accept
1	40 ºF	Reject	Reject	Reject	Reject	Reject	Reject	Accept	Accept	Accept
0.5	40 ºF	Reject	Reject	Reject	Reject	Reject	Reject	Accept	Accept	Accept
0.1	40 ºF	Reject	Reject	Reject	Reject	Reject	Reject	Accept	Accept	Accept
25	70 ºF	Accept	Accept	Reject	Accept	Accept	Reject	Accept	Accept	Accept
10	70 ºF	Accept	Accept	Reject	Accept	Accept	Reject	Accept	Accept	Accept
5	70 ºF	Accept	Accept	Reject	Accept	Accept	Reject	Accept	Accept	Accept
1	70 ºF	Accept	Accept	Accept	Accept	Accept	Reject	Accept	Accept	Accept
0.5	70 ºF	Accept	Accept	Accept	Accept	Accept	Reject	Accept	Accept	Accept
0.1	70 ºF	Accept	Accept	Accept	Accept	Accept	Reject	Accept	Accept	Accept
25	100 ºF	Accept	Reject	Reject	Accept	Reject	Reject	Accept	Accept	Accept
10	100 ºF	Accept	Reject	Reject	Accept	Reject	Reject	Accept	Accept	Accept
5	100 ºF	Accept	Reject	Reject	Accept	Reject	Reject	Accept	Accept	Accept
1	100 ºF	Accept	Accept	Reject	Accept	Accept	Reject	Accept	Accept	Accept
0.5	100 ºF	Accept	Accept	Reject	Accept	Accept	Reject	Accept	Accept	Accept
0.1	100 ºF	Accept	Accept	Reject	Accept	Accept	Reject	Accept	Accept	Accept
25	130 ºF	Accept	Accept	Accept	Accept	Accept	Accept	Accept	Accept	Accept
10	130 ºF	Accept	Accept	Accept	Accept	Accept	Accept	Accept	Accept	Accept
5	130 ºF	Accept	Accept	Accept	Accept	Accept	Accept	Accept	Accept	Accept
1	130 ºF	Accept	Accept	Accept	Accept	Accept	Accept	Accept	Accept	Accept
0.5	130 ºF	Accept	Accept	Accept	Accept	Accept	Accept	Accept	Accept	Accept
0.1	130 ºF	Accept	Accept	Accept	Accept	Accept	Accept	Accept	Accept	Accept

5.1.3 Variance

Following the test procedure for hypothesis testing for the variance as outlined in Table *30*, average values and variances found in Table *33 & 34* respectively were used for calculations. The F-statistic used for hypothesis testing was calculated for all scenarios using Equation (77) below.

$$F = \frac{\sum_{i=1}^{n} \frac{(x_i - \bar{x})^2}{n_x - 1}}{\sum_{i=1}^{n} \frac{(y_i - \bar{y})^2}{n_y - 1}} = \frac{S_x^2}{S_y^2} \tag{77}$$

The criteria for rejecting the hypothesis H: $(\sigma_1^2 = \sigma_2^2)$ is as follows. If the hypothesis is rejected the alternative, A: $(\sigma_1^2 \neq \sigma_2^2)$ must be accepted. Equation (78) was used to determine acceptance or rejection of the null hypothesis.

$$F \leq \frac{1}{F_{\frac{\alpha}{2}, n_y - 1, n_x - 1}} \text{ or } F \geq F_{\frac{\alpha}{2}, n_x - 1, n_y - 1} \tag{78}$$

Table *39* summarizes the calculated values for the F-test statistic at 14°F and all six frequencies. Complete tabular results for hypothesis tests can be found in Appendix D.

Table 39: Sample of Calculated F-statistics for Hypothesis Testing

Temp °F	Frequency Hz	|E*| (psi)			Log |E*|			Log Reduced Time (s)		
		F1	F2	F3	F1	F2	F3	F1	F2	F3
14 °F	25	0.2010	0.1437	0.0415	0.2931	0.2536	0.0987	0.6893	0.1687	0.4899
14 °F	10	0.3986	0.1680	0.0395	0.5057	0.2664	0.0905	0.8200	0.2305	0.6694
14 °F	5	0.3060	0.2328	0.0245	0.3872	0.3515	0.0609	0.6893	0.1687	0.4899
14 °F	1	0.2233	0.2572	0.0376	0.2814	0.3782	0.0827	0.6893	0.1687	0.4899
14 °F	0.5	0.2220	0.2817	0.0439	0.2802	0.4067	0.0933	0.6893	0.1687	0.4899
14 °F	0.1	0.2692	0.3634	0.1496	0.3308	0.5088	0.2664	0.6893	0.1687	0.4899

Since the degree of freedom is the same for each treatment the tabular value corresponding to each frequency and temperature is the same value for each scenario tested. Table *40* summarizes the values identified for each scenario. The results for the hypothesis test on the variance at 14°F is summarized in Table *41*.

Table 40: Tabular Value for the F-test

F Table |E*|
F(a/2,nx-1,ny-1) = F(a/2,ny-1,nx-1)
39.0000

Table 41: Results of Hypothesis Testing on Variance

		|E*| (psi)			Log|E*|			Log Reduced Time (s)		
Frequency Hz	**Temp °F**	**H:σ^2x = σ^2y1**	**H:σ^2x = σ^2y2**	**H:σ^2x = σ^2y3**	**H:σ^2x = σ^2y1**	**H:σ^2x = σ^2y2**	**H:σ^2x = σ^2y3**	**H:σ^2x = σ^2y1**	**H:σ^2x = σ^2y2**	**H:σ^2x = σ^2y3**
25	14 °F	Accept	Accept	Accept	Accept	Accept	Accept	Accept	Accept	Accept
10	14 °F	Accept	Accept	Accept	Accept	Accept	Accept	Accept	Accept	Accept
5	14 °F	Accept	Accept	Reject	Accept	Accept	Accept	Accept	Accept	Accept
1	14 °F	Accept	Accept	Accept	Accept	Accept	Accept	Accept	Accept	Accept
0.5	14 °F	Accept	Accept	Accept	Accept	Accept	Accept	Accept	Accept	Accept
0.1	14 °F	Accept	Accept	Accept	Accept	Accept	Accept	Accept	Accept	Accept

With the exception of one frequency-temperature combination, the acceptance of the null hypothesis verified that each button style is able to perform similarly to brass studs. Tests were performed with increasing confidence levels until full acceptance could be achieved, if possible. In addition to the previously presented 95% confidence level, tests were performed using confidence levels of 98%, 99%, and 99.9%. Table 36 below summarizes the results for 99.9% confidence levels for testing the mean, which still did not yield full acceptance. There are no values for a higher confidence level, therefore the values in Table *42* are to be considered the final values for the mean testing. The hypothesis test for variance yielded full acceptance at a 98% confidence level.

Table 42: F-statistic for Full Acceptance at 99.9% Confidence

F Table 99.9%
F(a/2,nx-1,ny-1) = F(a/2,ny-1,nx-1)
999.0000

Table 43: Results for Full Acceptance of Hypothesis Tests on the Mean and Variance of |E*| Data at $14°F$

		Mean Test at 99.9% Confidence			Variance Test at 98% Confidence		
Frequency Hz	**Temp ºF**	**H:σ^2x = σ^2y1**	**H:σ^2x = σ^2y2**	**H:σ^2x = σ^2y3**	**H:σ^2x = σ^2y1**	**H:σ^2x = σ^2y2**	**H:σ^2x = σ^2y3**
25	14 ºF	Accept	Accept	Accept	Accept	Accept	Accept
10	14 ºF	Accept	Accept	Accept	Accept	Accept	Accept
5	14 ºF	Accept	Accept	Accept	Accept	Accept	Accept
1	14 ºF	Accept	Accept	Accept	Accept	Accept	Accept
0.5	14 ºF	Accept	Accept	Accept	Accept	Accept	Accept
0.1	14 ºF	Accept	Accept	Accept	Accept	Accept	Accept

The values for |E*| were fully accepted by the null hypothesis for the mean at a 99.9% confidence level. The variance values fully accepted the null hypothesis at a 98% confidence level. Full acceptance of the null hypothesis verifies that each button style is able to perform similarly to brass studs.

5.2 Repeated Load Permanent Deformation

The process for hypothesis testing for the results of the Repeated Load Permanent Deformation tests is identical to that of Dynamic modulus. See Table *29 – 30* for the rejection criteria of the null hypothesis. Equations (72) – (78) were used for the determination of all parameters used for statistical analysis. The parameters tested from results of the Repeated Load Permanent Deformation tests were; flow number (Cycles), resilient Modulus (psi), axial permanent Strain at failure (%), axial resilient strain at

failure (%), and strain ratio (%). The following tables show the results of the hypothesis tests.

5.2.1 ANOVA for Flow Number

The results for ANOVA analysis performed on Flow Number results can be seen in Table *44*. The results show no significant difference in the performance of the mounting studs for each parameter tested.

Table 44. ANOVA Results for Flow Number

ANOVA for Flow Number				
Parameters				
Flow Number (Cycles)	Resilient Modulus at Failure (psi)	Axial Permanent Strain at Failure εp (%)	Axial Resilient Strain at Failure εr (%)	εp/εr (%)
NS	NS	NS	NS	NS

NS= Not Significant S= Significant

5.2.2 Mean

Table *45 - 46* summarize the results of the average values, variances, and test statistic values of all test parameters for the Repeated Load Permanent Deformation tests.

Table 45: Sample of Average Values for Hypothesis Testing on Flow Number Parameters

Parameter	**ACTUATOR**	**PLA**	**ABS**	**PC**
Flow Number (Cycles)	1340	1247	1426	1463
Resilient Modulus at Failure (psi)	104766	131288	144402	96760
Axial Permanent Strain at Failure εp (%)	1.2670	1.2297	1.2793	1.3487
Axial Resilient Strain at Failure εr (%)	0.0377	0.0360	0.0357	0.0443
εp/εr (%)	34.5617	33.9441	42.2885	30.9381

Table 46: Sample of Calculated Variance Values for Hypothesis Testing on Flow Number Parameters

Parameter	**ACTUATOR**	**PLA**	**ABS**	**PC**
Flow Number (Cycles)	44309	35008	31637	53056
Resilient Modulus at Failure (psi)	488313305	606556252	7030281592	188990182
Axial Permanent Strain at Failure εp (%)	0.0153	0.1050	0.0036	0.0026
Axial Resilient Strain at Failure εr (%)	0.00004	0.00005	0.00025	0.00004
εp/εr (%)	76.3788	16.4765	474.6960	26.9966

Table 47: Sample of Calculated Test Statistics and Degree of Freedom for Flow Number Parameters

Parameter	**t'1**	**t'2**	**t'3**	**Dof1**	**Dof2**	**Dof3**
Flow Number (Cycles)	0.5740	0.5363	0.6809	5.8915	5.7833	5.9360
Resilient Modulus at Failure (psi)	1.3883	0.7917	0.5328	5.9078	2.5530	4.6929
Axial Permanent Strain at Failure εp (%)	0.1864	0.1555	1.0586	3.1377	3.8020	3.3263
Axial Resilient Strain at Failure εr (%)	0.3143	0.2032	1.2856	5.8498	3.1200	5.9221
εp/εr (%)	0.1110	0.5701	0.6173	3.6490	3.2547	4.5136

To evaluate the tabulated value in which to compare the test statistic, $t_{0.025,\nu}$, must be used to locate the value in a standard table of values. For the hypothesis test on the mean, the degree of freedom was calculated and corresponds to varying values for each test. The tabulated solutions from the T-table that were used to compare the test statistic are summarized in Table *48*. The results of the hypothesis test for Flow Number parameters are summarized in Table *49*. Full acceptance of the null hypothesis verifies that each button style is able to perform similarly to brass studs.

Table 48: Tabulated T-table Values for α = 0.05 Used for Flow Number Parameters

Parameter	t'1	t'2	t'3
Flow Number (Cycles)	3.1671	3.1911	3.1572
Resilient Modulus at Failure (psi)	3.1635	5.6245	3.4823
Axial Permanent Strain at Failure εp (%)	4.4317	3.9042	4.2819
Axial Resilient Strain at Failure εr (%)	3.1764	4.4457	3.1603
εp/εr (%)	4.0257	4.3388	3.5508

Table 49: Results of Hypothesis Tests for the Mean of Flow Number Parameters.

Parameter	H:μx1 = μy1	H:μx2 = μy2	H:μx3 = μy3
Flow Number (Cycles)	Accept	Accept	Accept
Resilient Modulus at Failure (psi)	Accept	Accept	Accept
Axial Permanent Strain at Failure εp (%)	Accept	Accept	Accept
Axial Resilient Strain at Failure εr (%)	Accept	Accept	Accept
εp/εr (%)	Accept	Accept	Accept

5.2.3 Variance

Table *50* summarizes the calculated values for the F-test statistic for all tested parameters. Complete tabular results for hypothesis tests can be found in Appendix D.

Table 50: Sample of Calculated F-statistics for Hypothesis Testing on Flow Number Parameters

Parameter	F1	F2	F3
Flow Number (Cycles)	1.2657	1.4005	0.8351
Resilient Modulus at Failure (psi)	0.8051	0.0695	2.5838
Axial Permanent Strain at Failure εp (%)	0.1452	4.2015	5.8613
Axial Resilient Strain at Failure εr (%)	0.75694	0.14286	0.81955
εp/εr (%)	4.6356	0.1609	2.8292

Since the degree of freedom is the same for each treatment the tabular value corresponding to each frequency and temperature is the same value for each scenario tested. Table *51* summarizes the values identified for each scenario. The results for the hypothesis test, at 95% confidence for all parameters, is summarized in Table *52*.

Table 51: Tabular Value for the F-test on Flow Number Parameters

F Table |E*|
F(a/2,nx-1,ny-1) = F(a/2,ny-1,nx-1)
39.0000

Table 52: Results of Hypothesis Testing on Variance for Flow Number Parameters

Parameter	**H:σ^2x = σ^2y1**	**H:σ^2x = σ^2y2**	**H:σ^2x = σ^2y3**
Flow Number (Cycles)	Accept	Accept	Accept
Resilient Modulus at Failure (psi)	Accept	Accept	Accept
Axial Permanent Strain at Failure εp (%)	Accept	Accept	Accept
Axial Resilient Strain at Failure εr (%)	Accept	Accept	Accept
εp/εr (%)	Accept	Accept	Accept

Table 53: Results for Full Acceptance of Hypothesis Tests on the Mean and Variance of Flow Number Parameters

Parameter	Mean Test at 95% Confidence			Variance Test at 95% Confidence		
	H:μx1 = μy1	H:μx2 = μy2	H:μx3 = μy3	H:σ^2x = σ^2y1	H:σ^2x = σ^2y2	H:σ^2x = σ^2y3
Flow Number (Cycles)	Accept	Accept	Accept	Accept	Accept	Accept
Resilient Modulus at Failure (psi)	Accept	Accept	Accept	Accept	Accept	Accept
Axial Permanent Strain at Failure εp (%)	Accept	Accept	Accept	Accept	Accept	Accept
Axial Resilient Strain at Failure εr (%)	Accept	Accept	Accept	Accept	Accept	Accept
εp/εr (%)	Accept	Accept	Accept	Accept	Accept	Accept

As seen in Table *53* all parameters accepted the null hypothesis at a 95% confidence level. The results confirm that there is no statistical difference in the mean and variance values for all parameters tested. The conclusion is that high strain has no noticeable effect on the performance of any of the three thermoplastic studs. In terms of Flow Number, all stud types would perform similarly to the brass studs.

5.3 Axial Cyclic Fatigue

The ANOVA results for Axial Cyclic Fatigue is summarized in Table *54*. The results show no significant difference in the various treatments for each parameter tested.

Table 54. ANOVA Results for Axial Cyclic Fatigue

ANOVA for Axial Cyclic Fatigue						
Parameters						
Strain @ 10000	Strain @ 100000	Strain @ 1000000	Nf @ 100 με (100th Cycle)	Nf @ 200 με (100th Cycle)	Nf @ 300 με (100th Cycle)	Slope
NS	NS	NS	NS	NS	NS	NS

NS= Not Significant S= Significant

For hypothesis testing on fatigue model results a damage curve and failure curve were developed for each LVDT, for three samples per stud type. The mean and variances of several parameters were tested. The results do not show a clear pattern and can be considered inconclusive. Figure *36* shows a plot of the failure curves developed for each LVDT. Table *55* shows the results for each parameter tested. From hypothesis results it is difficult to isolate the variability of the performance of the mounting studs from other sources of variability inherent to asphalt concrete mixes and testing procedures.

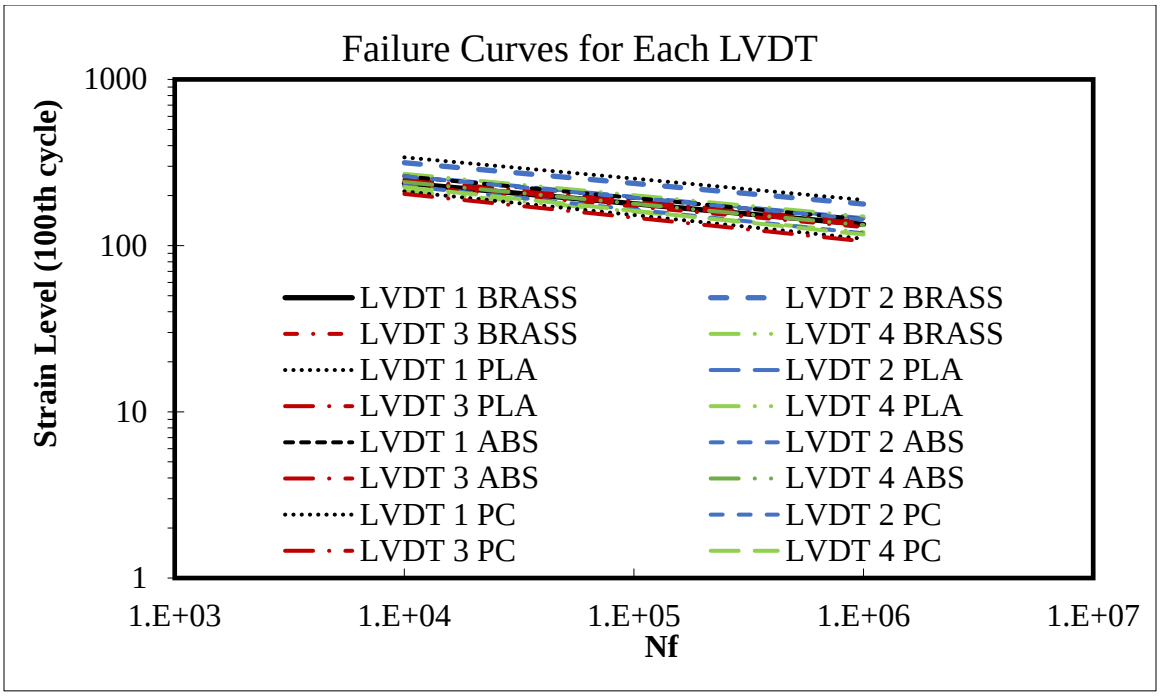

Figure 36. Failure Curves for Each LVDT

Table 55. Hypothesis Results for Axial Cyclic Fatigue

PARAMETERS	Mean	alpha =	0.01	Variance	alpha =	0.02
	H:μx1 = μy1	H:μx2 = μy2	H:μx3 = μy3	H:σ^2x = σ^2y1	H:σ^2x = σ^2y2	H:σ^2x = σ^2y3
Strain @ 10000	Accept	Accept	Reject	Accept	Accept	Accept
Strain @ 100000	Accept	Accept	Reject	Accept	Accept	Accept
Strain @ 1000000	Accept	Accept	Reject	Accept	Accept	Accept
Nf @ 100 με (100th Cycle)	Accept	Accept	Accept	Reject	Reject	Reject
Nf @ 200 με (100th Cycle)	Accept	Accept	Accept	Accept	Reject	Reject
Nf @ 300 με (100th Cycle)	Accept	Accept	Accept	Accept	Reject	Reject
Slope	Accept	Accept	Accept	Accept	Accept	Accept

6. DISCUSSION

6.1 Conclusion

From the results of hypothesis testing on the mean and variance of normally distributed |E*| data there is not a clear trend that can be identified. At a 95% confidence level all treatments were fully accepted at extreme temperatures but did not accept the hypothesis for mid-range temperatures. All treatments were fully rejected for all frequencies at $40°F$. Treatment 1 (PLA) and treatment 2 (ABS) only rejected at $40°F$ while treatment 3 (PC) rejected at $40°F$, $100°F$, and for three frequencies (25Hz, 10Hz, and 5Hz) at $70°F$. The variance, (σ^2) at $\alpha = 0.05$, only rejected treatment 3 (PC) at 5Hz at $14°F$, otherwise all other tests accepted the hypothesis.

For full acceptance of the null hypothesis for |E*| data, for the mean (μ), analysis was unable to identify a sufficient confidence. The variance (σ^2) fully accepted the null hypothesis at $\alpha = 0.002$ confidence level.

For analysis of Log |E*|, the mean (μ) at $\alpha = 0.05$, produced variable results and yielded no identifiable pattern. Treatment 3 (PC) produced the most rejection of the hypothesis which suggests the effect of temperature is strongest with this stud type. The variance (σ^2) at $\alpha = 0.05$ yielded full acceptance. For the hypothesis tests on Log Reduced Time (s), the mean (μ) $at\ \alpha = 0.05$, yielded full acceptance. Similar to hypothesis tests on Log |E*|, the variance (σ^2) at $\alpha = 0.05$, yielded full acceptance.

When considering testing under a wide range of temperatures, one can conclude from the results of the Dynamic Modulus tests performed that temperature could have a possible effect on the performance of thermoplastic mounting studs. However, more

considerations than measured performance must be taken into account. Variable results suggest possible errors could have occurred. Limitations with instrumentation and LVDT availability forced tests to be performed on each stud type one by one. Removal of the samples from the chamber to re-instrument could have affected sample placement on loading platens and produce variation in results. Operator errors are likely to have occurred as a result of the learning process of performing laboratory tests. Bonding errors between the glue and the thermoplastic studs could have added to variation in results. The use of fine threaded screws to affix instrumentation can cause stripping of stud threads if overtightened. Repeated testing of the same sample for dynamic modulus could have led to rejection of the null hypothesis for PC studs as they were the last stud type to be tested. It is suggested to perform more Dynamic Modulus tests on a variety of asphalt mixes performed by several operators to provide a more comprehensive study for the performance of thermoplastic studs.

When considering high strain scenarios, measured from Repeated Load Permanent Deformation tests, all thermoplastic studs performed as good as the brass studs. Average data from all three replicates produced very similar flow numbers. Statistical analysis on all parameters tested showed there was no significant difference in the mean and variance values measured for brass and thermoplastic studs. The results are a good indicator that thermoplastic mounting studs can be a suitable replacement for brass studs. Regardless of the results, it is suggested to perform more extensive testing using several different asphalt mixes by several different operators to provide more definitive results.

When considering the effect of high tensile and compressive stress measured from the Direct Tension Cyclic Fatigue test, the modeling process produced failure curves that did not facilitate statistical analysis. Any variation in the failure curves must be taken as variation in the results; However, additional research concentrating on isolation of variables to the mounting studs would provide a clearer understanding of material performance. Figure *34* shows the average micro-strain levels recorded for each material and is a decent indicator of variation in the results. It was observed that the failure curve for the ABS studs was almost identical to the failure curve for brass studs, indicating no discernable difference in the performance of the ABS studs under high stress. The failure curve for PC studs varied slightly from the failure curve for brass studs, especially at low values of load repetitions to failure. It is unclear if the amount of variation between brass and PC studs is significant enough to reject PC as a viable replacement stud. The highest variation observed was for PLA studs. The high variation suggests that PLA is not a god choice for stud fabrication when performing high stress testing.

Taking all tests and statistical analysis into consideration, the concept of using 3D printed thermoplastic for mounting stud fabrication is a promising option; although, the concept should be verified with more extensive research using a variety of asphalt mixes and performed by several operators to ensure no bias in the repeatability and reproducibility of test results.

Several aspects of material behavior were also taken into consideration when making a recommendation for replacement studs. During the printing process the bonding between layers is important for integrity of the final stud. If layers split, test results are

invalid. It was found that PC had a stronger layer bonding than ABS and PLA while printing. PC also has a higher glass transition temperature than both ABS and PLA, and can easily withstand all testing temperatures for SPT. The likelihood of stripping threads due to overtightening is reduced when using PC studs. Of the three thermoplastics tested. Polycarbonate (PC) was found to be the optimal material to utilize for mounting stud fabrication. The price of PC material, is approximately \$40.00/kg ($\approx \$0.04/stud$), which is double the cost of PLA or ABS, however, the benefits of the stronger material for SPT justify the additional cost. Regardless of the choice of thermoplastic, the option of using 3D printed studs greatly reduced the cost when compared to the \$2.00/Stud for brass.

Considering the variable nature of asphalt concrete and the results obtained from each test, it is apparent that variability exists between replicates using the same stud type. With a certain amount of expected variability using the same stud type, the variability of the results of comparison between stud type do not show an extreme difference in the performance of each thermoplastic stud. To further isolate the performance of mounting stud material it is recommended to eliminate as much variability as possible. Therefore, it is recommended to repeat each test, with each stud type, using a homogenous material such as a plexiglass or metal. Using a homogenous material to perform testing will provide data that does not consider the variability of the asphalt mix and will provide a more accurate representation of mounting stud performance.

For sustainability consideration, recycling the thermoplastic to form new filament is the most practical approach. After research into the effect of solvent used to clean brass studs (Acetone) on thermoplastic studs, it was found that the solvent affected all

thermoplastic studs to a degree that they are unsalvageable. However, opting to not use solvent for cleaning, one can easily remove, shred, and wash the thermoplastics, creating an ideal raw material to create filament which can be 3D printed into new mounting studs. The equipment necessary to complete the task is inexpensive and readily available.

6.2 Additional 3D Printing Applications

The above work only addressed one possible benefit of using 3D printing technology for asphalt research in a laboratory setting. In addition to the creation of mounting studs, this section demonstrates the use of other 3D printed objects for the research work in the laboratory. Several jigs and fixtures were fabricated to ease the burden of specimen preparation and/or various laboratory tests. For example, disks were created to measure ideal end sawing locations for cored gyratory samples. Figure *37* shows the measuring disks. The numbers incorporated into the design describe the height in millimeters for each disk. The use of these jigs minimizes human errors and saves time when measuring cored samples for end sawing. The following figures illustrate several items made to assist in laboratory testing at Arizona State University's Advanced Pavement Laboratory.

Figure 37: End Sawing Jigs for Cored Gyratory Samples

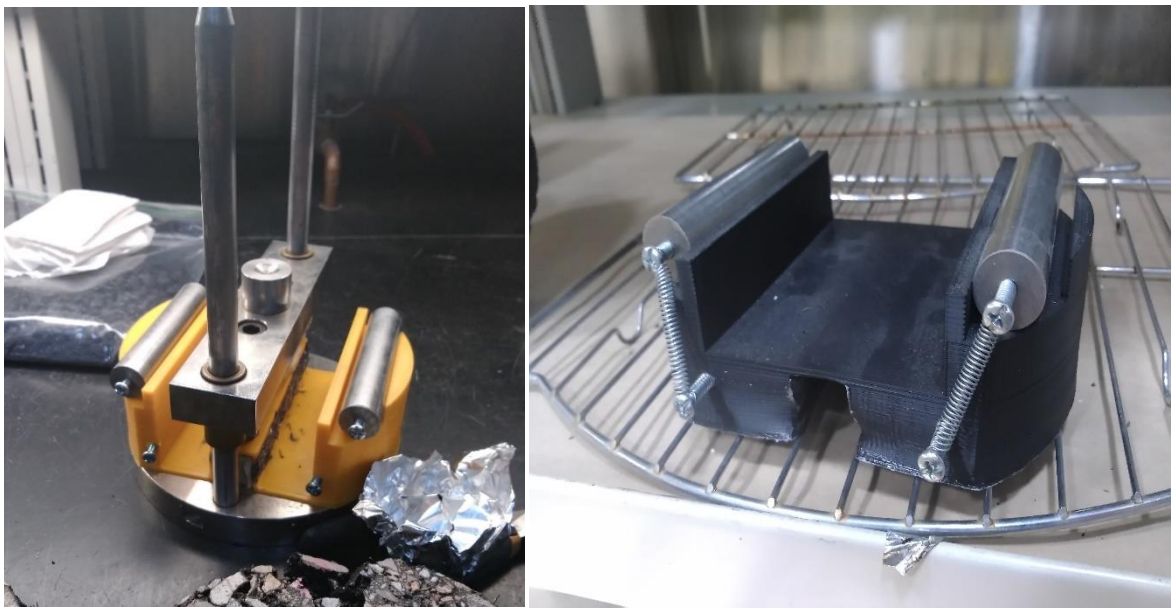

Figure 38. Semi-Circular Bending Device

Figure 39: Cutting Template for SCB Samples

Figure 40: Fiber Pull-out Testing Apparatus

Figure 41: Cutting Template for the Hamburg Wheel Test Samples

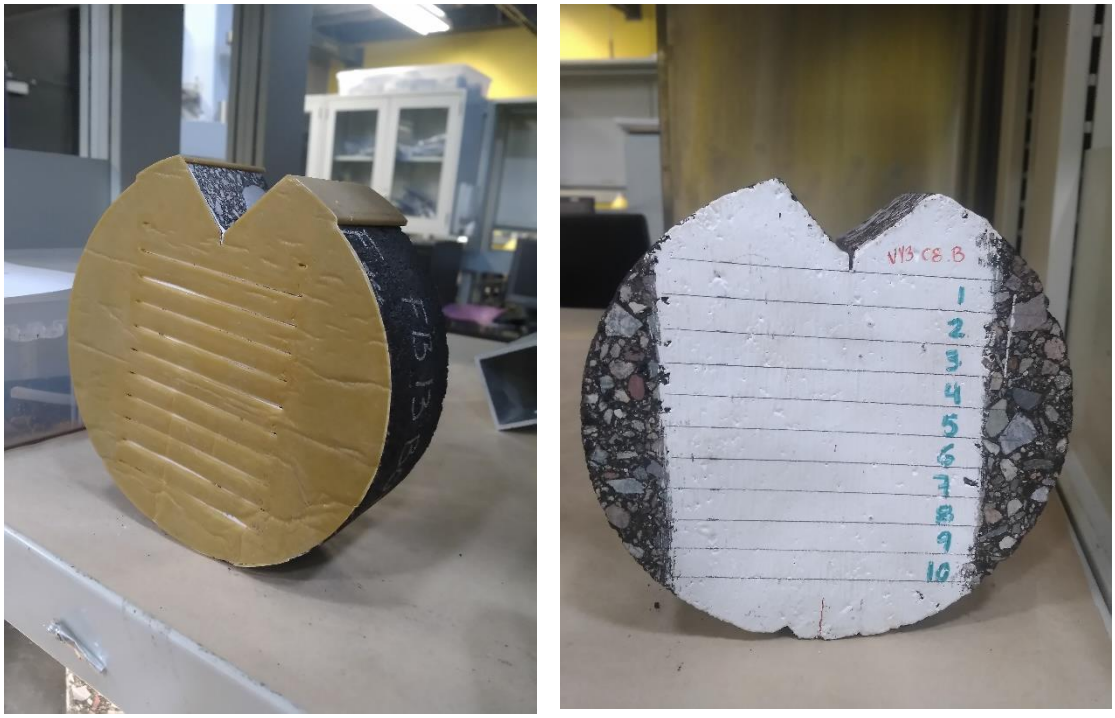

Figure 42: Marking Template for the C* Line Integral Test

Figure 43: Cell Phone Mount for IRI Measurements

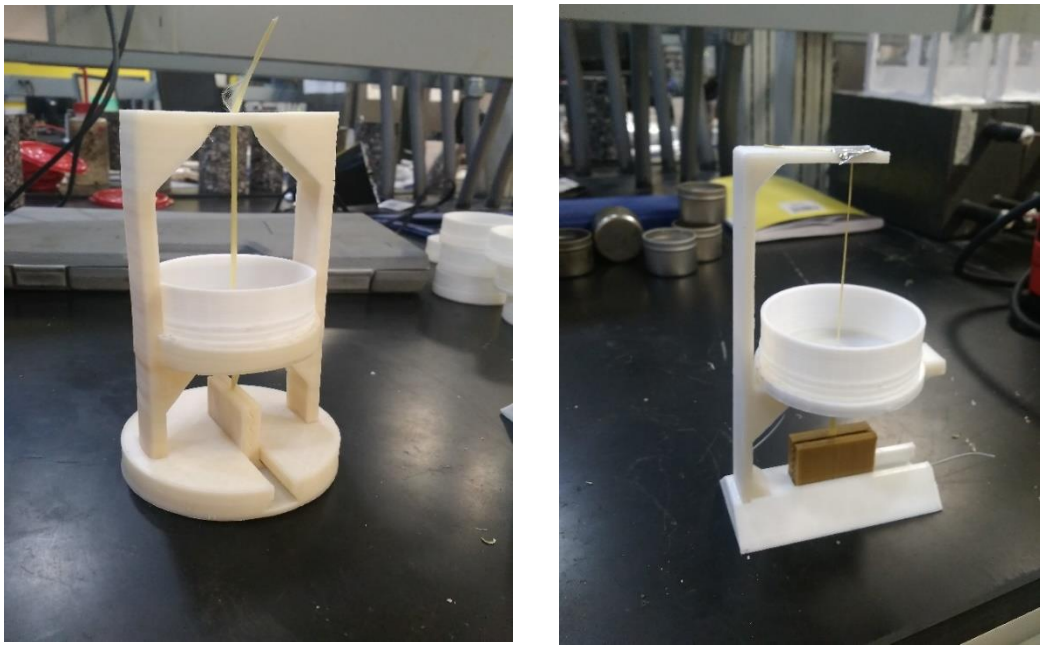

Figure 44: Fiber Alignment Apparatus Designs

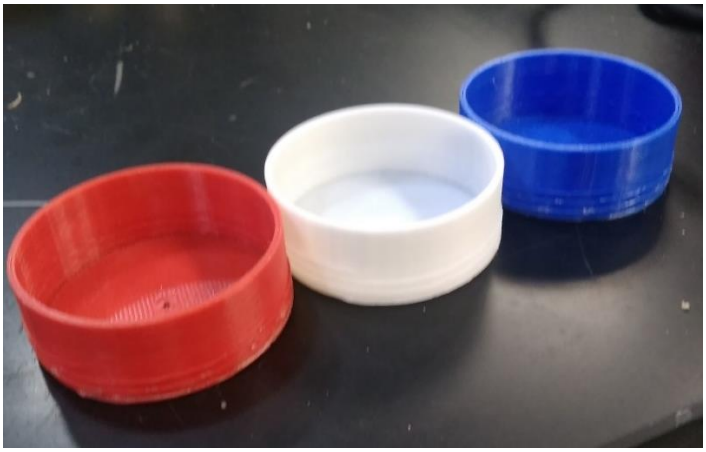

Figure 45: Binder Cups for Fiber Pull-out Test

Figure 46: Binder Cup Mount and Load Cell Spacer for Fiber Pull-out Test

Figure 47. Confinement Device for Circular Test Samples

REFERENCES

[1] R. J. Cominsky, "The Superpave Mix Design Manual for New Construction and Overlays," Strategic Highway Research Program National Research Council, Washington DC, 1994.

[2] WesTrack Forensic Team Consensus Report, "Superpave Mixture Design Guide," Federal Highway Administration, Wahington DC, 2001.

[3] K. E. Kaloush, "Simple Perofrmance Test for Permanent Deformation of Asphalt Mixtures," Arizona State University, Tempe, 2001.

[4] Witczak, M., Kaloush, K., Pellinen, T., El-Bayouny, M., and Von Quintas, H, "Simple Performance Test for Superpave Mix Design," NCHRP 465, 105 pages, Transportation Research Board, National Research Council, National Academy Press, Washington, D.C., 2002.

[5] Kaloush, K., Mirza, M.W., Uzan, J. and Witczak, M.W., "Specimen Instrumentation Techniques for Permanent Deformation Testing of Asphalt Mixtures," *Journal of Testing and Evaluation, ASTM,* vol. 29, no. No. 5, pp. 423-431, September 2001.

[6] Roque, R., R.L. Lytton, J. Uzan, E.G. Fernando, D. Hiltunen, and S.M. Stoffels. "Development and Validation of Performance Prediction Models and Specifications for Asphalt Binders and Paving Mixes," Strategic Highway Research Program, National Research Council, Washington DC, 1976.

[7] Witczak, M. W., and Kaloush, K., "Performance Evaluation of Asphalt Modified Mixtures Using Superpave and P-401 Mix Gradings" Maryland Port Administration, Baltimore, Maryland, March 1998.

[8] B. R. Elizabeth Matias, "3D Printing: On Its Historical Evolution and the Implications for Business," in *Management of the Technology Age*, New York, 2015.

[9] American Standards of Testing and Measurements ASTM, "Standard Test Methods for Dynamic Modulus of Asphalt Mixtures," ASTM International, West Conshohocken, PA, 2003.

[10] American Association of State Highway and Transportation Officials, "Determining the Dynamic Modulus of Hot Mix Asphalt (HMA)," American Association of State Highway and Transportation Officials, Washington DC, 2003.

[11] American Association of State Highway and Transportation Officials, "Standard Method of Test for Determining Dynamic Modulus and Flow Number for Asphalt Mixtures Using the Asphalt Mixture Performance Tester (AMPT)," American Association of State Highway and Transportation Officials, Washington DC, 2013.

[12] M. C. Rodezno, "Rutting Criteria for Asphalt Mixtures Based on Flow Number Analysis," Arizona State University, Tempe, AZ, 2010.

[13] B. Shane Underwood, "Manual of Practice for S-VECD Test and Analysis," 2010.

[14] American Association of State Highway and Transportation Officials, "Standard Method of Test for Determining the Damage Characteristic Curve of Asphalt Mixtures from Direct Tension Cyclic Fatigue Tests," American Association of State Highway and Transportation Officials, Washington DC, 2016.

[15] American Association of State Highway and Transportation Officials, "Standard Method of Test for Determining Dynamic Modulus of Hot Mix Asphalt (HMA)," American Association of State Highway and Transportation Officials, Washington D, 2011.

[16] Lieberman, A.H Bowker and G.J G. Lieberman, "Engineering Statistics," February 1963.

[17] "MakeItFrom.com," 2009-2016. [Online]. Available: http://www.makeitfrom.com/material-group/Thermoplastic. [Accessed 12 6 2017].

APPENDIX A

MIX DESIGN & SAMPLE PREPARATION

SOUTHWEST Asphalt
A DIVISION OF FISHER SAND & GRAVEL CO.

MARSHALL MIX DESIGN - 75 BLOW

SUPPLIER: Southwest Asphalt - PLANT NO. 4
PROJECT: 2016 Annual Mix Design El Mirage
LOCATION: Various
MIX DESIGNATION: COP C- "J" Marshall Asphalt Concrete
LAB NO: 4453

DATE: 02/09/2016
PROJECT NO: N/A
SWA PROJECT NO: 16-207
AGENCY: COP
PLANT NO.: 4
COMMODITY CODE: 432CH & 432DH

COMPOSITE GRADATION

Material I.D.	Material Source			% Used
[illegible] Sand	SR Tanner El Mirage Pit	1653	21	53.0
[illegible] Fines	SR Tanner El Mirage Pit	553	[illegible]	13.0
3/8 Inch Agg	SR Tanner El Mirage Pit	503	9	10.0
3/4 Inch Agg	SR Tanner El Mirage Pit	2022	31	40.0
Hydrated Lime	United North America	50	1	1.0

Sieve US/mm	w/o Admix % Passing	w/Admix % Passing	City of Phoenix Mix Design Target	Production Limits
1"/37.5	100	100		
1"/25	100	100	100	
3/4"/19	100	100	95	88 - 100
1/2"/12.5	89	89	85	78 - 92
3/8"/9.5	71	72	75	68 - 82
#4/4.75	59	59		
#8/2.36	55	56	50	51 - 65
#10/2.00	43	43	44	39 - 49
#16/1.18	31	32		
#30/.600	21	21	24	19 - 29
#40/.425	15	15		
#50/.300	10	11		
#100/.150	5	6		
#200/.075	3.7	4.8	4.0	2.0 - 6.0

ADDITIONAL DATA

Asphalt Binder Source	Western
Asphalt Binder Grade	PG 70-10
Asphalt Binder Specific Gravity	1.015
Mineral Admix Type	Hydrated Lime
Mineral Admix Specific Gravity	2.20
Recommended Lab Mixing Temperature	317°F to 328°F
Recommended Lab Compaction Temperature	297°F to 305°F
Actual Lab Mixing Temperature Used	322.5°F
Actual Lab Compaction Temperature Used	301°F

DESIGN DATA

	432CH	&	432DH
Traffic Loading	Heavy		Low
Total Binder Content (%)	5.0		5.5
Marshall Bulk Density (pcf)	144.4		147.3
Max Theoretical Specific Gravity	2.451		2.433
Max Theoretical Specific Density (pcf)	152.9		151.8
Stability	5,220		5,340
Marshall Flow (in.)	11		12
% Air Voids	4.2		3.9
% VMA	14.2		14.1
% Air Voids Filled	69.9		78.9
% Eff Asphalt Total Mix	4.29		4.79
Film Thickness (µ)	9		10
Dust/Bitumen Ratio	1.1		1.0

AGGREGATE PROPERTIES

Aggregate Property	Coarse Aggr.	Fine Aggr.	Comb. w/o Admix	Comb w/ Admix	Spec.
Bulk OD Specific Gravity	2.598	2.599	2.600	2.598	2.35-2.9
SSD Specific Gravity	2.650	2.634	2.642	2.636	
Apparent Specific Gravity	2.724	2.695	2.709	2.702	
Absorption (%)	1.832	1.376	1.505	1.485	0.00-2.5
Effective Specific Gravity (Gse)				2.649	
Sand Equivalent		62			55 Min
Plasticity Index		NP			NP
% 1 or More Fractured Face	99				92 Min
% 2 or More Fractured Face	96				85 Min
Uncompacted Voids		46.2			45 Min
Los Angeles Abrasion					
% Loss @ 100 Rev - Grading B	4				9 Max
% Loss @ 500 Rev - Grading B	19				40 Max
% Flat & Elongated (5:1 Ratio)	1.9				10 Max
% Soundness Loss (NaSO4)	2				
% Claylumps & Friable Particles	0.3	0.5			

Figure 48: High Volume City of Phoenix Mix Design

Table 56: Maximum Theoretical Specific Gravity (Gmm) for Mix Design

	Virgin Mix	
Trial 1	**Gmm**	**2.515848**
	Weight Sample (A)	1500.2
	Weight container+Water (B)	7584.5
	Weight Sample + Water ©	8488.4
Trial 2	**Gmm**	**2.513572**
	Weight Sample (A)	1500.1
	Weight container+Water (B)	7581.8
	Weight Sample + Water ©	8485.1
Trial 3	**Gmm**	**2.534628**
	Weight Sample (A)	1500.5
	Weight container+Water (B)	7584.1
	Weight Sample + Water ©	8492.6
	Average Gmm	**2.521349**

Table 57: Aggregate Specific Gravity

Material	3/4"	3/8"	CF	BS	CA	FA	Comb	Admix	Comb. Agg
% used	38	12	16.8	33.2	50	50	Aggr.	1.1	w/Admix
Bulk OD (Gsb)	2.659	2.620	2.645	2.610	2.650	2.622	2.636	2.2	2.630
SSD (Gssdb)	2.689	2.661	2.677	2.648	2.682	2.658	2.670	2.2	2.664
Apparent (Gsa)	2.741	2.733	2.732	2.714	2.739	2.720	2.730	2.2	2.722
Absorption (%)	1.13	1.57	1.19	1.46	1.211	1.357	1.280	0.9	1.274

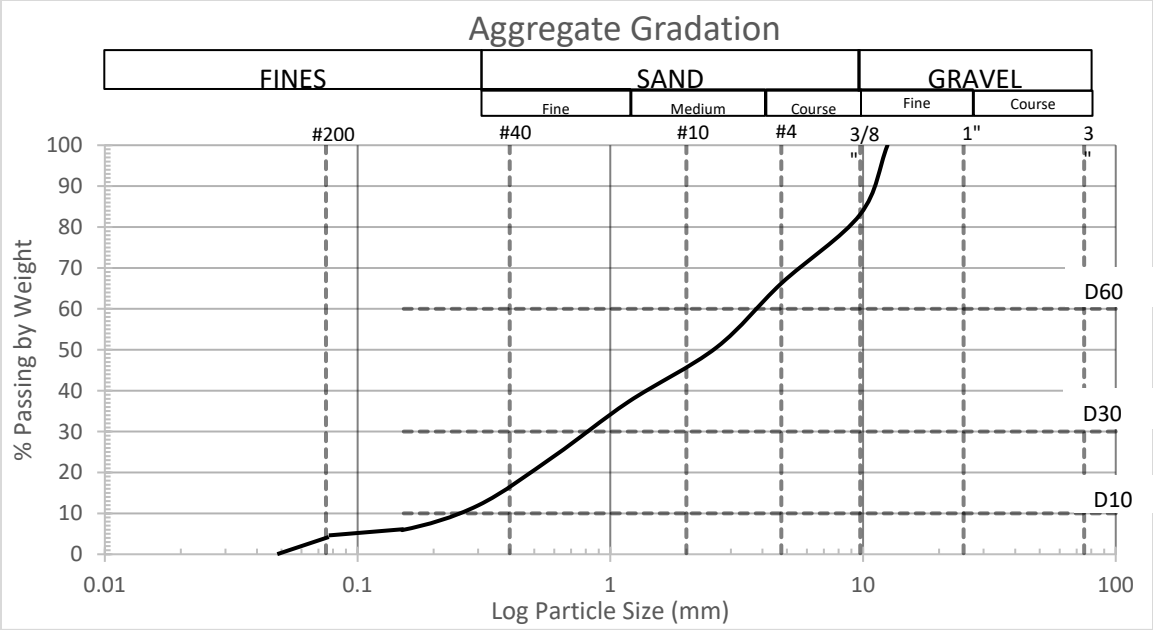

Figure 49: Aggregate Gradation Chart

Table 58: Volumetric Calculations

Sample	Pb	Mass	Heights at different N			Volume at different heights			Gmb (estimated)		
			N ini	N des	N max	N ini	N des	N max	ini	Des	max
4.5%, Control	4.5	4691.0	123.90	115.53	114.40	2189.5	2041.6	2021.6	2.143	2.298	2.320
4.5%, Control	4.5	4694.0	124.88	115.55	114.30	2206.8	2041.9	2019.8	2.127	2.299	2.324
5%, control	5.0	4692.0	122.55	114.17	112.98	2165.6	2017.6	1996.5	2.167	2.326	2.350
5%, control	5.0	4691.0	122.24	113.83	112.64	2160.2	2011.5	1990.5	2.172	2.332	2.357
5.5%, control	5.5	4691.0	121.55	113.07	111.91	2148.0	1998.1	1977.6	2.184	2.348	2.372
5.5%, control	5.5	4691.0	120.74	112.44	111.26	2133.7	1987.0	1966.1	2.199	2.361	2.386

Table 59: Volumetric Calculations (Continued)

Gmb	Correction	Gmb corrected			Gmm	%Gmm			% Air voids	%VFA
(measured)	factor	N ini	N des	N max		N ini	N des	N max	@Ndes	
2.347	1.011	2.167	2.324	2.347	2.477	87.5	93.8	94.8	6.2	60.5
2.356	1.014	2.157	2.331	2.356	2.477	87.1	94.1	95.1	5.9	61.7
2.381	1.013	2.195	2.356	2.381	2.458	89.3	95.8	96.9	4.2	72.1
2.385	1.012	2.198	2.360	2.385	2.458	89.4	96.0	97.0	4.0	73.0
2.404	1.013	2.213	2.379	2.404	2.440	90.7	97.5	98.5	2.5	82.7
2.407	1.009	2.218	2.382	2.407	2.440	90.9	97.6	98.6	2.4	83.4

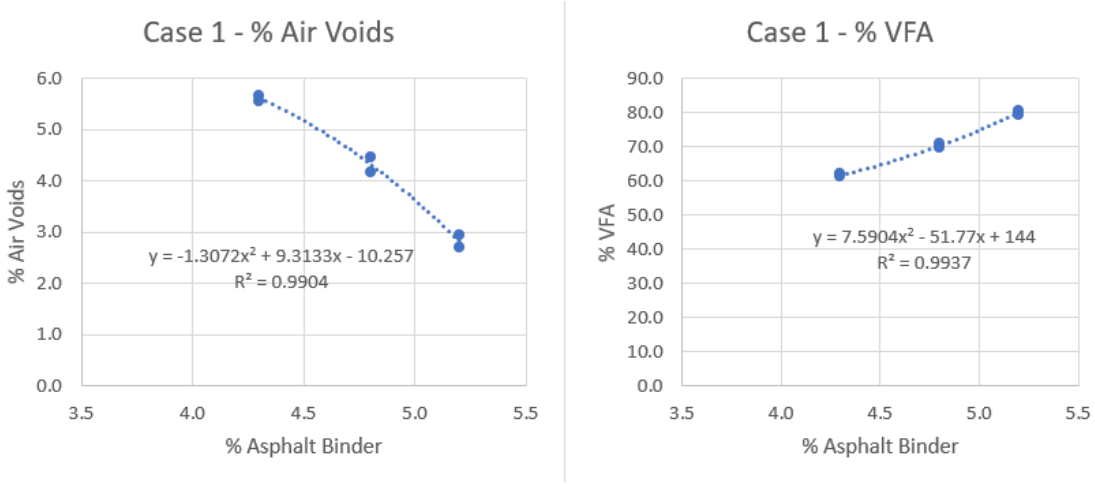

Figure 50: Case 1 Air Voids & VFA

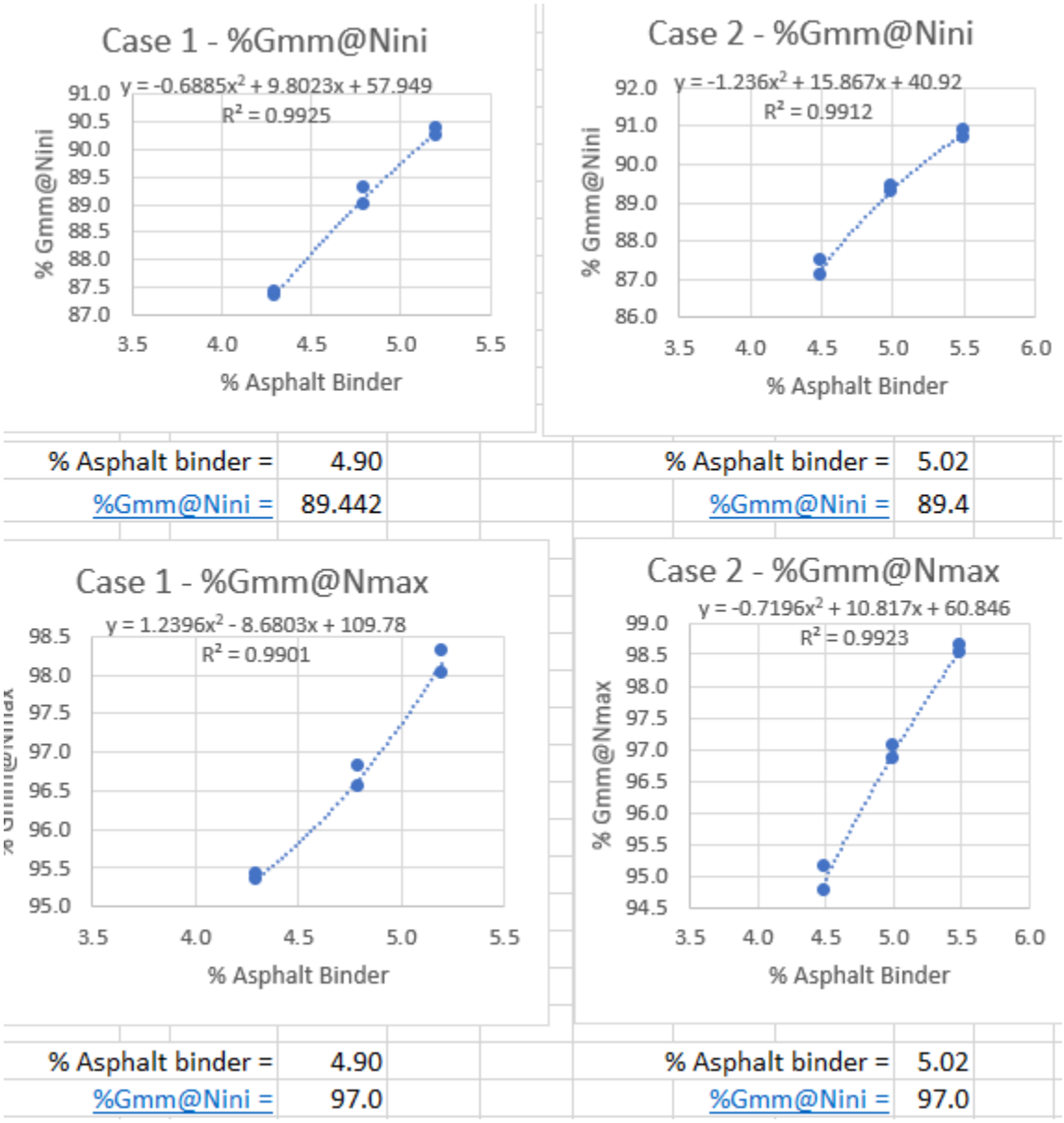

Figure 51: Case 1 & Case 2 Gmm

Table 60: Criteria for Trial 2

Mix Property	Criteria 3/4" Mix	**Trial 2**	Specifications
Asphalt Binder (%)		**5.02**	
Air Voids (%)	4.0+/-0.2	**4.00**	
VMA (%)	13 min.	**14.76**	Pass
VFA (%)	65 - 78	**72.59**	Pass
Absorbed Asphalt (%)	0 - 1.0	**0.38**	Pass
Dust Proportion	0.6 - 1.4	**1.03**	Pass
%Gmm@Nini = 7	less than 90.5	**89.4**	Pass
%Gmm@Nmax = 115	less than 98	**97.0**	Pass
Eff. Asphalt content (%)		**4.66**	
P0.075		**4.8**	

Table 61: Final Superpave Mix Design

			Required weight		7112	
Control Mix 0% RAP				Total mix weight		7300
Binder percentage		5.02		Binder weight		366.5
Aggregate %		94.98		Aggregate weight		6933.5
Sieves US	Cum % Passing	Cum % Retained	% retained	weight		
1"	100	0	0	0.0		
3/4"	100	0	0	0.0		
1/2"	86	14	14	970.7		
3/8"	72	28	14	970.7		
1/4"	59	41	13	901.4		
#4	56	44	3	208.0		
#8	43	57	13	901.4		
#16	32	68	11	762.7		
#30	21	79	11	762.7		
50	11	89	10	693.4		
100	6	94	5	346.7		
#200	4.8	95.2	1.2	83.2		
Pan			3.7	256.5		
Lime			1.1	76.3		
			100	6933.5		

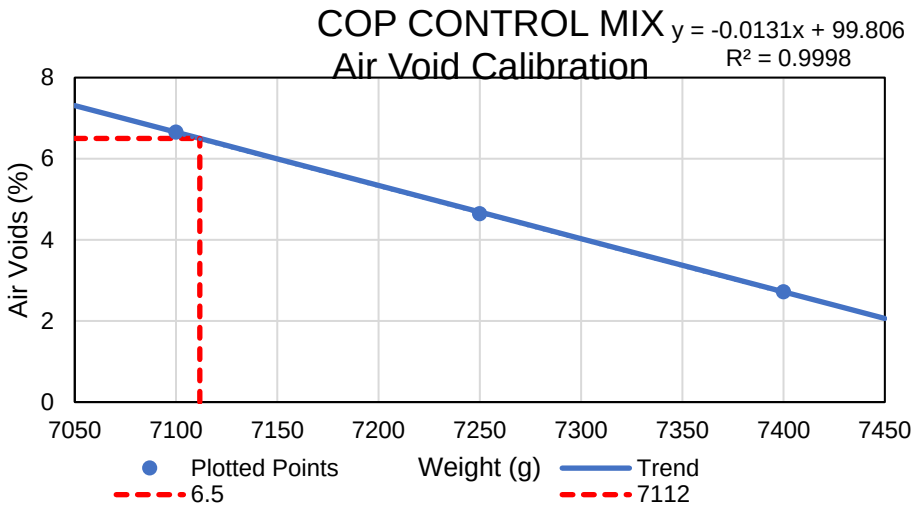

Figure 52: Air Void Calibration Chart

Sample Preparation

Table 62: Sample Properties for Stud Testing

Gmm	Set 1					
2.458	1	2	3	4	5	6
Wet weight (C)	1610	1634.6	1617.1	1614.7	1614	1628.3
SSD Weight (B)	2840	2871.1	2850.5	2842.3	2842.5	2865.5
Dry Weight [A]	2819.9	2851.3	2829.6	2832.2	2823.6	2844.5
Gmb	2.293	2.306	2.294	2.307	2.298	2.299
% Absorbed	1.634	1.601	1.695	0.823	1.538	1.697
% Air Voids	6.729	6.186	6.666	6.139	6.493	6.463
	Set 2					
	7	8	9	10	11	12
Wet weight (C)	1610.5	1632.6	1634.7	1635.8	1557	1623.4
SSD Weight (B)	2835.5	2868.8	2872.5	2879	2790.2	2867.4
Dry Weight [A]	2811	2848.7	2850	2851.1	2783.8	2840.1
Gmb	2.295	2.304	2.302	2.293	2.257	2.283
% Absorbed	2.000	1.626	1.818	2.244	0.519	2.195
% Air Voids	6.644	6.249	6.327	6.698	8.162	7.118
	Set 3					
	13	14	15	16	17	18
Wet weight (C)	1642.5	1659.1	1632.5	1617.1	1612.8	1595.2
SSD Weight (B)	2895.7	2907.4	2874.1	2850.7	2847.3	2831.3
Dry Weight [A]	2870.6	2869.7	2853.1	2828	2822.1	2805.8
Gmb	2.291	2.299	2.298	2.292	2.286	2.270
% Absorbed	2.003	3.020	1.691	1.840	2.041	2.063
% Air Voids	6.810	6.473	6.513	6.734	6.996	7.653

Table 63: Sample Properties for Stud Testing (Continued)

Gmm	Set 4						
2.458	**19**	**20**	**21**	**22**	**23**	**24**	
Wet weight (C)	1610	1634.6	1556.5	1512.9	1566	1647.3	
SSD Weight (B)	2840	2871.1	2778.8	2730.9	2786.8	2871.8	
Dry Weight [A]	2741.6	2797.8	2771.6	2721.6	2781.2	2869.3	
Gmb	2.229	2.263	2.268	2.234	2.278	2.343	
% Absorbed	8.000	5.928	0.589	0.764	0.459	0.204	
% Air Voids	9.319	7.946	7.749	9.093	7.316	4.669	
	Set 5						
	25	**26**	**27**	**28**	**29**	**30**	**31**
Wet weight (C)	1610	1634.6	1556.5	1512.9	1566	1647.3	885
SSD Weight (B)	2840	2871.1	2778.8	2730.9	2786.8	2871.8	1560.2
Dry Weight [A]	2741.6	2797.8	2771.6	2721.6	2781.2	2869.3	1544.7
Gmb	2.229	2.263	2.268	2.234	2.278	2.343	2.288
% Absorbed	8.000	5.928	0.589	0.764	0.459	0.204	2.296
% Air Voids	9.319	7.946	7.749	9.093	7.316	4.669	6.926

APPENDIX B

THERMOPLASTIC MATERIAL PROPERTIES

Material properties for all thermoplastics to be used can be found in Tables 1 through 3 [17]. The values presented are general properties for each material and are assumed to be consistent with the actual material utilized for production of buttons.

Table 64: Material Properties for PLA

PLA	
Density	1.3 g/cm3 (81 lb/ft3)
Elastic (Young's, Tensile) Modulus	3.5 GPa (0.51 x 106 psi)
Elongation at Break	6.0 %
Flexural Modulus	4.0 GPa (0.58 x 106 psi)
Flexural Strength	80 MPa (12 x 103 psi)
Glass Transition Temperature	60 °C (140 °F)
Heat Deflection Temperature At 455 kPa	(66 psi)65 °C (150 °F)
Melting Onset (Solidus)	160 °C (320 °F)
Shear Modulus	2.4 GPa (0.35 x 106 psi)
Specific Heat Capacity	1800 J/kg-K
Strength to Weight Ratio	38 kN-m/kg
Tensile Strength: Ultimate (UTS)	50 MPa (7.3 x 103 psi)
Thermal Conductivity	0.13 W/m-K
Thermal Diffusivity	0.056 m2/s

Table 65: Material Properties for ABS

ABS	
Density	1.0 to 1.4 g/cm3 (62 to 87 lb/ft3)
Dielectric Constant (Relative Permittivity) At 1 Hz	3.1 to 3.2
Dielectric Strength (Breakdown Potential)	15 to 16 kV/mm (0.59 to 0.63 V/mil)
Elastic (Young's, Tensile) Modulus	2.0 to 2.6 GPa (0.29 to 0.38 x 106 psi)
Elongation at Break	3.5 to 50 %
Flexural Modulus	2.1 to 7.6 GPa (0.3 to 1.1 x 106 psi)
Flexural Strength	72 to 97 MPa (10 to 14 x 103 psi)
Heat Deflection Temperature At 1.82 MPa (264 psi)	76 to 110 °C (170 to 230 °F)
Heat Deflection Temperature At 455 kPa (66 psi)	83 to 110 °C (180 to 230 °F)
Impact Strength: Notched Izod	70 to 370 J/m (1.3 to 6.9 ft-lb/in)
Rockwell R Hardness	100 to 110
Strength to Weight Ratio	37 to 79 kN-m/kg
Tensile Strength: Ultimate (UTS)	37 to 110 MPa (5.4 to 16 x 103 psi)
Thermal Expansion	81 to 95 µm/m-K

Table 66: Material Properties for PC

PC	
Density	1.2 to 1.4 g/cm3 (75 to 87 lb/ft3)
Elongation at Break	3.5 to 110 %
Flexural Modulus	2.3 to 10 GPa (0.33 to 1.5 x 106 psi)
Flexural Strength	92 to 160 MPa (13 to 23 x 103 psi)
Glass Transition Temperature	150 °C (300 °F)
Heat Deflection Temperature At 1.82 MPa (264 psi)	130 to 140 °C (270 to 280 °F)
Impact Strength: Notched Izod	140 to 440 J/m (2.6 to 8.2 ft-lb/in)
Specific Heat Capacity	1000 to 1200 J/kg-K
Strength to Weight Ratio	55 to 110 kN-m/kg
Tensile Strength: Ultimate (UTS)	66 to 160 MPa (9.6 to 23 x 103 psi)
Thermal Expansion	10 to 69 µm/m-K
Water Absorption at Saturation	0.16 to 0.19 %

APPENDIX C

RESULTS AND ANALYSIS DATA

Dynamic Modulus

Table 67: Master Curve Model Coefficients

Parameter	Starting Values	Final Values															
		Replicate 1				Replicate 2				Replicate 3				Average			
		Brass	PLA	ABS	PC	Brass	PLA	ABS	PC	Brass	PLA	ABS	PC	Brass	PLA	ABS	PC
δ	4.0702	-2.0345	1.8086	2.6954	3.4113	2.9286	3.1093	2.4247	2.3436	2.3379	-0.5080	-1.9252	1.7302	0.4954	0.0932	1.3922	2.4949
α	2.5636	8.9992	5.0551	4.2458	3.4638	3.9505	3.8528	4.4462	4.5387	4.4593	7.4775	9.0511	5.1785	6.4118	6.8474	5.5780	4.3924
β	-0.9307	-2.1469	-1.6612	-1.3451	-1.2990	-1.3000	-1.1773	-1.5754	-1.6253	-1.5814	-2.0000	-2.0658	-1.7500	-1.8366	-1.9172	-1.6752	-1.5768
γ	0.4992	0.2250	0.2952	0.3137	0.3686	0.3238	0.3648	0.3306	0.3235	0.3152	0.2396	0.2190	0.3101	0.2555	0.2597	0.2761	0.3304
α	0.0002	0.0000	0.0001	0.0000	0.0000	0.0000	0.0001	0.0004	0.0002	0.0002	0.0001	0.0002	0.0003	0.0001	0.0002	0.0002	0.0002
β	-0.1072	-0.0851	-0.1013	-0.0755	-0.0862	-0.0772	-0.0889	-0.1372	-0.1171	-0.1018	-0.1033	-0.1095	-0.1226	-0.0950	-0.1150	-0.1137	-0.1116
χ	6.5581	5.7633	6.4500	5.1989	5.8047	5.2672	5.5170	7.7785	7.0925	6.3354	6.5236	6.8639	7.2538	6.1095	6.9574	6.8852	6.8275

Table 68: Log Reduced Temperature

Temp., F		Log a(T)															
		Replicate 1				Replicate 2				Replicate 3				Average			
		Brass	PLA	ABS	PC	Brass	PLA	ABS	PC	Brass	PLA	ABS	PC	Brass	PLA	ABS	PC
T1	14	4.5793	5.0573	4.1449	4.6069	4.1918	4.3004	5.9309	5.4974	4.9412	5.1051	5.3627	5.5910	4.8007	5.3910	5.3366	5.3044
T2	40	2.4216	2.6066	2.2059	2.4309	2.2233	2.1908	2.8865	2.7689	2.5202	2.6212	2.7447	2.7838	2.4849	2.7136	2.6878	2.6844
T3	69.98	0.0000	0.0000	0.0000	0.0000	0.0000	0.0000	0.0000	0.0000	0.0000	0.0000	0.0000	0.0000	0.0000	0.0000	0.0000	0.0000
T4	100.04	-2.3568	-2.3779	-2.1797	-2.3533	-2.1793	-1.9367	-2.2231	-2.3705	-2.2352	-2.3671	-2.4572	-2.3039	-2.2921	-2.3189	-2.3008	-2.3294
T5	130	-4.6347	-4.5131	-4.3201	-4.6151	-4.3015	-3.6079	-3.7703	-4.3289	-4.1722	-4.4662	-4.6125	-4.1145	-4.3779	-4.2297	-4.2012	-4.2903

Table 69: Regression Model Coefficients

Regression Modeling Terms	
n	30
p	8
n-p	22
n-1	29

Table 70: Regression Coefficients for Log |E*|

Parameter	Replicate 1				Replicate 2				Replicate 3				Average			
	Brass	PLA	ABS	PC	Brass	PLA	ABS	PC	Brass	PLA	ABS	PC	Brass	PLA	ABS	PC
ΣSE	0.0514	0.0481	0.0563	0.0350	0.0576	0.0510	0.0289	0.0130	0.0189	0.0294	0.0287	0.0088	0.0308	0.0237	0.0149	0.0127
Se	0.0483	0.0468	0.0506	0.0399	0.0512	0.0482	0.0363	0.0243	0.0293	0.0365	0.0361	0.0200	0.0374	0.0328	0.0260	0.0240
Sy	0.6894	0.7017	0.6862	0.7053	0.6709	0.6833	0.6479	0.6899	0.6448	0.6714	0.7312	0.6777	0.6669	0.6836	0.6840	0.6899
Se/Sy	0.0701	0.0667	0.0737	0.0566	0.0763	0.0705	0.0560	0.0352	0.0454	0.0544	0.0494	0.0295	0.0561	0.0480	0.0380	0.0348
R2	0.9963	0.9966	0.9959	0.9976	0.9956	0.9962	0.9976	0.9991	0.9984	0.9978	0.9982	0.9993	0.9976	0.9983	0.9989	0.9991

Table 71: Regression Statistics for |E*|

Para meter	Replicate 1				Replicate 2				Replicate 3				Average			
	Brass	PLA	ABS	PC	Brass	PLA	ABS	PC	Brass	PLA	ABS	PC	Brass	PLA	ABS	PC
ΣSE	7.71E+11	7.93E+11	1.27E+12	6.93E+11	3.14E+12	2.10E+12	1.30E+12	2.06E+11	1.78E+11	9.05E+11	5.57E+11	2.47E+11	6.30E+11	2.92E+11	2.93E+11	2.12E+11
Se	1.87E+05	1.90E+05	2.41E+05	1.77E+05	3.78E+05	3.09E+05	2.43E+05	9.68E+04	9.00E+04	2.03E+05	1.59E+05	1.06E+05	1.69E+05	1.15E+05	1.15E+05	9.82E+04
Sy	1.65E+06	1.82E+06	1.93E+06	2.08E+06	1.82E+06	2.26E+06	2.22E+06	2.16E+06	1.62E+06	1.94E+06	2.49E+06	2.26E+06	1.69E+06	2.00E+06	2.21E+06	2.16E+06
Se/Sy	1.13E-01	1.05E-01	1.25E-01	8.55E-02	2.08E-01	1.37E-01	1.10E-01	4.47E-02	5.55E-02	1.04E-01	6.40E-02	4.70E-02	1.00E-01	5.75E-02	5.22E-02	4.54E-02
R2	9.90E-01	9.92E-01	9.88E-01	9.94E-01	9.67E-01	9.86E-01	9.91E-01	9.98E-01	9.98E-01	9.92E-01	9.97E-01	9.98E-01	9.92E-01	9.97E-01	9.98E-01	9.98E-01

Replicate 1 – CB1 Brass

Table 72: Master Curve Data for Replicate 1 with Brass Studs

METAL (Brass)													
Temp, °C	**Temp, °F**	**Frequency Hz**	**E* Mpa**	**E* ksi**	**E* psi**	**Log E* psi**	**Time, t s**	**Log Time s**	**Log Red Time, t_r**	**Pred Log E* psi**	**Pred E* psi**	**Error**	**Error^2**
-10.0	14 °F	25	33612	4875.00845	4.88E+06	6.6880	0.04	-1.397940009	-5.9773	6.6988	5.00E+06	-0.0108	0.0001
-10.0	14 °F	10	32343	4690.95556	4.69E+06	6.6713	0.1	-1	-5.5793	6.6747	4.73E+06	-0.0034	0.0000
-10.0	14 °F	5	31593	4582.177257	4.58E+06	6.6611	0.2	-0.698970004	-5.2783	6.6551	4.52E+06	0.0060	0.0000
-10.0	14 °F	1	29543	4284.849894	4.28E+06	6.6319	1	0	-4.5793	6.6045	4.02E+06	0.0275	0.0008
-10.0	14 °F	0.5	28639	4153.735779	4.15E+06	6.6184	2	0.301029996	-4.2783	6.5803	3.80E+06	0.0382	0.0015
-10.0	14 °F	0.1	26522	3846.690887	3.85E+06	6.5851	10	1	-3.5793	6.5181	3.30E+06	0.0670	0.0045
4.4	40 °F	25	22063	3199.967614	3.20E+06	6.5051	0.04	-1.397940009	-3.8196	6.5405	3.47E+06	-0.0353	0.0012
4.4	40 °F	10	20606	2988.647629	2.99E+06	6.4755	0.1	-1	-3.4216	6.5028	3.18E+06	-0.0273	0.0007
4.4	40 °F	5	19600	2842.739665	2.84E+06	6.4537	0.2	-0.698970004	-3.1206	6.4722	2.97E+06	-0.0184	0.0003
4.4	40 °F	1	16821	2439.679791	2.44E+06	6.3873	1	0	-2.4216	6.3936	2.48E+06	-0.0063	0.0000
4.4	40 °F	0.5	15845	2298.122959	2.30E+06	6.3614	2	0.301029996	-2.1206	6.3563	2.27E+06	0.0051	0.0000
4.4	40 °F	0.1	13304	1929.582066	1.93E+06	6.2855	10	1	-1.4216	6.2608	1.82E+06	0.0247	0.0006
21.1	70 °F	25	11472	1663.87293	1.66E+06	6.2211	0.04	-1.397940009	-1.3979	6.2573	1.81E+06	-0.0362	0.0013
21.1	70 °F	10	9864	1430.652248	1.43E+06	6.1555	0.1	-1	-1.0000	6.1967	1.57E+06	-0.0412	0.0017
21.1	70 °F	5	8773	1272.416076	1.27E+06	6.1046	0.2	-0.698970004	-0.6990	6.1478	1.41E+06	-0.0431	0.0019
21.1	70 °F	1	6554	950.5773349	9.51E+05	5.9780	1	0	0.0000	6.0232	1.05E+06	-0.0452	0.0020
21.1	70 °F	0.5	5711	828.3105218	8.28E+05	5.9182	2	0.301029996	0.3010	5.9646	9.22E+05	-0.0464	0.0021
21.1	70 °F	0.1	3978	576.9601218	5.77E+05	5.7611	10	1	1.0000	5.8160	6.55E+05	-0.0548	0.0030
38.7	100 °F	25	5474	793.9365779	7.94E+05	5.8998	0.04	-1.397940009	0.9589	5.8252	6.69E+05	0.0746	0.0056
38.7	100 °F	10	4403	638.6011604	6.39E+05	5.8052	0.1	-1	1.3568	5.7331	5.41E+05	0.0721	0.0052
38.7	100 °F	5	3690	535.1892532	5.35E+05	5.7285	0.2	-0.698970004	1.6578	5.6593	4.56E+05	0.0692	0.0048
38.7	100 °F	1	2286	331.5562691	3.32E+05	5.5206	1	0	2.3568	5.4738	2.98E+05	0.0467	0.0022
38.7	100 °F	0.5	1807	262.0831926	2.62E+05	5.4184	2	0.301029996	2.6578	5.3877	2.44E+05	0.0308	0.0009
38.7	100 °F	0.1	988	143.2972852	1.43E+05	5.1562	10	1	3.3568	5.1726	1.49E+05	-0.0164	0.0003
54.4	130 °F	25	1151	166.9384364	1.67E+05	5.2226	0.04	-1.397940009	3.2368	5.2110	1.63E+05	0.0115	0.0001
54.4	130 °F	10	797	115.5950772	1.16E+05	5.0629	0.1	-1	3.6347	5.0812	1.21E+05	-0.0182	0.0003
54.4	130 °F	5	605	87.74783149	8.77E+04	4.9432	0.2	-0.698970004	3.9357	4.9783	9.51E+04	-0.0351	0.0012
54.4	130 °F	1	321	46.5571139	4.66E+04	4.6680	1	0	4.6347	4.7243	5.30E+04	-0.0563	0.0032
54.4	130 °F	0.5	254	36.83958545	3.68E+04	4.5663	2	0.301029996	4.9357	4.6084	4.06E+04	-0.0420	0.0018
54.4	130 °F	0.1	168	24.36633999	2.44E+04	4.3868	10	1	5.6347	4.3248	2.11E+04	0.0620	0.0038
												ΣE	**-0.0012**	**0.0514**
													Unbiased	Biased

Table 73: Predicted Curve Data for Replicate 1 Using Brass Studs

Log Red Time, t_r	**Reduced Frequency, f_r**	**Predicted**	
		Log E* psi	**E* psi**
-8	8	6.7942	6,225,791
-7	7	6.7522	5,651,714
-6	6	6.7001	5,013,330
-5	5	6.6358	4,323,173
-4	4	6.5566	3,602,252
-3	3	6.4594	2,879,885
-2	2	6.3407	2,191,349
-1	1	6.1967	1,572,913
0	0	6.0232	1,054,878
1	-1	5.8160	654,598
2	-2	5.5710	372,415
3	-3	5.2850	192,764
4	-4	4.9558	90,331
5	-5	4.5831	38,294
6	-6	4.1689	14,755
7	-7	3.7180	5,224
8	-8	3.2381	1,730

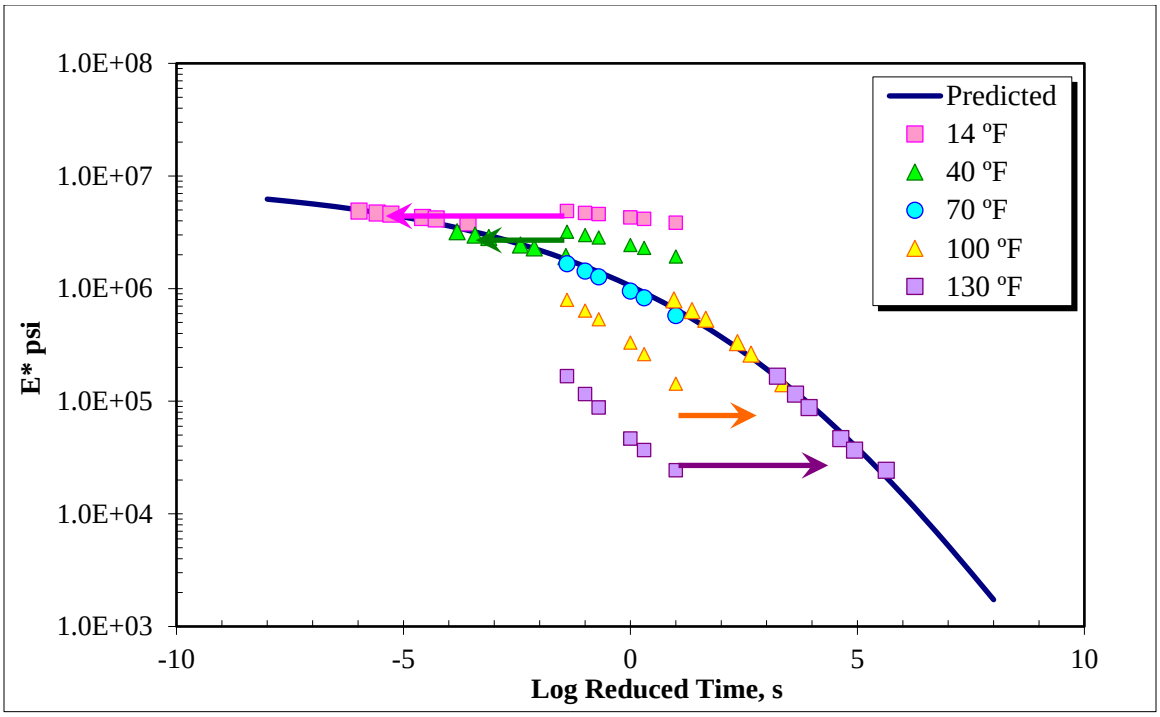

Figure 53: Initial Master Curve for Replicate 1 using Brass Studs

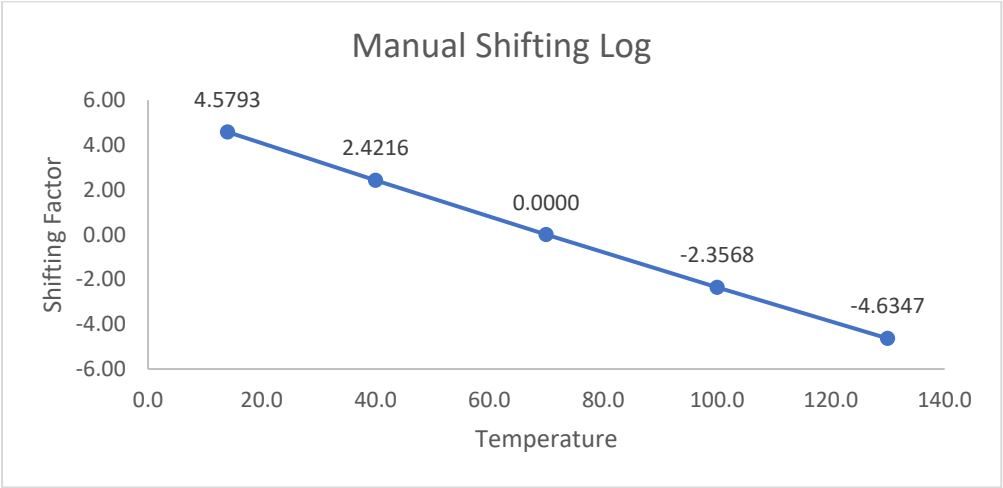

Figure 54: Manual Shifting Log for Replicate 1 Using Brass Studs

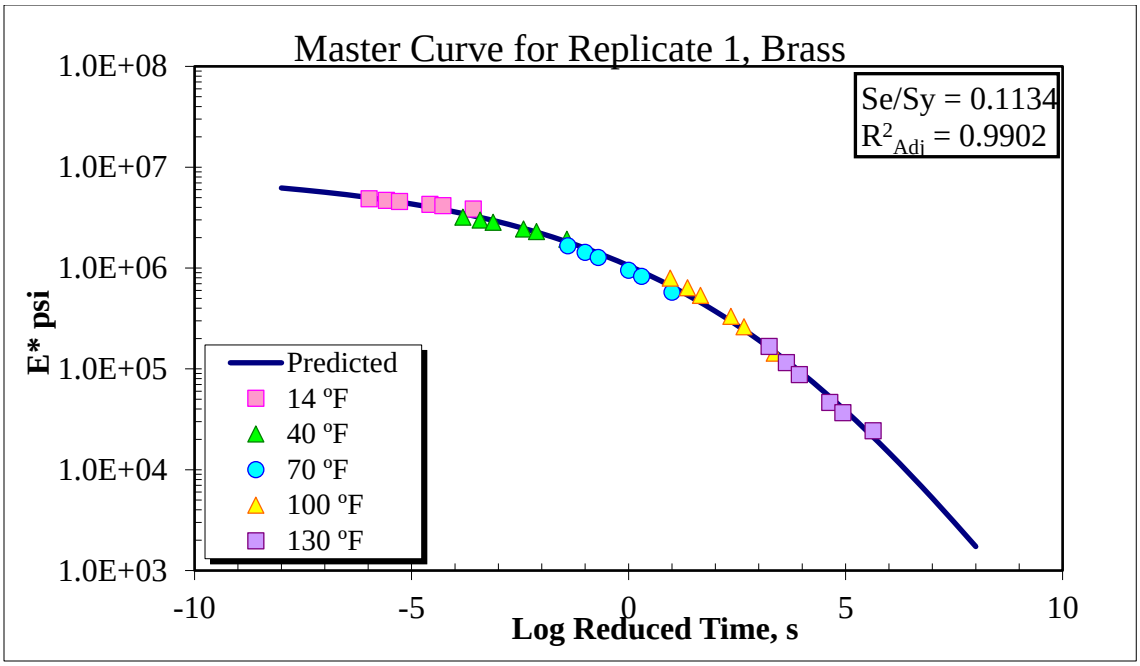

Figure 55: Final Master Curve for Replicate 1 Using Brass Studs

Replicate 2 – CB3 Brass

Table 74: Master Curve Data for Replicate 2 with Brass Studs

METAL (Brass)													
Temp, °C	Temp, °F	Frequency Hz	E* Mpa	E* ksi	E* psi	Log E* psi	Time, t s	Log Time s	Log Red Time, t_r	Pred Log E* psi	Pred E* psi	Error	Error^2
-10.0	14 ºF	25	36824	5340.869664	5.34E+06	6.7276	0.04	-1.39794	-5.5897	6.7104	5.13E+06	0.0172	0.0003
-10.0	14 ºF	10	36005	5222.083757	5.22E+06	6.7178	0.1	-1	-5.1918	6.6883	4.88E+06	0.0295	0.0009
-10.0	14 ºF	5	35658	5171.755662	5.17E+06	6.7136	0.2	-0.69897	-4.8907	6.6698	4.68E+06	0.0438	0.0019
-10.0	14 ºF	1	33134	4805.680411	4.81E+06	6.6818	1	0	-4.1918	6.6202	4.17E+06	0.0616	0.0038
-10.0	14 ºF	0.5	32102	4656.001466	4.66E+06	6.6680	2	0.30103	-3.8907	6.5956	3.94E+06	0.0725	0.0052
-10.0	14 ºF	0.1	29805	4322.849781	4.32E+06	6.6358	10	1	-3.1918	6.5299	3.39E+06	0.1059	0.0112
4.4	40 ºF	25	21389	3102.212178	3.10E+06	6.4917	0.04	-1.39794	-3.6212	6.5717	3.73E+06	-0.0801	0.0064
4.4	40 ºF	10	20124	2918.73944	2.92E+06	6.4652	0.1	-1	-3.2233	6.5332	3.41E+06	-0.0680	0.0046
4.4	40 ºF	5	19195	2783.999381	2.78E+06	6.4447	0.2	-0.69897	-2.9223	6.5011	3.17E+06	-0.0565	0.0032
4.4	40 ºF	1	16542	2399.214262	2.40E+06	6.3801	1	0	-2.2233	6.4164	2.61E+06	-0.0363	0.0013
4.4	40 ºF	0.5	15536	2253.306298	2.25E+06	6.3528	2	0.30103	-1.9223	6.3751	2.37E+06	-0.0222	0.0005
4.4	40 ºF	0.1	13042	1891.582179	1.89E+06	6.2768	10	1	-1.2233	6.2669	1.85E+06	0.0099	0.0001
21.1	70 ºF	25	12148	1761.918441	1.76E+06	6.2460	0.04	-1.39794	-1.3979	6.2956	1.98E+06	-0.0496	0.0025
21.1	70 ºF	10	10600	1537.400023	1.54E+06	6.1868	0.1	-1	-1.0000	6.2285	1.69E+06	-0.0418	0.0017
21.1	70 ºF	5	9421	1366.40053	1.37E+06	6.1356	0.2	-0.69897	-0.6990	6.1738	1.49E+06	-0.0383	0.0015
21.1	70 ºF	1	7028	1019.325223	1.02E+06	6.0083	1	0	0.0000	6.0331	1.08E+06	-0.0248	0.0006
21.1	70 ºF	0.5	6156	892.8523152	8.93E+05	5.9508	2	0.30103	0.3010	5.9665	9.26E+05	-0.0157	0.0002
21.1	70 ºF	0.1	4325	627.2882169	6.27E+05	5.7975	10	1	1.0000	5.7981	6.28E+05	-0.0007	0.0000
38.7	100 ºF	25	5291	767.3946718	7.67E+05	5.8850	0.04	-1.39794	0.7813	5.8528	7.13E+05	0.0322	0.0010
38.7	100 ºF	10	4284	621.3416696	6.21E+05	5.7933	0.1	-1	1.1793	5.7520	5.65E+05	0.0414	0.0017
38.7	100 ºF	5	3553	515.3190831	5.15E+05	5.7121	0.2	-0.69897	1.4803	5.6718	4.70E+05	0.0402	0.0016
38.7	100 ºF	1	2207	320.0982878	3.20E+05	5.5053	1	0	2.1793	5.4743	2.98E+05	0.0310	0.0010
38.7	100 ºF	0.5	1725	250.1900981	2.50E+05	5.3983	2	0.30103	2.4803	5.3848	2.43E+05	0.0134	0.0002
38.7	100 ºF	0.1	950	137.7858511	1.38E+05	5.1392	10	1	3.1793	5.1696	1.48E+05	-0.0304	0.0009
54.4	130 ºF	25	1341	194.4956067	1.94E+05	5.2889	0.04	-1.39794	2.9035	5.2556	1.80E+05	0.0333	0.0011
54.4	130 ºF	10	957	138.8011153	1.39E+05	5.1424	0.1	-1	3.3015	5.1311	1.35E+05	0.0113	0.0001
54.4	130 ºF	5	760	110.2286809	1.10E+05	5.0423	0.2	-0.69897	3.6025	5.0357	1.09E+05	0.0066	0.0000
54.4	130 ºF	1	405	58.74028389	5.87E+04	4.7689	1	0	4.3015	4.8124	6.49E+04	-0.0435	0.0019
54.4	130 ºF	0.5	324	46.99222711	4.70E+04	4.6720	2	0.30103	4.6025	4.7166	5.21E+04	-0.0446	0.0020
54.4	130 ºF	0.1	214	31.03807593	3.10E+04	4.4919	10	1	5.3015	4.4984	3.15E+04	-0.0065	0.0000
											ΣE	**-0.0088**	**0.0576**
												Unbiased	Biased

Table 75: Predicted Curve Data for Replicate 2 Using Brass Studs.

Log Red Time, t_r	**Reduced Frequency, f_r**	**Predicted**	
		Log E* psi	**E* psi**
-8	8	6.8000	6,309,136
-7	7	6.7705	5,895,844
-6	6	6.7306	5,377,757
-5	5	6.6767	4,750,425
-4	4	6.6047	4,024,697
-3	3	6.5096	3,233,277
-2	2	6.3860	2,432,301
-1	1	6.2285	1,692,544
0	0	6.0331	1,079,135
1	-1	5.7981	628,234
2	-2	5.5263	336,007
3	-3	5.2256	168,121
4	-4	4.9087	81,049
5	-5	4.5916	39,050
6	-6	4.2902	19,507
7	-7	4.0174	10,408
8	-8	3.7812	6,043

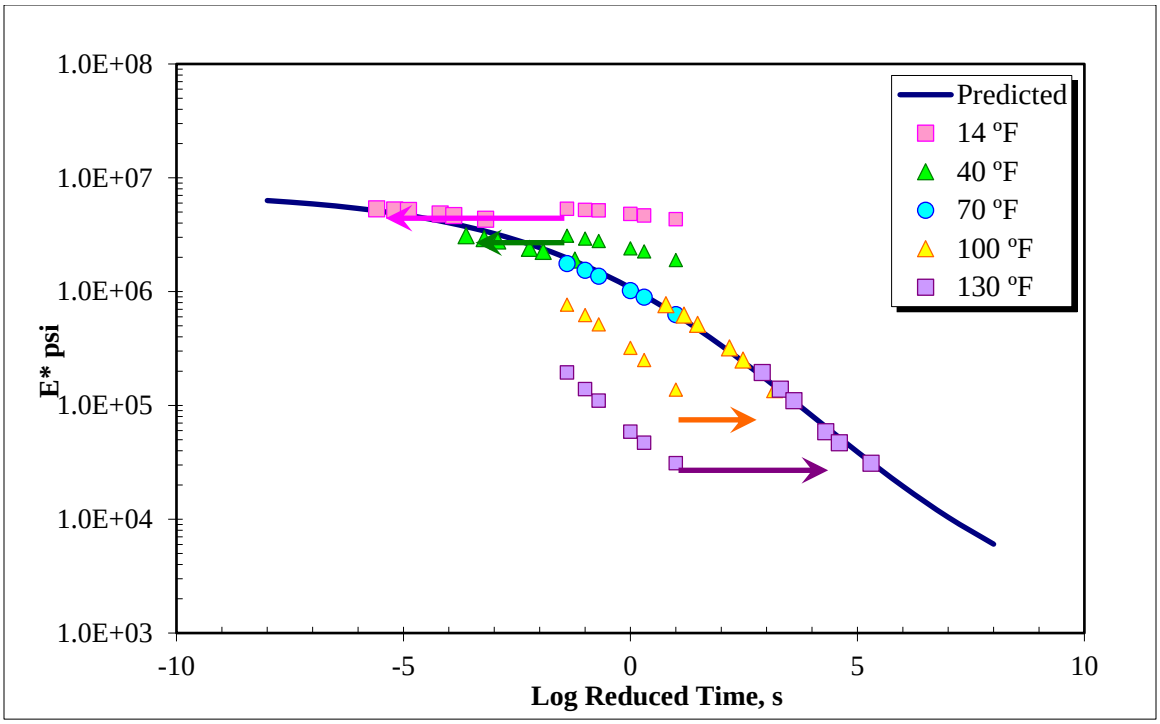

Figure 56: Initial Master Curve for Replicate 2 Using Brass Studs

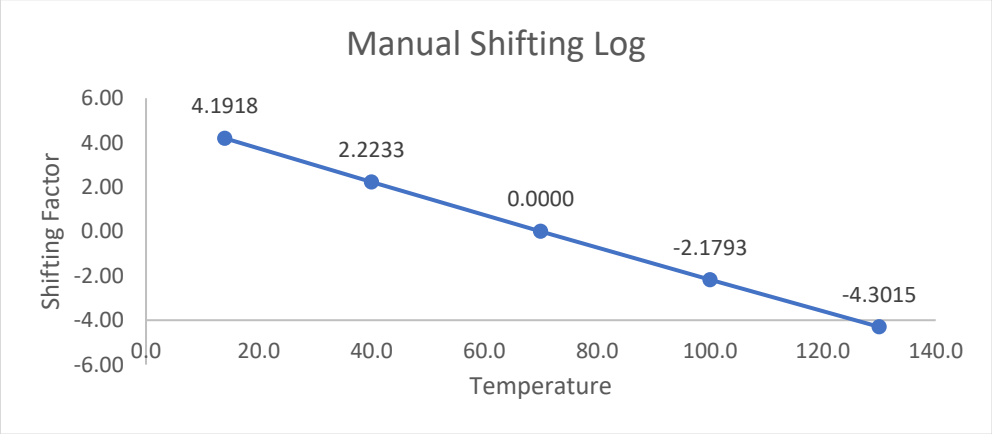

Figure 57: Manual Shifting Log for Replicate 2 Using Brass Studs

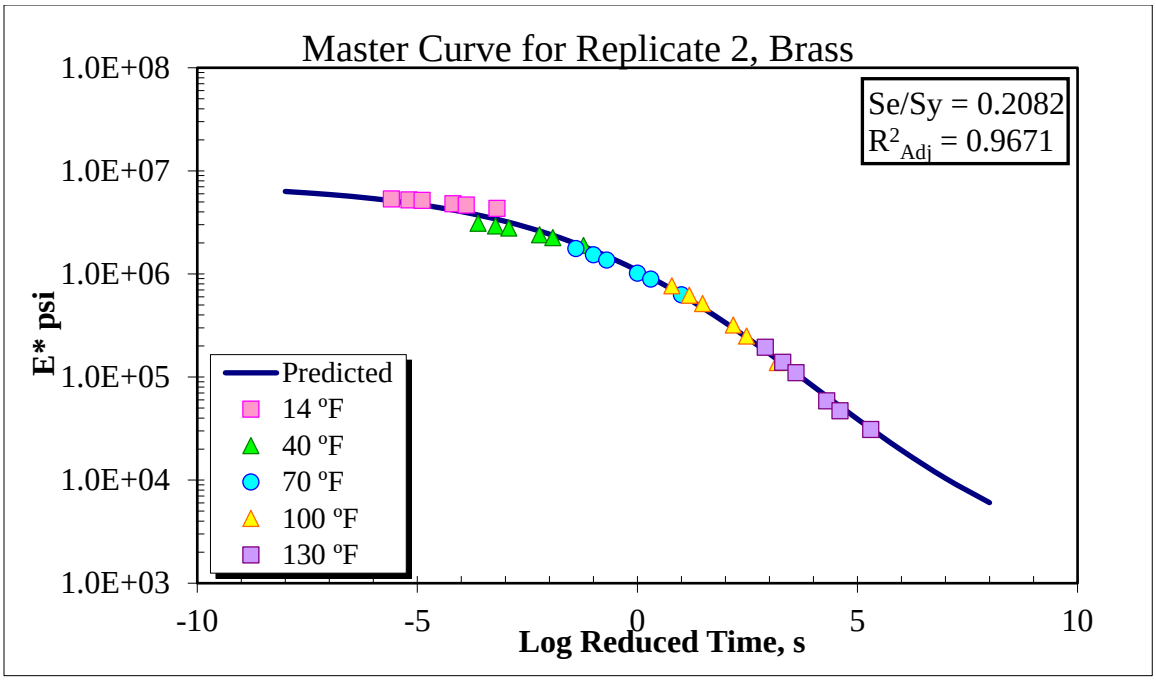

Figure 58: Final Master Curve for Replicate 2 Using Brass Studs

Replicate 3 – CB10 Brass

Table 76: Master Curve Data for Replicate 3 with Brass Studs

METAL (Brass)													
Temp, °C	Temp, °F	Frequency Hz	E* Mpa	E* ksi	E* psi	Log E* psi	Time, t s	Log Time s	Log Red Time, t_r	Pred Log E* psi	Pred E* psi	Error	Error^2
-10.0	14 °F	25	31850	4619.451956	4.62E+06	6.6646	0.04	-1.39794	-6.3392	6.6763	4.75E+06	-0.0117	0.0001
-10.0	14 °F	10	31372	4550.123917	4.55E+06	6.6580	0.1	-1	-5.9412	6.6606	4.58E+06	-0.0026	0.0000
-10.0	14 °F	5	30745	4459.185255	4.46E+06	6.6493	0.2	-0.69897	-5.6402	6.6474	4.44E+06	0.0018	0.0000
-10.0	14 °F	1	28762	4171.575421	4.17E+06	6.6203	1	0	-4.9412	6.6120	4.09E+06	0.0083	0.0001
-10.0	14 °F	0.5	27832	4036.690324	4.04E+06	6.6060	2	0.30103	-4.6402	6.5944	3.93E+06	0.0116	0.0001
-10.0	14 °F	0.1	25548	3705.424131	3.71E+06	6.5688	10	1	-3.9412	6.5473	3.53E+06	0.0216	0.0005
4.4	40 °F	25	23632	3427.531825	3.43E+06	6.5350	0.04	-1.39794	-3.9182	6.5455	3.51E+06	-0.0106	0.0001
4.4	40 °F	10	22297	3233.906444	3.23E+06	6.5097	0.1	-1	-3.5202	6.5140	3.27E+06	-0.0043	0.0000
4.4	40 °F	5	21215	3076.975612	3.08E+06	6.4881	0.2	-0.69897	-3.2192	6.4878	3.07E+06	0.0003	0.0000
4.4	40 °F	1	18391	2667.38904	2.67E+06	6.4261	1	0	-2.5202	6.4180	2.62E+06	0.0081	0.0001
4.4	40 °F	0.5	17279	2506.107075	2.51E+06	6.3990	2	0.30103	-2.2192	6.3838	2.42E+06	0.0152	0.0002
4.4	40 °F	0.1	14755	2140.031824	2.14E+06	6.3304	10	1	-1.5202	6.2934	1.97E+06	0.0370	0.0014
21.1	70 °F	25	12181	1766.704687	1.77E+06	6.2472	0.04	-1.39794	-1.3979	6.2759	1.89E+06	-0.0288	0.0008
21.1	70 °F	10	10418	1511.003155	1.51E+06	6.1793	0.1	-1	-1.0000	6.2153	1.64E+06	-0.0361	0.0013
21.1	70 °F	5	9353	1356.537964	1.36E+06	6.1324	0.2	-0.69897	-0.6990	6.1656	1.46E+06	-0.0332	0.0011
21.1	70 °F	1	6954	1008.59243	1.01E+06	6.0037	1	0	0.0000	6.0365	1.09E+06	-0.0328	0.0011
21.1	70 °F	0.5	6078	881.5393716	8.82E+05	5.9452	2	0.30103	0.3010	5.9748	9.44E+05	-0.0295	0.0009
21.1	70 °F	0.1	4315	625.8378395	6.26E+05	5.7965	10	1	1.0000	5.8166	6.56E+05	-0.0202	0.0004
38.7	100 °F	25	5368	778.5625776	7.79E+05	5.8913	0.04	-1.39794	0.8372	5.8553	7.17E+05	0.0360	0.0013
38.7	100 °F	10	4284	621.3416696	6.21E+05	5.7933	0.1	-1	1.2352	5.7588	5.74E+05	0.0346	0.0012
38.7	100 °F	5	3600	522.1358568	5.22E+05	5.7178	0.2	-0.69897	1.5362	5.6813	4.80E+05	0.0365	0.0013
38.7	100 °F	1	2256	327.2051369	3.27E+05	5.5148	1	0	2.2352	5.4870	3.07E+05	0.0278	0.0008
38.7	100 °F	0.5	1807	262.0831926	2.62E+05	5.4184	2	0.30103	2.5362	5.3976	2.50E+05	0.0209	0.0004
38.7	100 °F	0.1	1008	146.1980399	1.46E+05	5.1649	10	1	3.2352	5.1779	1.51E+05	-0.0129	0.0002
54.4	130 °F	25	1515	219.7321731	2.20E+05	5.3419	0.04	-1.39794	2.7742	5.3245	2.11E+05	0.0174	0.0003
54.4	130 °F	10	1077	156.2056438	1.56E+05	5.1937	0.1	-1	3.1722	5.1983	1.58E+05	-0.0046	0.0000
54.4	130 °F	5	827	119.9462093	1.20E+05	5.0790	0.2	-0.69897	3.4732	5.0997	1.26E+05	-0.0208	0.0004
54.4	130 °F	1	459	66.57232175	6.66E+04	4.8233	1	0	4.1722	4.8629	7.29E+04	-0.0396	0.0016
54.4	130 °F	0.5	365	52.93877437	5.29E+04	4.7238	2	0.30103	4.4732	4.7584	5.73E+04	-0.0346	0.0012
54.4	130 °F	0.1	249	36.11439676	3.61E+04	4.5577	10	1	5.1722	4.5132	3.26E+04	0.0444	0.0020
											ΣE	**-0.0008**	**0.0189**
												Unbiased	Biased

Table 77: Predicted Curve Data for Replicate 3 Using Brass Studs.

Log Red Time, t_r	**Reduced Frequency, f_r**	**Predicted**	
		Log E* psi	**E* psi**
-8	8	6.7248	5,305,965
-7	7	6.6985	4,994,596
-6	6	6.6630	4,602,691
-5	5	6.6153	4,123,846
-4	4	6.5516	3,561,233
-3	3	6.4673	2,933,029
-2	2	6.3571	2,275,806
-1	1	6.2153	1,641,892
0	0	6.0365	1,087,728
1	-1	5.8166	655,602
2	-2	5.5546	358,559
3	-3	5.2535	179,275
4	-4	4.9221	83,573
5	-5	4.5737	37,473
6	-6	4.2251	16,791
7	-7	3.8928	7,812
8	-8	3.5905	3,895

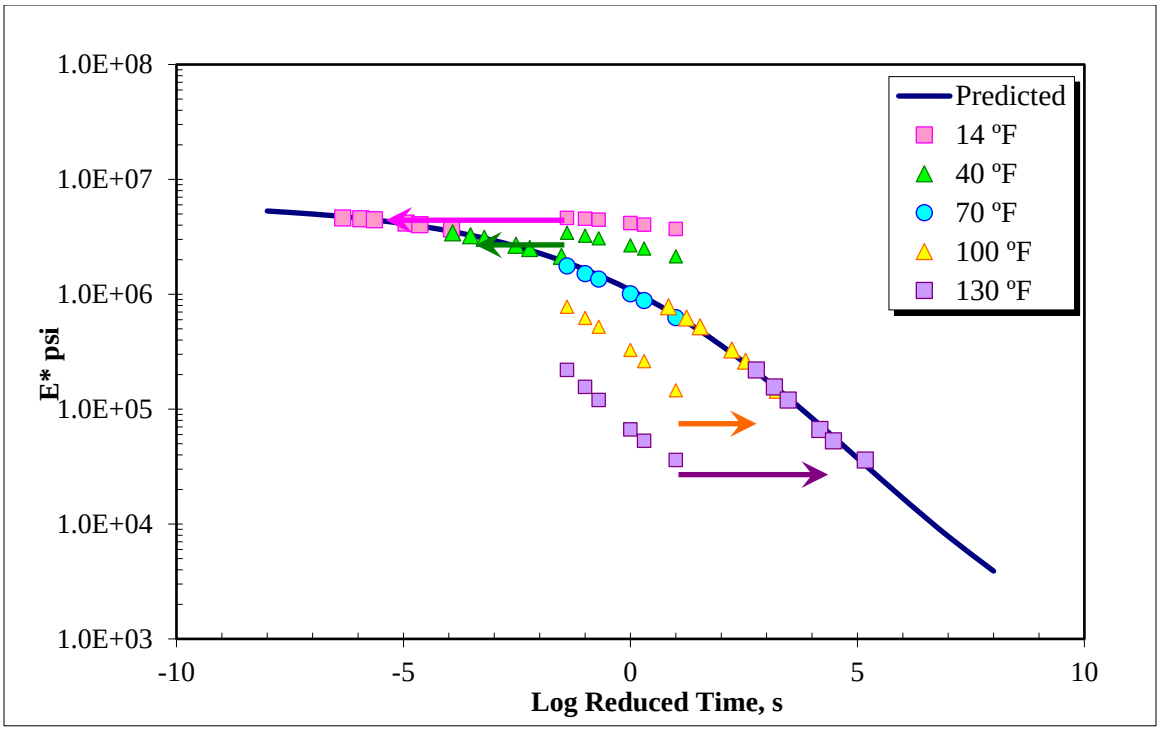

Figure 59: Initial Master Curve for Replicate 3 Using Brass Studs

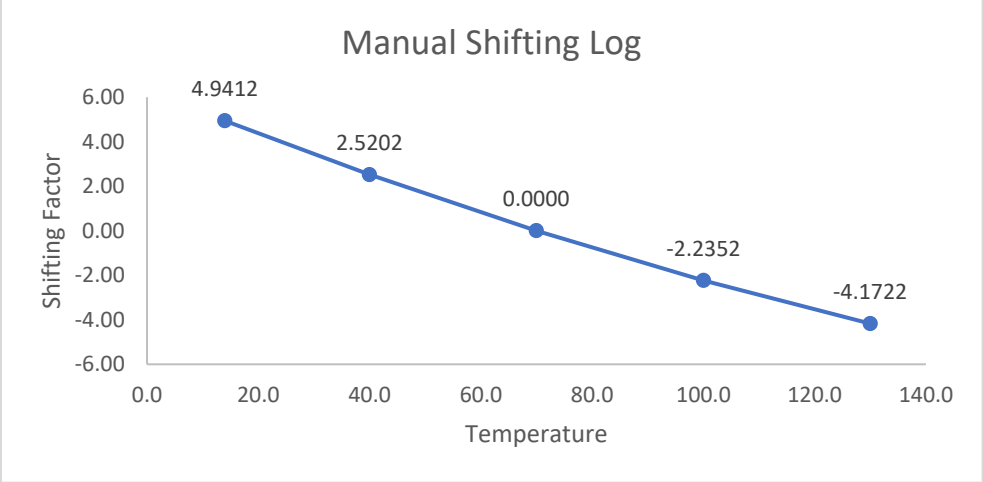

Figure 60: Manual Shifting Log for Replicate 3 Using Brass Studs.

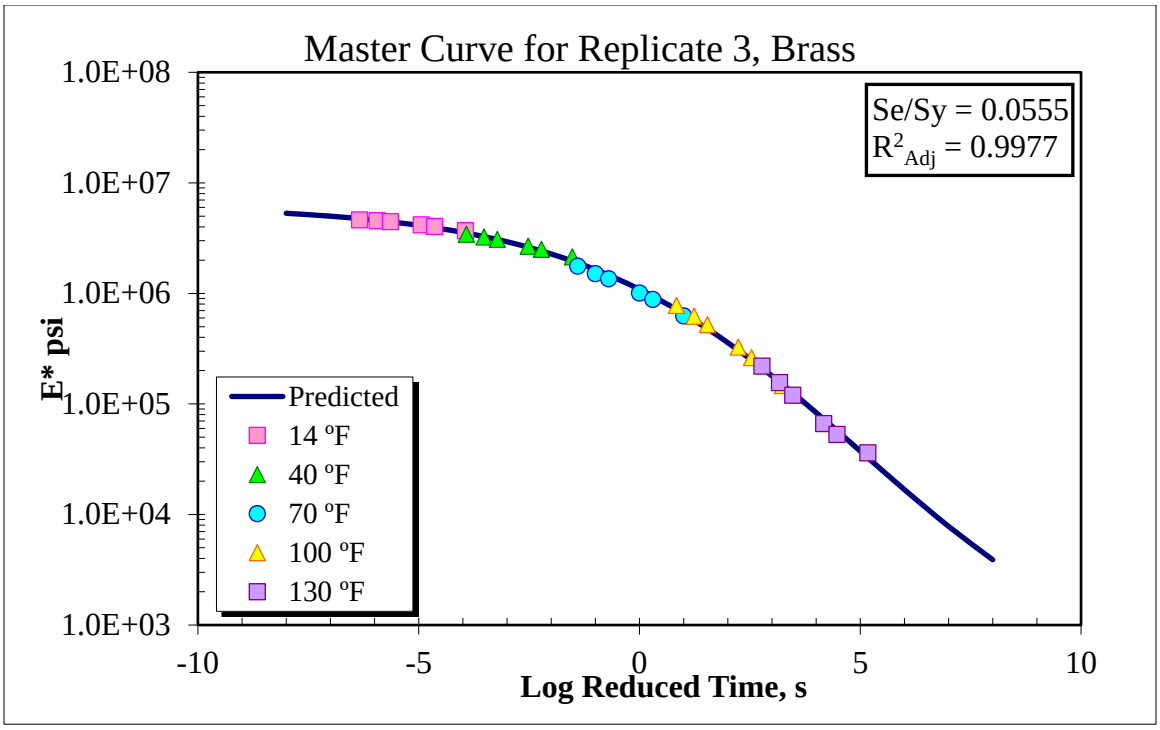

Figure 61: Final Master Curve for Replicate 3 Using Brass Studs.

Replicate 1 – CB1 PLA

Table 78: Master Curve Data for Replicate 1 with PLA Studs

PLA													
Temp, °C	**Temp, °F**	**Frequency Hz**	**E* Mpa**	**E* ksi**	**E* psi**	**Log E* psi**	**Time, t s**	**Log Time s**	**Log Red Time, t_r**	**Pred Log E* psi**	**Pred E* psi**	**Error**	**Error^2**
-10.0	14 °F	25	36462	5288.366003	5.29E+06	6.7233	0.04	-1.397940009	-6.4552	6.7247	5.31E+06	-0.0014	0.0000
-10.0	14 °F	10	33905	4917.504507	4.92E+06	6.6917	0.1	-1	-6.0573	6.7079	5.10E+06	-0.0162	0.0003
-10.0	14 °F	5	32937	4777.107977	4.78E+06	6.6792	0.2	-0.698970004	-5.7563	6.6940	4.94E+06	-0.0148	0.0002
-10.0	14 °F	1	30205	4380.864877	4.38E+06	6.6416	1	0	-5.0573	6.6567	4.54E+06	-0.0151	0.0002
-10.0	14 °F	0.5	29215	4237.277516	4.24E+06	6.6271	2	0.301029996	-4.7563	6.6383	4.35E+06	-0.0112	0.0001
-10.0	14 °F	0.1	26779	3883.965586	3.88E+06	6.5893	10	1	-4.0573	6.5895	3.89E+06	-0.0002	0.0000
4.4	40 °F	25	28369	4114.57559	4.11E+06	6.6143	0.04	-1.397940009	-4.0046	6.5854	3.85E+06	0.0289	0.0008
4.4	40 °F	10	26242	3806.080321	3.81E+06	6.5805	0.1	-1	-3.6066	6.5529	3.57E+06	0.0276	0.0008
4.4	40 °F	5	24973	3622.027431	3.62E+06	6.5590	0.2	-0.698970004	-3.3056	6.5259	3.36E+06	0.0330	0.0011
4.4	40 °F	1	21308	3090.464121	3.09E+06	6.4900	1	0	-2.6066	6.4548	2.85E+06	0.0352	0.0012
4.4	40 °F	0.5	20084	2912.93793	2.91E+06	6.4643	2	0.301029996	-2.3056	6.4202	2.63E+06	0.0442	0.0020
4.4	40 °F	0.1	17110	2481.595697	2.48E+06	6.3947	10	1	-1.6066	6.3293	2.13E+06	0.0654	0.0043
21.1	70 °F	25	11374	1649.659232	1.65E+06	6.2174	0.04	-1.397940009	-1.3979	6.2991	1.99E+06	-0.0817	0.0067
21.1	70 °F	10	10344	1500.270362	1.50E+06	6.1762	0.1	-1	-1.0000	6.2375	1.73E+06	-0.0613	0.0038
21.1	70 °F	5	9523	1381.194379	1.38E+06	6.1403	0.2	-0.698970004	-0.6990	6.1871	1.54E+06	-0.0469	0.0022
21.1	70 °F	1	6891	999.4550526	9.99E+05	5.9998	1	0	0.0000	6.0568	1.14E+06	-0.0571	0.0033
21.1	70 °F	0.5	6145	891.2569001	8.91E+05	5.9500	2	0.301029996	0.3010	5.9948	9.88E+05	-0.0448	0.0020
21.1	70 °F	0.1	4296	623.0821225	6.23E+05	5.7945	10	1	1.0000	5.8362	6.86E+05	-0.0416	0.0017
38.7	100 °F	25	5298	768.409936	7.68E+05	5.8856	0.04	-1.397940009	0.9800	5.8410	6.93E+05	0.0446	0.0020
38.7	100 °F	10	4289	622.0668583	6.22E+05	5.7938	0.1	-1	1.3779	5.7418	5.52E+05	0.0520	0.0027
38.7	100 °F	5	3537	512.9984793	5.13E+05	5.7101	0.2	-0.698970004	1.6789	5.6624	4.60E+05	0.0478	0.0023
38.7	100 °F	1	2206	319.95325	3.20E+05	5.5051	1	0	2.3779	5.4634	2.91E+05	0.0417	0.0017
38.7	100 °F	0.5	1731	251.0603245	2.51E+05	5.3998	2	0.301029996	2.6789	5.3716	2.35E+05	0.0281	0.0008
38.7	100 °F	0.1	950	137.7858511	1.38E+05	5.1392	10	1	3.3779	5.1459	1.40E+05	-0.0067	0.0000
54.4	130 °F	25	1225	177.6712291	1.78E+05	5.2496	0.04	-1.397940009	3.1151	5.2328	1.71E+05	0.0168	0.0003
54.4	130 °F	10	852	123.5721528	1.24E+05	5.0919	0.1	-1	3.5131	5.1004	1.26E+05	-0.0085	0.0001
54.4	130 °F	5	664	96.30505804	9.63E+04	4.9836	0.2	-0.698970004	3.8141	4.9971	9.93E+04	-0.0134	0.0002
54.4	130 °F	1	341	49.45786866	4.95E+04	4.6942	1	0	4.5131	4.7484	5.60E+04	-0.0541	0.0029
54.4	130 °F	0.5	272	39.45026474	3.95E+04	4.5960	2	0.301029996	4.8141	4.6383	4.35E+04	-0.0423	0.0018
54.4	130 °F	0.1	186	26.97701927	2.70E+04	4.4310	10	1	5.5131	4.3791	2.39E+04	0.0519	0.0027
											ΣE	**0.0000**	**0.0481**
												Unbiased	Biased

Table 79: Predicted Curve Data for Replicate 1 Using PLA Studs

Log Red Time, t_r	**Reduced Frequency, f_r**	**Predicted**	
		Log E* psi	**E* psi**
-8	8	6.7747	5,952,196
-7	7	6.7449	5,557,252
-6	6	6.7054	5,074,166
-5	5	6.6533	4,500,835
-4	4	6.5851	3,846,465
-3	3	6.4964	3,135,977
-2	2	6.3823	2,411,523
-1	1	6.2375	1,727,841
0	0	6.0568	1,139,843
1	-1	5.8362	685,727
2	-2	5.5734	374,473
3	-3	5.2701	186,246
4	-4	4.9320	85,512
5	-5	4.5698	37,134
6	-6	4.1976	15,761
7	-7	3.8313	6,781
8	-8	3.4859	3,061

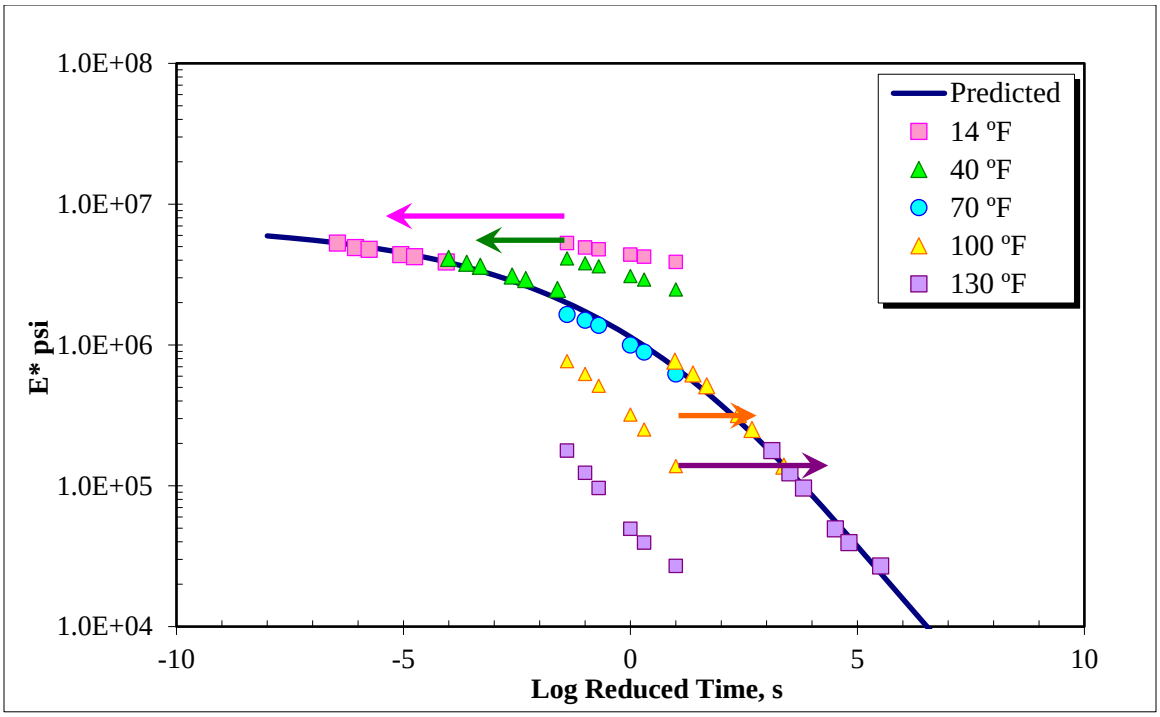

Figure 62: Initial Master Curve for Replicate 1 Using PLA Studs

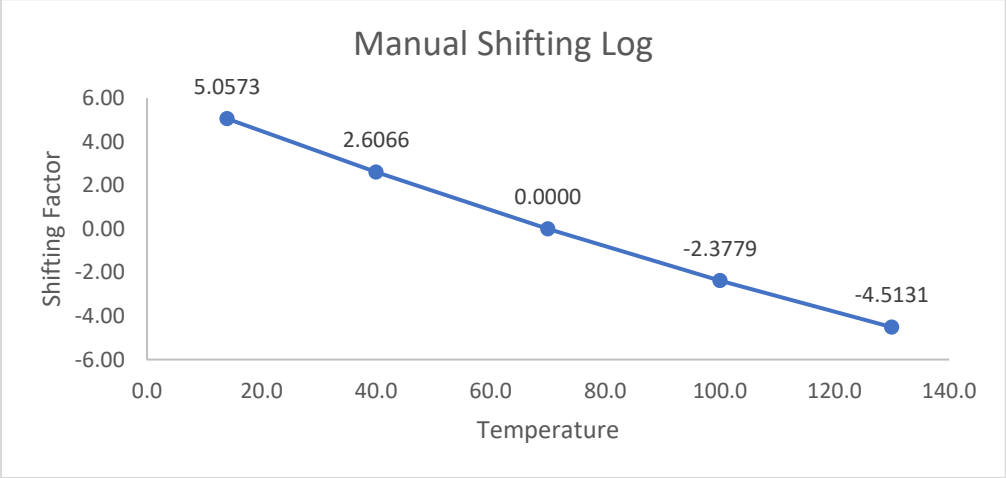

Figure 63: Manual Shifting Log for Replicate 1 Using PLA Studs

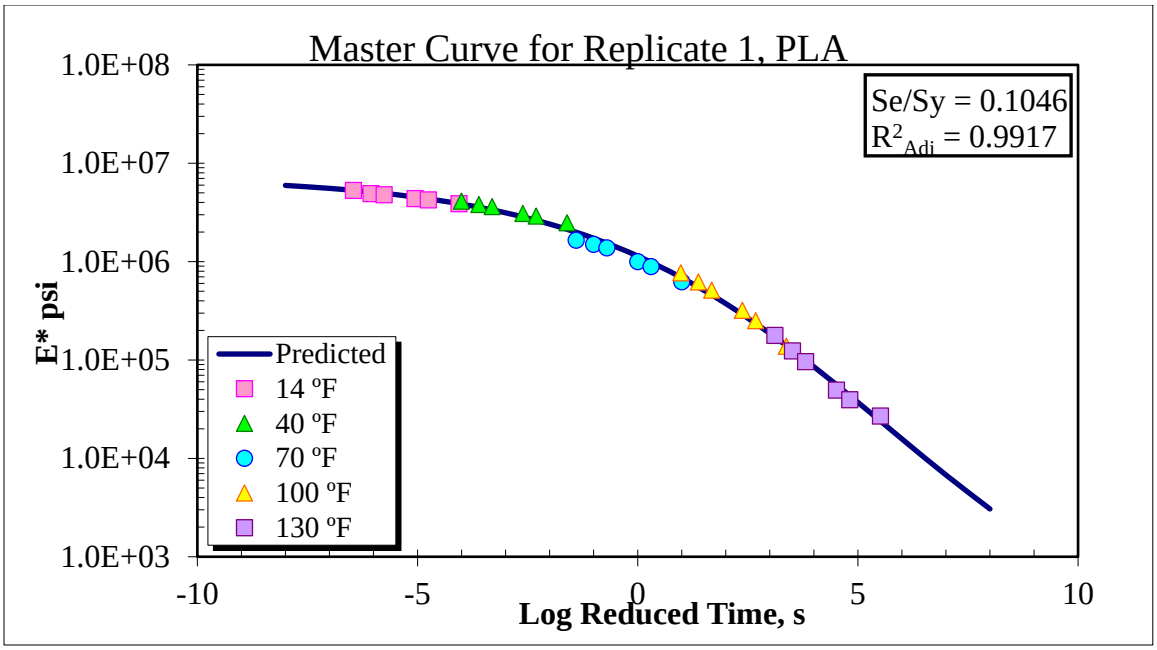

Figure 64: Final Master Curve for Replicate 1 Using PLA Studs

Replicate 2 – CB3 PLA

Table 80: Master Curve Data for Replicate 2 with PLA Studs

PLA													
Temp, °C	Temp, °F	Frequency Hz	E* Mpa	E* ksi	E* psi	Log E* psi	Time, t s	Log Time s	Log Red Time, t_r	Pred Log E* psi	Pred E* psi	Error	Error^2
-10.0	14 ºF	25	46607	6759.773855	6.76E+06	6.8299	0.04	-1.39794	-5.6983	6.8191	6.59E+06	0.0108	0.0001
-10.0	14 ºF	10	42448	6156.561903	6.16E+06	6.7893	0.1	-1	-5.3004	6.7978	6.28E+06	-0.0084	0.0001
-10.0	14 ºF	5	42431	6154.096261	6.15E+06	6.7892	0.2	-0.69897	-4.9993	6.7796	6.02E+06	0.0096	0.0001
-10.0	14 ºF	1	40066	5811.082011	5.81E+06	6.7643	1	0	-4.3004	6.7298	5.37E+06	0.0345	0.0012
-10.0	14 ºF	0.5	38841	5633.410782	5.63E+06	6.7508	2	0.30103	-3.9993	6.7046	5.07E+06	0.0462	0.0021
-10.0	14 ºF	0.1	35354	5127.66419	5.13E+06	6.7099	10	1	-3.3004	6.6361	4.33E+06	0.0738	0.0054
4.4	40 ºF	25	29126	4224.369157	4.22E+06	6.6258	0.04	-1.39794	-3.5887	6.6662	4.64E+06	-0.0404	0.0016
4.4	40 ºF	10	27566	3998.110286	4.00E+06	6.6019	0.1	-1	-3.1908	6.6240	4.21E+06	-0.0221	0.0005
4.4	40 ºF	5	26137	3790.851358	3.79E+06	6.5787	0.2	-0.69897	-2.8898	6.5886	3.88E+06	-0.0098	0.0001
4.4	40 ºF	1	22440	3254.646841	3.25E+06	6.5125	1	0	-2.1908	6.4933	3.11E+06	0.0192	0.0004
4.4	40 ºF	0.5	20898	3030.998649	3.03E+06	6.4816	2	0.30103	-1.8898	6.4461	2.79E+06	0.0355	0.0013
4.4	40 ºF	0.1	18016	2612.999888	2.61E+06	6.4171	10	1	-1.1908	6.3212	2.10E+06	0.0959	0.0092
21.1	70 ºF	25	12977	1882.154726	1.88E+06	6.2747	0.04	-1.39794	-1.3979	6.3606	2.29E+06	-0.0859	0.0074
21.1	70 ºF	10	11159	1618.476118	1.62E+06	6.2091	0.1	-1	-1.0000	6.2831	1.92E+06	-0.0740	0.0055
21.1	70 ºF	5	9983	1447.911739	1.45E+06	6.1607	0.2	-0.69897	-0.6990	6.2195	1.66E+06	-0.0588	0.0035
21.1	70 ºF	1	7388	1071.538808	1.07E+06	6.0300	1	0	0.0000	6.0546	1.13E+06	-0.0246	0.0006
21.1	70 ºF	0.5	6534	947.6765801	9.48E+05	5.9767	2	0.30103	0.3010	5.9762	9.47E+05	0.0004	0.0000
21.1	70 ºF	0.1	4636	672.3949534	6.72E+05	5.8276	10	1	1.0000	5.7779	6.00E+05	0.0497	0.0025
38.7	100 ºF	25	5533	802.4938044	8.02E+05	5.9044	0.04	-1.39794	0.5387	5.9113	8.15E+05	-0.0069	0.0000
38.7	100 ºF	10	4250	616.4103865	6.16E+05	5.7899	0.1	-1	0.9367	5.7968	6.26E+05	-0.0069	0.0000
38.7	100 ºF	5	3527	511.548102	5.12E+05	5.7089	0.2	-0.69897	1.2377	5.7056	5.08E+05	0.0033	0.0000
38.7	100 ºF	1	2138	310.0906839	3.10E+05	5.4915	1	0	1.9367	5.4810	3.03E+05	0.0105	0.0001
38.7	100 ºF	0.5	1675	242.9382112	2.43E+05	5.3855	2	0.30103	2.2377	5.3797	2.40E+05	0.0058	0.0000
38.7	100 ºF	0.1	924	134.0148699	1.34E+05	5.1272	10	1	2.9367	5.1377	1.37E+05	-0.0105	0.0001
54.4	130 ºF	25	1929	279.7777966	2.80E+05	5.4468	0.04	-1.39794	2.2100	5.3891	2.45E+05	0.0577	0.0033
54.4	130 ºF	10	1357	196.8162105	1.97E+05	5.2941	0.1	-1	2.6079	5.2524	1.79E+05	0.0417	0.0017
54.4	130 ºF	5	1015	147.2133041	1.47E+05	5.1679	0.2	-0.69897	2.9089	5.1474	1.40E+05	0.0205	0.0004
54.4	130 ºF	1	518	75.12954829	7.51E+04	4.8758	1	0	3.6079	4.9021	7.98E+04	-0.0263	0.0007
54.4	130 ºF	0.5	393	56.99983104	5.70E+04	4.7559	2	0.30103	3.9089	4.7974	6.27E+04	-0.0415	0.0017
54.4	130 ºF	0.1	231	33.50371748	3.35E+04	4.5251	10	1	4.6079	4.5606	3.64E+04	-0.0355	0.0013
											ΣE	**0.0634**	**0.0510**
												Unbiased	Biased

Table 81: Predicted Curve Data for Replicate 2 Using PLA Studs.

Log Red Time, t_r	**Reduced Frequency, f_r**	**Predicted**	
		Log E* psi	**E* psi**
-8	8	6.8991	7,925,945
-7	7	6.8719	7,446,169
-6	6	6.8336	6,816,345
-5	5	6.7796	6,020,460
-4	4	6.7047	5,065,911
-3	3	6.6019	3,998,607
-2	2	6.4638	2,909,636
-1	1	6.2831	1,919,266
0	0	6.0546	1,134,040
1	-1	5.7779	599,671
2	-2	5.4599	288,309
3	-3	5.1155	130,464
4	-4	4.7659	58,336
5	-5	4.4336	27,140
6	-6	4.1368	13,701
7	-7	3.8860	7,691
8	-8	3.6840	4,831

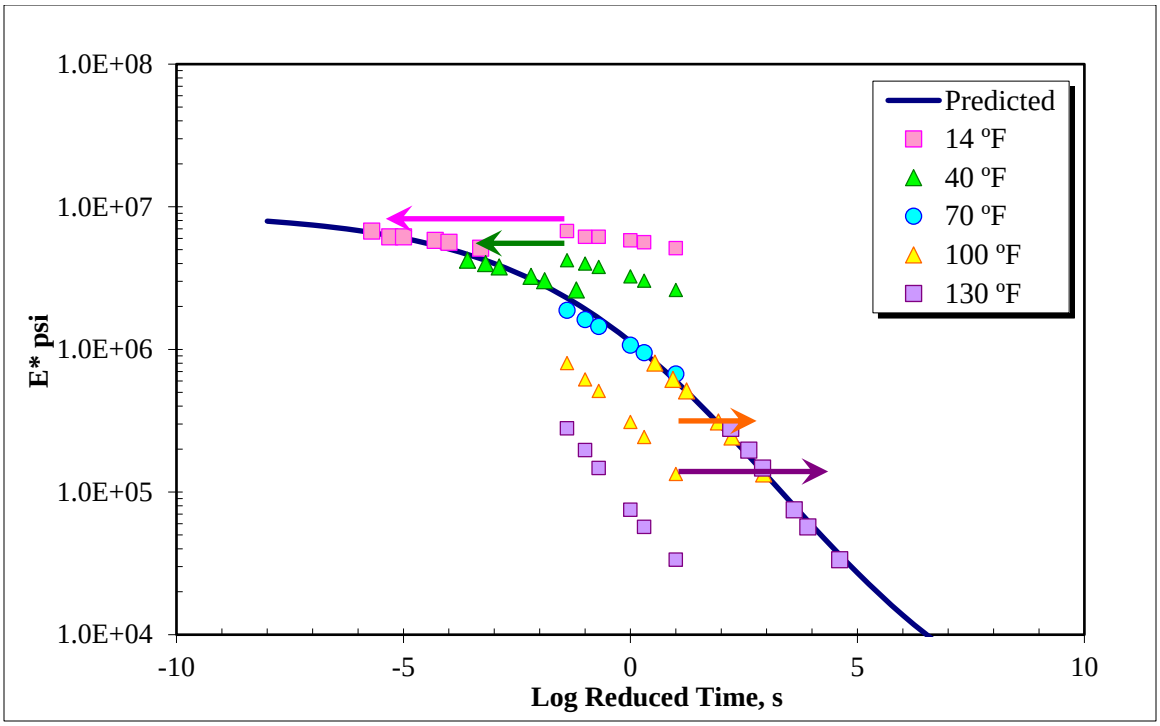

Figure 65: Initial Master Curve for Replicate 2 Using PLA Studs

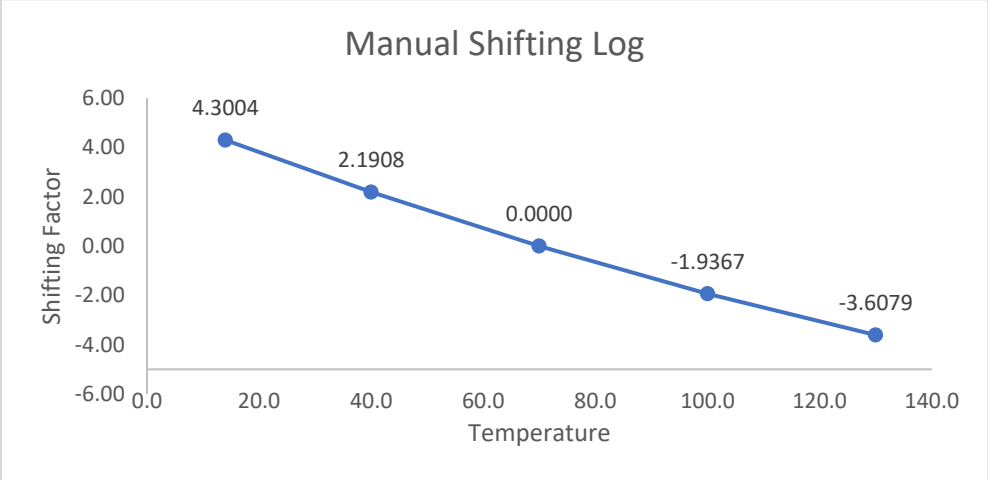

Figure 66: Manual Shifting Log for Replicate 2 Using Brass Studs

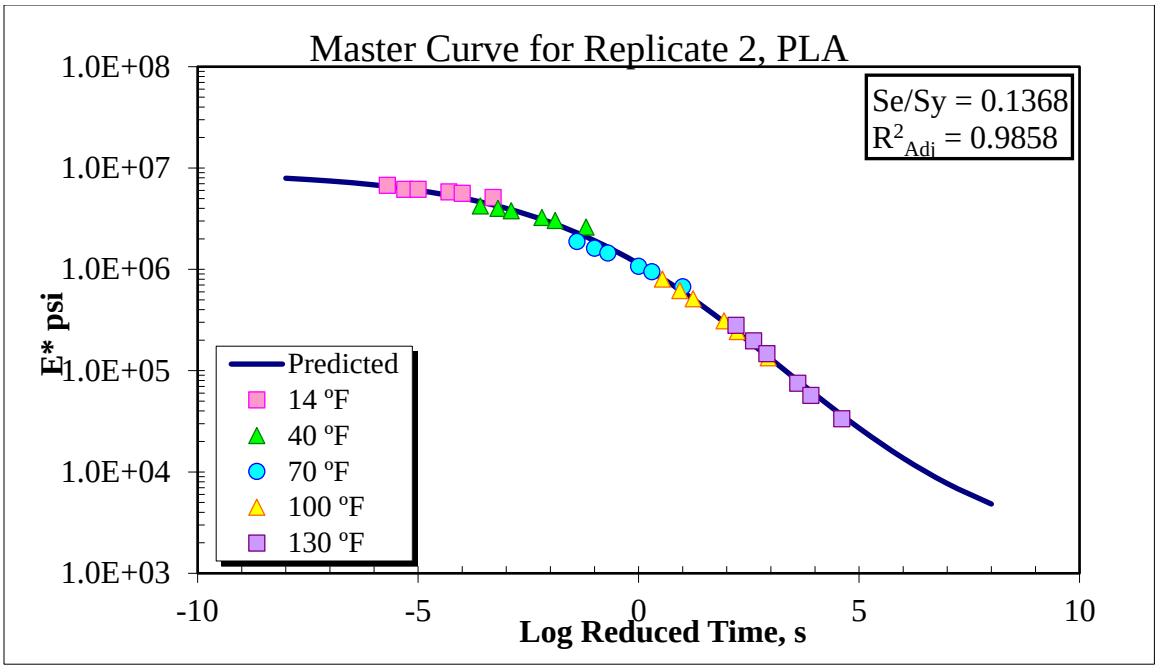

Figure 67: Final Master Curve for Replicate 2 Using PLA Studs

Replicate 3 – CB10 PLA

Table 82: Master Curve Data for Replicate 3 with PLA studs

PLA													
Temp, °C	Temp, °F	Frequency Hz	E* Mpa	E* ksi	E* psi	Log E* psi	Time, t s	Log Time s	Log Red Time, t_r	Pred Log E* psi	Pred E* psi	Error	Error^2
-10.0	14 ºF	25	37324.0000	5413.3885	5.41E+06	6.7335	0.04	-1.39794	-6.5030	6.7624	5.79E+06	-0.0289	0.0008
-10.0	14 ºF	10	38352.0000	5562.4873	5.56E+06	6.7453	0.1	-1	-6.1051	6.7423	5.52E+06	0.0030	0.0000
-10.0	14 ºF	5	37827.0000	5486.3425	5.49E+06	6.7393	0.2	-0.69897	-5.8041	6.7259	5.32E+06	0.0134	0.0002
-10.0	14 ºF	1	35472.0000	5144.7786	5.14E+06	6.7114	1	0	-5.1051	6.6831	4.82E+06	0.0282	0.0008
-10.0	14 ºF	0.5	34212.0000	4962.0311	4.96E+06	6.6957	2	0.30103	-4.8041	6.6626	4.60E+06	0.0331	0.0011
-10.0	14 ºF	0.1	31611.0000	4584.7879	4.58E+06	6.6613	10	1	-4.1051	6.6093	4.07E+06	0.0520	0.0027
4.4	40 ºF	25	25534.0000	3703.3936	3.70E+06	6.5686	0.04	-1.39794	-4.0192	6.6022	4.00E+06	-0.0336	0.0011
4.4	40 ºF	10	24109.0000	3496.7148	3.50E+06	6.5437	0.1	-1	-3.6212	6.5674	3.69E+06	-0.0238	0.0006
4.4	40 ºF	5	23016.0000	3338.1886	3.34E+06	6.5235	0.2	-0.69897	-3.3202	6.5391	3.46E+06	-0.0156	0.0002
4.4	40 ºF	1	19869.0000	2881.7548	2.88E+06	6.4597	1	0	-2.6212	6.4659	2.92E+06	-0.0062	0.0000
4.4	40 ºF	0.5	18652.0000	2705.2439	2.71E+06	6.4322	2	0.30103	-2.3202	6.4309	2.70E+06	0.0013	0.0000
4.4	40 ºF	0.1	15685.0000	2274.9169	2.27E+06	6.3570	10	1	-1.6212	6.3410	2.19E+06	0.0160	0.0003
21.1	70 ºF	25	12844.0000	1862.8647	1.86E+06	6.2702	0.04	-1.39794	-1.3979	6.3095	2.04E+06	-0.0393	0.0015
21.1	70 ºF	10	11581.0000	1679.6820	1.68E+06	6.2252	0.1	-1	-1.0000	6.2498	1.78E+06	-0.0246	0.0006
21.1	70 ºF	5	10328.0000	1497.9498	1.50E+06	6.1755	0.2	-0.69897	-0.6990	6.2015	1.59E+06	-0.0260	0.0007
21.1	70 ºF	1	7706.0000	1117.6608	1.12E+06	6.0483	1	0	0.0000	6.0781	1.20E+06	-0.0298	0.0009
21.1	70 ºF	0.5	6795.0000	985.5314	9.86E+05	5.9937	2	0.30103	0.3010	6.0199	1.05E+06	-0.0263	0.0007
21.1	70 ºF	0.1	4864.0000	705.4636	7.05E+05	5.8485	10	1	1.0000	5.8722	7.45E+05	-0.0237	0.0006
38.7	100 ºF	25	5882.0000	853.1120	8.53E+05	5.9310	0.04	-1.39794	0.9692	5.8791	7.57E+05	0.0519	0.0027
38.7	100 ºF	10	4759.0000	690.2346	6.90E+05	5.8390	0.1	-1	1.3671	5.7872	6.13E+05	0.0518	0.0027
38.7	100 ºF	5	4007.0000	581.1662	5.81E+05	5.7643	0.2	-0.69897	1.6681	5.7137	5.17E+05	0.0506	0.0026
38.7	100 ºF	1	2500.0000	362.5943	3.63E+05	5.5594	1	0	2.3671	5.5288	3.38E+05	0.0306	0.0009
38.7	100 ºF	0.5	1987.0000	288.1900	2.88E+05	5.4597	2	0.30103	2.6681	5.4430	2.77E+05	0.0167	0.0003
38.7	100 ºF	0.1	1115.0000	161.7171	1.62E+05	5.2088	10	1	3.3671	5.2294	1.70E+05	-0.0207	0.0004
54.4	130 ºF	25	1481.0000	214.8009	2.15E+05	5.3320	0.04	-1.39794	3.0682	5.3232	2.10E+05	0.0088	0.0001
54.4	130 ºF	10	1076.0000	156.0606	1.56E+05	5.1933	0.1	-1	3.4662	5.1975	1.58E+05	-0.0042	0.0000
54.4	130 ºF	5	825.0000	119.6561	1.20E+05	5.0779	0.2	-0.69897	3.7672	5.0982	1.25E+05	-0.0202	0.0004
54.4	130 ºF	1	437.0000	63.3815	6.34E+04	4.8020	1	0	4.4662	4.8535	7.14E+04	-0.0515	0.0027
54.4	130 ºF	0.5	352.0000	51.0533	5.11E+04	4.7080	2	0.30103	4.7672	4.7424	5.53E+04	-0.0343	0.0012
54.4	130 ºF	0.1	230.0000	33.3587	3.34E+04	4.5232	10	1	5.4662	4.4719	2.96E+04	0.0513	0.0026
											ΣE	**-0.0001**	**0.0294**
												Unbiased	Biased

Table 83: Predicted Curve Data for Replicate 3 Using PLA Studs.

Log Red Time, t_r	**Reduced Frequency, f_r**	**Predicted**	
		Log E* psi	**E* psi**
-8	8	6.8236	6,661,772
-7	7	6.7851	6,096,212
-6	6	6.7367	5,453,523
-5	5	6.6761	4,743,631
-4	4	6.6006	3,986,478
-3	3	6.5069	3,212,757
-2	2	6.3913	2,462,045
-1	1	6.2498	1,777,453
0	0	6.0781	1,197,140
1	-1	5.8722	745,071
2	-2	5.6284	424,966
3	-3	5.3441	220,865
4	-4	5.0188	104,427
5	-5	4.6541	45,097
6	-6	4.2548	17,980
7	-7	3.8285	6,737
8	-8	3.3856	2,430

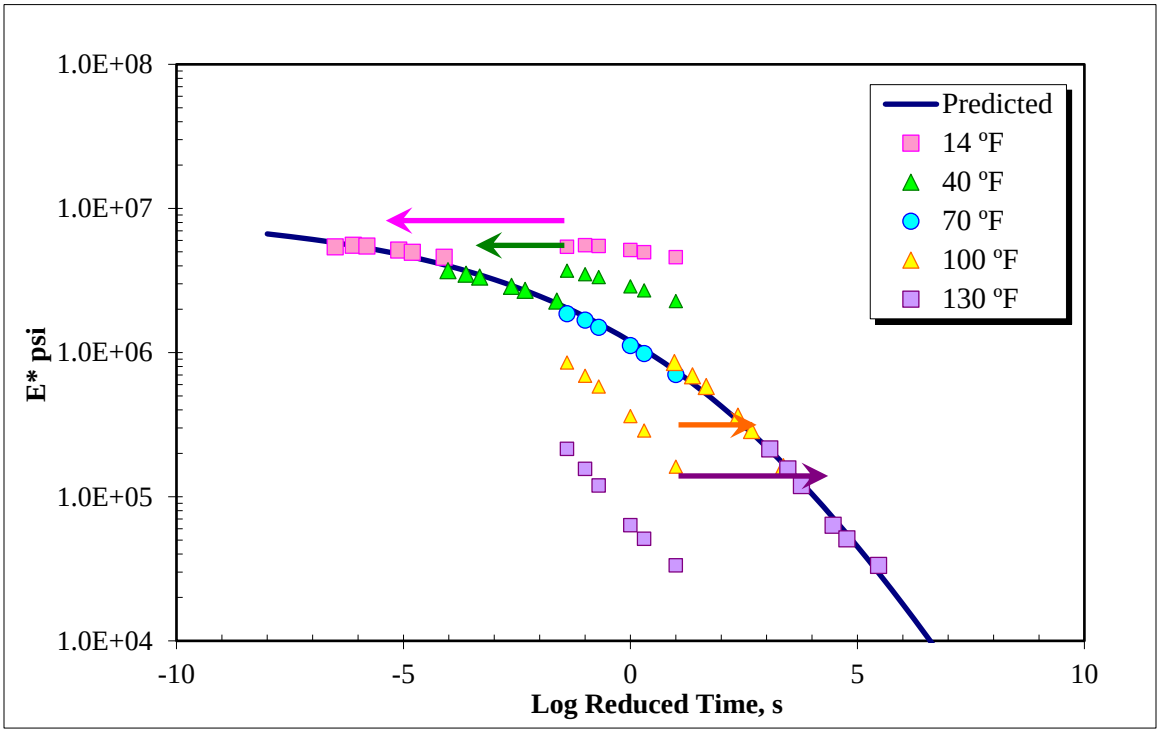

Figure 68: Initial Master Curve for Replicate 3 Using PLA Studs

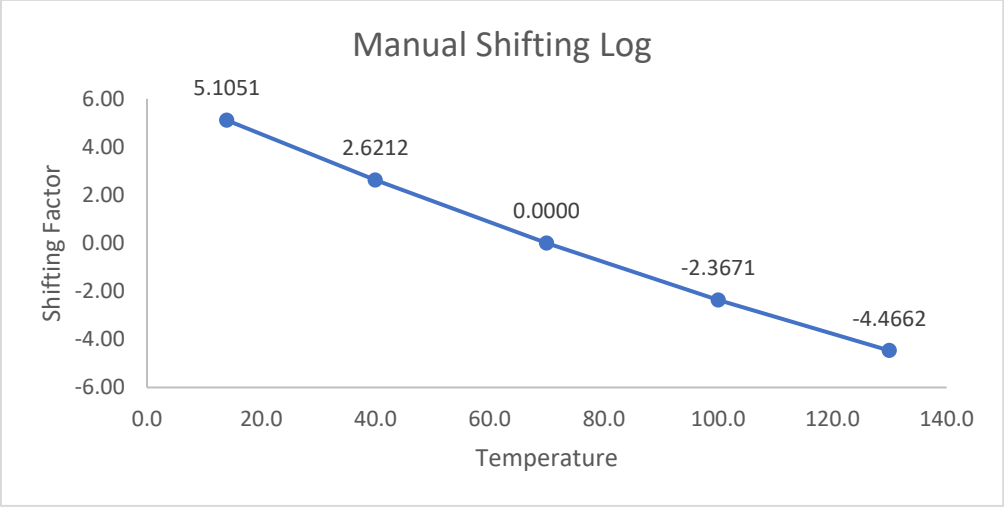

Figure 69: Manual Shifting Log for Replicate 3 Using PLA Studs.

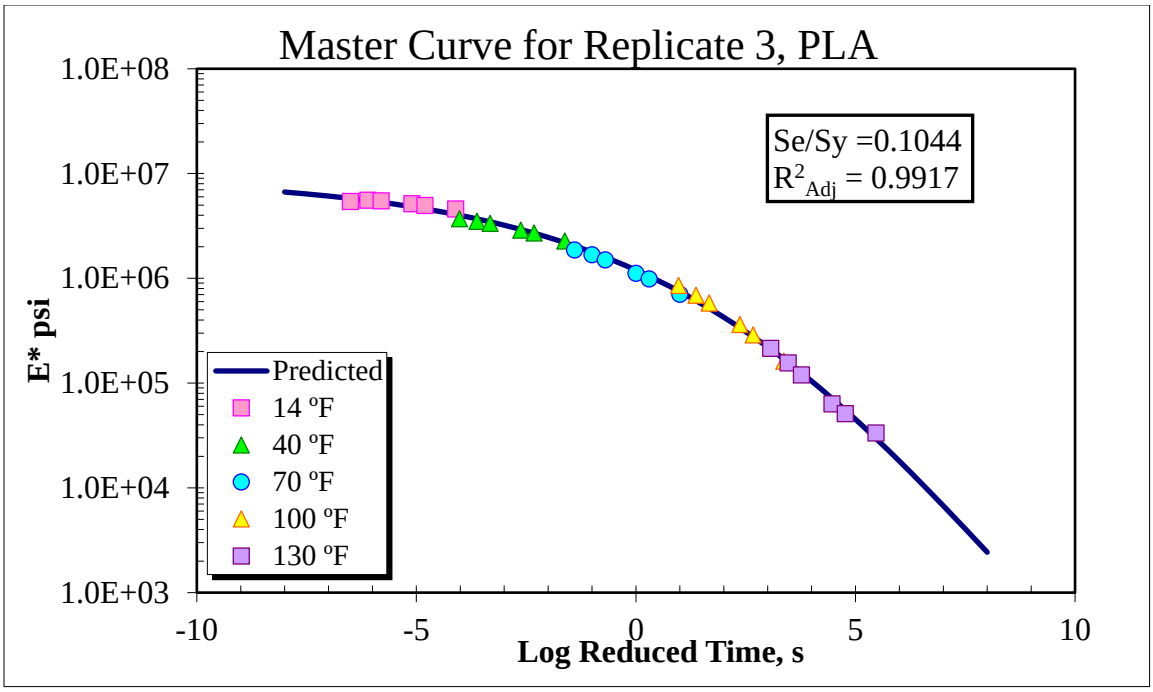

Figure 70: Final Master Curve for Replicate 3 Using PLA Studs.

Replicate 1 – CB1 ABS

Table 84: Master Curve Data for Replicate 1 with ABS Studs

ABS													
Temp, °C	Temp, °F	Frequency Hz	E* Mpa	E* ksi	E* psi	Log E* psi	Time, t s	Log Time s	Log Red Time, t_r	Pred Log E* psi	Pred E* psi	Error	Error^2
-10.0	14 ºF	25	39377	5711.15101	5.71E+06	6.7567	0.04	-1.397940009	-5.5428	6.7553	5.69E+06	0.0014	0.0000
-10.0	14 ºF	10	36418	5281.984343	5.28E+06	6.7228	0.1	-1	-5.1449	6.7319	5.39E+06	-0.0091	0.0001
-10.0	14 ºF	5	35988	5219.618115	5.22E+06	6.7176	0.2	-0.698970004	-4.8439	6.7122	5.16E+06	0.0054	0.0000
-10.0	14 ºF	1	33479	4855.718431	4.86E+06	6.6863	1	0	-4.1449	6.6598	4.57E+06	0.0264	0.0007
-10.0	14 ºF	0.5	32311	4686.314353	4.69E+06	6.6708	2	0.301029996	-3.8439	6.6340	4.31E+06	0.0369	0.0014
-10.0	14 ºF	0.1	29650	4300.368932	4.30E+06	6.6335	10	1	-3.1449	6.5653	3.68E+06	0.0682	0.0046
4.4	40 ºF	25	27596	4002.461418	4.00E+06	6.6023	0.04	-1.397940009	-3.6039	6.6118	4.09E+06	-0.0095	0.0001
4.4	40 ºF	10	26100	3785.484962	3.79E+06	6.5781	0.1	-1	-3.2059	6.5718	3.73E+06	0.0063	0.0000
4.4	40 ºF	5	24466	3548.493298	3.55E+06	6.5500	0.2	-0.698970004	-2.9049	6.5387	3.46E+06	0.0113	0.0001
4.4	40 ºF	1	20997	3045.357385	3.05E+06	6.4836	1	0	-2.2059	6.4514	2.83E+06	0.0322	0.0010
4.4	40 ºF	0.5	19460	2822.434382	2.82E+06	6.4506	2	0.301029996	-1.9049	6.4090	2.56E+06	0.0416	0.0017
4.4	40 ºF	0.1	16240	2355.412865	2.36E+06	6.3721	10	1	-1.2059	6.2983	1.99E+06	0.0738	0.0054
21.1	70 ºF	25	11921	1728.994875	1.73E+06	6.2378	0.04	-1.397940009	-1.3979	6.3304	2.14E+06	-0.0927	0.0086
21.1	70 ºF	10	10566	1532.46874	1.53E+06	6.1854	0.1	-1	-1.0000	6.2622	1.83E+06	-0.0768	0.0059
21.1	70 ºF	5	9419	1366.110454	1.37E+06	6.1355	0.2	-0.698970004	-0.6990	6.2066	1.61E+06	-0.0711	0.0051
21.1	70 ºF	1	6964	1010.042807	1.01E+06	6.0043	1	0	0.0000	6.0637	1.16E+06	-0.0594	0.0035
21.1	70 ºF	0.5	6037	875.5928243	8.76E+05	5.9423	2	0.301029996	0.3010	5.9962	9.91E+05	-0.0539	0.0029
21.1	70 ºF	0.1	4201	609.3035374	6.09E+05	5.7848	10	1	1.0000	5.8254	6.69E+05	-0.0405	0.0016
38.7	100 ºF	25	5754	834.5471445	8.35E+05	5.9215	0.04	-1.397940009	0.7817	5.8808	7.60E+05	0.0407	0.0017
38.7	100 ºF	10	4645	673.700293	6.74E+05	5.8285	0.1	-1	1.1797	5.7784	6.00E+05	0.0501	0.0025
38.7	100 ºF	5	3847	557.9601781	5.58E+05	5.7466	0.2	-0.698970004	1.4807	5.6970	4.98E+05	0.0496	0.0025
38.7	100 ºF	1	2330	337.9379296	3.38E+05	5.5288	1	0	2.1797	5.4958	3.13E+05	0.0331	0.0011
38.7	100 ºF	0.5	1840	266.8694379	2.67E+05	5.4263	2	0.301029996	2.4807	5.4044	2.54E+05	0.0219	0.0005
38.7	100 ºF	0.1	1029	149.2438324	1.49E+05	5.1739	10	1	3.1797	5.1836	1.53E+05	-0.0097	0.0001
54.4	130 ºF	25	1352	196.0910218	1.96E+05	5.2925	0.04	-1.397940009	2.9221	5.2662	1.85E+05	0.0262	0.0007
54.4	130 ºF	10	934	135.4652473	1.35E+05	5.1318	0.1	-1	3.3201	5.1381	1.37E+05	-0.0063	0.0000
54.4	130 ºF	5	745	108.0531148	1.08E+05	5.0336	0.2	-0.698970004	3.6211	5.0395	1.10E+05	-0.0059	0.0000
54.4	130 ºF	1	402	58.30517068	5.83E+04	4.7657	1	0	4.3201	4.8076	6.42E+04	-0.0419	0.0018
54.4	130 ºF	0.5	319	46.26703842	4.63E+04	4.6653	2	0.301029996	4.6211	4.7074	5.10E+04	-0.0421	0.0018
54.4	130 ºF	0.1	221	32.0533401	3.21E+04	4.5059	10	1	5.3201	4.4775	3.00E+04	0.0283	0.0008
											ΣE	**0.0345**	**0.0563**
												Unbiased	Biased

Table 85: Predicted Curve Data for Replicate 1 Using ABS Studs

Log Red Time, t_r	**Reduced Frequency, f_r**	**Predicted**	
		Log E* psi	**E* psi**
-8	8	6.8531	7,130,940
-7	7	6.8216	6,631,555
-6	6	6.7792	6,014,947
-5	5	6.7226	5,279,849
-4	4	6.6476	4,442,695
-3	3	6.5495	3,543,686
-2	2	6.4227	2,646,840
-1	1	6.2622	1,829,052
0	0	6.0637	1,158,071
1	-1	5.8254	668,913
2	-2	5.5490	354,009
3	-3	5.2414	174,336
4	-4	4.9141	82,048
5	-5	4.5821	38,206
6	-6	4.2615	18,259
7	-7	3.9660	9,247
8	-8	3.7052	5,073

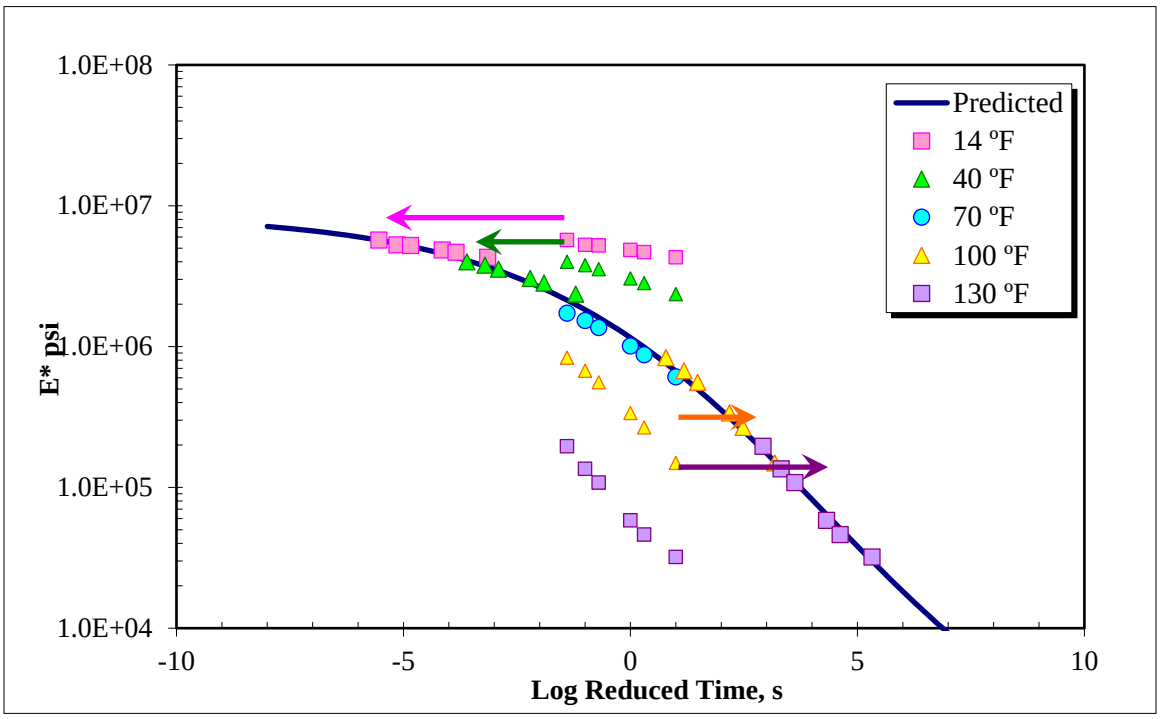

Figure 71: Initial Master Curve for Replicate 1 Using ABS Studs

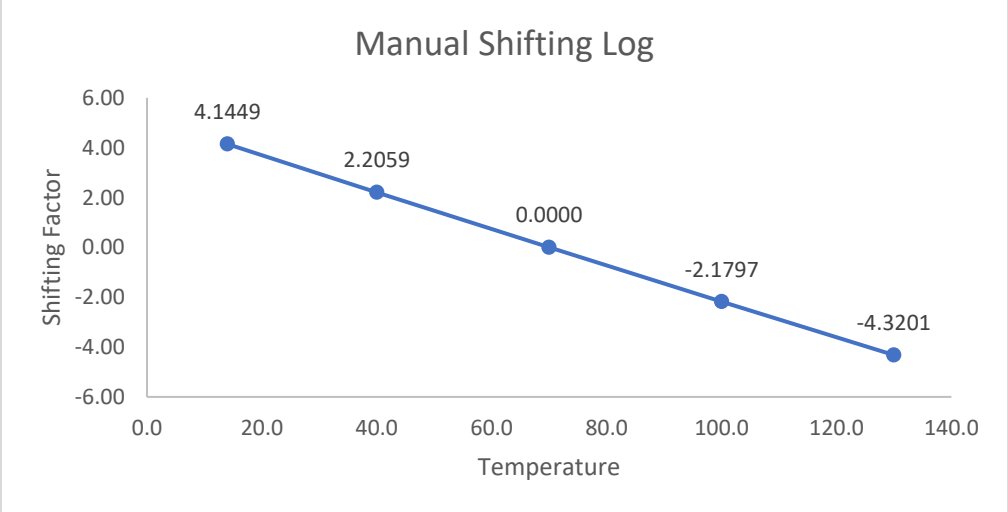

Figure 72: Manual Shifting Log for Replicate 1 Using ABS Studs

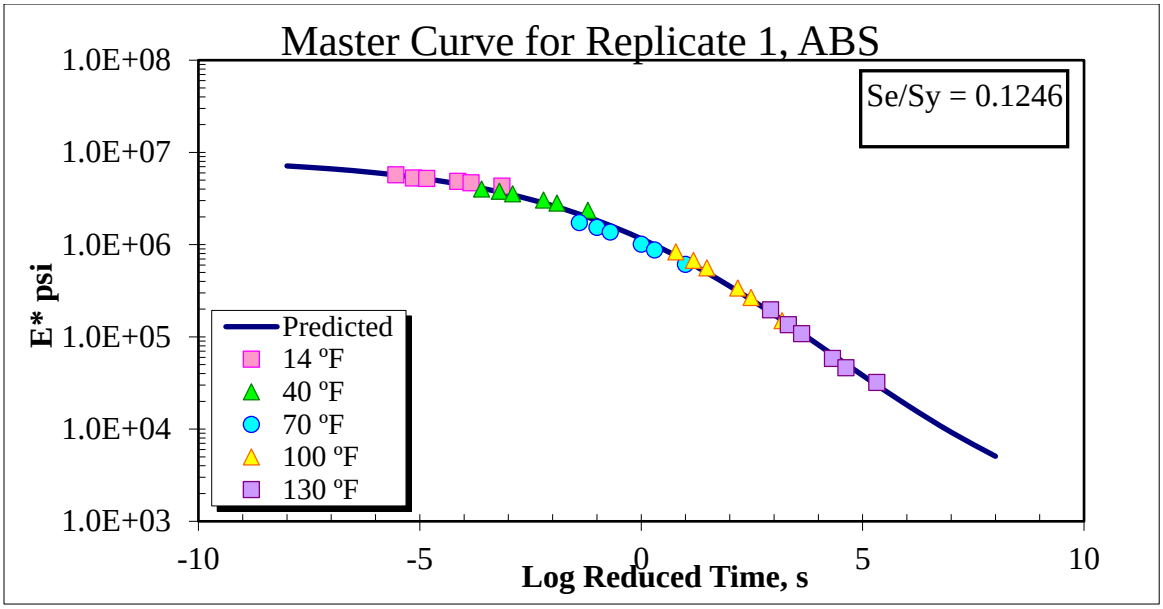

Figure 73: Final Master Curve for Replicate 1 Using ABS Studs

Replicate 2 – CB3 ABS

Table 86: Master Curve Data for Replicate 2 with ABS sSuds

ABS													
Temp, °C	Temp, °F	Frequency Hz	E* Mpa	E* ksi	E* psi	Log E* psi	Time, t s	Log Time s	Log Red Time, t_r	Pred Log E* psi	Pred E* psi	Error	Error^2
-10.0	14 ºF	25	45967	6666.949703	6.67E+06	6.8239	0.04	-1.39794	-7.3289	6.7908	6.18E+06	0.0331	0.0011
-10.0	14 ºF	10	44092	6395.003944	6.40E+06	6.8058	0.1	-1	-6.9309	6.7798	6.02E+06	0.0261	0.0007
-10.0	14 ºF	5	42849	6214.722036	6.21E+06	6.7934	0.2	-0.69897	-6.6299	6.7705	5.89E+06	0.0230	0.0005
-10.0	14 ºF	1	39389	5712.891462	5.71E+06	6.7569	1	0	-5.9309	6.7451	5.56E+06	0.0118	0.0001
-10.0	14 ºF	0.5	38121	5528.983611	5.53E+06	6.7426	2	0.30103	-5.6299	6.7323	5.40E+06	0.0103	0.0001
-10.0	14 ºF	0.1	35216	5107.648982	5.11E+06	6.7082	10	1	-4.9309	6.6977	4.99E+06	0.0105	0.0001
4.4	40 ºF	25	28572	4144.01825	4.14E+06	6.6174	0.04	-1.39794	-4.2844	6.6584	4.55E+06	-0.0410	0.0017
4.4	40 ºF	10	26343	3820.729132	3.82E+06	6.5821	0.1	-1	-3.8865	6.6301	4.27E+06	-0.0480	0.0023
4.4	40 ºF	5	25198	3654.660922	3.65E+06	6.5628	0.2	-0.69897	-3.5855	6.6064	4.04E+06	-0.0436	0.0019
4.4	40 ºF	1	21882	3173.715783	3.17E+06	6.5016	1	0	-2.8865	6.5427	3.49E+06	-0.0412	0.0017
4.4	40 ºF	0.5	20546	2979.945365	2.98E+06	6.4742	2	0.30103	-2.5855	6.5112	3.24E+06	-0.0370	0.0014
4.4	40 ºF	0.1	17496	2537.580264	2.54E+06	6.4044	10	1	-1.8865	6.4270	2.67E+06	-0.0226	0.0005
21.1	70 ºF	25	16209	2350.916695	2.35E+06	6.3712	0.04	-1.39794	-1.3979	6.3582	2.28E+06	0.0131	0.0002
21.1	70 ºF	10	14311	2075.635069	2.08E+06	6.3172	0.1	-1	-1.0000	6.2954	1.97E+06	0.0217	0.0005
21.1	70 ºF	5	12823	1859.818914	1.86E+06	6.2695	0.2	-0.69897	-0.6990	6.2437	1.75E+06	0.0258	0.0007
21.1	70 ºF	1	9536	1383.07987	1.38E+06	6.1408	1	0	0.0000	6.1086	1.28E+06	0.0323	0.0010
21.1	70 ºF	0.5	8336	1209.034584	1.21E+06	6.0824	2	0.30103	0.3010	6.0437	1.11E+06	0.0388	0.0015
21.1	70 ºF	0.1	5997	869.7913148	8.70E+05	5.9394	10	1	1.0000	5.8767	7.53E+05	0.0627	0.0039
38.7	100 ºF	25	5644	818.5929933	8.19E+05	5.9131	0.04	-1.39794	0.8252	5.9206	8.33E+05	-0.0075	0.0001
38.7	100 ºF	10	4509	653.9751607	6.54E+05	5.8156	0.1	-1	1.2231	5.8186	6.59E+05	-0.0030	0.0000
38.7	100 ºF	5	3745	543.1663288	5.43E+05	5.7349	0.2	-0.69897	1.5242	5.7366	5.45E+05	-0.0017	0.0000
38.7	100 ºF	1	2265	328.5104766	3.29E+05	5.5165	1	0	2.2231	5.5306	3.39E+05	-0.0141	0.0002
38.7	100 ºF	0.5	1762	255.5564944	2.56E+05	5.4075	2	0.30103	2.5242	5.4356	2.73E+05	-0.0281	0.0008
38.7	100 ºF	0.1	972	140.9766813	1.41E+05	5.1491	10	1	3.2231	5.2025	1.59E+05	-0.0534	0.0028
54.4	130 ºF	25	2266	328.6555143	3.29E+05	5.5167	0.04	-1.39794	2.3723	5.4840	3.05E+05	0.0328	0.0011
54.4	130 ºF	10	1578	228.8695506	2.29E+05	5.3596	0.1	-1	2.7703	5.3554	2.27E+05	0.0042	0.0000
54.4	130 ºF	5	1203	174.4803988	1.74E+05	5.2417	0.2	-0.69897	3.0713	5.2545	1.80E+05	-0.0128	0.0002
54.4	130 ºF	1	672	97.46535994	9.75E+04	4.9889	1	0	3.7703	5.0102	1.02E+05	-0.0213	0.0005
54.4	130 ºF	0.5	520	75.41962376	7.54E+04	4.8775	2	0.30103	4.0713	4.9017	7.97E+04	-0.0242	0.0006
54.4	130 ºF	0.1	345	50.03801961	5.00E+04	4.6993	10	1	4.7703	4.6460	4.43E+04	0.0533	0.0028
											ΣE	**0.0000**	**0.0289**
												Unbiased	Biased

Table 87: Predicted Curve Data for Replicate 2 Using ABS Studs.

Log Red Time, t_r	**Reduced Frequency, f_r**	**Predicted**	
		Log E* psi	**E* psi**
-8	8	6.8065	6,404,999
-7	7	6.7818	6,050,524
-6	6	6.7478	5,595,518
-5	5	6.7015	5,028,708
-4	4	6.6385	4,350,429
-3	3	6.5540	3,580,755
-2	2	6.4418	2,765,559
-1	1	6.2954	1,974,300
0	0	6.1086	1,284,084
1	-1	5.8767	752,845
2	-2	5.5986	396,864
3	-3	5.2787	189,968
4	-4	4.9275	84,629
5	-5	4.5616	36,440
6	-6	4.2003	15,859
7	-7	3.8620	7,278
8	-8	3.5608	3,637

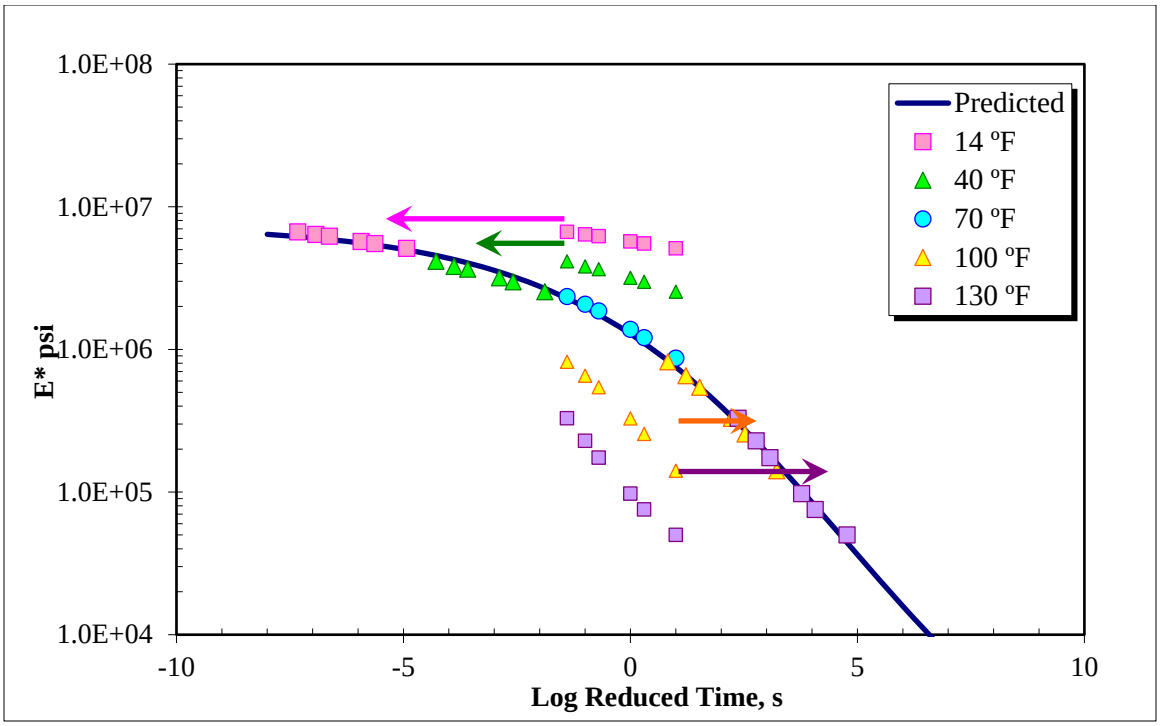

Figure 74: Initial Master Curve for Replicate 2 Using ABS Studs

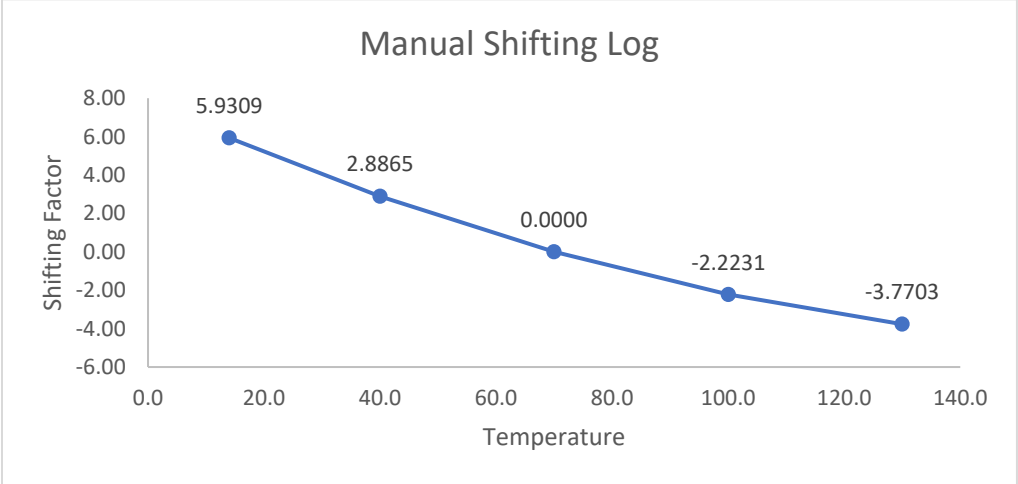

Figure 75: Manual Shifting Log for Replicate 2 Using ABS Studs

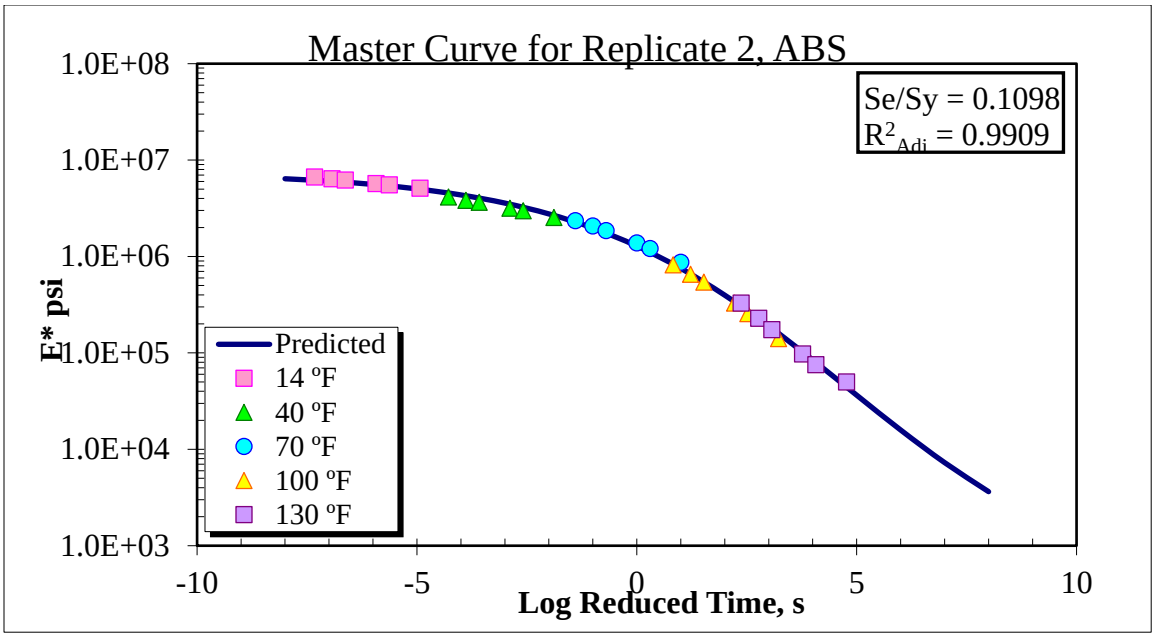

Figure 76: Final Master Curve for Replicate 2 Using ABS Studs

Replicate 3 – CB10 ABS

Table 88: Master Curve Data for Replicate 3 with ABS Studs

ABS													
Temp, °C	Temp, °F	Frequency Hz	E* Mpa	E* ksi	E* psi	Log E* psi	Time, t s	Log Time s	Log Red Time, t_r	Pred Log E* psi	Pred E* psi	Error	Error^2
-10.0	14 ºF	25	52684	7641.168189	7.64E+06	6.8832	0.04	-1.39794	-6.7606	6.872320353	7.45E+06	0.0108	0.0001
-10.0	14 ºF	10	49517	7181.833673	7.18E+06	6.8562	0.1	-1	-6.3627	6.849931182	7.08E+06	0.0063	0.0000
-10.0	14 ºF	5	46738	6778.773799	6.78E+06	6.8312	0.2	-0.69897	-6.0617	6.831733801	6.79E+06	-0.0006	0.0000
-10.0	14 ºF	1	42534	6169.035148	6.17E+06	6.7902	1	0	-5.3627	6.784902463	6.09E+06	0.0053	0.0000
-10.0	14 ºF	0.5	40647	5895.348937	5.90E+06	6.7705	2	0.30103	-5.0617	6.762594306	5.79E+06	0.0079	0.0001
-10.0	14 ºF	0.1	36656	5316.503324	5.32E+06	6.7256	10	1	-4.3627	6.705283883	5.07E+06	0.0203	0.0004
4.4	40 ºF	25	30612	4439.895236	4.44E+06	6.6474	0.04	-1.39794	-4.1426	6.685522196	4.85E+06	-0.0381	0.0015
4.4	40 ºF	10	29985	4348.956574	4.35E+06	6.6384	0.1	-1	-3.7447	6.647535659	4.44E+06	-0.0092	0.0001
4.4	40 ºF	5	28120	4078.461193	4.08E+06	6.6105	0.2	-0.69897	-3.4436	6.616765693	4.14E+06	-0.0063	0.0000
4.4	40 ºF	1	24417	3541.386449	3.54E+06	6.5492	1	0	-2.7447	6.538006627	3.45E+06	0.0112	0.0001
4.4	40 ºF	0.5	22986	3333.837446	3.33E+06	6.5229	2	0.30103	-2.4436	6.500704899	3.17E+06	0.0222	0.0005
4.4	40 ºF	0.1	19634	2847.670948	2.85E+06	6.4545	10	1	-1.7447	6.405505583	2.54E+06	0.0490	0.0024
21.1	70 ºF	25	14228	2063.596936	2.06E+06	6.3146	0.04	-1.39794	-1.3979	6.353515375	2.26E+06	-0.0389	0.0015
21.1	70 ºF	10	12083	1752.490988	1.75E+06	6.2437	0.1	-1	-1.0000	6.289670241	1.95E+06	-0.0460	0.0021
21.1	70 ºF	5	11044	1601.796779	1.60E+06	6.2046	0.2	-0.69897	-0.6990	6.238263701	1.73E+06	-0.0337	0.0011
21.1	70 ºF	1	8155	1182.782753	1.18E+06	6.0729	1	0	0.0000	6.107928891	1.28E+06	-0.0350	0.0012
21.1	70 ºF	0.5	7150	1037.019827	1.04E+06	6.0158	2	0.30103	0.3010	6.046817264	1.11E+06	-0.0310	0.0010
21.1	70 ºF	0.1	5013	727.0741806	7.27E+05	5.8616	10	1	1.0000	5.89261787	7.81E+05	-0.0310	0.0010
38.7	100 ºF	25	5755	834.6921822	8.35E+05	5.9215	0.04	-1.39794	1.0593	5.878725102	7.56E+05	0.0428	0.0018
38.7	100 ºF	10	4708	682.8376705	6.83E+05	5.8343	0.1	-1	1.4572	5.782003834	6.05E+05	0.0523	0.0027
38.7	100 ºF	5	3920	568.547933	5.69E+05	5.7548	0.2	-0.69897	1.7582	5.704787044	5.07E+05	0.0500	0.0025
38.7	100 ºF	1	2391	346.7852316	3.47E+05	5.5401	1	0	2.4572	5.511608238	3.25E+05	0.0285	0.0008
38.7	100 ºF	0.5	1921	278.6174947	2.79E+05	5.4450	2	0.30103	2.7582	5.422289151	2.64E+05	0.0227	0.0005
38.7	100 ºF	0.1	1065	154.465191	1.54E+05	5.1888	10	1	3.4572	5.200399482	1.59E+05	-0.0116	0.0001
54.4	130 ºF	25	1386	201.0223049	2.01E+05	5.3032	0.04	-1.39794	3.2146	5.279727405	1.90E+05	0.0235	0.0006
54.4	130 ºF	10	969	140.5415681	1.41E+05	5.1478	0.1	-1	3.6125	5.148323556	1.41E+05	-0.0005	0.0000
54.4	130 ºF	5	712	103.2668695	1.03E+05	5.0140	0.2	-0.69897	3.9136	5.044529277	1.11E+05	-0.0306	0.0009
54.4	130 ºF	1	379	54.9693027	5.50E+04	4.7401	1	0	4.6125	4.789085463	6.15E+04	-0.0490	0.0024
54.4	130 ºF	0.5	300	43.5113214	4.35E+04	4.6386	2	0.30103	4.9136	4.672974589	4.71E+04	-0.0344	0.0012
54.4	130 ºF	0.1	187	27.12205701	2.71E+04	4.4333	10	1	5.6125	4.389831124	2.45E+04	0.0435	0.0019
											ΣE	**0.0006**	**0.0287**
												Unbiased	Biased

Table 89: Predicted Curve Data for Replicate 3 Using ABS Studs.

Log Red Time, t_r	**Reduced Frequency, f_r**	**Predicted**	
		Log E* psi	**E* psi**
-8	8	6.9313	8,537,024
-7	7	6.8849	7,672,339
-6	6	6.8279	6,727,692
-5	5	6.7579	5,726,057
-4	4	6.6723	4,701,653
-3	3	6.5680	3,698,387
-2	2	6.4417	2,765,207
-1	1	6.2897	1,948,365
0	0	6.1079	1,282,121
1	-1	5.8926	780,941
2	-2	5.6402	436,705
3	-3	5.3478	222,762
4	-4	5.0140	103,282
5	-5	4.6390	43,548
6	-6	4.2251	16,794
7	-7	3.7776	5,992
8	-8	3.3039	2,013

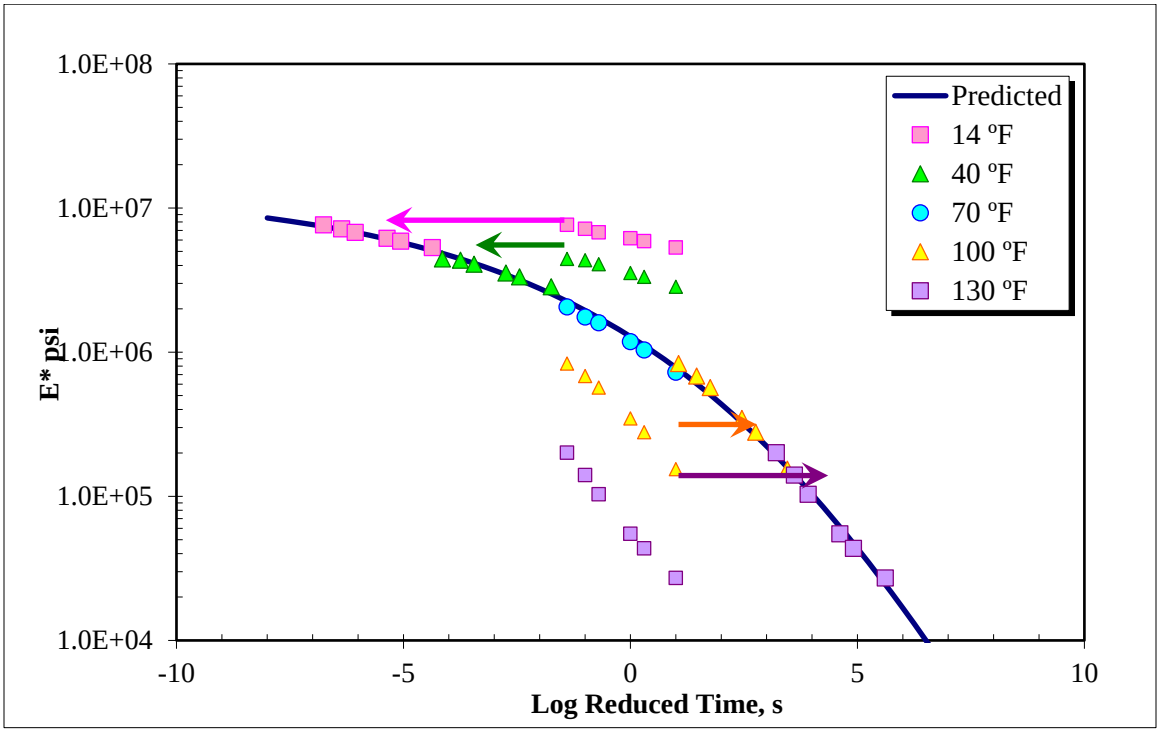

Figure 77: Initial Master Curve for Replicate 3 Using ABS Studs

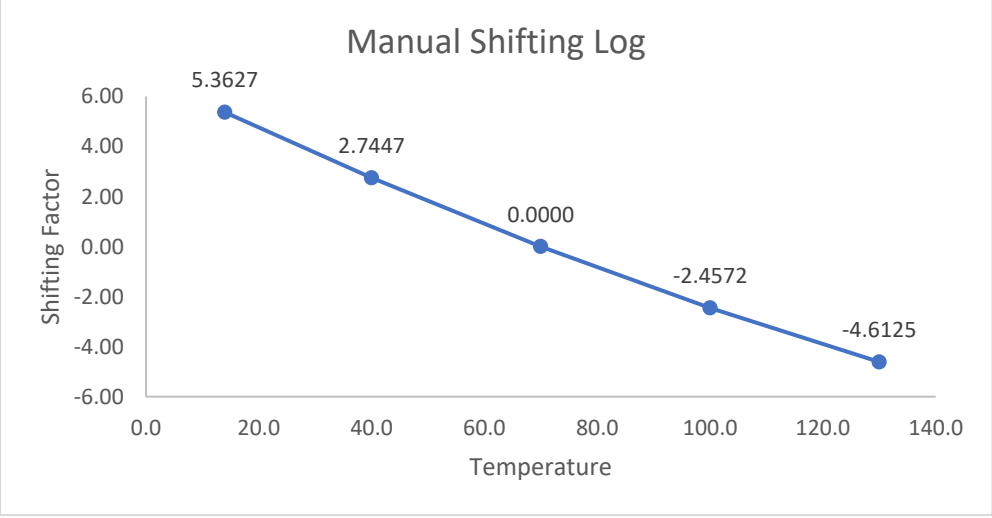

Figure 78: Manual Shifting Log for Replicate 3 Using ABS Studs.

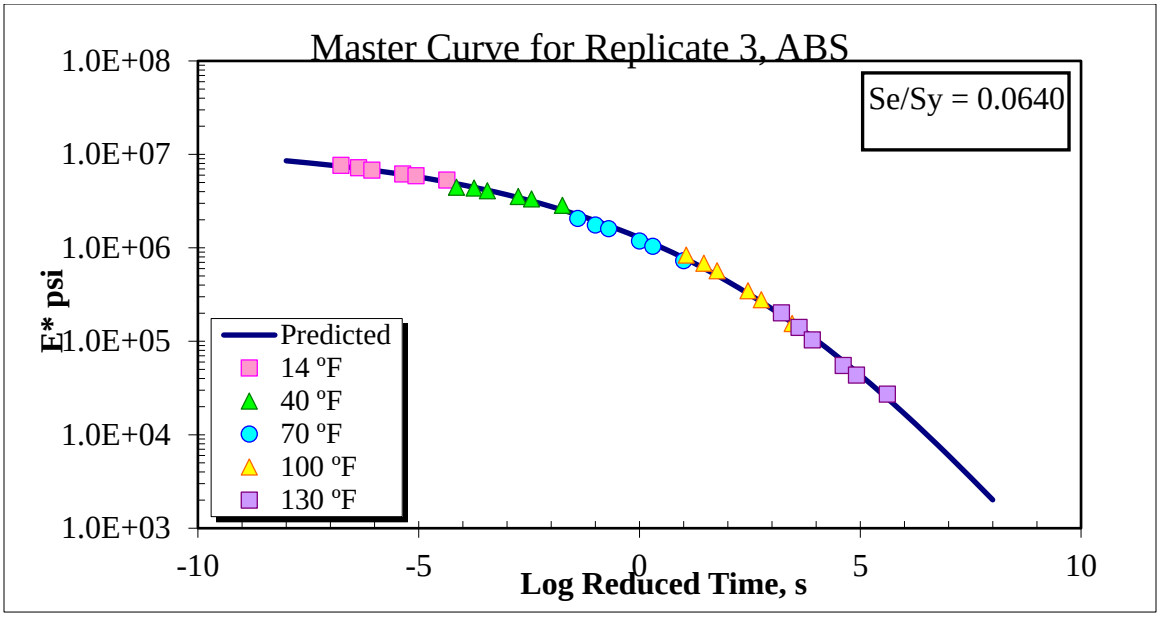

Figure 79: Final Master Curve for Replicate 3 Using ABS Studs.

Replicate 1 – CB1 PC

Table 90: Master Curve Data for Replicate 1 with PC Studs

PC													
Temp, °C	Temp, °F	Frequency Hz	E* Mpa	E* ksi	E* psi	Log E* psi	Time, t s	Log Time s	Log Red Time, t_r	Pred Log E* psi	Pred E* psi	Error	Error^2
-10.0	14 ºF	25	41342	5996.150165	6.00E+06	6.7779	0.04	-1.397940009	-6.0048	6.7748	5.95E+06	0.0031	0.0000
-10.0	14 ºF	10	38436	5574.670498	5.57E+06	6.7462	0.1	-1	-5.6069	6.7594	5.75E+06	-0.0132	0.0002
-10.0	14 ºF	5	37691	5466.617383	5.47E+06	6.7377	0.2	-0.698970004	-5.3059	6.7464	5.58E+06	-0.0087	0.0001
-10.0	14 ºF	1	34970	5071.969698	5.07E+06	6.7052	1	0	-4.6069	6.7104	5.13E+06	-0.0052	0.0000
-10.0	14 ºF	0.5	33822	4905.466375	4.91E+06	6.6907	2	0.301029996	-4.3059	6.6921	4.92E+06	-0.0014	0.0000
-10.0	14 ºF	0.1	31450	4561.43686	4.56E+06	6.6591	10	1	-3.6069	6.6419	4.38E+06	0.0172	0.0003
4.4	40 ºF	25	31430	4558.536106	4.56E+06	6.6588	0.04	-1.397940009	-3.8288	6.6591	4.56E+06	-0.0002	0.0000
4.4	40 ºF	10	30534	4428.582292	4.43E+06	6.6463	0.1	-1	-3.4309	6.6274	4.24E+06	0.0189	0.0004
4.4	40 ºF	5	28756	4170.705194	4.17E+06	6.6202	0.2	-0.698970004	-3.1299	6.6006	3.99E+06	0.0196	0.0004
4.4	40 ºF	1	24585	3565.752789	3.57E+06	6.5522	1	0	-2.4309	6.5280	3.37E+06	0.0241	0.0006
4.4	40 ºF	0.5	23108	3351.53205	3.35E+06	6.5252	2	0.301029996	-2.1299	6.4918	3.10E+06	0.0334	0.0011
4.4	40 ºF	0.1	19833	2876.533458	2.88E+06	6.4589	10	1	-1.4309	6.3948	2.48E+06	0.0641	0.0041
21.1	70 ºF	25	14333	2078.825899	2.08E+06	6.3178	0.04	-1.397940009	-1.3979	6.3897	2.45E+06	-0.0719	0.0052
21.1	70 ºF	10	13034	1890.421877	1.89E+06	6.2766	0.1	-1	-1.0000	6.3252	2.11E+06	-0.0487	0.0024
21.1	70 ºF	5	11229	1628.62876	1.63E+06	6.2118	0.2	-0.698970004	-0.6990	6.2719	1.87E+06	-0.0601	0.0036
21.1	70 ºF	1	8423	1221.652867	1.22E+06	6.0869	1	0	0.0000	6.1327	1.36E+06	-0.0457	0.0021
21.1	70 ºF	0.5	7357	1067.042639	1.07E+06	6.0282	2	0.301029996	0.3010	6.0659	1.16E+06	-0.0377	0.0014
21.1	70 ºF	0.1	5167	749.4099923	7.49E+05	5.8747	10	1	1.0000	5.8954	7.86E+05	-0.0206	0.0004
38.7	100 ºF	25	6049	877.3332772	8.77E+05	5.9432	0.04	-1.397940009	0.9554	5.9069	8.07E+05	0.0363	0.0013
38.7	100 ºF	10	4778	692.9903122	6.93E+05	5.8407	0.1	-1	1.3533	5.8013	6.33E+05	0.0394	0.0016
38.7	100 ºF	5	3931	570.1433481	5.70E+05	5.7560	0.2	-0.698970004	1.6544	5.7174	5.22E+05	0.0386	0.0015
38.7	100 ºF	1	2400	348.0905712	3.48E+05	5.5417	1	0	2.3533	5.5112	3.24E+05	0.0305	0.0009
38.7	100 ºF	0.5	1875	271.9457588	2.72E+05	5.4345	2	0.301029996	2.6544	5.4184	2.62E+05	0.0161	0.0003
38.7	100 ºF	0.1	1049	152.1445872	1.52E+05	5.1823	10	1	3.3533	5.1976	1.58E+05	-0.0154	0.0002
54.4	130 ºF	25	1342	194.6406444	1.95E+05	5.2892	0.04	-1.397940009	3.2171	5.2410	1.74E+05	0.0482	0.0023
54.4	130 ºF	10	943	136.7705869	1.37E+05	5.1360	0.1	-1	3.6151	5.1141	1.30E+05	0.0219	0.0005
54.4	130 ºF	5	710	102.976794	1.03E+05	5.0127	0.2	-0.698970004	3.9161	5.0182	1.04E+05	-0.0055	0.0000
54.4	130 ºF	1	393	56.99983104	5.70E+04	4.7559	1	0	4.6151	4.7995	6.30E+04	-0.0437	0.0019
54.4	130 ºF	0.5	317	45.97696295	4.60E+04	4.6625	2	0.301029996	4.9161	4.7083	5.11E+04	-0.0458	0.0021
54.4	130 ºF	0.1	228	33.06860427	3.31E+04	4.5194	10	1	5.6151	4.5069	3.21E+04	0.0125	0.0002
											ΣE	**0.0000**	**0.0350**
												Unbiased	Biased

Table 91: Predicted Curve Data for Replicate 1 Using PC Studs

Log Red Time, t_r	**Reduced Frequency, f_r**	**Predicted**	
		Log E* psi	**E* psi**
-8	8	6.8263	6,702,874
-7	7	6.8049	6,381,818
-6	6	6.7746	5,951,035
-5	5	6.7317	5,390,876
-4	4	6.6715	4,693,450
-3	3	6.5883	3,874,924
-2	2	6.4752	2,986,632
-1	1	6.3252	2,114,616
0	0	6.1327	1,357,305
1	-1	5.8954	785,892
2	-2	5.6172	414,238
3	-3	5.3099	204,141
4	-4	4.9916	98,092
5	-5	4.6833	48,231
6	-6	4.4035	25,321
7	-7	4.1641	14,590
8	-8	3.9694	9,319

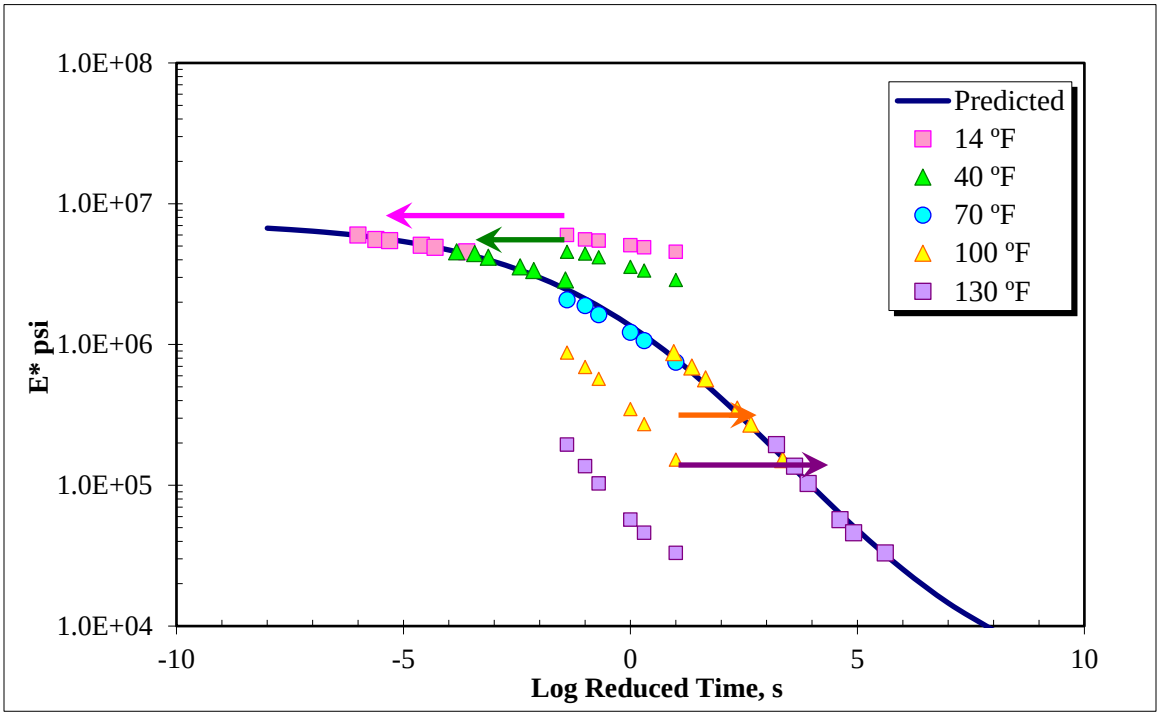

Figure 80: Initial Master Curve for Replicate 1 Using PC Studs

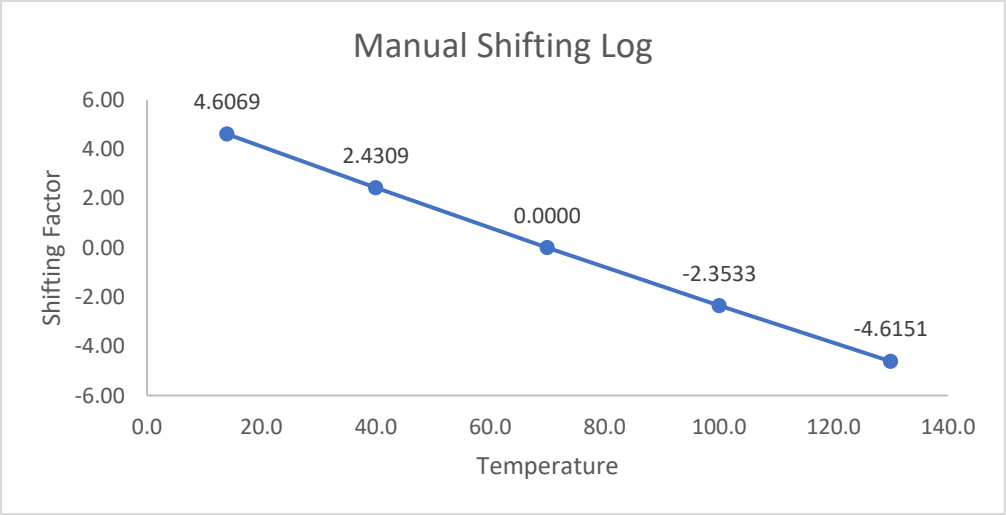

Figure 81: Manual Shifting Log for Replicate 1 Using PC Studs

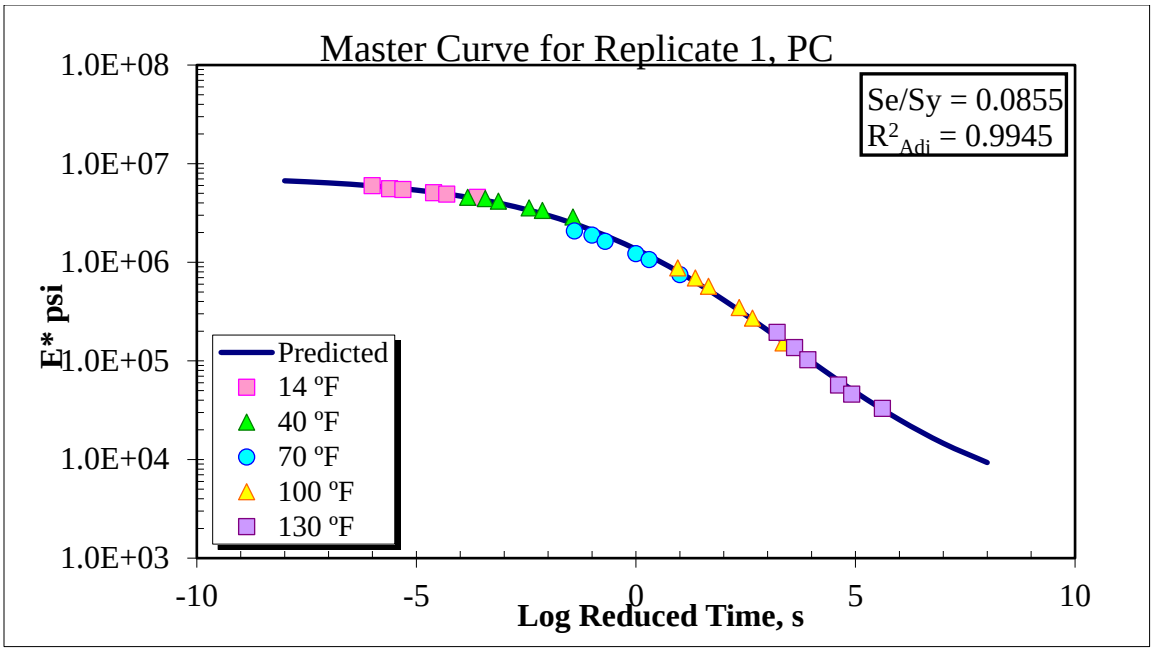

Figure 82: Final Master Curve for Replicate 1 Using PC Studs

Replicate 2 – CB3 PC

Table 92: Master Curve Data for Replicate 2 with PC Studs

PC													
Temp, °C	Temp, °F	Frequency Hz	E* Mpa	E* ksi	E* psi	Log E* psi	Time, t s	Log Time s	Log Red Time, t_r	Pred Log E* psi	Pred E* psi	Error	Error^2
-10.0	14 ºF	25	44204	6411.248171	6.41E+06	6.8069	0.04	-1.39794	-6.8954	6.7882	6.14E+06	0.0187	0.0004
-10.0	14 ºF	10	41131.5	5965.619721	5.97E+06	6.7757	0.1	-1	-6.4974	6.7756	5.97E+06	0.0000	0.0000
-10.0	14 ºF	5	39892	5785.845445	5.79E+06	6.7624	0.2	-0.69897	-6.1964	6.7650	5.82E+06	-0.0026	0.0000
-10.0	14 ºF	1	36985.5	5364.293259	5.36E+06	6.7295	1	0	-5.4974	6.7362	5.45E+06	-0.0067	0.0000
-10.0	14 ºF	0.5	35745	5184.373945	5.18E+06	6.7147	2	0.30103	-5.1964	6.7218	5.27E+06	-0.0071	0.0001
-10.0	14 ºF	0.1	32843.5	4763.546948	4.76E+06	6.6779	10	1	-4.4974	6.6829	4.82E+06	-0.0049	0.0000
4.4	40 ºF	25	31836.5	4617.493946	4.62E+06	6.6644	0.04	-1.39794	-4.1668	6.6614	4.59E+06	0.0030	0.0000
4.4	40 ºF	10	30096.5	4365.128282	4.37E+06	6.6400	0.1	-1	-3.7689	6.6328	4.29E+06	0.0072	0.0001
4.4	40 ºF	5	28537	4138.94193	4.14E+06	6.6169	0.2	-0.69897	-3.4679	6.6088	4.06E+06	0.0081	0.0001
4.4	40 ºF	1	24313.5	3526.375043	3.53E+06	6.5473	1	0	-2.7689	6.5446	3.50E+06	0.0027	0.0000
4.4	40 ºF	0.5	22879	3318.318408	3.32E+06	6.5209	2	0.30103	-2.4679	6.5129	3.26E+06	0.0081	0.0001
4.4	40 ºF	0.1	19568.5	2838.170976	2.84E+06	6.4530	10	1	-1.7689	6.4285	2.68E+06	0.0245	0.0006
21.1	70 ºF	25	15058	2183.978259	2.18E+06	6.3392	0.04	-1.39794	-1.3979	6.3771	2.38E+06	-0.0378	0.0014
21.1	70 ºF	10	13571.5	1968.379661	1.97E+06	6.2941	0.1	-1	-1.0000	6.3163	2.07E+06	-0.0222	0.0005
21.1	70 ºF	5	11932.5	1730.662809	1.73E+06	6.2382	0.2	-0.69897	-0.6990	6.2663	1.85E+06	-0.0281	0.0008
21.1	70 ºF	1	9051.5	1312.809086	1.31E+06	6.1182	1	0	0.0000	6.1357	1.37E+06	-0.0175	0.0003
21.1	70 ºF	0.5	7936.5	1151.092008	1.15E+06	6.0611	2	0.30103	0.3010	6.0730	1.18E+06	-0.0119	0.0001
21.1	70 ºF	0.1	5625.5	815.9097952	8.16E+05	5.9116	10	1	1.0000	5.9116	8.16E+05	0.0001	0.0000
38.7	100 ºF	25	6070.5	880.4515886	8.80E+05	5.9447	0.04	-1.39794	0.9726	5.9183	8.29E+05	0.0264	0.0007
38.7	100 ºF	10	4832	700.8223501	7.01E+05	5.8456	0.1	-1	1.3705	5.8170	6.56E+05	0.0287	0.0008
38.7	100 ºF	5	3997	579.7158388	5.80E+05	5.7632	0.2	-0.69897	1.6716	5.7355	5.44E+05	0.0277	0.0008
38.7	100 ºF	1	2445	354.6172694	3.55E+05	5.5498	1	0	2.3705	5.5312	3.40E+05	0.0186	0.0003
38.7	100 ºF	0.5	1905	276.2968909	2.76E+05	5.4414	2	0.30103	2.6716	5.4370	2.74E+05	0.0044	0.0000
38.7	100 ºF	0.1	1062	154.0300778	1.54E+05	5.1876	10	1	3.3705	5.2057	1.61E+05	-0.0181	0.0003
54.4	130 ºF	25	1647	238.8771545	2.39E+05	5.3782	0.04	-1.39794	2.9310	5.3531	2.25E+05	0.0251	0.0006
54.4	130 ºF	10	1145	166.06821	1.66E+05	5.2203	0.1	-1	3.3289	5.2199	1.66E+05	0.0003	0.0000
54.4	130 ºF	5	856.5	124.2248226	1.24E+05	5.0942	0.2	-0.69897	3.6300	5.1161	1.31E+05	-0.0219	0.0005
54.4	130 ºF	1	466.5	67.66010478	6.77E+04	4.8303	1	0	4.3289	4.8669	7.36E+04	-0.0366	0.0013
54.4	130 ºF	0.5	366	53.08381211	5.31E+04	4.7250	2	0.30103	4.6300	4.7573	5.72E+04	-0.0323	0.0010
54.4	130 ºF	0.1	242.5	35.17165147	3.52E+04	4.5462	10	1	5.3289	4.5010	3.17E+04	0.0452	0.0020
												ΣE	**0.0010**	**0.0130**
													Unbiased	Biased

Table 93: Predicted Curve Data for Replicate 2 Using PC Studs.

Log Red Time, t_r	**Reduced Frequency, f_r**	**Predicted**	
		Log E* psi	**E* psi**
-8	8	6.8161	6,547,368
-7	7	6.7913	6,184,362
-6	6	6.7575	5,721,491
-5	5	6.7117	5,148,189
-4	4	6.6498	4,465,094
-3	3	6.5672	3,691,621
-2	2	6.4581	2,871,642
-1	1	6.3163	2,071,718
0	0	6.1357	1,366,857
1	-1	5.9116	815,755
2	-2	5.6421	438,629
3	-3	5.3304	213,978
4	-4	4.9853	96,682
5	-5	4.6217	41,847
6	-6	4.2575	18,094
7	-7	3.9113	8,152
8	-8	3.5977	3,960

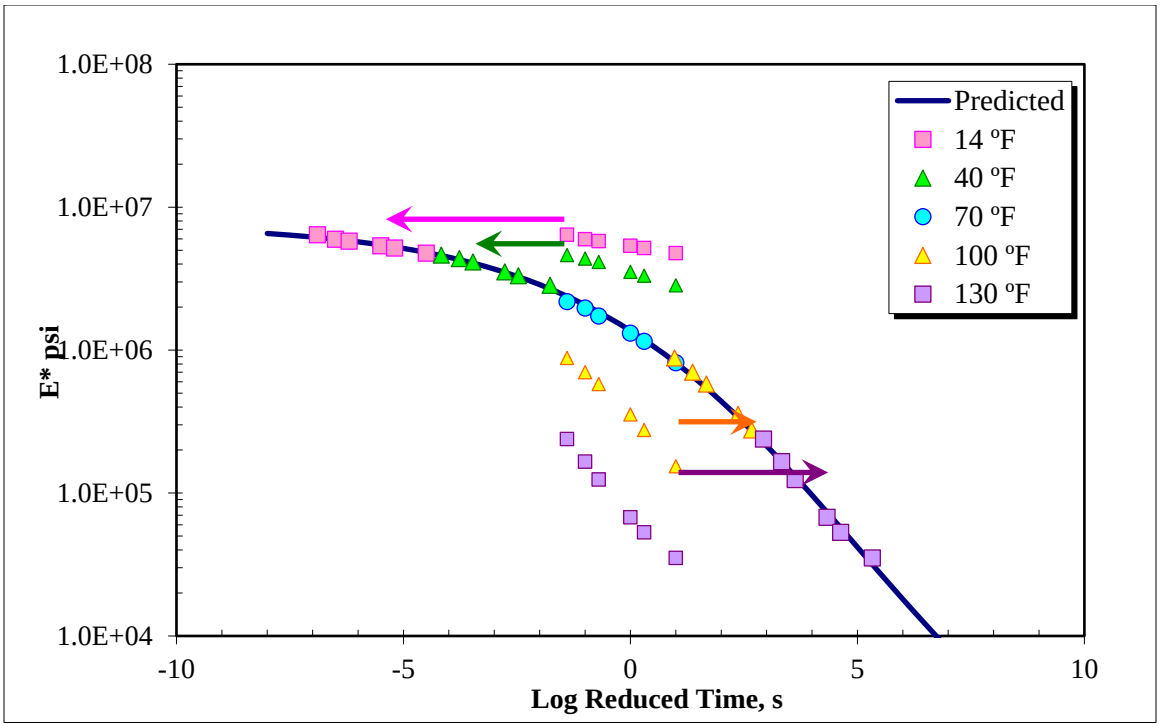

Figure 83: Initial Master Curve for Replicate 2 Using PC Studs

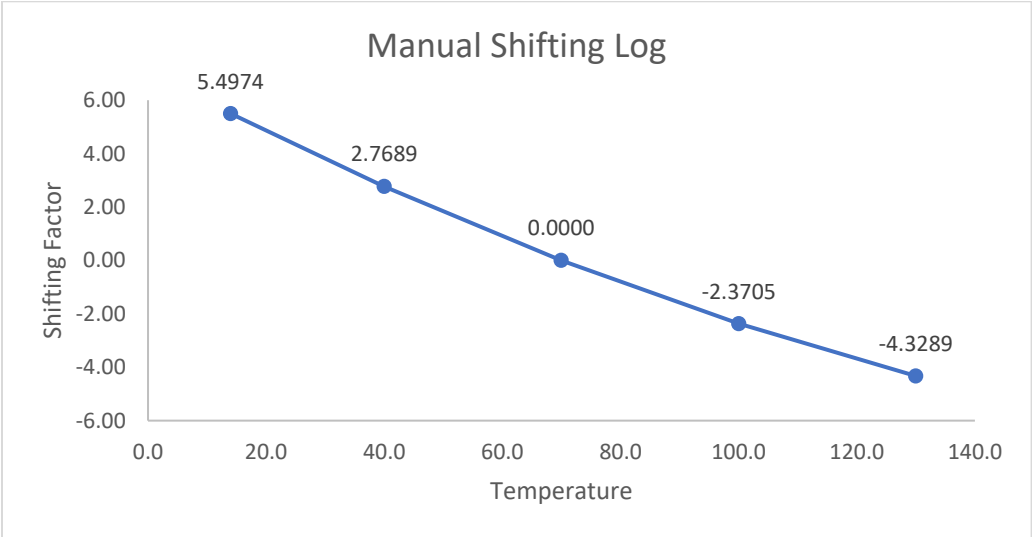

Figure 84: Manual Shifting Log for Replicate 2 Using PC Studs

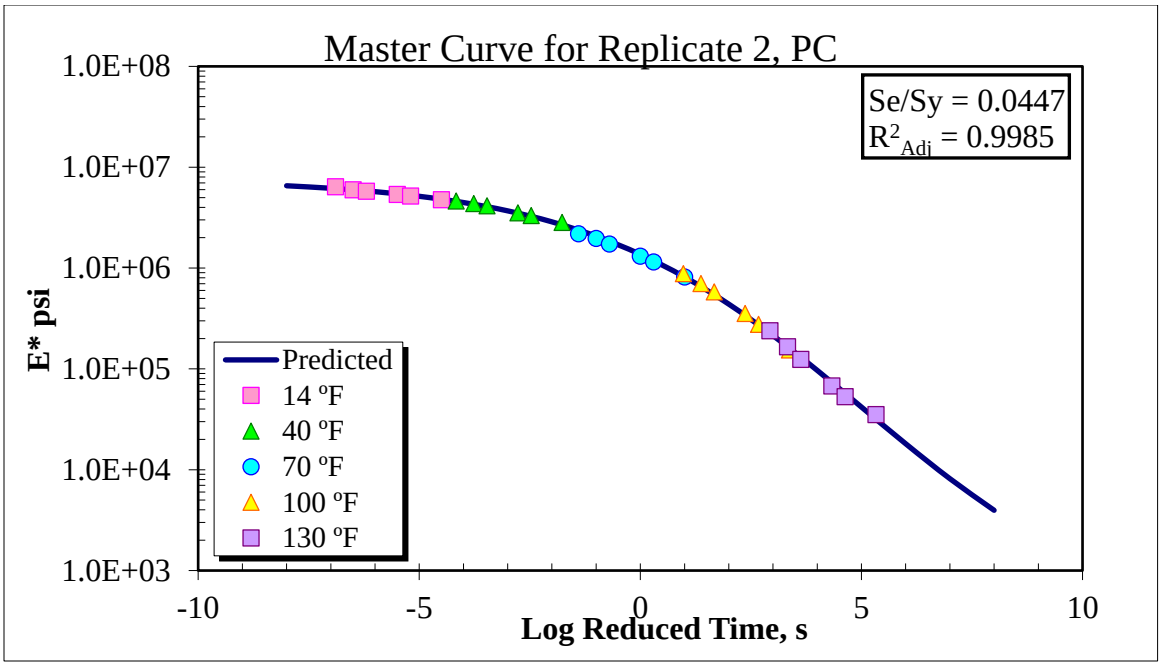

Figure 85: Final Master Curve for Replicate 2 Using PC Studs

Replicate 3 – CB10 PC

Table 94: Master Curve Data for Replicate 3 with PC Studs

PC													
Temp, °C	Temp, °F	Frequency Hz	E* Mpa	E* ksi	E* psi	Log E* psi	Time, t s	Log Time s	Log Red Time, t_r	Pred Log E* psi	Pred E* psi	Error	Error^2
-10.0	14 °F	25	47066	6826.346177	6.83E+06	6.8342	0.04	-1.39794	-6.9889	6.8077	6.42E+06	0.0265	0.0007
-10.0	14 °F	10	43827	6356.568944	6.36E+06	6.8032	0.1	-1	-6.5910	6.7947	6.23E+06	0.0085	0.0001
-10.0	14 °F	5	42093	6105.073506	6.11E+06	6.7857	0.2	-0.69897	-6.2900	6.7839	6.08E+06	0.0018	0.0000
-10.0	14 °F	1	39001	5656.61682	5.66E+06	6.7526	1	0	-5.5910	6.7545	5.68E+06	-0.0020	0.0000
-10.0	14 °F	0.5	37668	5463.281515	5.46E+06	6.7375	2	0.30103	-5.2900	6.7399	5.49E+06	-0.0025	0.0000
-10.0	14 °F	0.1	34237	4965.657036	4.97E+06	6.6960	10	1	-4.5910	6.7007	5.02E+06	-0.0047	0.0000
4.4	40 °F	25	32243	4676.451787	4.68E+06	6.6699	0.04	-1.39794	-4.1817	6.6738	4.72E+06	-0.0039	0.0000
4.4	40 °F	10	29659	4301.674272	4.30E+06	6.6336	0.1	-1	-3.7838	6.6446	4.41E+06	-0.0109	0.0001
4.4	40 °F	5	28318	4107.178665	4.11E+06	6.6135	0.2	-0.69897	-3.4827	6.6202	4.17E+06	-0.0066	0.0000
4.4	40 °F	1	24042	3486.997297	3.49E+06	6.5425	1	0	-2.7838	6.5551	3.59E+06	-0.0126	0.0002
4.4	40 °F	0.5	22650	3285.104766	3.29E+06	6.5165	2	0.30103	-2.4827	6.5231	3.33E+06	-0.0065	0.0000
4.4	40 °F	0.1	19304	2799.808494	2.80E+06	6.4471	10	1	-1.7838	6.4382	2.74E+06	0.0089	0.0001
21.1	70 °F	25	15783	2289.130619	2.29E+06	6.3597	0.04	-1.39794	-1.3979	6.3844	2.42E+06	-0.0248	0.0006
21.1	70 °F	10	14109	2046.337446	2.05E+06	6.3110	0.1	-1	-1.0000	6.3234	2.11E+06	-0.0124	0.0002
21.1	70 °F	5	12636	1832.696857	1.83E+06	6.2631	0.2	-0.69897	-0.6990	6.2731	1.88E+06	-0.0100	0.0001
21.1	70 °F	1	9680	1403.965304	1.40E+06	6.1474	1	0	0.0000	6.1421	1.39E+06	0.0053	0.0000
21.1	70 °F	0.5	8516	1235.141377	1.24E+06	6.0917	2	0.30103	0.3010	6.0791	1.20E+06	0.0126	0.0002
21.1	70 °F	0.1	6084	882.409598	8.82E+05	5.9457	10	1	1.0000	5.9168	8.26E+05	0.0289	0.0008
38.7	100 °F	25	6092	883.5698999	8.84E+05	5.9462	0.04	-1.39794	0.9059	5.9400	8.71E+05	0.0063	0.0000
38.7	100 °F	10	4886	708.6543879	7.09E+05	5.8504	0.1	-1	1.3039	5.8390	6.90E+05	0.0114	0.0001
38.7	100 °F	5	4063	589.2883295	5.89E+05	5.7703	0.2	-0.69897	1.6049	5.7576	5.72E+05	0.0127	0.0002
38.7	100 °F	1	2490	361.1439676	3.61E+05	5.5577	1	0	2.3039	5.5520	3.56E+05	0.0056	0.0000
38.7	100 °F	0.5	1935	280.648023	2.81E+05	5.4482	2	0.30103	2.6049	5.4565	2.86E+05	-0.0084	0.0001
38.7	100 °F	0.1	1075	155.9155684	1.56E+05	5.1929	10	1	3.3039	5.2197	1.66E+05	-0.0268	0.0007
54.4	130 °F	25	1952	283.1136646	2.83E+05	5.4520	0.04	-1.39794	2.7165	5.4201	2.63E+05	0.0319	0.0010
54.4	130 °F	10	1347	195.3658331	1.95E+05	5.2908	0.1	-1	3.1145	5.2859	1.93E+05	0.0050	0.0000
54.4	130 °F	5	1003	145.4728512	1.45E+05	5.1628	0.2	-0.69897	3.4155	5.1801	1.51E+05	-0.0173	0.0003
54.4	130 °F	1	540	78.32037852	7.83E+04	4.8939	1	0	4.1145	4.9222	8.36E+04	-0.0284	0.0008
54.4	130 °F	0.5	415	60.19066127	6.02E+04	4.7795	2	0.30103	4.4155	4.8068	6.41E+04	-0.0272	0.0007
54.4	130 °F	0.1	257	37.27469867	3.73E+04	4.5714	10	1	5.1145	4.5316	3.40E+04	0.0398	0.0016
											ΣE	**0.0001**	**0.0088**
												Unbiased	Biased

Table 95: Predicted Curve Data for Replicate 3 Using PC Studs.

Log Red Time, t_r	**Reduced Frequency, f_r**	**Predicted**	
		Log E* psi	**E* psi**
-8	8	6.8345	6,831,594
-7	7	6.8081	6,427,738
-6	6	6.7724	5,921,251
-5	5	6.7246	5,304,085
-4	4	6.6609	4,580,077
-3	3	6.5765	3,771,748
-2	2	6.4661	2,924,827
-1	1	6.3234	2,105,610
0	0	6.1421	1,387,042
1	-1	5.9168	825,626
2	-2	5.6442	440,802
3	-3	5.3251	211,421
4	-4	4.9655	92,366
5	-5	4.5772	37,772
6	-6	4.1768	15,023
7	-7	3.7831	6,069
8	-8	3.4137	2,592

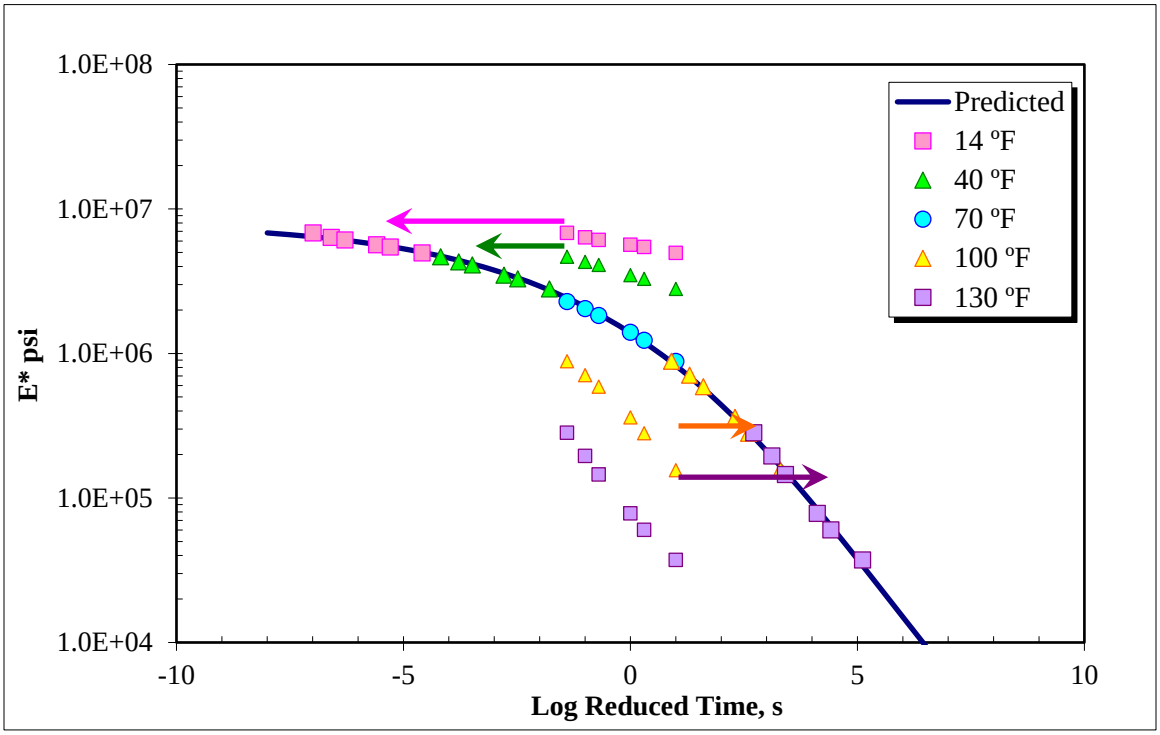

Figure 86: Initial Master Curve for Replicate 3 Using PC Studs

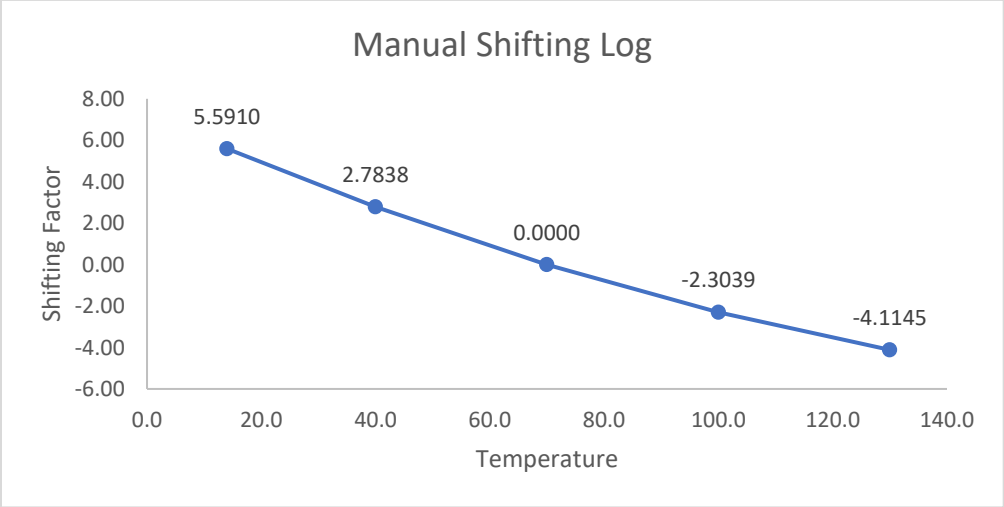

Figure 87: Manual Shifting Log for Replicate 3 Using PC Studs.

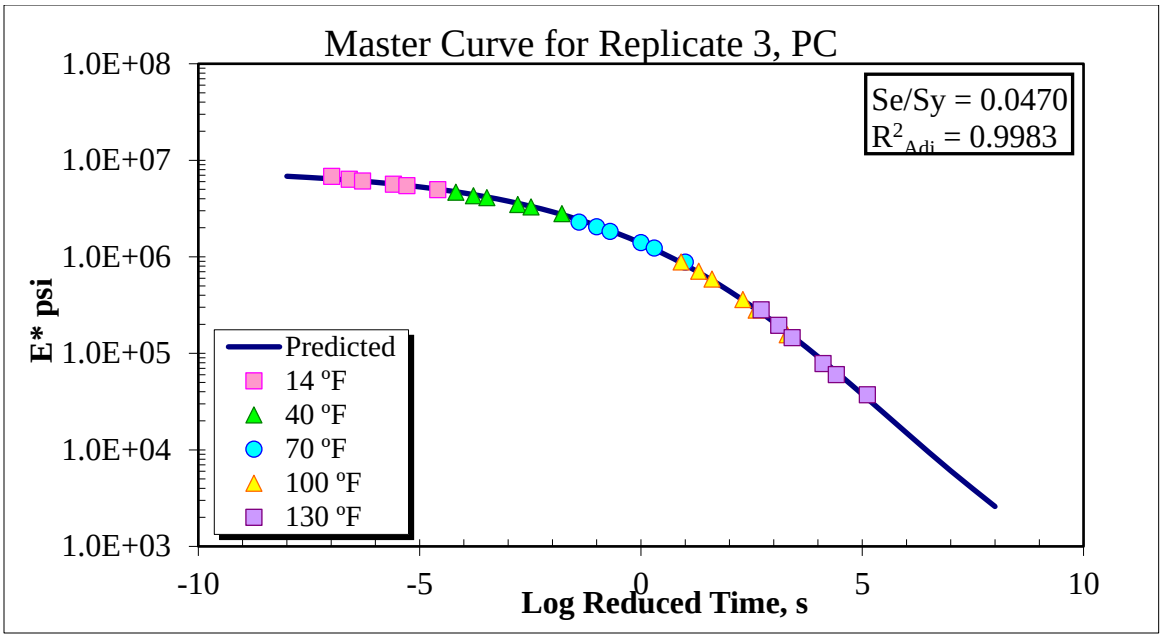

Figure 88: Final Master Curve for Replicate 3 Using PC Studs.

Flow Number

Repeated Load Permanent Deformation

Replicate 1 – CB5

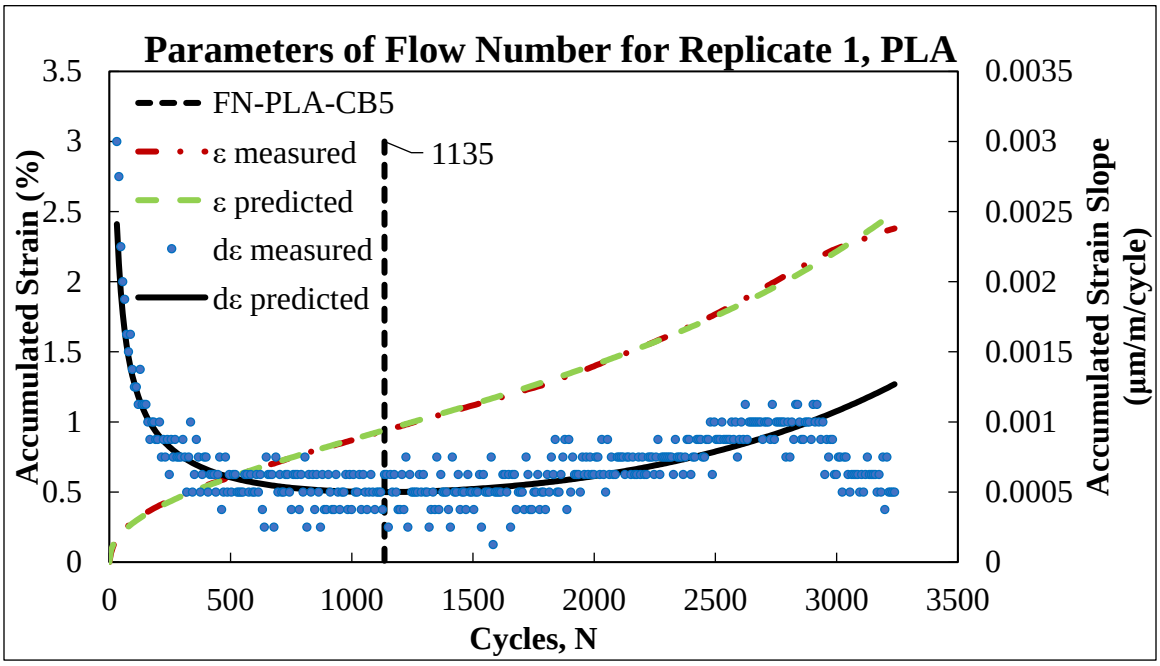

Figure 89: Parameters of Flow Number for Replicate 1, PLA

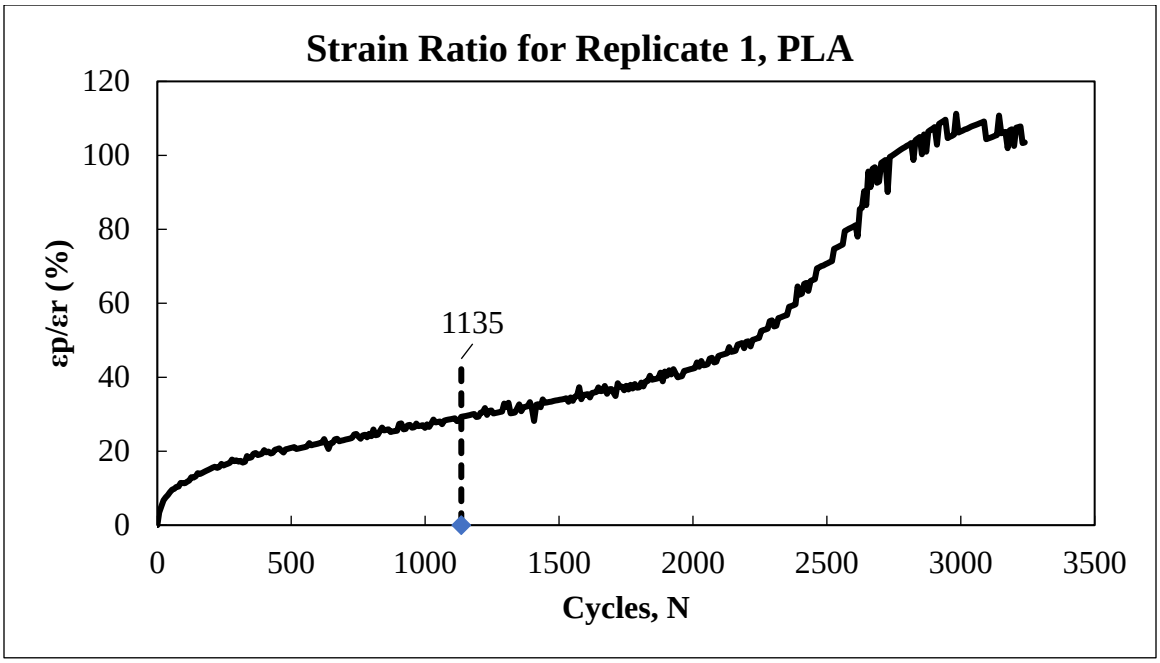

Figure 90: Strain Ratio for Replicate 1, PLA

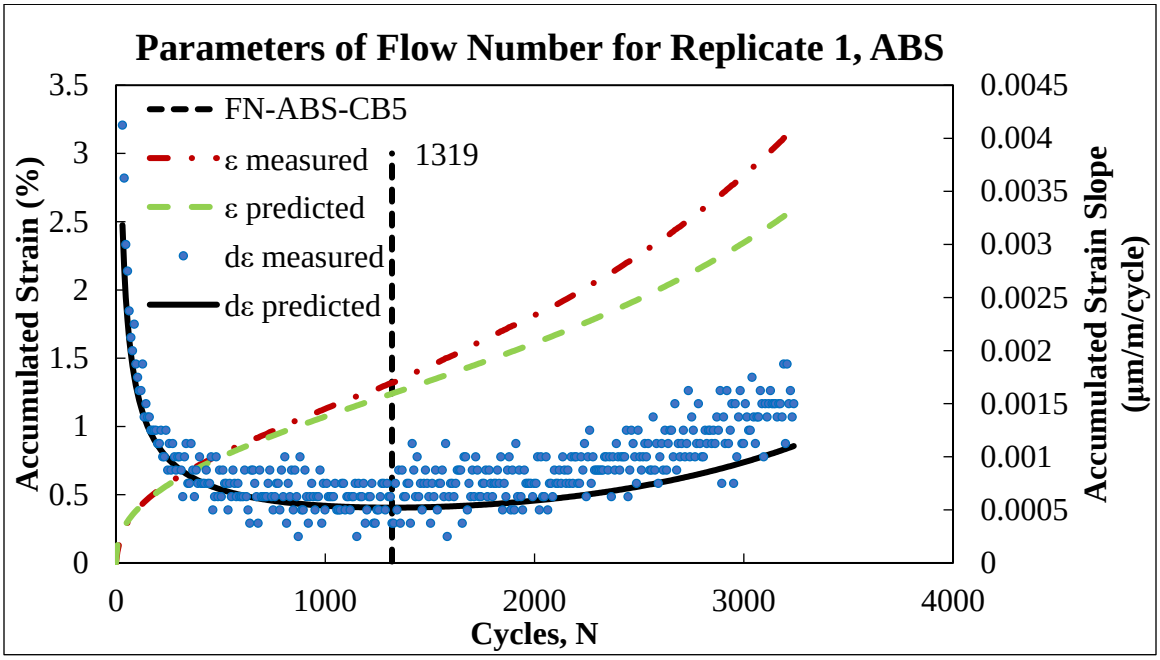

Figure 91: Parameters of Flow Number for Replicate 1, ABS

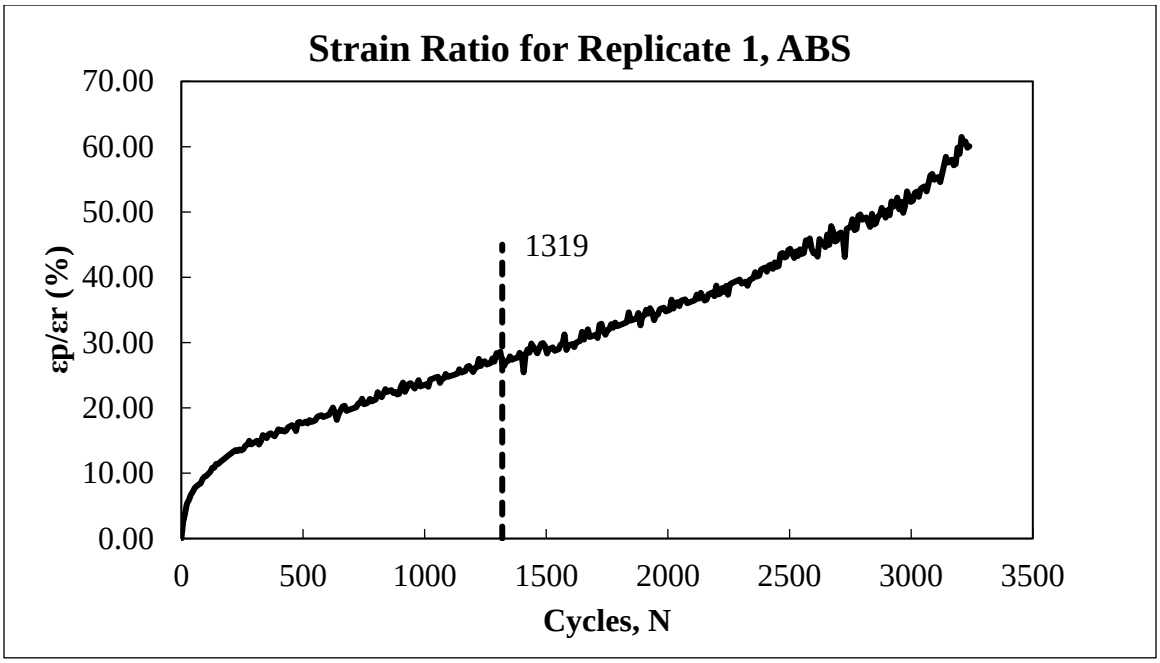

Figure 92: Strain Ratio for Replicate 1, ABS

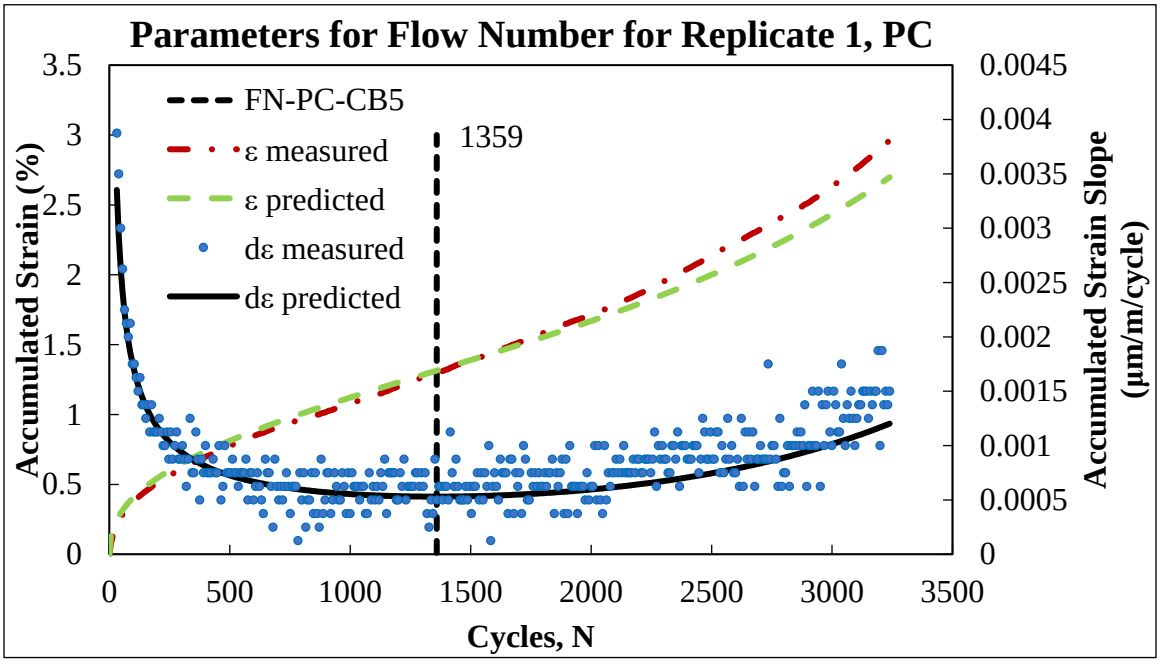

Figure 93: Parameters for Flow Number for Replicate 1, PC

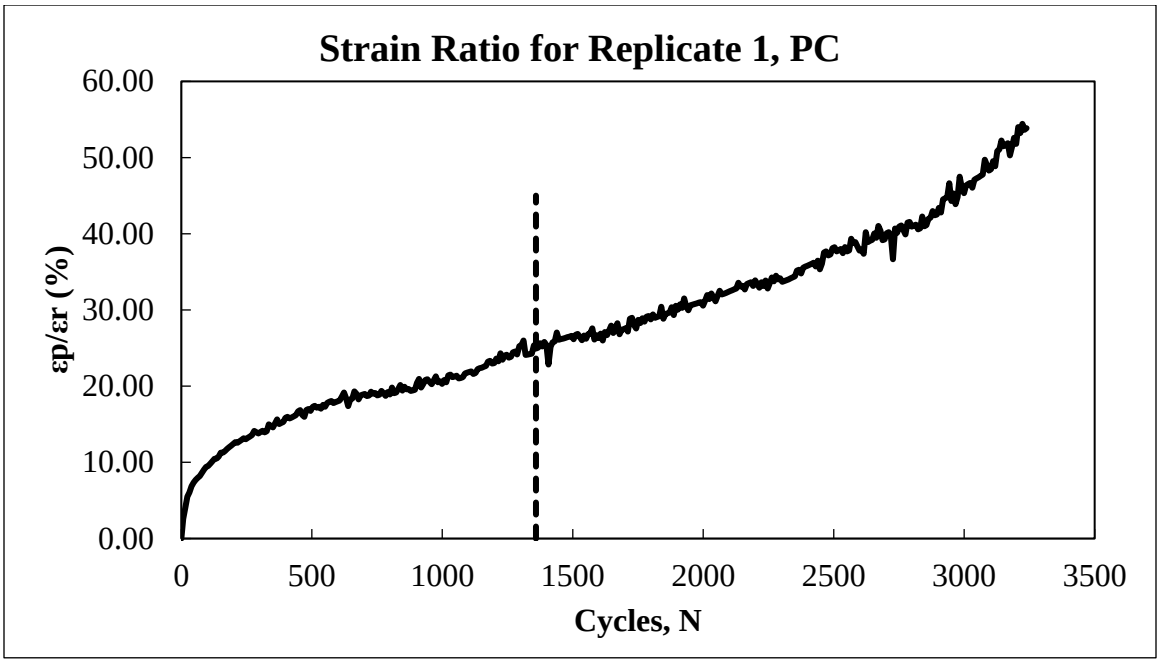

Figure 94: Strain Ratio for Replicate 1, PC

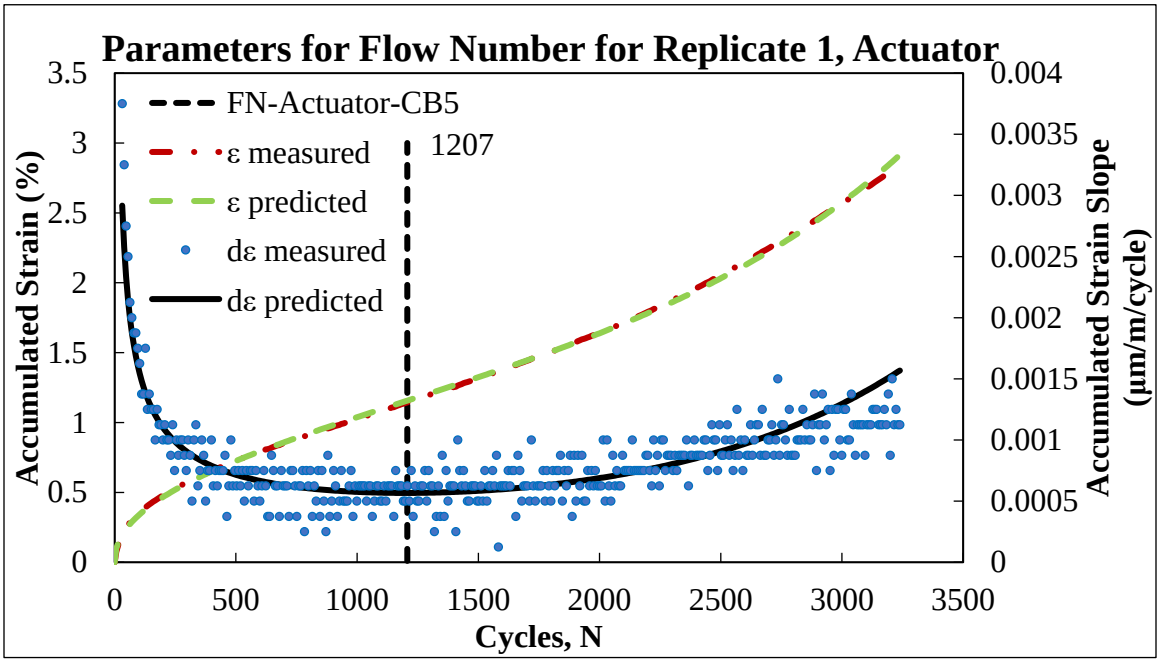

Figure 95: Parameters for Flow Number for Replicate 1, Actuator

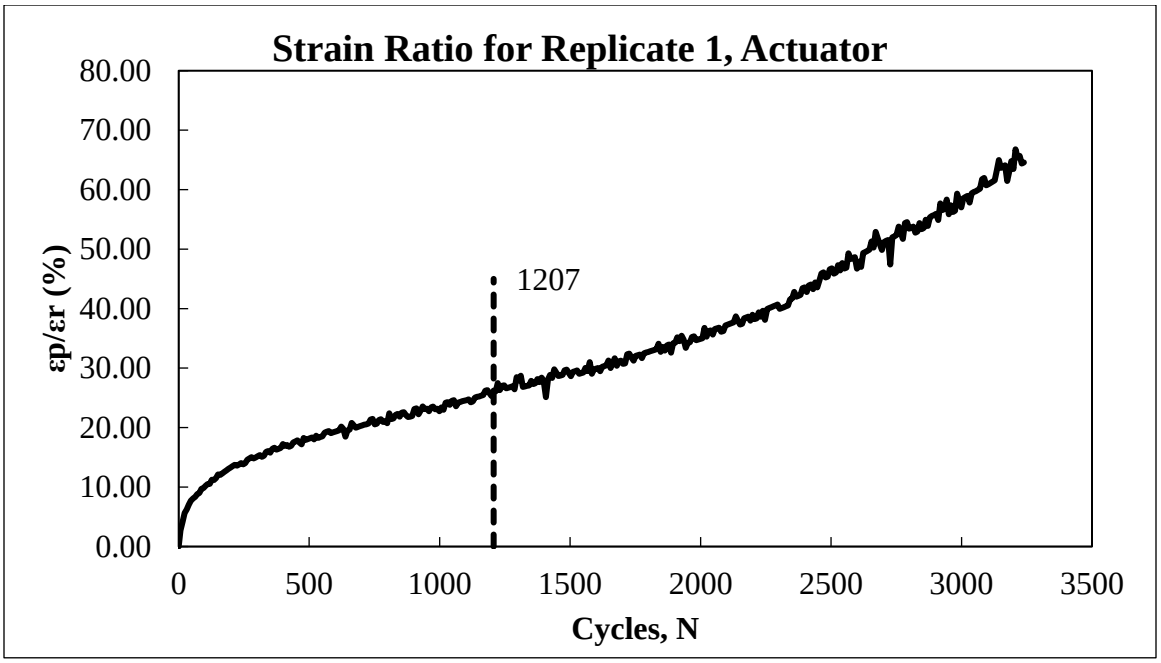

Figure 96: Strain Ratio for Replicate 1, Actuator

Replicate 2 – CB6

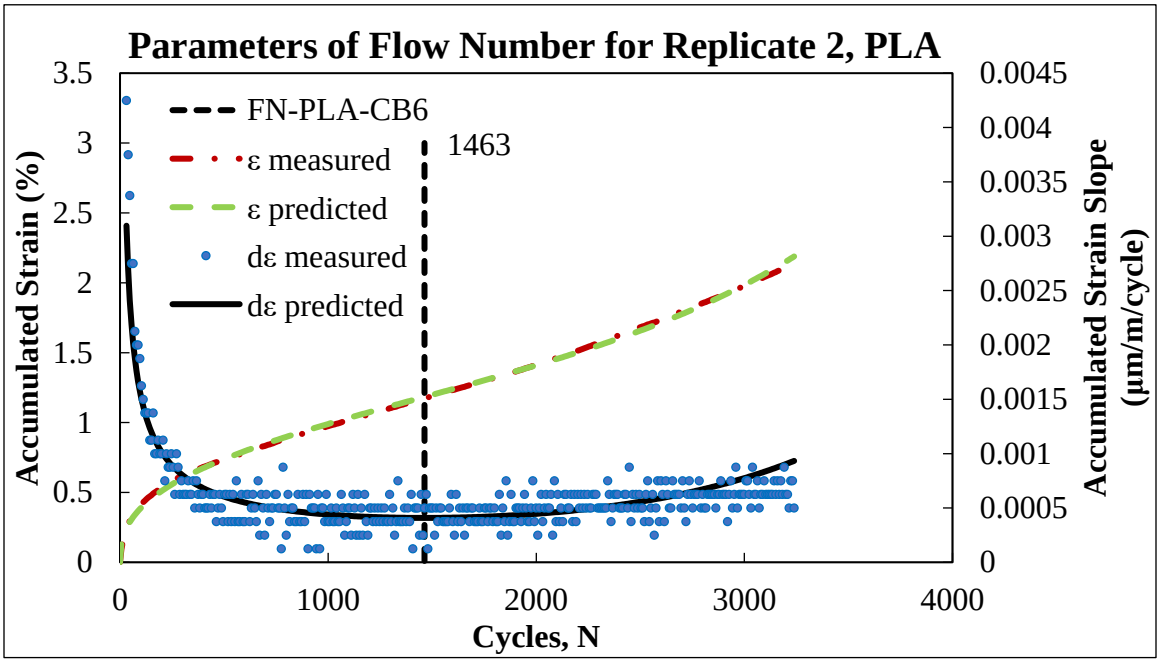

Figure 97: Parameters of Flow Number for Replicate 2, PLA

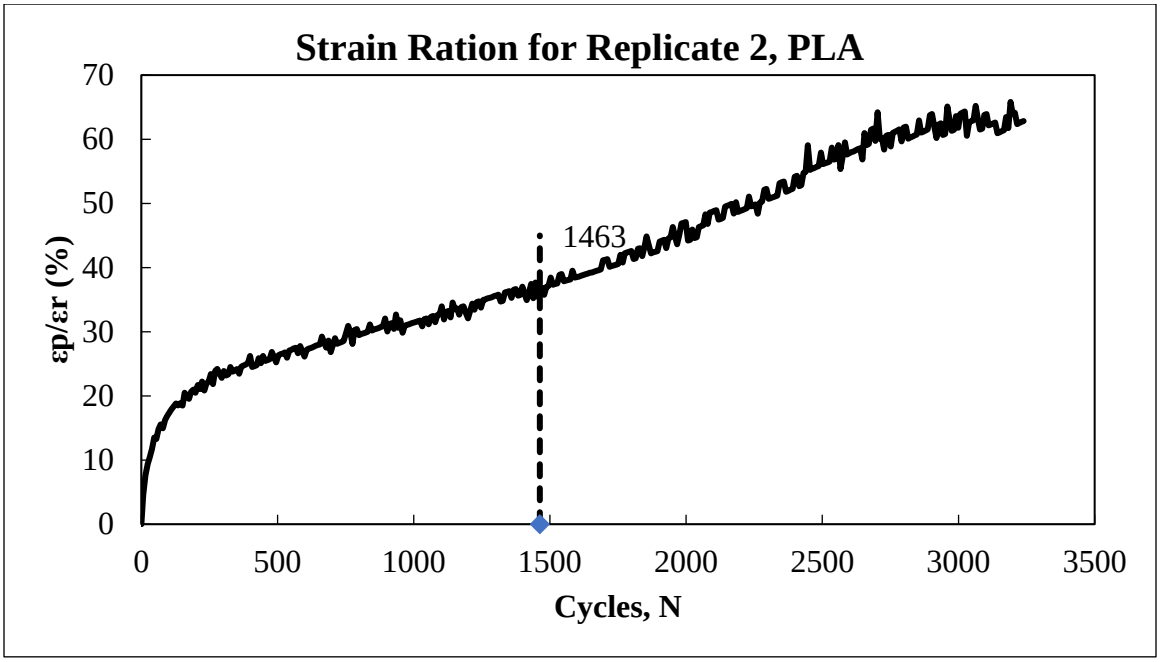

Figure 98: Strain Ration for Replicate 2, PLA

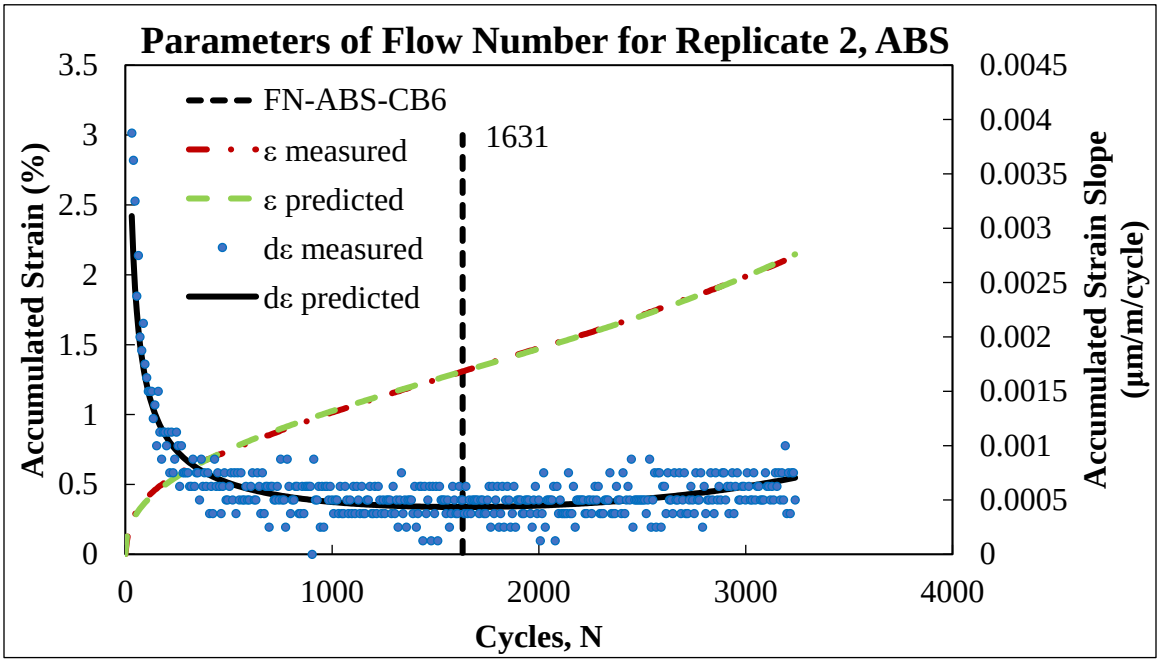

Figure 99: Parameters of Flow Number for Replicate 2, ABS

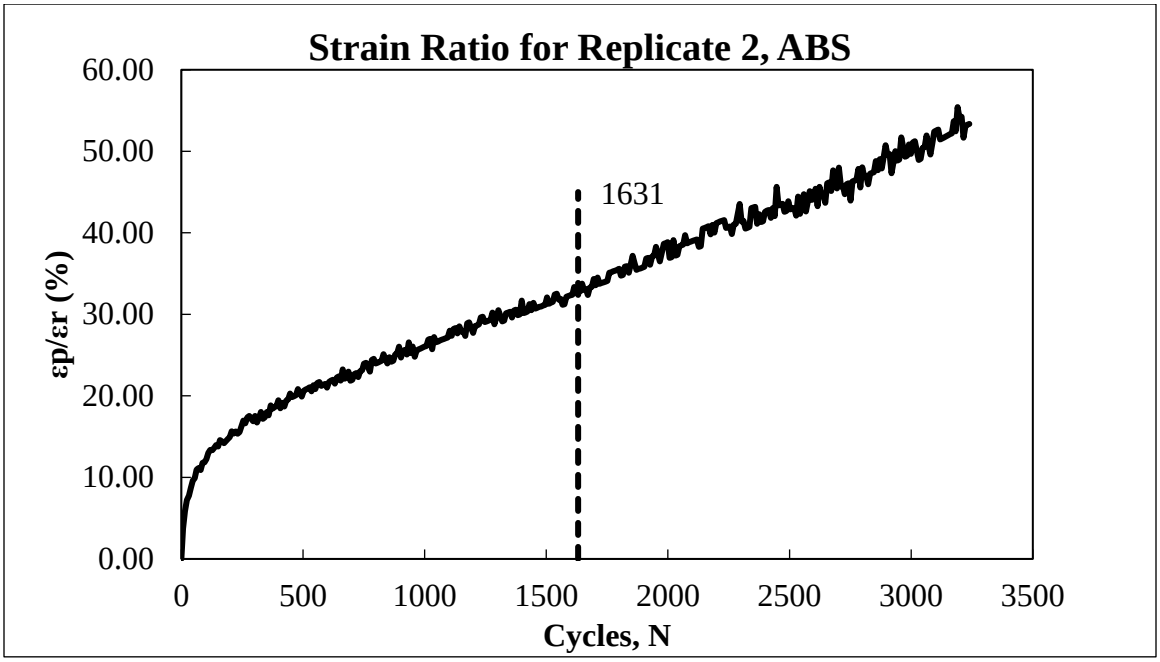

Figure 100: Strain Ratio for Replicate 2, ABS

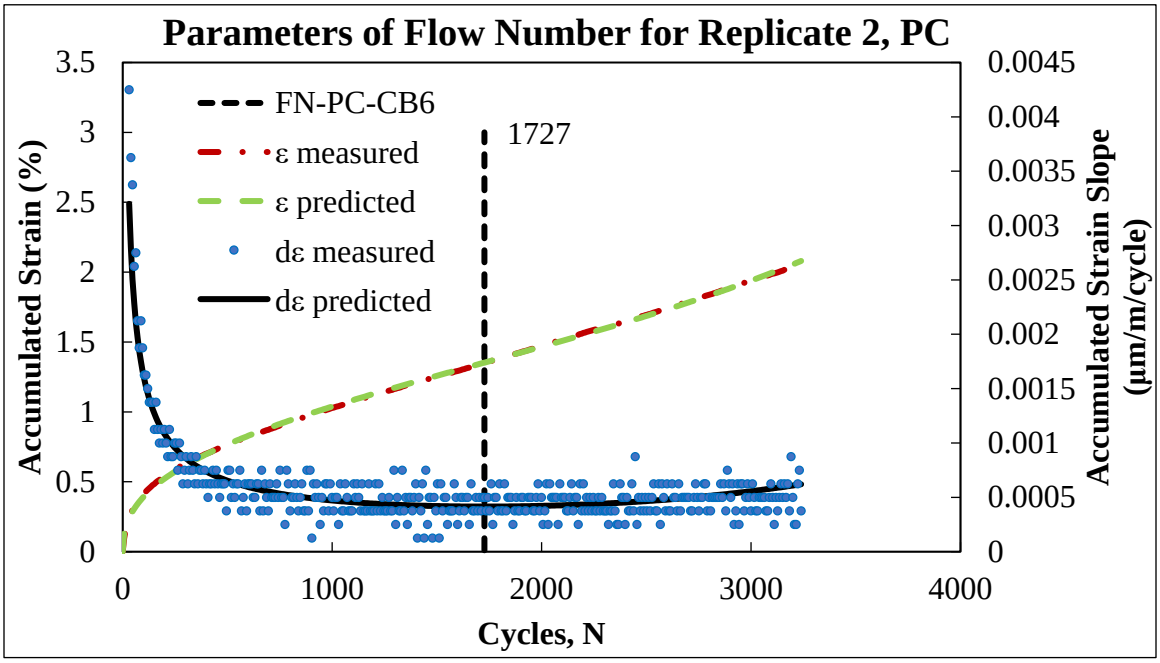

Figure 101: Parameters of Flow Number for Replicate 2, PC

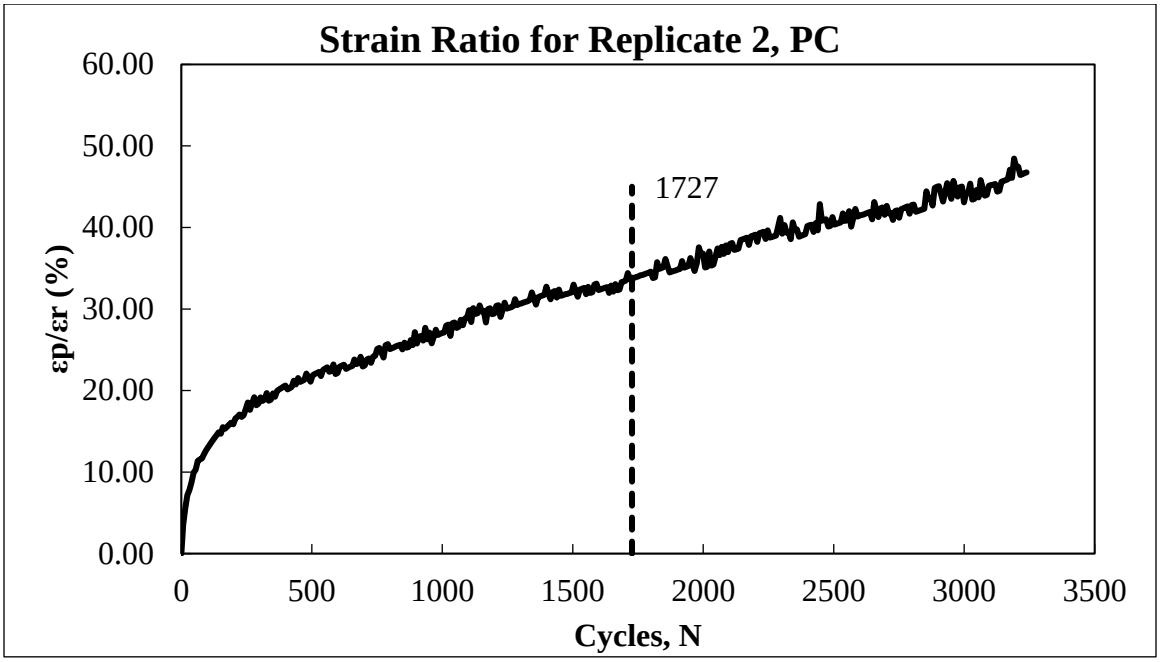

Figure 102: Strain Ratio for Replicate 2, PC

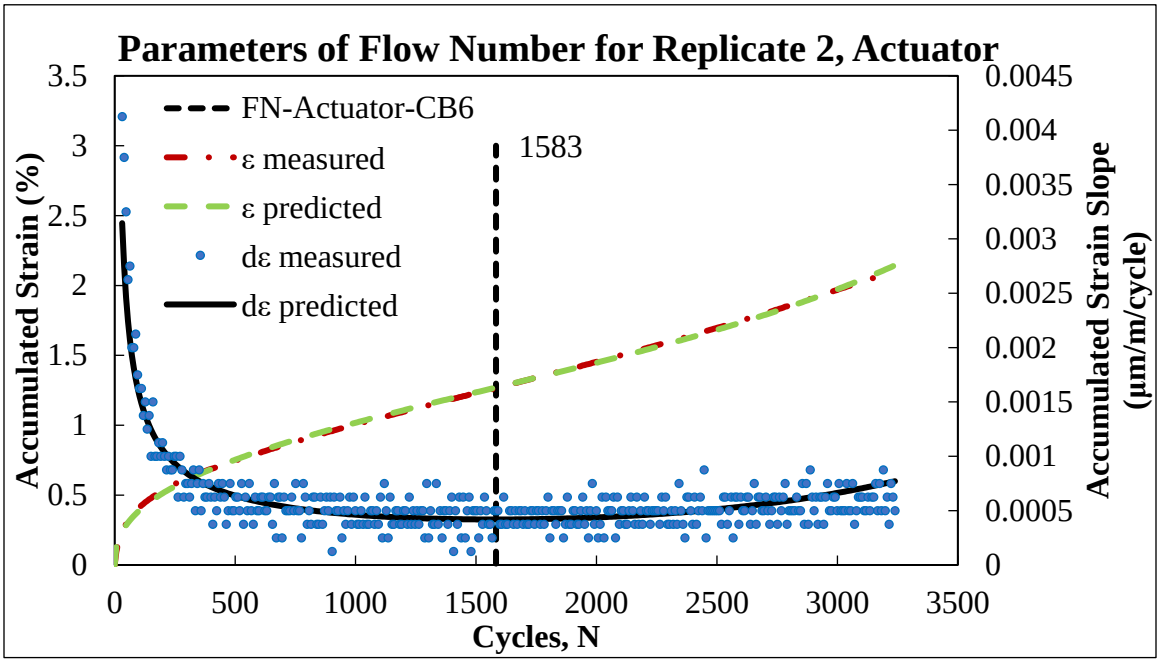

Figure 103:Parameters of Flow Number for Replicate 2, Actuator

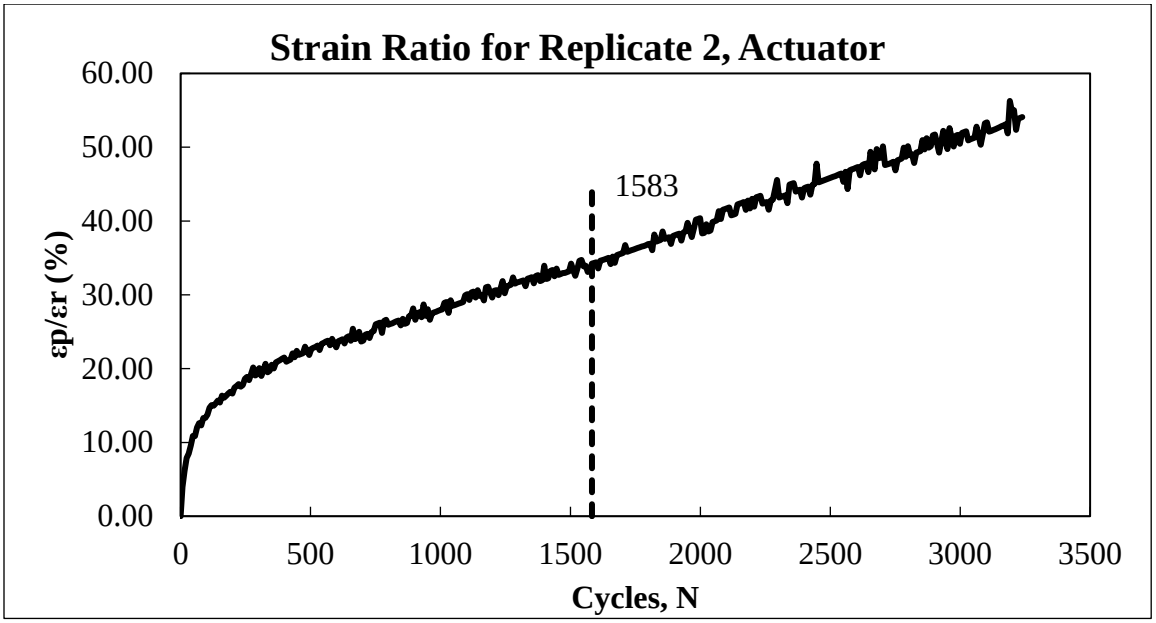

Figure 104: Strain Ratio for Replicate 2, Actuator

Replicate 3 – CB14

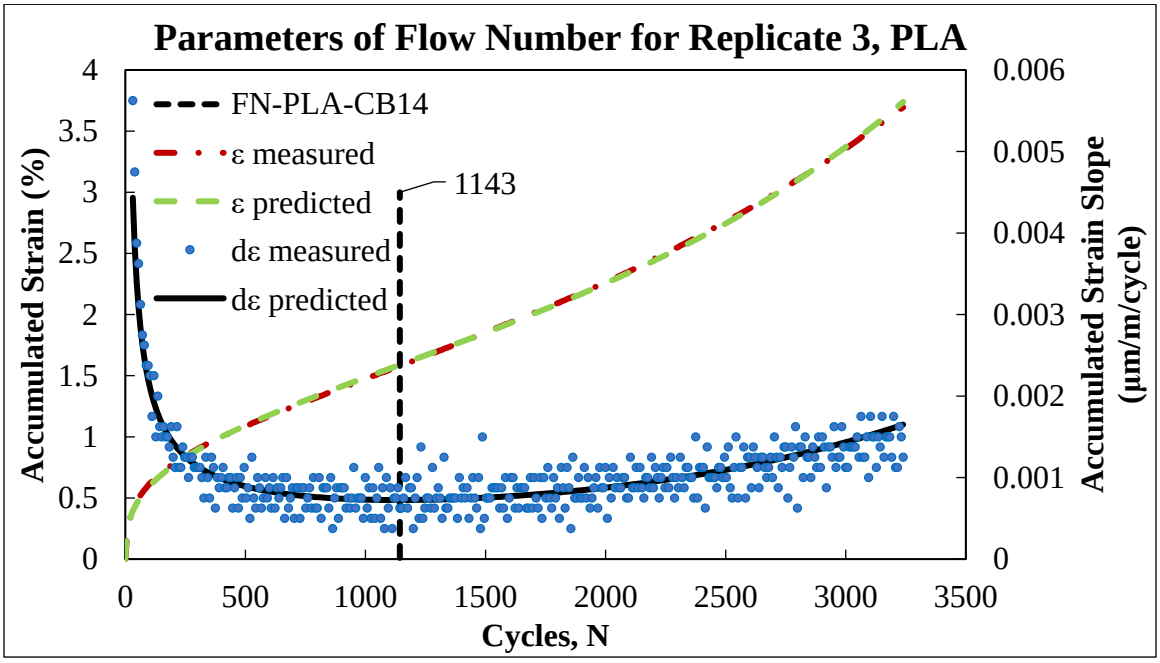

Figure 105: Parameters of Flow Number for Replicate 3, PLA

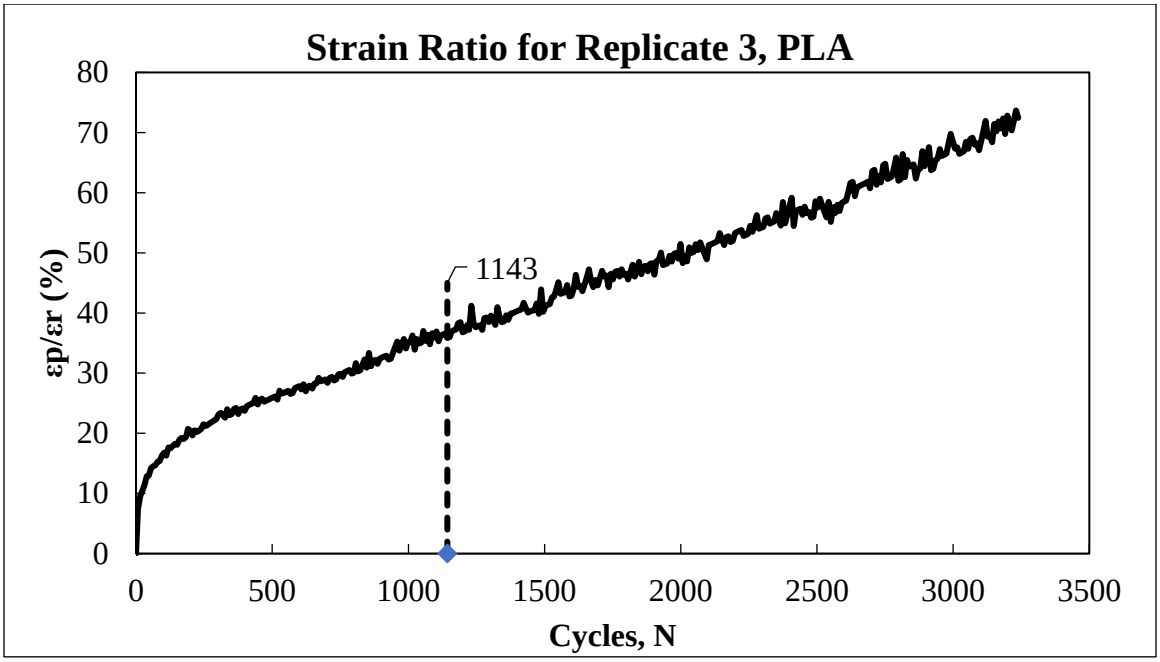

Figure 106: Strain Ratio for Replicate 3, PLA

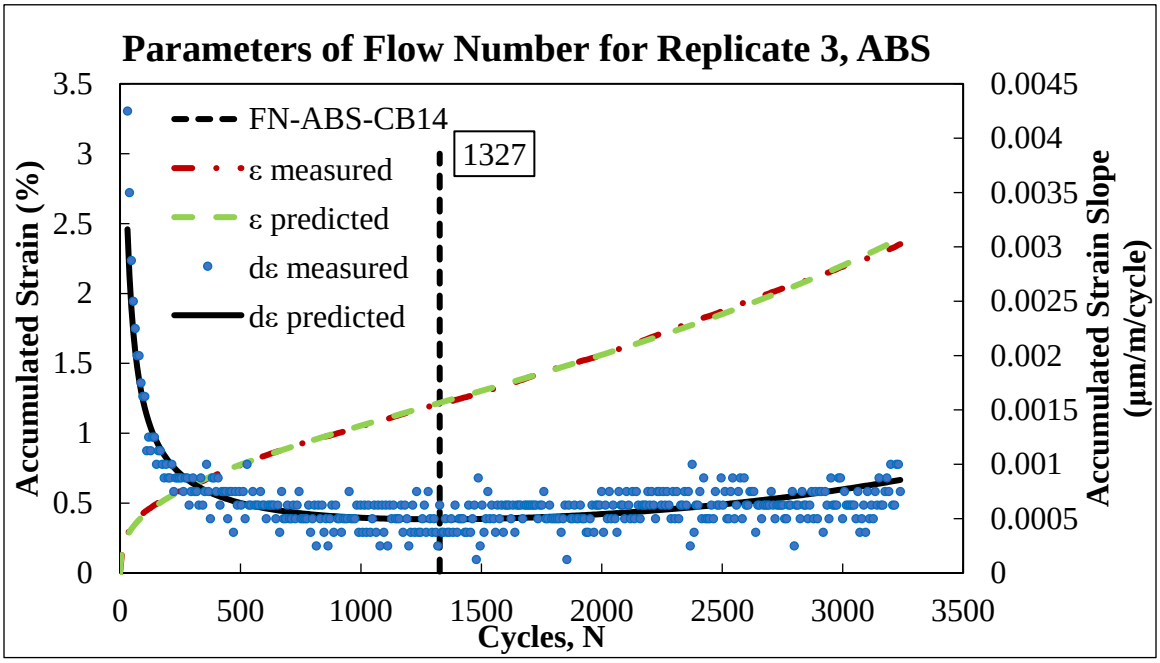

Figure 107: Parameters of Flow Number for Replicate 3, ABS

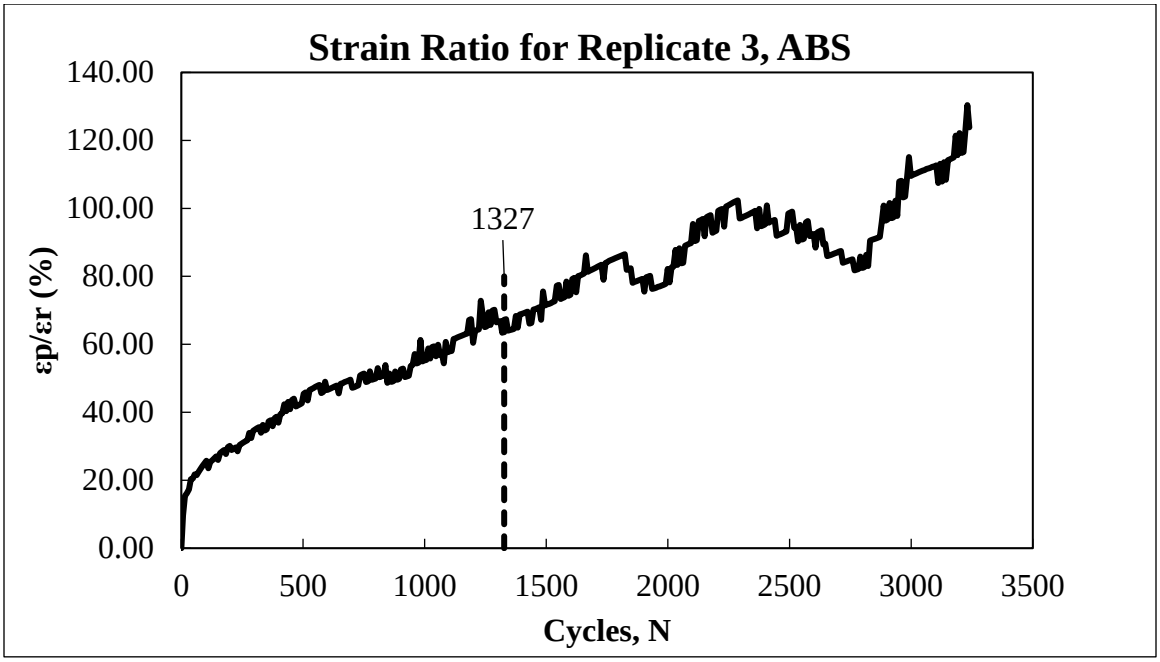

Figure 108: Strain Ratio for Replicate 3, ABS

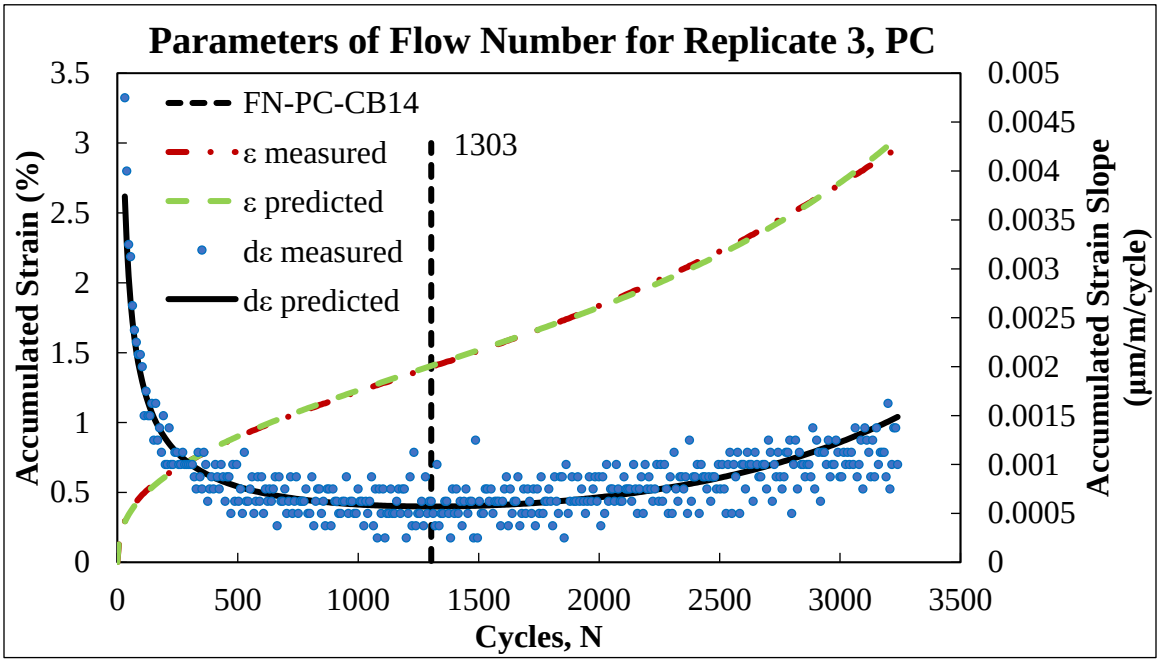

Figure 109: Parameters of Flow Number for Replicate 3, PC

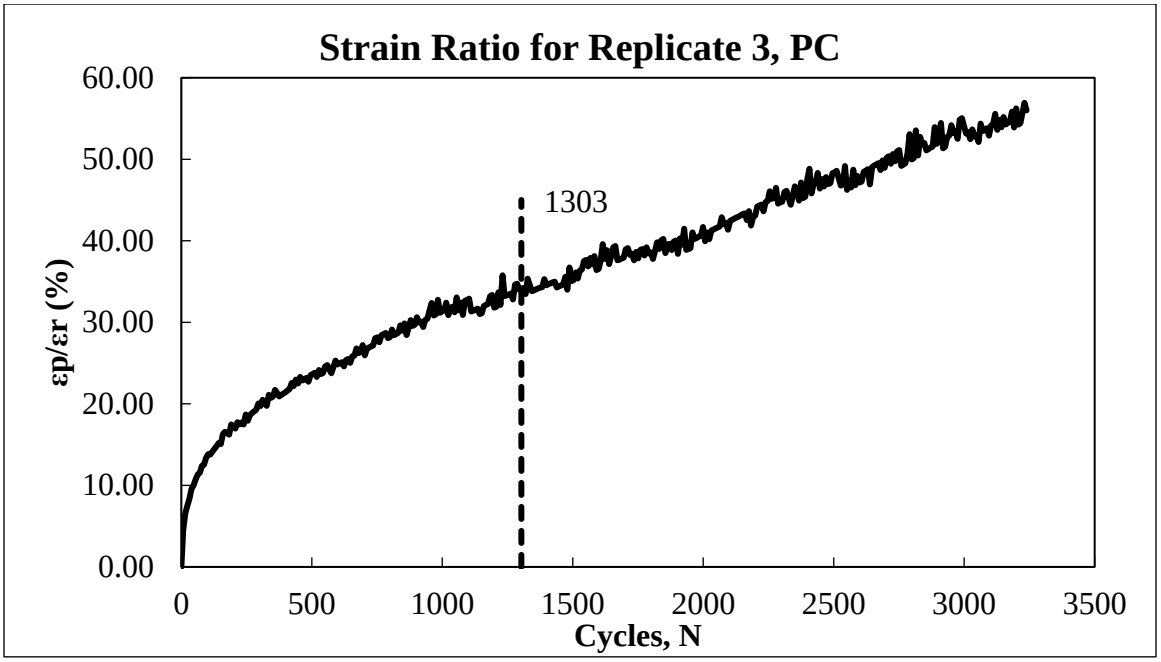

Figure 110: Strain Ratio for Replicate 3, PC

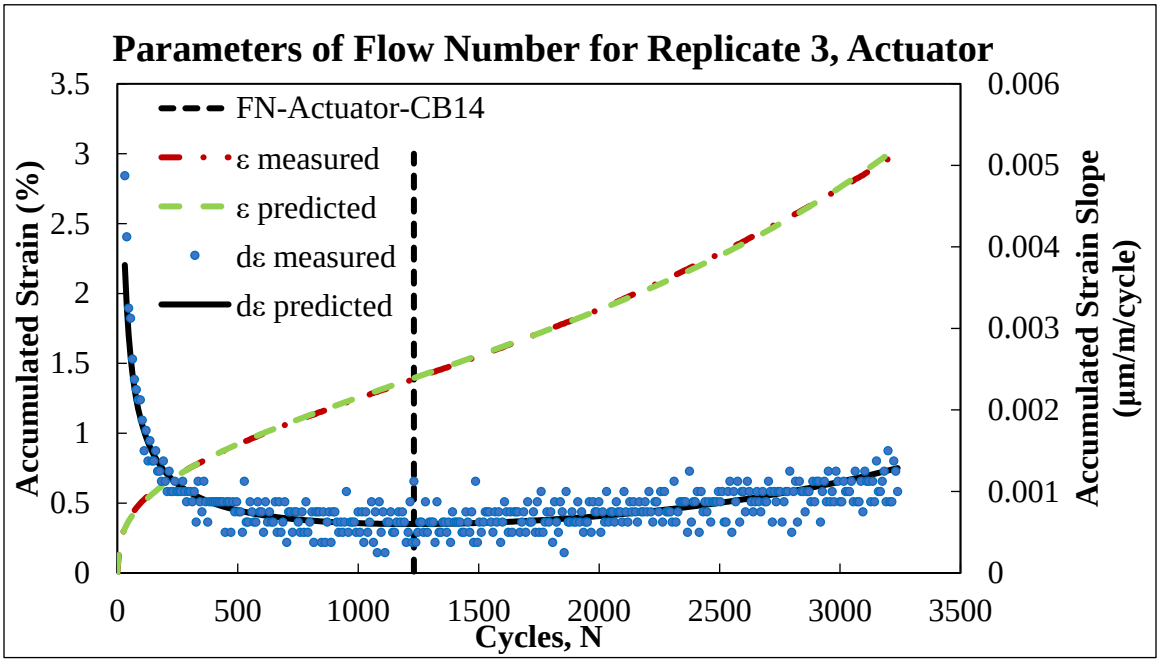

Figure 111: Parameters of Flow Number for Replicate 3, Actuator

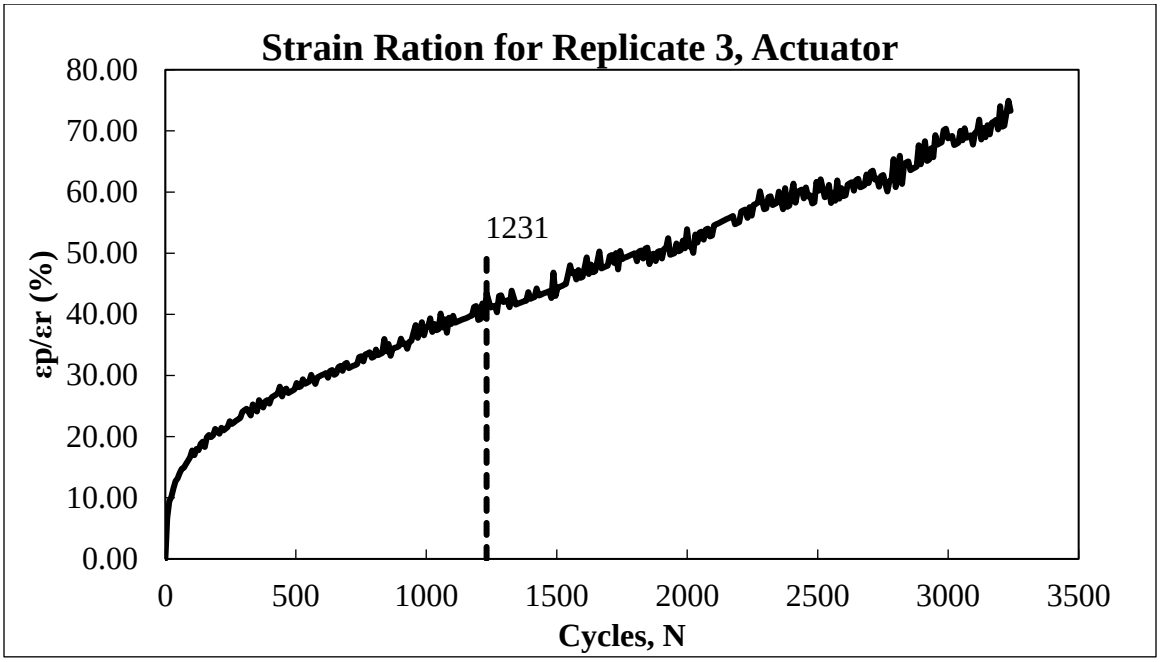

Figure 112: Strain Ration for Replicate 3, Actuator

Direct Tension Cyclic Fatigue

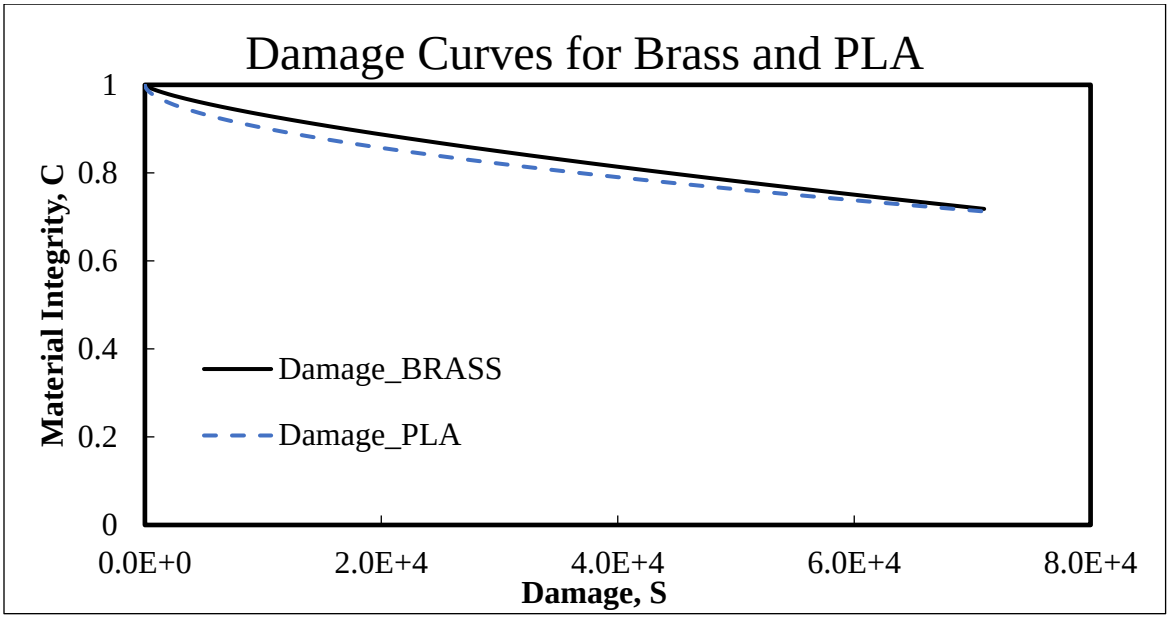

Figure 113: Damage Curves for Brass and PLA

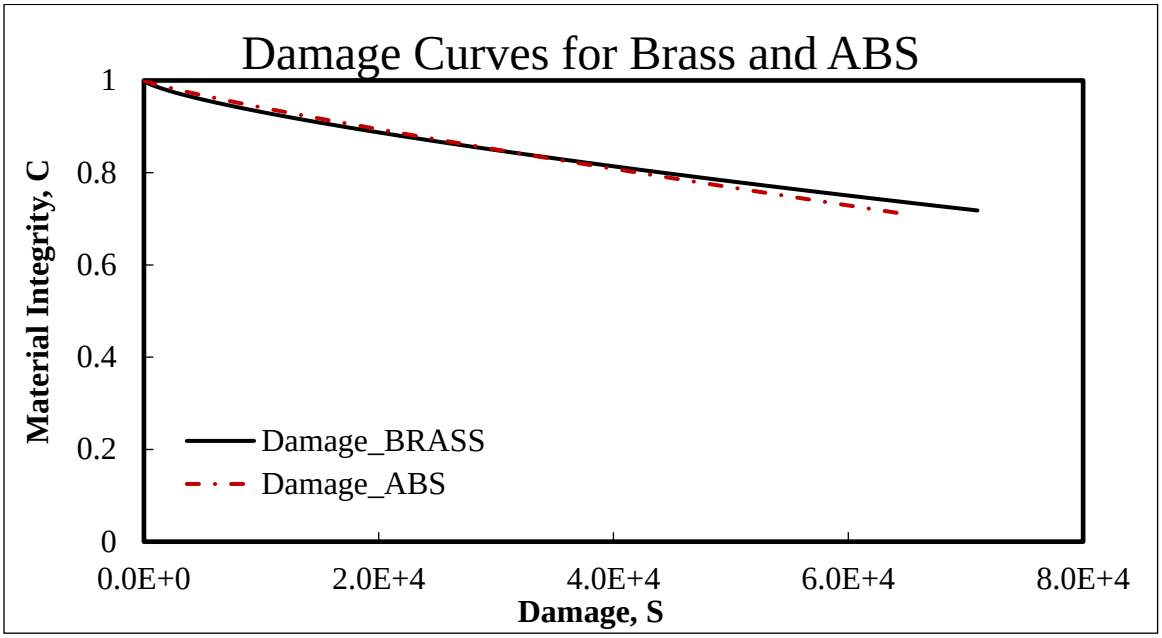

Figure 114: Damage Curves for Brass and ABS

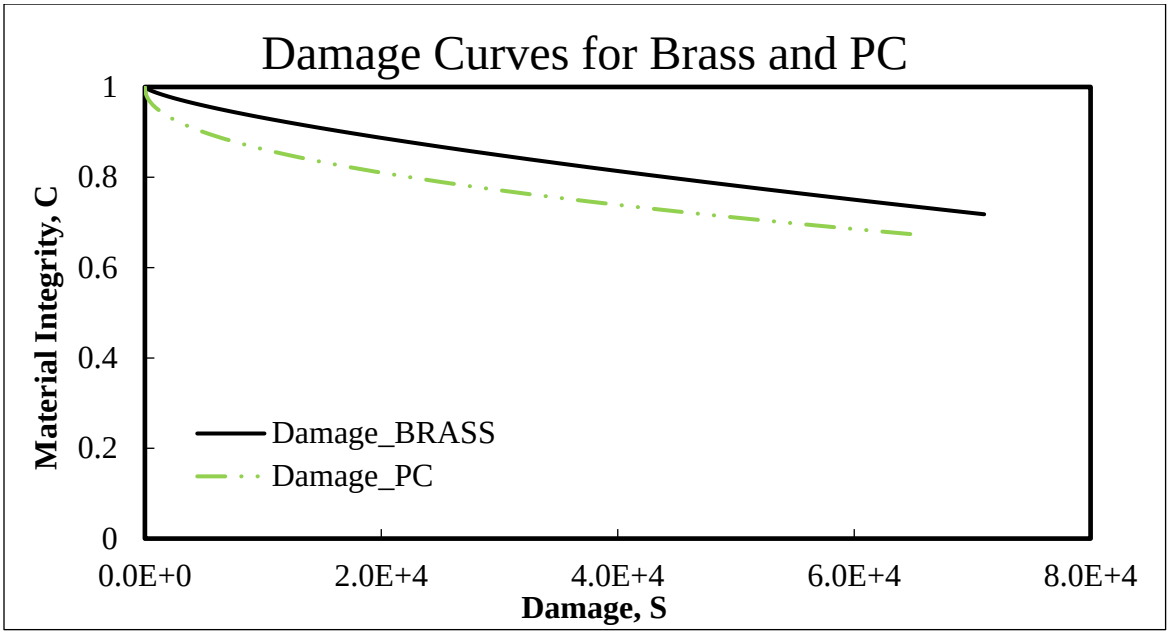

Figure 115: Damage Curves for Brass and PC

APPENDIX D

STATISTICAL DATA

Dynamic Modulus

Mean

Table 96: Average Values for Hypothesis Testing

Temp. (°F)	Freq. (Hz)	|E*| (psi)				Log| E*|				Log Reduced Time (s)			
		METAL	**PLA**	**ABS**	**PC**	**METAL**	**PLA**	**ABS**	**PC**	**METAL**	**PLA**	**ABS**	**PC**
14	25	4945	5821	6673	7419	3.6934	3.7622	3.8213	3.8623	-5.9687	-6.2189	-6.5441	-6.6189
	10	4957	5537	6286	7080	3.6946	3.7405	3.7950	3.8394	-5.3855	-5.6788	-6.1462	-6.2209
	5	4738	5473	6071	7180	3.6747	3.7359	3.7807	3.8407	-5.2697	-5.5199	-5.8451	-5.9199
	1	4421	5112	5579	6356	3.6447	3.7057	3.7444	3.7930	-4.5708	-4.8209	-5.1462	-5.2209
	0.5	4282	4944	5370	6077	3.6308	3.6912	3.7280	3.7746	-4.2697	-4.5199	-4.8451	-4.9199
	0.1	3958	4532	4908	5232	3.5966	3.6535	3.6891	3.7151	-3.5708	-3.8209	-4.1462	-4.2209
40	25	3243	4014	4195	4389	3.5106	3.6029	3.6224	3.6411	-3.7863	-3.8708	-4.0103	-4.0425
	10	3047	3767	3985	4081	3.4835	3.5753	3.5996	3.6085	-3.3884	-3.4729	-3.6124	-3.6446
	5	2901	3584	3761	3898	3.4622	3.5537	3.5745	3.5890	-3.0874	-3.1719	-3.3113	-3.3435
	1	2502	3076	3253	3346	3.3978	3.4874	3.5115	3.5233	-2.3884	-2.4729	-2.6124	-2.6446
	0.5	2353	2883	3045	3150	3.3711	3.4594	3.4826	3.4970	-2.0874	-2.1719	-2.3113	-2.3435
	0.1	1987	2457	2580	2679	3.2976	3.3896	3.4103	3.4263	-1.3884	-1.4729	-1.6124	-1.6446
70	25	1731	1798	2048	2112	3.2381	3.2541	3.3079	3.3239	-1.3979	-1.3979	-1.3979	-1.3979
	10	1493	1599	1787	1893	3.1739	3.2035	3.2487	3.2761	-1.0000	-1.0000	-1.0000	-1.0000
	5	1332	1442	1609	1672	3.1242	3.1588	3.2032	3.2223	-0.6990	-0.6990	-0.6990	-0.6990
	1	993	1063	1192	1257	2.9967	3.0260	3.0727	3.0978	0.0000	0.0000	0.0000	0.0000
	0.5	868	941	1041	1100	2.9381	2.9734	3.0135	3.0398	0.3010	0.3010	0.3010	0.3010
	0.1	610	667	735	782	2.7850	2.8235	2.8619	2.8914	1.0000	1.0000	1.0000	1.0000
100	25	780	808	829	862	2.8920	2.9070	2.9187	2.9355	0.8591	0.8293	0.8887	0.9030
	10	627	643	670	695	2.7973	2.8076	2.8261	2.8419	1.2571	1.2272	1.2867	1.3009
	5	524	535	557	577	2.7195	2.7278	2.7454	2.7608	1.5581	1.5283	1.5877	1.6019
	1	326	331	338	351	2.5136	2.5187	2.5285	2.5446	2.2571	2.2272	2.2867	2.3009
	0.5	258	261	267	273	2.4117	2.4150	2.4263	2.4358	2.5581	2.5283	2.5877	2.6019
	0.1	142	145	148	153	2.1535	2.1584	2.1706	2.1846	3.2571	3.2272	3.2867	3.3009
130	25	194	224	242	250	2.2845	2.3428	2.3708	2.3918	2.9715	2.7978	2.8363	2.8468
	10	137	159	168	176	2.1330	2.1931	2.2131	2.2401	3.3695	3.1957	3.2343	3.2447
	5	106	121	129	132	2.0215	2.0765	2.0964	2.1159	3.6705	3.4967	3.5353	3.5457
	1	57	63	70	73	1.7534	1.7907	1.8316	1.8549	4.3695	4.1957	4.2343	4.2447
	0.5	46	49	55	57	1.6540	1.6866	1.7271	1.7535	4.6705	4.4967	4.5353	4.5457
	0.1	31	31	36	38	1.4788	1.4931	1.5462	1.5750	5.3695	5.1957	5.2343	5.2447

Table 97: Calculated Variance Values Used for Hypothesis Testing

Temp. (°F)	Freq. (Hz)	|E*| (psi)				Log| E*|				Log Reduced Time (s)			
		METAL	**PLA**	**ABS**	**PC**	**METAL**	**PLA**	**ABS**	**PC**	**METAL**	**PLA**	**ABS**	**PC**
14	25	133797	665571	931270	3221157	0.0010	0.0035	0.0040	0.0103	0.1405	0.2038	0.8326	0.2867
	10	153103	384140	911224	3876224	0.0012	0.0024	0.0045	0.0134	0.1919	0.2341	0.8326	0.2867
	5	145081	474168	623225	5931261	0.0012	0.0030	0.0033	0.0193	0.1405	0.2038	0.8326	0.2867
	1	114364	512174	444602	3038135	0.0011	0.0038	0.0028	0.0129	0.1405	0.2038	0.8326	0.2867
	0.5	108253	487534	384347	2467791	0.0011	0.0038	0.0026	0.0115	0.1405	0.2038	0.8326	0.2867
	0.1	104650	388775	287975	699722	0.0012	0.0037	0.0024	0.0046	0.1405	0.2038	0.8326	0.2867
40	25	27862	75423	49822	160056	0.0005	0.0009	0.0005	0.0017	0.0229	0.0597	0.1289	0.0353
	10	27395	63997	99628	246998	0.0005	0.0009	0.0011	0.0030	0.0229	0.0597	0.1289	0.0353
	5	24025	52328	78624	175818	0.0005	0.0008	0.0010	0.0023	0.0229	0.0597	0.1289	0.0353
	1	20901	34927	66284	98716	0.0006	0.0007	0.0011	0.0018	0.0229	0.0597	0.1289	0.0353
	0.5	18196	27199	68597	86070	0.0006	0.0006	0.0014	0.0017	0.0229	0.0597	0.1289	0.0353
	0.1	17910	29047	61943	77670	0.0008	0.0009	0.0017	0.0022	0.0229	0.0597	0.1289	0.0353
70	25	3368	16647	96883	26562	0.0002	0.0010	0.0045	0.0011	0.0000	0.0000	0.0000	0.0000
	10	3091	8318	74644	23262	0.0003	0.0006	0.0044	0.0012	0.0000	0.0000	0.0000	0.0000
	5	2668	3431	60979	20652	0.0003	0.0003	0.0045	0.0014	0.0000	0.0000	0.0000	0.0000
	1	1368	3549	34852	17639	0.0003	0.0006	0.0047	0.0020	0.0000	0.0000	0.0000	0.0000
	0.5	1188	2251	27805	14788	0.0003	0.0005	0.0049	0.0022	0.0000	0.0000	0.0000	0.0000
	0.1	821	1719	17015	7863	0.0004	0.0007	0.0060	0.0023	0.0000	0.0000	0.0000	0.0000
100	25	178	1816	86	998	0.0001	0.0005	0.0000	0.0003	0.0082	0.0633	0.0223	0.0029
	10	99	1688	218	162	0.0000	0.0007	0.0001	0.0001	0.0082	0.0633	0.0223	0.0029
	5	102	1583	163	122	0.0001	0.0010	0.0001	0.0001	0.0082	0.0633	0.0223	0.0029
	1	33	779	84	93	0.0001	0.0013	0.0001	0.0001	0.0082	0.0633	0.0223	0.0029
	0.5	47	582	133	55	0.0001	0.0015	0.0004	0.0001	0.0082	0.0633	0.0223	0.0029
	0.1	18	226	46	7	0.0002	0.0019	0.0004	0.0001	0.0082	0.0633	0.0223	0.0029
130	25	697	2671	5648	2318	0.0036	0.0098	0.0160	0.0080	0.0569	0.2597	0.1829	0.1059
	10	415	1347	2759	1168	0.0043	0.0102	0.0162	0.0081	0.0569	0.2597	0.1829	0.1059
	5	273	649	1584	651	0.0049	0.0085	0.0159	0.0080	0.0569	0.2597	0.1829	0.1059
	1	102	165	558	184	0.0062	0.0083	0.0187	0.0075	0.0569	0.2597	0.1829	0.1059
	0.5	66	80	313	105	0.0064	0.0067	0.0171	0.0066	0.0569	0.2597	0.1829	0.1059
	0.1	35	14	145	25	0.0074	0.0029	0.0189	0.0033	0.0569	0.2597	0.1829	0.1059

Table 98: Test Statistics Used for Hypothesis Testing

Temp. (°F)	Freq. (Hz)	|E*| (psi)			Log| E*|			Log Reduced Time (s)		
		t'1	**t'2**	**t'3**	**t'1**	**t'2**	**t'3**	**t'1**	**t'2**	**t'3**
14	25	1.7822	3.1271	2.7519	1.7822	3.1271	2.7519	0.7384	1.0103	1.7229
	10	1.3272	2.2934	2.0779	1.3272	2.2934	2.0779	0.7783	1.3016	2.0913
	5	1.6344	2.7340	2.0105	1.6344	2.7340	2.0105	0.7384	1.0103	1.7229
	1	1.5182	2.7733	2.1744	1.5182	2.7733	2.1744	0.7384	1.0103	1.7229
	0.5	1.4909	2.7592	2.2178	1.4909	2.7592	2.2178	0.7384	1.0103	1.7229
	0.1	1.4084	2.6666	2.6976	1.4084	2.6666	2.6976	0.7384	1.0103	1.7229
40	25	4.2632	6.0710	4.8831	4.2632	6.0710	4.8831	0.5092	0.9956	1.8399
	10	4.2371	4.9073	3.6291	4.2371	4.9073	3.6291	0.5092	0.9956	1.8399
	5	4.3841	4.9554	4.1076	4.3841	4.9554	4.1076	0.5092	0.9956	1.8399
	1	4.2773	4.6925	4.4620	4.2773	4.6925	4.4620	0.5092	0.9956	1.8399
	0.5	4.3585	4.3590	4.5153	4.3585	4.3590	4.5153	0.5092	0.9956	1.8399
	0.1	3.8078	3.8656	4.0711	3.8078	3.8656	4.0711	0.5092	0.9956	1.8399
70	25	0.7894	1.7629	4.0908	0.7894	1.7629	4.0908	1.5958	2.5884	0.1287
	10	1.7195	1.9067	4.5821	1.7195	1.9067	4.5821	1.5958	2.5884	0.1287
	5	2.4410	1.9786	4.1919	2.4410	1.9786	4.1919	1.5958	2.5884	0.1287
	1	1.7256	1.8762	3.6458	1.7256	1.8762	3.6458	1.5958	2.5884	0.1287
	0.5	2.1819	1.8089	3.5026	2.1819	1.8089	3.5026	1.5958	2.5884	0.1287
	0.1	1.9528	1.6651	3.5186	1.9528	1.6651	3.5186	1.5958	2.5884	0.1287
100	25	1.0816	5.2075	4.2477	1.0816	5.2075	4.2477	0.1932	0.2934	0.7189
	10	0.6322	4.2292	7.3634	0.6322	4.2292	7.3634	0.1932	0.2934	0.7189
	5	0.4399	3.4616	6.0869	0.4399	3.4616	6.0869	0.1932	0.2934	0.7189
	1	0.2408	1.8384	3.7878	0.2408	1.8384	3.7878	0.1932	0.2934	0.7189
	0.5	0.1379	1.1412	2.5111	0.1379	1.1412	2.5111	0.1932	0.2934	0.7189
	0.1	0.1851	1.2418	3.5744	0.1851	1.2418	3.5744	0.1932	0.2934	0.7189
130	25	0.8739	1.0691	1.7306	0.8739	1.0691	1.7306	0.5348	0.4781	0.5354
	10	0.8626	0.9684	1.6609	0.8626	0.9684	1.6609	0.5348	0.4781	0.5354
	5	0.8223	0.8987	1.4376	0.8223	0.8987	1.4376	0.5348	0.4781	0.5354
	1	0.5351	0.8573	1.5034	0.5351	0.8573	1.5034	0.5348	0.4781	0.5354
	0.5	0.4922	0.8244	1.5096	0.4922	0.8244	1.5096	0.5348	0.4781	0.5354
	0.1	0.2439	0.7191	1.6087	0.2439	0.7191	1.6087	0.5348	0.4781	0.5354

Table 99: Calculated Degree of Freedom Used for Hypothesis Testing

Temp. (°F)	Freq. (Hz)	|E*| (psi)			Log |E*|			Log Reduced Time (s)		
		Dof1	**Dof2**	**Dof3**	**Dof1**	**Dof2**	**Dof3**	**Dof1**	**Dof2**	**Dof3**
14	25	3.5457	3.1261	2.3317	4.1595	3.9063	2.7819	5.7382	3.3123	5.1607
	10	4.7514	3.3072	2.3155	5.2215	3.9902	2.7177	5.9225	3.7511	5.6981
	5	4.2382	3.7666	2.1956	4.6938	4.5027	2.4856	5.7382	3.3123	5.1607
	1	3.7015	3.9301	2.3007	4.0858	4.6470	2.6568	5.7382	3.3123	5.1607
	0.5	3.6929	4.0876	2.3503	4.0782	4.7918	2.7403	5.7382	3.3123	5.1607
	0.1	4.0079	4.5681	3.1703	4.3853	5.2335	3.9902	5.7382	3.3123	5.1607
40	25	4.6004	5.4081	3.3517	5.3344	5.9908	4.1855	4.6712	3.3759	5.6513
	10	4.8942	4.0451	2.8765	5.6016	5.1167	3.3971	4.6712	3.3759	5.6513
	5	5.0336	4.2358	3.0732	5.7019	5.2667	3.7130	4.6712	3.3759	5.6513
	1	5.5250	4.2945	3.6212	5.9616	5.3225	4.4836	4.6712	3.3759	5.6513
	0.5	5.6972	3.9825	3.6189	5.9969	4.9658	4.4876	4.6712	3.3759	5.6513
	0.1	5.5739	4.1346	3.7516	5.9757	5.1215	4.6629	4.6712	3.3759	5.6513
70	25	3.5550	2.2778	2.9984	3.6321	2.3849	3.5115	3.5983	3.1220	4.6307
	10	4.6124	2.3308	3.0447	4.8825	2.4865	3.6550	3.5983	3.1220	4.6307
	5	5.8766	2.3493	3.0165	5.9883	2.5148	3.6425	3.5983	3.1220	4.6307
	1	4.6844	2.3135	2.6167	4.9688	2.4572	3.0301	3.5983	3.1220	4.6307
	0.5	5.3023	2.3411	2.6385	5.6019	2.4931	3.0723	3.5983	3.1220	4.6307
	0.1	5.1108	2.3850	2.8260	5.4679	2.5701	3.4297	3.5983	3.1220	4.6307
100	25	2.7748	5.1296	3.3794	2.8348	4.9048	3.6256	3.0233	4.6023	4.5127
	10	2.4689	5.0214	5.5613	2.5049	5.2470	5.8367	3.0233	4.6023	4.5127
	5	2.5132	5.6012	5.9354	2.5533	5.7590	5.9996	3.0233	4.6023	4.5127
	1	2.3431	4.7614	4.5426	2.3678	4.9053	4.8542	3.0233	4.6023	4.5127
	0.5	2.6438	4.5199	5.9499	2.6949	4.6837	5.9984	3.0233	4.6023	4.5127
	0.1	2.6429	4.7321	4.6594	2.7011	4.8874	4.3489	3.0233	4.6023	4.5127
130	25	3.9551	2.9728	4.2066	4.5740	3.7026	4.9874	3.6738	4.2712	5.3373
	10	4.2517	3.1771	4.5251	4.8793	4.0037	5.3240	3.6738	4.2712	5.3373
	5	4.8563	3.3375	4.8527	5.4738	4.2598	5.5724	3.6738	4.2712	5.3373
	1	5.5724	3.4106	5.3830	5.8326	4.3912	5.9326	3.6738	4.2712	5.3373
	0.5	5.9332	3.6230	5.6137	5.9962	4.6349	5.9989	3.6738	4.2712	5.3373
	0.1	4.7592	3.8062	5.8055	4.7054	4.7235	4.9713	3.6738	4.2712	5.3373

Table 100: Tabulated T-table Values for $\alpha = 0.05$ Used for Hypothesis Testing

Temp. (°F)	Freq. (Hz)	|E*| (psi)			Log | E*|			Log Reduced Time (s)		
		t Table 1	**t Table 2**	**t Table 3**	**t Table 1**	**t Table 2**	**t Table 3**	**t Table 1**	**t Table 2**	**t Table 3**
14	25	2.9604	3.1308	3.9311	2.7433	2.8140	3.4265	2.4795	3.0552	2.5511
	10	2.6220	3.0573	3.9493	2.5435	2.7800	3.4984	2.4566	2.8771	2.4844
	5	2.7272	2.8708	4.0838	2.6338	2.6729	3.7587	2.4795	3.0552	2.5511
	1	2.8972	2.8044	3.9659	2.7584	2.6434	3.5667	2.4795	3.0552	2.5511
	0.5	2.9007	2.7580	3.9104	2.7600	2.6137	3.4731	2.4795	3.0552	2.5511
	0.1	2.7744	2.6595	3.1129	2.6970	2.5420	2.7800	2.4795	3.0552	2.5511
40	25	2.6529	2.5204	3.0392	2.5295	2.4481	2.7380	2.6384	3.0294	2.4902
	10	2.5927	2.7667	3.3204	2.4964	2.5565	3.0208	2.6384	3.0294	2.4902
	5	2.5668	2.7277	3.1523	2.4840	2.5379	2.8925	2.6384	3.0294	2.4902
	1	2.5059	2.7156	2.9298	2.4518	2.5310	2.6769	2.6384	3.0294	2.4902
	0.5	2.4845	2.7831	2.9307	2.4474	2.5780	2.6760	2.6384	3.0294	2.4902
	0.1	2.4998	2.7484	2.8769	2.4500	2.5559	2.6401	2.6384	3.0294	2.4902
70	25	2.9567	3.9916	3.1837	2.9254	3.8715	2.9743	2.9391	3.1325	2.6467
	10	2.6505	3.9322	3.1639	2.5951	3.7577	2.9161	2.9391	3.1325	2.6467
	5	2.4623	3.9114	3.1753	2.4485	3.7259	2.9212	2.9391	3.1325	2.6467
	1	2.6357	3.9516	3.6117	2.5774	3.7905	3.1698	2.9391	3.1325	2.6467
	0.5	2.5335	3.9206	3.5873	2.4964	3.7502	3.1527	2.9391	3.1325	2.6467
	0.1	2.5573	3.8715	3.3771	2.5130	3.6639	3.0075	2.9391	3.1325	2.6467
100	25	3.4345	2.5549	3.0280	3.3672	2.5905	2.9280	3.1725	2.6525	2.6709
	10	3.7773	2.5683	2.5014	3.7370	2.5404	2.4672	3.1725	2.6525	2.6709
	5	3.7277	2.4965	2.4550	3.6827	2.4769	2.4471	3.1725	2.6525	2.6709
	1	3.9184	2.6199	2.6648	3.8907	2.5904	2.6009	3.1725	2.6525	2.6709
	0.5	3.5813	2.6694	2.4532	3.5240	2.6358	2.4472	3.1725	2.6525	2.6709
	0.1	3.5823	2.6259	2.6408	3.5170	2.5941	2.7045	3.1725	2.6525	2.6709
130	25	2.7942	3.2125	2.7337	2.6583	2.8967	2.5736	2.9084	2.7204	2.5292
	10	2.7244	3.1101	2.6684	2.5957	2.7752	2.5308	2.9084	2.7204	2.5292
	5	2.6005	3.0450	2.6012	2.5122	2.7227	2.5000	2.9084	2.7204	2.5292
	1	2.5000	3.0153	2.5235	2.4678	2.6958	2.4554	2.9084	2.7204	2.5292
	0.5	2.4553	2.9291	2.4949	2.4475	2.6459	2.4471	2.9084	2.7204	2.5292
	0.1	2.6204	2.8547	2.4711	2.6314	2.6277	2.5769	2.9084	2.7204	2.5292

Table 101: CV % Values for All Stud Types

		CV (%)			
Temp, ºF	Frequency Hz	x	y1	y2	y3
		METAL	**PLA**	**ABS**	**PC**
14 ºF	25	7.396845	14.01638921	14.46142	24.19021
	10	7.894326	11.19354126	15.18515	27.80935
	5	8.039652	12.58284705	13.00348	33.9204
	1	7.649863	13.99901495	11.95123	27.42168
	1	7.683488	14.12222466	11.54436	25.85054
	0	8.172555	13.75771101	10.93346	15.98746
40 ºF	25	5.146721	6.841694317	5.32022	9.115216
	10	5.431857	6.715628266	7.920556	12.17948
	5	5.342583	6.383191152	7.456373	10.75821
	1	5.778046	6.076447744	7.913243	9.38889
	1	5.733931	5.720305015	8.600181	9.313467
	0	6.73498	6.938006786	9.645836	10.40369
70 ºF	25	3.353164	7.175059004	15.19947	7.716421
	10	3.723998	5.702019712	15.2899	8.058348
	5	3.878315	4.061138907	15.34501	8.59371
	1	3.725175	5.605136834	15.66217	10.56553
	1	3.972579	5.038930396	16.02509	11.05141
	0	4.696079	6.215594033	17.73792	11.3387
100 ºF	25	1.708588	5.274611389	1.115825	3.664362
	10	1.589037	6.390845943	2.201135	1.833071
	5	1.926098	7.432579379	2.290642	1.917239
	1	1.772662	8.43361592	2.705865	2.75517
	1	2.660202	9.25316235	4.318561	2.72536
	0	3.000187	10.39685402	4.588405	1.7233
130 ºF	25	13.63054	23.06387827	31.06488	19.27046
	10	14.88612	23.10827129	31.2094	19.39036
	5	15.58437	21.05026607	30.95291	19.26868
	1	17.60541	20.5106178	33.64015	18.72859
	1	17.85615	18.15298105	32.10789	17.85472
	0	19.31424	11.9151245	33.13247	13.29124

Table 102: Results of Hypothesis Tests for the Mean of the Control Treatment to Alternative Treatments.

Frequency Hz	Temp ºF	|E*| (psi)			Log |E*|			Log Reduced Time (s)		
		H:μx = μy1	**H:μx = μy2**	**H:μx = μy3**	**H:μx = μy1**	**H:μx = μy2**	**H:μx = μy3**	**H:μx = μy1**	**H:μx = μy2**	**H:μx = μy3**
25	14 ºF	Accept	Accept	Accept	Accept	Reject	Accept	Accept	Accept	Accept
10	14 ºF	Accept	Accept	Accept	Accept	Accept	Accept	Accept	Accept	Accept
5	14 ºF	Accept	Accept	Accept	Accept	Reject	Accept	Accept	Accept	Accept
1	14 ºF	Accept	Accept	Accept	Accept	Reject	Accept	Accept	Accept	Accept
0.5	14 ºF	Accept	Accept	Accept	Accept	Reject	Accept	Accept	Accept	Accept
0.1	14 ºF	Accept	Accept	Accept	Accept	Reject	Accept	Accept	Accept	Accept
25	40 ºF	Reject	Reject	Reject	Reject	Reject	Reject	Accept	Accept	Accept
10	40 ºF	Reject	Reject	Reject	Reject	Reject	Reject	Accept	Accept	Accept
5	40 ºF	Reject	Reject	Reject	Reject	Reject	Reject	Accept	Accept	Accept
1	40 ºF	Reject	Reject	Reject	Reject	Reject	Reject	Accept	Accept	Accept
0.5	40 ºF	Reject	Reject	Reject	Reject	Reject	Reject	Accept	Accept	Accept
0.1	40 ºF	Reject	Reject	Reject	Reject	Reject	Reject	Accept	Accept	Accept
25	70 ºF	Accept	Accept	Reject	Accept	Accept	Reject	Accept	Accept	Accept
10	70 ºF	Accept	Accept	Reject	Accept	Accept	Reject	Accept	Accept	Accept
5	70 ºF	Accept	Accept	Reject	Accept	Accept	Reject	Accept	Accept	Accept
1	70 ºF	Accept	Accept	Accept	Accept	Accept	Reject	Accept	Accept	Accept
0.5	70 ºF	Accept	Accept	Accept	Accept	Accept	Reject	Accept	Accept	Accept
0.1	70 ºF	Accept	Accept	Accept	Accept	Accept	Reject	Accept	Accept	Accept
25	100 ºF	Accept	Reject	Reject	Accept	Reject	Reject	Accept	Accept	Accept
10	100 ºF	Accept	Reject	Reject	Accept	Reject	Reject	Accept	Accept	Accept
5	100 ºF	Accept	Reject	Reject	Accept	Reject	Reject	Accept	Accept	Accept
1	100 ºF	Accept	Accept	Reject	Accept	Accept	Reject	Accept	Accept	Accept
0.5	100 ºF	Accept	Accept	Reject	Accept	Accept	Reject	Accept	Accept	Accept
0.1	100 ºF	Accept	Accept	Reject	Accept	Accept	Reject	Accept	Accept	Accept
25	130 ºF	Accept	Accept	Accept	Accept	Accept	Accept	Accept	Accept	Accept
10	130 ºF	Accept	Accept	Accept	Accept	Accept	Accept	Accept	Accept	Accept
5	130 ºF	Accept	Accept	Accept	Accept	Accept	Accept	Accept	Accept	Accept
1	130 ºF	Accept	Accept	Accept	Accept	Accept	Accept	Accept	Accept	Accept
0.5	130 ºF	Accept	Accept	Accept	Accept	Accept	Accept	Accept	Accept	Accept
0.1	130 ºF	Accept	Accept	Accept	Accept	Accept	Accept	Accept	Accept	Accept

Variance

Table 103: Summary of Calculated F-statistics for Hypothesis Testing

Frequency Hz	Temp ºF	|E*| (psi)			Log |E*|			Log Reduced Time (s)		
		F1	F2	F3	F1	F2	F3	F1	F2	F3
25	14 ºF	0.2010	0.1437	0.0415	0.2931	0.2536	0.0987	0.6893	0.1687	0.4899
10	14 ºF	0.3986	0.1680	0.0395	0.5057	0.2664	0.0905	0.8200	0.2305	0.6694
5	14 ºF	0.3060	0.2328	0.0245	0.3872	0.3515	0.0609	0.6893	0.1687	0.4899
1	14 ºF	0.2233	0.2572	0.0376	0.2814	0.3782	0.0827	0.6893	0.1687	0.4899
0.5	14 ºF	0.2220	0.2817	0.0439	0.2802	0.4067	0.0933	0.6893	0.1687	0.4899
0.1	14 ºF	0.2692	0.3634	0.1496	0.3308	0.5088	0.2664	0.6893	0.1687	0.4899
25	40 ºF	0.3694	0.5592	0.1741	0.5370	0.9345	0.2973	0.3828	0.1774	0.6481
10	40 ºF	0.4281	0.2750	0.1109	0.6274	0.4790	0.1803	0.3828	0.1774	0.6481
5	40 ºF	0.4591	0.3056	0.1366	0.6712	0.5178	0.2250	0.3828	0.1774	0.6481
1	40 ºF	0.5984	0.3153	0.2117	0.8701	0.5335	0.3481	0.3828	0.1774	0.6481
0.5	40 ºF	0.6690	0.2653	0.2114	0.9611	0.4437	0.3488	0.3828	0.1774	0.6481
0.1	40 ºF	0.6166	0.2891	0.2306	0.8953	0.4801	0.3812	0.3828	0.1774	0.6481
25	70 ºF	0.2023	0.0348	0.1268	0.2133	0.0482	0.1962	4.7970	6.9873	2.6659
10	70 ºF	0.3717	0.0414	0.1329	0.4256	0.0610	0.2166	4.7970	6.9873	2.6659
5	70 ºF	0.7775	0.0437	0.1292	0.9262	0.0646	0.2148	4.7970	6.9873	2.6659
1	70 ºF	0.3854	0.0392	0.0775	0.4444	0.0573	0.1310	4.7970	6.9873	2.6659
0.5	70 ºF	0.5278	0.0427	0.0803	0.6275	0.0619	0.1365	4.7970	6.9873	2.6659
0.1	70 ºF	0.4775	0.0482	0.1044	0.5786	0.0716	0.1848	4.7970	6.9873	2.6659
25	100 ºF	0.0978	2.0741	0.1779	0.1055	2.3237	0.2124	0.1301	0.3698	2.8305
10	100 ºF	0.0588	0.4563	0.6118	0.0634	0.5125	0.7477	0.1301	0.3698	2.8305
5	100 ºF	0.0644	0.6272	0.8344	0.0695	0.7003	1.0148	0.1301	0.3698	2.8305
1	100 ºF	0.0430	0.4006	0.3587	0.0461	0.4304	0.4196	0.1301	0.3698	2.8305
0.5	100 ºF	0.0810	0.3546	0.8529	0.0875	0.3853	0.9720	0.1301	0.3698	2.8305
0.1	100 ºF	0.0809	0.3947	2.6276	0.0883	0.4266	3.0814	0.1301	0.3698	2.8305
25	130 ºF	0.2610	0.1234	0.3008	0.3645	0.2235	0.4486	0.2193	0.3114	0.5378
10	130 ºF	0.3082	0.1505	0.3555	0.4249	0.2685	0.5340	0.2193	0.3114	0.5378
5	130 ºF	0.4200	0.1721	0.4193	0.5806	0.3095	0.6160	0.2193	0.3114	0.5378
1	130 ºF	0.6160	0.1822	0.5515	0.7449	0.3318	0.8312	0.2193	0.3114	0.5378
0.5	130 ºF	0.8319	0.2120	0.6323	0.9573	0.3759	0.9773	0.2193	0.3114	0.5378
0.1	130 ºF	2.4992	0.2386	1.3749	2.5676	0.3930	2.2475	0.2193	0.3114	0.5378

Table 104: Results of Hypothesis Testing on Variance

		|E*| (psi)			Log |E*|			Log Reduced Time (s)		
Frequency Hz	**Temp °F**	**H:σ^2x = σ^2y1**	**H:σ^2x = σ^2y2**	**H:σ^2x = σ^2y3**	**H:σ^2x = σ^2y1**	**H:σ^2x = σ^2y2**	**H:σ^2x = σ^2y3**	**H:σ^2x = σ^2y1**	**H:σ^2x = σ^2y2**	**H:σ^2x = σ^2y3**
25	14 °F	Accept	Accept	Accept	Accept	Accept	Accept	Accept	Accept	Accept
10	14 °F	Accept	Accept	Accept	Accept	Accept	Accept	Accept	Accept	Accept
5	14 °F	Accept	Accept	Reject	Accept	Accept	Accept	Accept	Accept	Accept
1	14 °F	Accept	Accept	Accept	Accept	Accept	Accept	Accept	Accept	Accept
0.5	14 °F	Accept	Accept	Accept	Accept	Accept	Accept	Accept	Accept	Accept
0.1	14 °F	Accept	Accept	Accept	Accept	Accept	Accept	Accept	Accept	Accept
25	40 °F	Accept	Accept	Accept	Accept	Accept	Accept	Accept	Accept	Accept
10	40 °F	Accept	Accept	Accept	Accept	Accept	Accept	Accept	Accept	Accept
5	40 °F	Accept	Accept	Accept	Accept	Accept	Accept	Accept	Accept	Accept
1	40 °F	Accept	Accept	Accept	Accept	Accept	Accept	Accept	Accept	Accept
0.5	40 °F	Accept	Accept	Accept	Accept	Accept	Accept	Accept	Accept	Accept
0.1	40 °F	Accept	Accept	Accept	Accept	Accept	Accept	Accept	Accept	Accept
25	70 °F	Accept	Accept	Accept	Accept	Accept	Accept	Accept	Accept	Accept
10	70 °F	Accept	Accept	Accept	Accept	Accept	Accept	Accept	Accept	Accept
5	70 °F	Accept	Accept	Accept	Accept	Accept	Accept	Accept	Accept	Accept
1	70 °F	Accept	Accept	Accept	Accept	Accept	Accept	Accept	Accept	Accept
0.5	70 °F	Accept	Accept	Accept	Accept	Accept	Accept	Accept	Accept	Accept
0.1	70 °F	Accept	Accept	Accept	Accept	Accept	Accept	Accept	Accept	Accept
25	100 °F	Accept	Accept	Accept	Accept	Accept	Accept	Accept	Accept	Accept
10	100 °F	Accept	Accept	Accept	Accept	Accept	Accept	Accept	Accept	Accept
5	100 °F	Accept	Accept	Accept	Accept	Accept	Accept	Accept	Accept	Accept
1	100 °F	Accept	Accept	Accept	Accept	Accept	Accept	Accept	Accept	Accept
0.5	100 °F	Accept	Accept	Accept	Accept	Accept	Accept	Accept	Accept	Accept
0.1	100 °F	Accept	Accept	Accept	Accept	Accept	Accept	Accept	Accept	Accept
25	130 °F	Accept	Accept	Accept	Accept	Accept	Accept	Accept	Accept	Accept
10	130 °F	Accept	Accept	Accept	Accept	Accept	Accept	Accept	Accept	Accept
5	130 °F	Accept	Accept	Accept	Accept	Accept	Accept	Accept	Accept	Accept
1	130 °F	Accept	Accept	Accept	Accept	Accept	Accept	Accept	Accept	Accept
0.5	130 °F	Accept	Accept	Accept	Accept	Accept	Accept	Accept	Accept	Accept
0.1	130 °F	Accept	Accept	Accept	Accept	Accept	Accept	Accept	Accept	Accept

Table 105: Results for Full Acceptance of Hypothesis Tests on the Mean and Variance of |E*| Data

Frequency Hz	Temp °F	Mean Test at 99.9% Confidence			Variance Test at 98% Confidence		
		H:σ^2x = σ^2y1	H:σ^2x = σ^2y2	H:σ^2x = σ^2y3	H:σ^2x = σ^2y1	H:σ^2x = σ^2y2	H:σ^2x = σ^2y3
25	14 °F	Accept	Accept	Accept	Accept	Accept	Accept
10	14 °F	Accept	Accept	Accept	Accept	Accept	Accept
5	14 °F	Accept	Accept	Accept	Accept	Accept	Accept
1	14 °F	Accept	Accept	Accept	Accept	Accept	Accept
0.5	14 °F	Accept	Accept	Accept	Accept	Accept	Accept
0.1	14 °F	Accept	Accept	Accept	Accept	Accept	Accept
25	40 °F	Accept	Accept	Accept	Accept	Accept	Accept
10	40 °F	Accept	Accept	Accept	Accept	Accept	Accept
5	40 °F	Accept	Accept	Accept	Accept	Accept	Accept
1	40 °F	Accept	Accept	Accept	Accept	Accept	Accept
0.5	40 °F	Accept	Accept	Accept	Accept	Accept	Accept
0.1	40 °F	Accept	Accept	Accept	Accept	Accept	Accept
25	70 °F	Accept	Accept	Accept	Accept	Accept	Accept
10	70 °F	Accept	Accept	Accept	Accept	Accept	Accept
5	70 °F	Accept	Accept	Accept	Accept	Accept	Accept
1	70 °F	Accept	Accept	Accept	Accept	Accept	Accept
0.5	70 °F	Accept	Accept	Accept	Accept	Accept	Accept
0.1	70 °F	Accept	Accept	Accept	Accept	Accept	Accept
25	100 °F	Accept	Accept	Accept	Accept	Accept	Accept
10	100 °F	Accept	Accept	Reject	Accept	Accept	Accept
5	100 °F	Accept	Accept	Reject	Accept	Accept	Accept
1	100 °F	Accept	Accept	Accept	Accept	Accept	Accept
0.5	100 °F	Accept	Accept	Accept	Accept	Accept	Accept
0.1	100 °F	Accept	Accept	Accept	Accept	Accept	Accept
25	130 °F	Accept	Accept	Accept	Accept	Accept	Accept
10	130 °F	Accept	Accept	Accept	Accept	Accept	Accept
5	130 °F	Accept	Accept	Accept	Accept	Accept	Accept
1	130 °F	Accept	Accept	Accept	Accept	Accept	Accept
0.5	130 °F	Accept	Accept	Accept	Accept	Accept	Accept
0.1	130 °F	Accept	Accept	Accept	Accept	Accept	Accept

Repeated Load Permanent Deformation

Table 106. CV (%) Values for Flow Number Parameters

CV (%) Values for Flow Number Parameters				
	Actuator	**PLA**	**ABS**	**PC**
Flow Number (Cycles)	15.70	15.00	12.48	15.74
Resilient Modulus at Failure (psi)	17.94	15.32	58.06	14.21
Axial Permanent Strain at Failure εp (%)	9.75	26.36	4.71	3.78
Axial Resilient Strain at Failure εr (%)	16.00	19.25	44.71	15.02
εp/εr (%)	25.29	11.96	51.52	16.79

Axial Cyclic Fatigue

Table 107. CV (%) Values for Flow Number Parameters

CV (%) for Fatigue Parameters				
	BRASS	**PLA**	**ABS**	**PC**
Strain @ 10000	13.037	8.633	8.876	6.240
Strain @ 100000	13.037	8.633	8.876	6.240
Strain @ 1000000	13.037	13.096	8.876	6.240
Nf @ 100 με (100th Cycle)	136.980	38.521	40.260	27.347
Nf @ 200 με (100th Cycle)	107.039	78.719	64.780	51.121
Nf @ 300 με (100th Cycle)	120.041	125.704	82.491	71.485
Slope	-13.031	-9.658	-8.870	-6.240